IJHSR International Journal of High School Research

February 2022 | Volume 4 | Issue 1

ijhighschoolresearch.org

ISSN (Print) 2642-1046

ISSN (Online) 2642-1054

Marine Biology Research at Bahamas

Unique and exclusive partnership with the Gerace Research Center (GRC) in San Salvador, Bahamas to offer marine biology research opportunities for high school teachers and students.

- Terra has exclusive rights to offer the program to high school teachers and students around world.
- All trips entail extensive snorkeling in Bahamian reefs as well as other scientific and cultural activities.
- Terra will schedule the program with GRC and book the flights from US to the GRC site.
- Fees include travel within the US to Island, lodging, meals, and hotels for transfers, and courses.
- For more information, please visit terraed.org/bahamas.html

Terra is a N.Y. based 501.c.3 non-profit organization
dedicated for improving K-16 education

Table of Contents

February 2022| Volume 4| Issue 1

Editorial Board

International Journal of High School Research

IJHSR
ijhighschoolresearch.org
■ RESEARCH ARTICLE

Coronavirus Disease 2019: Why Some Countries Appear to be Relatively Spared

Ahmed J. Aldeeb

Doha College, Al Mansoura, Doha, Doha, PO Box 7506 , QATAR; ahmedjehaddev@gmail.com

ABSTRACT: The COVID-19 pandemic has affected numerous countries worldwide, however some countries appear relatively spared when compared to others. There are countless factors affecting the spread of the virus and its distribution. This study aimed to characterize factors such as: population density, age of the population, climate & immunology, and strategies/measures used by nations to combat the spread of the virus. Whilst these factors play substantial roles in explaining the possible reasons for the uneven distribution around the world, there were a few exceptions to each of the findings. Furthermore, precautionary measures and effective strategies to limit and combat the spread of COVID-19 have played a significant role regardless of factors such as regional climates, population density, and more. Above all, it is important to note that with additional knowledge and information about the virus, scientists and researchers will be able to develop more effective approaches in responding to such a virus, and even future diseases.

KEYWORDS: Biology; COVID-19; population age; climate; Immunology; population density; inflammation; medicine.

■ Introduction

COVID-19 was first identified on 31 December 2019, following a report of a cluster of cases of "viral pneumonia" in Wuhan, People's Republic of China. The World Health Organization proclaimed the outbreak a "Public Health Emergency of International Concern" in January 2020, and in March 2020 declared it a pandemic. As of the 19th of December 2020, 5:22 pm CET, there have been 74,299,042 ± total cases globally; with the Americas accounting for about 43% of the cases (globally), and Europe accounting for about 32% of the total cases (globally), while the Eastern Mediterranean, Africa, South East Asia, and the Western Pacific regions combined account for just around 25% percent, despite housing around 6,283,110,834± people which is about 4 times more compared to the Americas' and Europe's population of 1550260479±. In this report (Figure 1),[1,2] the reasons behind this significant difference will be investigated and specific countries will be explored further to thoroughly understand and examine examples of how some factors might come into play.

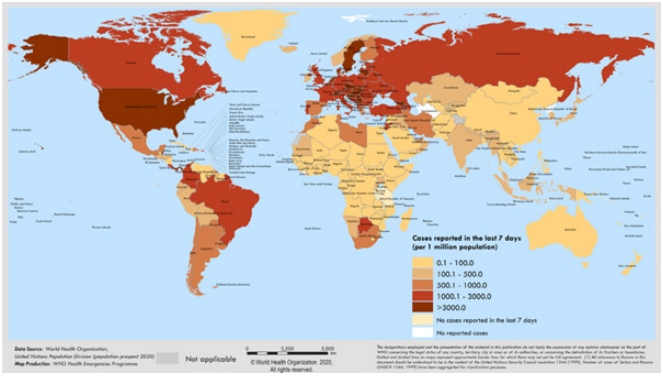

Figure 1: Map displaying total cases reported (per 1 million population) in the last 7 days, as of 2020/12/19, 5:22pm CET.[1]

Based on the data, the Americas had the most cases, 31,925,704, and following that Europe, with 23,457,397 cases, Southeast Asia, 11,572,247, Eastern Mediterranean at 4,641,968, Africa at 1,701,091, and finally the Western Pacific region at 999,891. However, what is unusual is the great difference in population between the regions. For instance, the Americas account for 802,409,370± (approximately 10.2%) of the global population (at the time of writing is 7,833,371,313),[2] and Europe with 747,851,109± (approximately 9.5%) of the population. In contrast, all of the other regions, in spite of having a population of 6,283,110,834± (more than 4 times as much as the population of the Americas and Europe); report fewer cases compared to the Americas and Europe (Figure 2). This might be due to efficient practices and measures, political aspects, availability of healthcare, environmental aspects, and numerous other factors.

Population Density:

Population density is the number of individuals per unit geographic area, numerous politicians and public figures have argued that population density affects the transmission of the virus (Figure 3).[3] However, it is one of many factors that affect the transmission rate of the 2019-nCoV, that should be taken into account while understanding the reasons behind this abnormal distribution of cases in different countries.

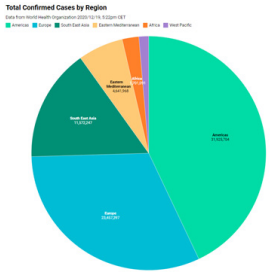

Figure 2: Pie chart displaying the total confirmed cases by region according to the World Health Organization.[1]

DOI: 10.36838/v4i1.1

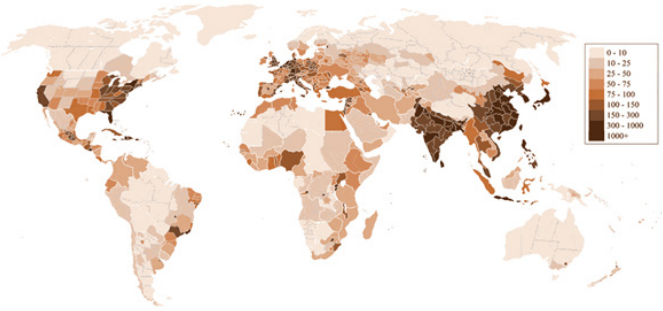

Figure 3: Map displaying population density of countries and states around the world according to the CIA World Factbook.[4]

According to the World Health Organization, Singapore, Hong Kong, Bahrain, Malta, Bangladesh, Palestine, Lebanon, Taiwan, South Korea, Rwanda (excluding island nations or territories, *read notice*) place the top ten most densely populated countries in the world.[1]

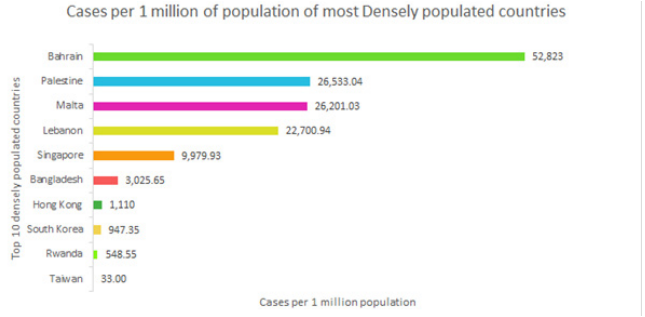

Figure 4: Graph displaying the total cases per 1 million population of most densely populated countries around the world.[1, 4]

As shown in Figure 4, the included countries all belong either to the Eastern Mediterranean, Southeast Asia, Africa, and Western Pacific regions (with the exception of Malta, an island country in the Mediterranean Sea and part of the EU politically, however geographically speaking part of Africa). It can also be seen that countries that are located in the Eastern Mediterranean account for more cases per 1 million population. However, it should be noted that the top 4 countries have a smaller population compared to the rest. For example, Bahrain has 1.569 million people, while Taiwan has 23.78 million people; so, if a number of cases appear, the cases per million population would be higher in Bahrain than in Taiwan. This method is more efficient and accurate in comparing countries rather than using the number of total cases, as every country has a different population. According to the data, it can be observed that countries like Rwanda, South Korea, Hong Kong, and Taiwan are responding exceptionally well to the COVID-19 pandemic.

Similarly, in less densely populated countries, it was observed that countries in the Americas, and Europe have the highest cases per 1 million population (with the exception of Libya, an eastern Mediterranean country). While countries like Australia, and Mongolia (Western Pacific) had fewer cases, with the African countries following (Figure 5).

As Mongolia, Australia, Suriname, Iceland, Guyana, Libya, Mauritania, Botswana, Canada, and Russia place the top ten least populated countries in the world respectively; we can clearly show that population density doesn't affect the cases per 1 million population, just like in the previous example (Figure 5).

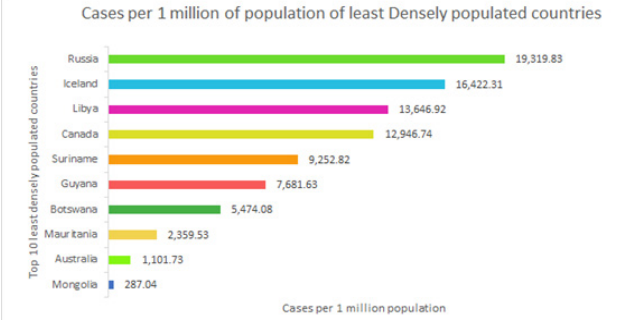

Figure 5: Graph displaying the total cases per 1 million population of least densely populated countries around the world.[1, 4]

As a whole, despite being more densely populated, some countries like South Korea, Rwanda, Hong Kong, and Taiwan managed to have fewer cases per 1 million population than less densely populated countries. This shows that population density does not necessarily play a role in a country's cases. Furthermore, the Americas, Europe, and some Eastern-Mediterranean countries performed worse than Western-Pacific, and African countries.

Young Population:

Additionally, aging might be a contributing factor in the uneven distribution of cases around the globe (Figure 6).

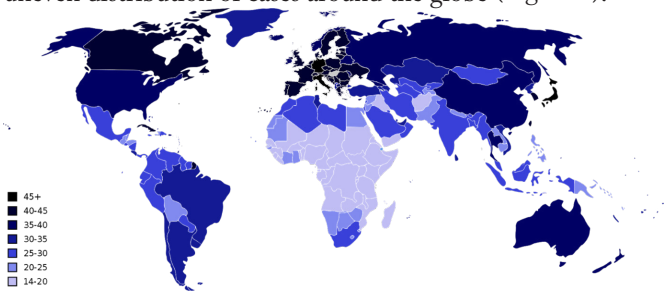

Figure 6: Map displaying Median age by country, according to CIA World Factbook 2018 est.

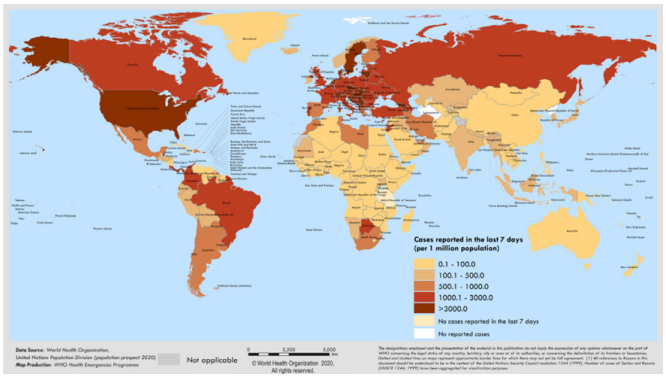

Figure 7: Map displaying total cases reported (per 1 million population) in the last 7 days, as of 2020/12/19, 5:22pm CET.

Comparing Figures 6 and 7, it can be clearly seen that there is a moderate relation between the median age of countries and the reported cases in the last 7 days, from the time of this writing. There are some outliers, such; as Australia, New Zealand, China, Ireland, etc., however in the majority of countries, a pattern can be noticed, the older the population,

DOI: 10.36838/v4i1.1

the more cases, and the younger the population, the fewer the cases.

In addition, African, Eastern Mediterranean, Western Pacific, and South-East Asian regions appear to be relatively spared compared to the Americas and Europe.

To further investigate the matter, I decided to take the newly reported cases in the last seven days from the top 10 countries with the youngest and oldest populations (according to CIA World Factbook 2018 estimate),[4] and compare them with each other and point out the differences and similarities between the cases and age, and the possible causes.

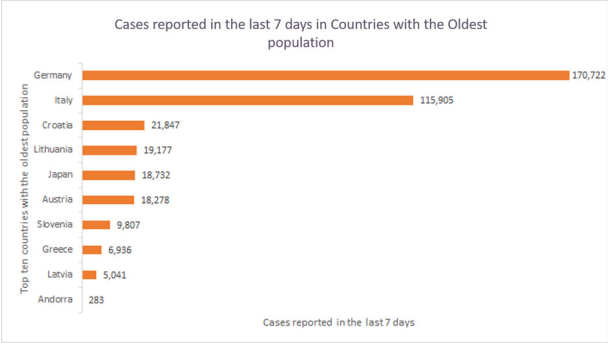

Figure 8: Graph representing the cases reported in the last 7 days in countries with the oldest population.

Based on Figure 8, all of the countries, except Japan, are in Europe, and Western Europe seems to be more affected than Eastern Europe and the Balkans. The country that was most affected was Germany, with 170,722 cases reported in the last 7 days. While the least affected country Andorra, which only has a population of 76,177± people, reported 283 cases in the last 7 days.

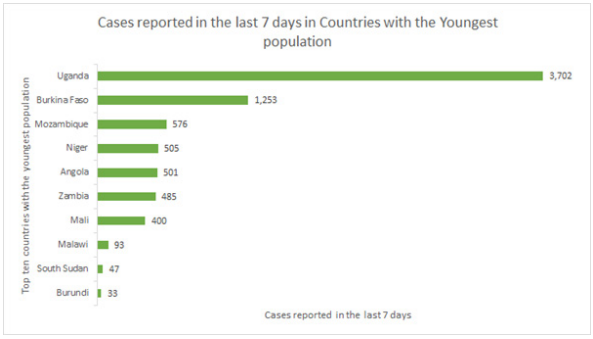

Figure 9: Graph representing the cases reported in the last 7 days in countries with the oldest populatios.

Based on Figure 9, all of the 10 countries are from Africa, which does explain why they are spared more when compared to other regions. The country with the highest number of cases reported in the last 7 days was Uganda, with 3,702 cases reported in the last 7 days, while Burundi accounted for the least number of cases (in the last 7 days), for a total of 33.

The difference can be clearly observed, which confirms that the age of a country's population does affect the case count to varying degrees and does not apply in all circumstances. In addition, Uganda, with 3,702 cases, accounts for fewer cases reported (in the last 7 days) than the top ten countries with the oldest populations (with the exception of Andorra) in the world. From the data, Africa's young population has clearly helped it to accumulate fewer cases. The same can also be said for most of Asia. This is clearly the result of declining mortality, and the high fertility rate amongst people, especially in Africa.[6] Despite the information gathered, the reasons behind the probability of catching the virus in varying ages needs to be explained thoroughly, as a lack of available information regarding the probability of different age groups catching the virus, is present.

Although there have been several studies on this matter, the research records the number of cases reported from each age group, as seen below (Figure 10) from the Georgia Department of Public Health, and not the immunity of different ages catching the virus.[7]

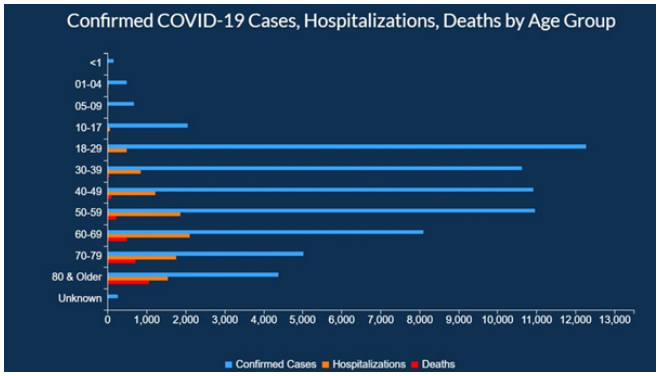

Figure 10: Graph representing and comparing the cases, hospitalizations, and deaths by age groups, according to the Georgia Department of Public Health.[7]

What is not ideal in this method is that it is obvious that people of ages, 18-59, spend more time outside,[8] than children, teenagers, and the elderly. This of course varies but is true for the majority of people. Therefore, this does not measure the immunity towards the virus, but instead the age groups and their cases and deaths.[9]

Nonetheless, the difference between the younger and older populations is believed to be a result of the aging immune system. However, information about this has not been thoroughly explored as minimal research has been done in this area.

Aging Immune System:

An aging immune system may have an effect on the probability of catching a virus and responding to it. The immune system protects the body from external and internal stressors (harmful substances, germs, and cell changes that could make a person ill).[10] It is beneficial for fighting pathogens like bacteria, viruses, parasites, or fungi, as well as for recognizing and neutralizing harmful substances from the environment. In addition, the immune system is responsible for fighting off disease-causing changes in the body, such as cancer cells or in this case COVID-19 infected cells.

As people age, the immune system changes in several ways. Immunosenescence, the aging process that leads to dysregulation of immunity and a person's adaptive response to pathogen exposure, is one major factor in the changes the immune system goes through in the process of aging. Another noteworthy process is Inflammaging, which is a chronic increase in systemic inflammation, that attacks mainly the macrophage as one of its major target cells in this process.[11]

DOI: 10.36838/v4i1.1

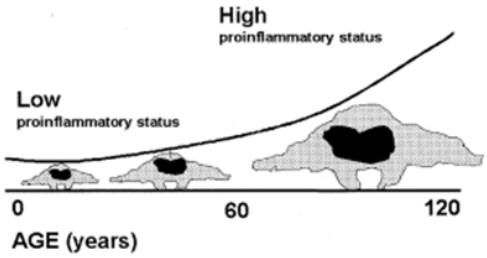

Figure 11: Inflamm-aging as a consequence of macroph-aging.[11]

As seen above (Figure 11), this prediction conveys a relation between age and macrophage activation, which is mostly responsible for the presence of a subclinical chronic inflammatory process in the elderly. Though, macrophages are not the only cell involved in this process, as cells like lymphocytes are also affected by immunosenescence.

As a whole, immunosenescence, and inflammaging affect the immune system during aging. This could be a factor attributed to the distribution of cases throughout countries depending on ages.

Climate and immunolog:

Climate and Immunology can be a noteworthy consideration for the spread of the coronavirus among countries.

A coronavirus is a single-stranded RNA-enveloped virus. Non-enveloped viruses -- such as coxsackieviruses, poliovirus, and rotavirus – cannot survive for extended periods of time on surfaces and can be affected by heat, moisture, or pH. On the other hand, enveloped viruses (such as the coronavirus); can remain infectious on surfaces for several days. The persistence of viruses, for example the coronavirus, can be affected by environmental conditions and factors like heat, moisture, pH, and the type of surface.[12] Furthermore, conditions such as heat can be found in the principle behind inactivated vaccines; where viruses such as measles, mumps, and rubella are inactivated with heat or formaldehyde -- a notable example is the BBIBP-CorV vaccine from Sinopharm.[13] Evidently, the virulence of coronaviruses (including SARS-CoV-2) appears to attenuate or get completely inactivated by heat; in our case the Tropical Sun.

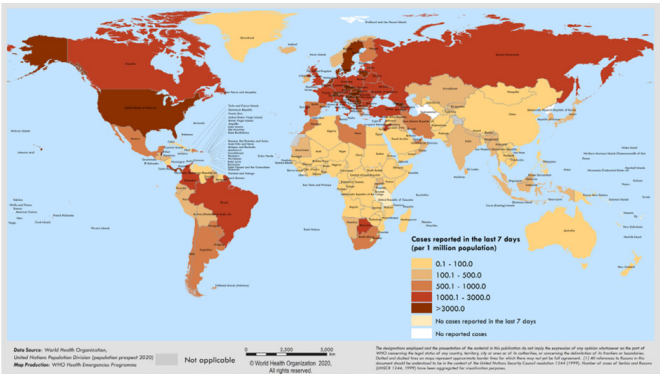

In the above image, it can be seen that the tropics, sub-Saharan, and Sahelian regions; spanning from Mauritania, Morocco, and the Western Sahara region to Egypt and eastern African countries, through the Middle East, and into South-East Asia, appear to be relatively spared. Other regions, such as the Malay Archipelago and the Western Pacific (Oceanic) regions also appear to be spared in mortality rates and cases (Figure 12).

As such, this evidence might also aid in the understanding of why certain regions appear to be spared in case count and mortality rates. Due to the nature of the virus being incapable of withstanding heat, the coronavirus would not be able to remain on surfaces as long compared to regions with relatively colder temperatures. This helps explain why there is a significant difference in cases between countries that are located in regions with hotter temperatures and countries with relatively colder temperatures.

How countries are battling the spread of the virus:

Various countries have implemented different strategies into battling the spread and effects of the virus. However, only a few countries have managed to conduct notable measures into limiting the development of the problem. One of many examples is Hong Kong, which has maintained a profoundly low numbers of cases and deaths, despite close proximity to China, and its reputation as a major transport and economic hub. Its sustainable measures and its fixed attitude amongst its people and culture (for instance, citizens wear masks to keep their faces warm in the winter and offer a sense of protection from air pollution, including any airborne germs prior to the pandemic) have helped the state to overcome any major problems that can be caused by the pandemic.[14]

Hong Kong:

Hong Kong is a country that imposes a great example of dealing with the coronavirus. This can be seen by the relatively low case count compared to many other countries, despite its remarkable status as an international transport hub. Evidently, this can be attributed to several implementations and procedures the government imposed on its population.

To begin with, experts believe the habit of wearing masks in public since the 2003 SARS epidemic has helped keep the number of cases relatively low. Additionally, border restrictions, quarantine and isolation, social distancing, and behavioral changes (such as wearing masks) may have had a role in containing the spread of the virus.[15]

Subsequently, during the 4th wave, schools were suspended until further notice, and businesses' working hours were reduced; to further reduce the spread. In addition to this, a mandate for authorities to order partial lockdowns on locations with multiple cases of COVID-19 until all residents were tested.[16]

From late January 2021, the government repeatedly locked down residential buildings to conduct mass testing. Steps have also been taken to limit the spread and death count by vaccination, as a free mass vaccination program has been launched from the 26th of February.[16]

There are numerous other examples of countries that have been able to contain the spread of the virus, in similar strategies to that of Hong Kong-- like Taiwan, South Korea, and more -- which also demonstrated outstanding results after implementation.[17]

Vacciness:

This paper has explored how inactivated vaccines may be able to protect against infection through exposure to heat. It

is important to note, that vaccine pioneers can also inactivate a version of a virus through radiation and chemicals, or by containing a similar virus that resembles the real one.[18] This is seen in vaccines offered by Sinovac, Bharat Biotech, and Sinopharm.[18] However, there are numerous other types of vaccines, such as RNA, Viral Vector Vaccines, and Protein subunit vaccines. RNA vaccines work by the concept of messenger RNA, which is a sequence of genetic code that communicates with our cells to ensure the necessary proteins are built.[19] In such vaccines, scientists develop a synthetic version of the virus' messenger RNA. When injected into the body, cells read the instructions and start building the necessary viral proteins; prompting the immune system to respond so it can learn to protect itself against future COVID-19 infection. This technology is used by Moderna and Pfizer-BioNTech, and have reported high levels of efficacy- around 95%.[20]

Conclusion

Future directions:

Above all, the coronavirus has affected the majority of countries around the world, with some nations being relatively more spared than others. However, many factors can affect the number of cases and deaths in countries. As discussed in this research paper; the population density of the country, the age of the population, immunology, climate, and precautionary measures could potentially help explain the reasons behind the disproportionate distribution of cases among countries in the world. Factors such as the coronavirus' persistence based on temperature, can help aid in the understanding of how it might react and can help develop an understanding of the virus. These factors therefore potentially allow the production of inactivated vaccines with the help of heat or formaldehyde. Additionally, precautionary measures taken by countries around the world can be used as an influential example for other countries and people to implement. Nevertheless, some factors cannot be changed such as the age of the population and the population density of a country. However, this can help us to study and comprehend how individuals and age groups are affected, as well as the environments people live in. The foregoing factors that were included in this paper are only a few of many reasons and factors that affect the spread and mortality rate of the virus. Despite this, more information and relating factors would be able to provide additional details and information to assist in the understanding of a phenomenon such as COVID-19. For the foreseeable future, more information would assist in the development of cures, vaccines, and precautionary measures and help prevent a phenomenon similar to this from occurring again.

References

1. https://drive.google.com/file/d/1cqd6uZMmj4G09RgqZZogQ_W1lwOJNd0c6/view?usp=sharing
2. https://www.worldometers.info/world-population/2020/12/19, 5:22pm CET
3. https://www.medrxiv.org/content/10.1101/2020.10.16.20213892v2.full
4. https://www.cia.gov/library/publications/resources/the-world-factbook/fields/343rank.html
5. https://en.wikipedia.org/wiki/List_of_countries_by_median_age
6. https://qz.com/africa/1099546/population-growth-africans-will-be-a-third-of-all-people-on-earth-by-2100/
7. https://www.11alive.com/article/news/health/coronavirus/coronavirus-numbers/georgia-age-group-most-covid-19-cases-18-29/85-277d5702-25fa-4ff8-8b5e-7f803b925adc
8. https://e360.yale.edu/digest/u-s-study-shows-widening-disconnect-with-nature-and-potential-solutions
9. http://phmovement.or.kr/south-korean-kids-get-just-34-minutes-of-outside-play-time-a-dayhankyoreh/
10. https://www.ncbi.nlm.nih.gov/books/NBK279364
11. https://d1wqtxts1xzle7.cloudfront.net/49787813/j.1749-6632.2000.tb06651.x20161022-14279-1s1v7mo-with-cover-page-v2.pdf?Expires=1640930139&Signature=AR0ZsHEIbt24PcbXekDKX4GVuF5ihdw9K9GOwMx01at7IRgDf3KxSektJA5POFKMpEMqoXPeWjs0GoUao-4C4psIvDPlgRLcNtAVujdIVTcvFL5AWt0EKUO1~BxknIgCqPYXUm1aqyYum4eAxdFauCnF5808wZIOYM2Y8qCy2oqY5uRKy8N6wNCZSBSy7iGrcgSWAoIRk9G710v31Pw4x-n-mU-ziDH7cGKvdx-zL6w6YQPECLNxkAdFh2iIs3p4p1NCOKJafWYnutKDigsrBCtjPY6Qr~tzppW6kYJ~y8QsXOmrbgsjz3PWd4zEXmlWsnLA9gxmQUKEYmoUtltBIA__&Key-Pair-Id=APKAJLOHF5GGSLRBV4ZA
12. https://www.jstage.jst.go.jp/article/jsme2/30/2/30_ME14145/_pdf/-char/en
13. https://www.medicalnewstoday.com/articles/covid-19-how-do-inactivated-vaccines-work#Making-inactivated-vaccines
14. https://www.voanews.com/science-health/coronavirus-outbreak/not-just-coronavirus-asians-have-worn-face-masks-decades
15. /https://www.scmp.com/news/hong-kong/health-environment/article/3078437/mask-or-not-mask-who-makes-u-turn-while-us
16. https://hongkongfp.com/2020/12/08/hong-kong-plans-partial-lockdowns-for-covid-19-hotpots-and-more-tests-as-number-of-new-infections-surges/.
17. https://healthmanagement.org/c/hospital/news/where-are-the-most-effective-anti-covid-19-strategies
18. https://www.thelancet.com/article/S1473-3099%2820%2930843-4/fulltext
19. https://www.cdc.gov/coronavirus/2019-ncov/vaccines/different-vaccines/mrna.html#:~:text=mRNA%20vaccines%20teach%20our%20cells,getting%20sick%20with%20COVID%2D19.
20. https://pubmed.ncbi.nlm.nih.gov/33629336/

Author

Ahmed Aldeeb is a 13-year-old student who is interested in researching COVID-19 and its effects on a global magnitude, and the creator of the coronavirus-tracking website www.coronaviruslive.io.

DOI: 10.36838/v4i1.1

IJHSR
ijhighschoolresearch.org
■ RESEARCH ARTICLE

Protection of Deep Neural Networks for Face Recognition with Adversarial Attacks

Alice Guo

Morgantown High School, 109 Wilson Ave, Morgantown, WV 26501, USA; aliceguo168@gmail.com

ABSTRACT: Artificial Intelligence (AI) is a transformative technology with the potential to revolutionize our entire lives. The discovery of deep neural networks (DNNs), which give computers the ability to outperform humans in many things, including face recognition, was a milestone that has made AI so inviting. However, scientists have discovered very recently that DNN networks are especially vulnerable to attacks, i.e., the so-called adversarial examples, which are imperceptible to humans but can fool DNNs easily. In this project, a novel approach is proposed to defend against these adversaries, which is much more efficient than the often-used defense methods based on adversarial learning. The newly proposed idea utilizes the attacks themselves as a defense mechanism. The task of face recognition is used to experimentally validate the novel idea and approaches. Based on a large dataset with 6,000 pairs of face images, this new defense handles the adversarial attacks efficiently, improving the face recognition accuracies from about 0% under attack to over 80% after defense.

KEYWORDS: Deep learning; Deep Neural Networks; Adversarial attacks; Defense; Face recognition.

■ Introduction

The field of artificial intelligence is essentially when machines do tasks that typically require human intelligence. It encompasses machine learning, where machines can learn through experience. Deep learning[1,2] is a subset of machine learning where artificial neural networks, inspired by the human brain, learn from large amounts of data. Deep learning is referred to as such because the neural networks have various (deep) layers that enable learning. The application of deep learning has affected almost every aspect of our daily lives. Deep Neural Networks (DNNs) have become the preferred choice as a means of solving many challenging tasks in face recognition, image classification, speech recognition, and natural language processing.[1]

Recent advances in deep learning allow neural networks to achieve the state-of-the-art results for most machine learning tasks. However, it has been shown that neural networks are vulnerable to adversarial examples.[3,6] It is easy to modify inputs so that they indistinguishable from the original data for humans, and yet classified incorrectly by the network. Figure 1 shows an example of an adversarial attack where the image of a panda has been misclassified as a gibbon. Adversarial attacks such as shown in Figure 1 make it difficult to apply deep learning models in security-critical environments. Because of this, adversarial attacks and their defenses have drawn increasing attention in recent years.

Most research focusing on adversarial attacks and defenses involve developing algorithms for the problem of image classification, based on the datasets, e.g., MNIST, CIFAR-10, CIFAR-100, ImageNet, and developed algorithms, e.g., Fast Gradient Sign Method (FGSM),[3] or C&W's attack,[5] usually do not consider the specific image content, like a human face or a special object. On the other hand, human face recognition (FR) is a different problem with many practical applications. Deep networks developed for face recognition could be attacked as well. Currently, there are a small number of approaches to attacking face recognition systems, which are specially designed for perturbation of face images to attack FR systems,[7,9] by modifying facial features and/or by facial landmark manipulations. Thus, a question is raised: is the development of special attacks against face images needed in order to attack face recognition systems? In other words, are the attacks developed for image classification applicable to effectively attack face recognition?

It is unclear whether the attacks developed for image classification apply to face images without detecting any facial content or details. A knowledge gap exists, which is one of the motivations for this work. The purpose of this project is to examine whether the attack methods take effect on face images without searching any facial content or details. If the answer is yes, researchers should make efforts to deal with these general attacks for face recognition systems; in contrast, if the answer is no, there should be less concern about face recognition attacks, and the focus should be on developing special attacks to face images by utilizing the facial features or landmarks in order to attack the FR systems.

Therefore, it was of great importance to investigate the representative attacks developed for image classification for their effect on face recognition. Additionally, a new scheme based on positively utilizing the attacks themselves is developed to protect deep networks for face recognition under attack.

The main contributions of this work include:

• An investigation and selection of the representative adversarial attack methods originally developed for image classification, but applied to a different problem domain- face recognition;

DOI: 10.36838/v4i1.2

• An exploration of the selected attack methods' effect and performance on face recognition;

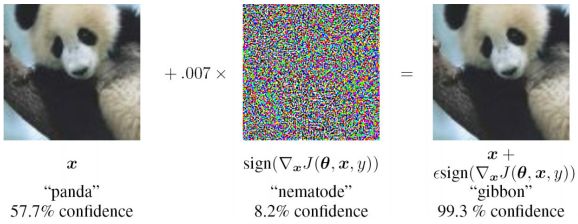

Figure 1: An adversarial image generated by Fast Gradient Sign Method:[3] left: a clean image of panda; middle: the adversarial perturbation; right: adversarial image, classified as a gibbon.

• A proposed and validated new scheme based on a smart and positive use of the attacks to make face recognition systems more robust against adversarial attacks.

In the following paragraphs, Section 2 presents some representative methods for adversarial attacks in image classification. Section 3 describes a new investigation of the attacks on face recognition and proposes a new scheme for defense. Experimental validations are conducted in Section 4. Finally, some conclusions are given.

■ Methods for Adversarial Attacks

Quite a few methods have been developed to perform adversarial attacks to deep networks[10] with typical attack applications on image classification. After careful examination of various attack methods, three were selected for the investigation on face recognition, and brief descriptions of the selected methods are presented here, followed by a short overview of defense approaches.

Fast Gradient Sign Method (FGSM):

Goodfellow *et al.* proposed a method called Fast Gradient Sign Method (FGSM),[3] which performs one-step gradient updates along the sign direction of the gradient at each pixel. The algorithm can be expressed as:

$$x^{adv} = x + \epsilon \cdot sign(\nabla_x L(x, y, \theta)), \qquad (1)$$

where ε is the magnitude of the perturbation and $L(x, y, \theta)$ is the original loss function (such as the cross-entropy loss for image classification). x is the clean image, y is the ground truth label, θ is the set of parameters, and x^{adv} is the adversarial example after the attack.

FGSM updates each pixel location of image x by a magnitude of ε following the direction that increases the original loss function. Targeted attack towards a given label l is also easy to perform, only requiring a flipped sign in Eq. (1) and changing the ground truth label y to the targeted label l.

Projected Gradient Descent (PGD):

A more powerful adversary is the multi-step variant $FGSM^k$, which is essentially projected gradient descent (PGD) on the negative loss function:[4]

$$x_{k+1}^{adv} = x_k^{adv} + \alpha \cdot sign(\nabla_{x_k^{adv}} L(x_k^{adv}, y, \theta)), \quad (2)$$

where the PGD first finds the adversarial example by iteratively adding the gradient sign with the previous adversarial example in Eq. (2). α in the equation is a small constant. Also, small, random noise is added to the clean image before the first iteration, which may slightly improve the attack success rate.

One main difference between PGD and many other adversarial methods is that PGD only uses adversarial data to update the parameters of the model, rather than using both the clean and adversarial data as in many other methods.

C&W's Attack (C&W:

The C&W's Attack (CW)[5] is with a new adversarial loss function,

$$\min_{\delta} \ ||\delta||_p + c \cdot g(x + \delta) \qquad (3)$$

$$s.t. \ \ x + \delta \in [0, 1]^d \qquad (4)$$

where $g(x^{adv}) \geq 0$ if and only if $f(x^{adv}) = l$. Here l is the targetted attack label, δ is the pixel perturbation, p is the norm control, c is a constant, and d is the image size.

The distance along the penalty term can be easily optimized with any gradient-based method (FGSM, PGD, etc.). Several different objective functions can be used for $g(x)$. One of the most commonly used is:

$$g(x^{adv}) = \max(\max_{i \neq l}(f_i(x^{adv})) - f_l(x^{adv}), \ -k) \qquad (5)$$

Where $f(x)$ denotes the output from Softmax function. This objective pushes the Softmax score for targeted attack class l to be higher than all other classes i by a margin k.

Adversarial Defenses:

Adversarial defense mainly follows two approaches. These methods differ in the stage where defense is applied: either at the data input stage or at the model stage. Currently, the most effective defense methods are model stage defenses. An example of this is adversarial training,[4,11] where models are trained with adversarial examples, and thus, become more robust to adversarial attack during the test time. In practice, however, adversarial training can take a very long time, e.g. days to learn with a robust model.

Unlike model stage defense, input stage defense does not make any changes to the original model. Such defense methods either detect for an adversarial example before feeding it into the model,[12,13] or reconstruct the input data so that the adversarial perturbation is removed.[14,15]

One major concern with input stage defense is that the defense accuracy tends to drop significantly when the attacker knows the detection or reconstruction pipeline and modifies the attack accordingly.[10] It is also quite hard to remove the perturbations and recover the clean images from the attacked adversarial examples.

■ New Attacks

So far, there are only a small number of approaches related to attack and defense for face recognition. Existing approaches[7,9] are specially designed for attacking face images, using facial properties or landmarks, while a number of methods were developed for attack and defense to image classification. It was worth investigating a whether the attack and defense methods developed for natural image classification can be applied to face recognition or not since face recognition is considered a different task from image classification.[7,9]

DOI: 10.36838/v4i1.2

Attacks to Face Recognition:

After a careful examination of the attack methods, three representative methods were selected among those attacks, the FGSM,[3] PGD,[4] and C&W,[5] as presented in the previous section, applying to attacking face recognition. Reasons for selecting these three representatives are: (1) The FGSM is a classical one-step attack method, which can be computed effectively based on the gradient operation; (2) The PGD and C&W are two effective iterative methods with multiple iterations in attacking image classification systems. The three selected examples are sufficiently representative for attacks to image classification.

The benefits of examining the image classification attacks on face recognition include: (1) If the attacks developed for image classification can be applied to face recognition effectively, one may not need to pursue the use of special properties from facial regions in designing the face attack algorithms; Instead, one may just treat the face images as some "general" images; (2) On the other hand, if the attacks designed for image classification have no effect on face recognition, one may not need to worry about those attacks in developing a face recognition system. Therefore, it is of great importance to investigate the effect on face recognition on the attacks designed to attack image classification systems.

Defenses for Face Recognition:

In addition to applying the attacks on face recognition and investigating the attack effects, it is also useful to develop an approach to defend the attacks on face recognition.

A novel defense idea is presented here utilizes the attacks to change the clean face images of the adversarial images, and then the face matching is changed to measure the similarity between two adversarial face images, rather than between one clean face image and one attacked image.

By applying the adversarial attack to the query face image and gallery database face image, both images are converted into adversarial images, and the problem is reformulated as matching between two adversarial images. In this way, it not only avoids the need to retrain the face recognition model with adversarial examples, which could take days or weeks even for a relatively small dataset,[4] but also circumvents the unnecessary trade-off between robustness and model accuracy, as in previous approaches.[16] So, there are some useful properties for the proposed new approach as compared to adversarial training and other complex defense methods developed so far.

■ Results and Discussion

The datasets and the deep networks used for face recognition are introduced first. Then the validation of the selected attacks on face recognition are presented. Next, the new scheme for defense is evaluated.

Dataset and Deep Networks:

Web-collected data sets were used, including CASIA-WebFace with 453,453 images over 10,575 identities (a cleaned version of the original dataset), and LFW with 6000 pairs of face images, including 3000 pairs of the same person (positive pairs) and 3000 pairs of different people (negative pairs). In the experiments, CASIA-WebFace was used to train the deep model for face recognition, and then the LFW was used to evaluate the trained model for face verification.

All the faces in images were aligned by MTCNN algorithm[17] and cropped to 160 x 160 RGB images for FaceNet[18] and 112x112 for CosFace.[19] Following convention, each pixel (in [0, 255]) in RGB images was normalized by subtracting 127.5 and then dividing by 128 in testing. For training, random flipping and per-data whitening was used.

The network used was the same as the used in FaceNet + CosFace with the SphereFace Network.[20] The pre-trained model was provided by the inventors, which was trained on CASIA-WebFace and tested on LFW. For face verification, an input image was fed to a pre-trained model, and the extracted feature of that image was a size of 512 for FaceNet and 1024 for CosFace. Then, the distance, or similarity, was computed for every pair of images. As a result, the verification accuracy was 98.9% for FaceNet and 99.3% for CosFace, showing that the face models can work very well for face recognition without attacks. For the following experiments, only the CosFace model was used, because of its higher accuracy.

Attacks on Face Recognition:

The most commonly used adversarial attack methods, FGSM, PGD, and C&W attacks, originally proposed for image classification tasks, were selected for examining their effect on face recognition.

In the experimental validation, all perturbations were added onto the face images in LFW dataset for the face verification task. For experimental results, the accuracies of verification were compared between two cases: before attacking and after attacking, to evaluate the attack methods' capability to attack face recognition. For all attacks, the perturbations of images were constrained within the pixel value difference of 2, 4, and 8 (for the 0 to 255 range). FGSM is a one-step attack, which means the perturbation is executed only once. However, the PGD and C&W are iterative; thus, the perturbation calculations are done many times. In the end, the accuracies for face verification with adversarial attacks on the LFW are shown in Table 1.

From Table 1, it is clear that the three selected attack methods can disrupt the face recognition system significantly. For instance, even the one-step attack method FGSM can reduce the face recognition accuracy from 99.3% to 7.5% when the perturbation range is within 4 pixel values, and can be reduced further to 2.9% when the perturbation is allowed to have 8 pixel values. The iterative methods PGD and C&W can be more effective than the FGSM in attacking. For example, the face recognition accuracy can be reduced from 99.3% to 0.0% when the perturbations are within 4 pixel values. Based on these experimental results, one can see clearly that the attack methods originally developed for image classification can attack the face recognition systems significantly without identifying any special facial properties or manipulating any facial landmarks. So, based on the results here, effective attack methods can be develop for face recognition systems without utilizing the facial fiducial points or any other special features

or properties in those methods to attack face recognition.

Table 1: Face verification accuracy after attacks. The separate accuracies for positive and negative pairs are reported, in addition to the accuracy for all pairs. Some key parameter settings are reported as well.

Attack Method		Acc.(%)	Acc.(%) (pos.)	Acc.(%) (neg.)
FGSM	eps=2.0	30.20	30.80	29.50
	eps=4.0	7.50	7.30	7.70
	eps=8.0	2.90	1.80	3.90
PGD (Iter 10)	step size=0.5 eps=2.0	3.40	3.50	3.30
	step size=1.0 eps=4.0	0.00	0.00	0.00
	step.size=2.0 eps=8.0	0.00	0.00	0.00
C&W (Iter 10)	step size=0.5 eps=2.0	3.40	3.50	3.30
	step size=1.0 eps=4.0	0.00	0.00	0.00
	step size=2.0 eps=8.0	0.00	0.00	0.00

Defenses for Face Recognition Systems:

After showing the effectiveness of the selected attack methods on face recognition, a further question arises: how do we develop effective defense methods to deal with those attacks and make the face recognition systems more robust?

In the field of image classification, the most commonly used defense methods are based on the adversarial training[3,21] by adding the adversarial examples with the clean images in the training stage. However, adversarial training can be very time consuming, may take days or weeks even on a relatively small dataset,[4] and also has to trade-off between robustness and model accuracy.[16]

Table 2: Face verification accuracy after using PGD defense.

	num_step: 10 step_size: 2.0			num_step: 20 step_size: 1.0			num_step: 40 step_size: 0.5		
	Acc. (%) overall	Acc. (%) (pos.)	Acc. (%) (neg.)	Acc. (%) overall	Acc. (%) (pos.)	Acc. (%) (neg.)	Acc. (%) overall	Acc. (%) (pos.)	Acc. (%) (neg.)
PGD vs PGD	2.70	1.00	4.40	37.9	34.2	41.7	71.4	65.9	76.9
FGSM+PGD vs PGD	26.0	16.9	35.1	58.8	50.5	67.2	80.6	74.7	86.6
PGD + PGD vs PGD	45.2	37.7	52.6	73.8	68.7	78.9	88.0	84.5	91.5
C&W+PGD vs PGD	45.2	37.5	52.8	74.1	69.0	79.2	87.8	84.4	91.2

Table 3: Face verification accuracy after using C&W defense.

	num_step: 10 step_size: 2.0			num_step: 20 step_size: 1.0			num_step: 40 step_size: 0.5		
	Acc. (%) overall	Acc. (%) (pos.)	Acc. (%) (neg.)	Acc. (%) overall	Acc. (%) (pos.)	Acc. (%) (neg.)	Acc. (%) overall	Acc. (%) (pos.)	Acc. (%) (neg.)
C&W vs C&W	13.5	11.4	11.6	43.4	38.1	48.2	72.1	66.4	77.8
FGSM+C&W vs C&W	26.0	16.9	35.2	59.0	49.9	68.1	80.8	74.3	87.3
PGD+C&W vs C&W	45.4	37.7	53.0	74.4	69.9	79.0	88.1	84.7	91.6
C&W+C&W vs C&W	45.1	37.2	52.9	74.4	69.3	79.4	87.9	84.6	91.2

In this exploration to develop a defense for face recognition systems, the author takes a unique approach to using the attacks to create a novel and effective defense. The key idea is to apply the attack to clean face images before matching in such a way that the face matching is between two attacked face images rather than between an attacked image and a clean one.

The defense results are shown in Tables 2, 3, and 4. In each table, the results are shown for face matching of "Query" vs "Gallery", which indicates what attack methods were applied to the query face image and gallery image, respectively. For example, the first row in Table 2: "PGD vs PGD", means that the PGD attack was applied to the query face image and gallery face image, individually. In the first row of each of the three tables, the results were to show the case when the same attack methods are applied to the query and gallery face images separately. That is, assuming that the attack methods were known (to the query), and the same attack methods were applied to the gallery face images as well. In this case, both the PGD and C&W methods did well for defense. For instance, after 40 iterations, the face recognition accuracies can be raised from 0% to 71.4% for the PGD method and to 72.1% for the C&W method. However, as shown in Table 4, the FGSM method did not raise the face recognition accuracy. So, to use the attacks to perform defense, the FGSM attack did not work while the PGD and C&W methods improved the face recognition accuracies significantly.

In practice, the attacks may not be known to the defense system. To perform the defense for unknown attacks, the three attack methods were validated with a different setting. No matter what the attack method was on the query face image, a specified attack method (one of the FGSM, PGD, and C&W) was applied to the query image again, and the same attack method was applied to the gallery face image as well.

The experimental results using this approach are shown in Tables 2, 3 and 4 in rows 2-4. For example, in Table 2 row 2: the FGSM attack was applied to the query face image which was unknown to the defense system. The PGD attack method was the specified method by the defense system, so the PGD attack was applied to the query face image (already attacked by the FGSM), and also applied to the gallery face image. The face recognition accuracy was raised from 0% to 80.6% by using the PGD attack as the specified defense and the recognition accuracy was improved significantly.

Table 4: Face verification accuracy after using FGSM defense.

	num_step: 10 step_size: 2.0			num_step: 20 step_size: 1.0			num_step: 40 step_size: 0.5		
	Acc. (%) overall	Acc. (%) (pos.)	Acc. (%) (neg.)	Acc. (%) overall	Acc. (%) (pos.)	Acc. (%) (neg.)	Acc. (%) overall	Acc. (%) (pos.)	Acc. (%) (neg.)
FGSM vs FGSM	6.20	12.2	0.20	0.10	0.20	0.00	0.00	0.00	0.00
FGSM+FGSM vs FGSM	0.00	0.00	0.00	0.00	0.00	0.00	0.00	0.00	0.00
PGD+FGSM vs FGSM	0.00	0.00	0.00	0.00	0.00	0.00	0.00	0.00	0.00
FGSM+FGSM vs FGSM	0.00	0.00	0.00	0.00	0.00	0.00	0.00	0.00	0.00

Similarly, a check of other rows in the three tables, shows that even when the attacks were unknown to the defense system, the PGD and C&W methods (Tables 2 and 3) still worked well for defense. All recognition accuracies were raised above 80% by both methods. However, the FGSM method did not work, since almost all accuracies were about 0%, as shown in Table 4.

To summarize the experimental results, both the PGD and C&W attack methods work quite well in serving as a defense, whether the attacks to the query face images are known or unknown. The FGSM attack does not work for any defense.

■ Conclusion

Adversarial attacks on face recognition were investigated with three representative attacks, the FGSM, PGD, and C&W, selected to perform attacks on face recognition. The validations revealed that the three attacks can make face recognition performance worse, reducing the recognition accuracies from about 99% to 0%. This result is of great importance, showing that the design of attacks to face recognition systems does not need to use special facial properties or landmarks, which were utilized previously to attack face recognition. Furthermore, a novel use of the attacks was proposed and performed for defense. Experimental results show that the PGD and C&W attacks can be used to perform defense effectively, raising face reecognition accuracies from 0% to around 80% or above, regardless of whether the attacks are known or unknown; this is of great significance in practice, since the attacks can be used positively for defense result. Future research could show deeper insights into the mechanism of attacks and defense, and validate future attacks developed for defense purposes.

DOI: 10.36838/v4i1.2

Acknowledgements

The author thanks X. Xu and C. Chen for some help on coding and running experiments and reviewers for previewing the paper.

References

1. Yann LeCun, Yoshua Bengio, and Geoffrey Hinton. Deep learning. *nature*, 521(7553):436, 2015.
2. Ian Goodfellow, Yoshua Bengio, and Aaron Courville. *Deep learning*. MIT press, 2016.
3. Ian J Goodfellow, Jonathon Shlens, and Christian Szegedy. Explaining and harnessing adversarial examples. *arXiv preprint arXiv:1412.6572*, 2014.
4. Aleksander Madry, Aleksandar Makelov, Ludwig Schmidt, Dimitris Tsipras, and Adrian Vladu. To- wards deep learning models resistant to adversarial attacks. *arXiv preprint arXiv:1706.06083*, 2017..
5. Nicholas Carlini and David Wagner. Towards evaluating the robustness of neural networks. In *Symposium on Security and Privacy*, pages 39–57. IEEE, 2017
6. Nicolas Papernot, Patrick McDaniel, Ian Goodfel- low, Somesh Jha, Z Berkay Celik, and Ananthram Swami. Practical black-box attacks against ma- chine learning. *In Proceedings of the 2017 ACM on Asia Conf. on Computer and Communications Security*, pages 506–519. ACM, 2017.
7. Qing Song, Yingqi Wu, and Lu Yang. Attacks on state-of-the-art face recognition using attentional adversarial attack generative network. *arXiv preprint arXiv*:1811.12026, 2018.
8. Mahmood Sharif, Sruti Bhagavatula, Lujo Bauer, and Michael K Reiter. Adversarial generative nets: Neural network attacks on state-of-the-art face recognition. *arXiv preprint arXiv:1801.00349*, 2017..
9. Ali Dabouei, Sobhan Soleymani, Jeremy Dawson, and Nasser M Nasrabadi. Fast geometrically- perturbed adversarial faces. *arXiv preprint arXiv:1809.08999*, 2018.
10. Anish Athalye, Nicholas Carlini, and David Wagner. Obfuscated gradients give a false sense of security: Circumventing defenses to adversarial examples. *arXiv preprint arXiv:1802.00420*, 2018.
11. Florian Tram`er, Alexey Kurakin, Nicolas Paper- not, Ian Goodfellow, Dan Boneh, and Patrick Mc- Daniel. Ensemble adversarial training: Attacks and defenses. *arXiv preprint arXiv:1705.07204*, 2017.
12. Jan Hendrik Metzen, Tim Genewein, Volker Fischer, and Bastian Bischoff. On detecting adversarial perturbations. *arXiv preprint arXiv:1702.04267*, 2017.
13. Reuben Feinman, Ryan R Curtin, Saurabh Shintre, and Andrew B Gardner. Detecting adversarial samples from artifacts. *arXiv preprint arXiv*:1703.00410, 2017.
14. Arjun Nitin Bhagoji, Daniel Cullina, and Prateek Mittal. Dimensionality reduction as a defense against evasion attacks on machine learning classifiers. *arXiv preprint arXiv:1704.02654*, 2017.
15. Dongyu Meng and Hao Chen. Magnet: a two- pronged defense against adversarial examples. In *Proceedings of the 2017 ACM SIGSAC Conference on Computer and Communications Security, pages 135–147*. ACM, 2017.
16. Dimitris Tsipras, Shibani Santurkar, Logan Engstrom, Alexander Turner, and Aleksander Madry. Robustness may be at odds with accuracy. *stat, 1050:11*, 2018.
17. K. Zhang, Z. Zhang, Z. Li, and Y. Qiao. Joint face detection and alignment using multitask cascaded convolutional networks. *IEEE Signal Processing Letters, 23(10):1499–1503*, 2016.
18. Florian Schroff, Dmitry Kalenichenko, and James Philbin. Facenet: A unified embedding for face recognition and clustering. In *Proceedings of the IEEE conference on computer vision and pattern recognition*, pages 815–823, 2015.
19. Hao Wang, Yitong Wang, Zheng Zhou, Xing Ji, Dihong Gong, Jingchao Zhou, Zhifeng Li, and Wei Liu. Cosface: Large margin cosine loss for deep face recognition. In *Proceedings of the IEEE Conference on Computer Vision and Pattern Recognition*, pages 5265–5274, 2018.
20. Weiyang Liu, Yandong Wen, Zhiding Yu, Ming Li, Bhiksha Raj, and Le Song. Sphereface: Deep hypersphere embedding for face recognition. In *Proceedings of the IEEE conference on computer vision and pattern recognition*, pages 212–220, 2017.
21. Ruitong Huang, Bing Xu, Dale Schuurmans, and Csaba Szepesv´ari. Learning with a strong adversary. *arXiv preprint arXiv:1511.03034*, 2015.

Author

Alice Guo is currently a senior at Morgantown High School in Morgantown, WV, but completed this research project as a freshman. She is the recipient of research awards at the international level and has been recognized by organizations and government agencies for her work. With strong interests in computer programming, artificial intelligence, mathematics, and writing, she plans to major in Computer Science in college.

IJHSR
ijhighschoolresearch.org

■ REVIEW ARTICLE

Scientific and Medical Research Involvement amongst High School Students and Career Exploration Initiatives: A Scoping Review

Abramo Aziz Rizk, Mohid Farooqi, John Sarga, Mahmoud Al-Izzi, Monica Elzawy, Ahmed Al-Izzi, Abanoub Aziz Rizk

Bishop P. F. Reding Catholic Secondary School, 1120 Main St E, Milton, Ontario, L9T 6HT, CANADA; abramorizk@gmail.com.

ABSTRACT: Involvement by high school students in scientific inquiry expands experiences and enriches education. Research experiences can be utilized in high school education in an attempt to improve students' critical thinking skills through introducing the following interventions: science fairs, in-class experimentations, and research papers. The aim of this study was to collect current data and discuss the efficacy, drawbacks, and future goals for these interventions. The objective of this study was to develop an outline of how research might be introduced into the high school curriculum and present the strengths as well as limitations of such initiatives. This review was written in a scoping review format using the five stages of the proposed approach by Arksey and O'Malley and advanced by Levac, Colquhoun, and O'Brien. PubMed and Gale Academic OneFile databases were used to search for articles related to high school students engaging in research. While each method of implementation of research into the high school curriculum has its strengths and limitations, they can be used in conjunction to complement each other. Implementing research into the curriculum may improve education at the high school level if it is incorporated correctly. Additionally, providing more opportunities for high school students to get involved in research may help guide interested students toward a suitable career path and may even spark new interests in some students.

KEYWORDS: High school; Students; Curriculum; Education; Research; Scientific inquiry; STEM.

■ Introduction

Research, which is the act of inferring new ideas based on past knowledge and investigating the truth of those ideas using observations, is an important aspect of science that allows for the evolution of human knowledge.[1] A study suggested that high school students' performance in science education has been on a downward trend, suggesting that the importance of science is being diminished over time.[1] Teaching students how to conduct research may have the potential to improve many basic skills one might need in life, such as critical thinking skills and the ability to consult multiple sources before making conclusions on a subject.

In Canada, high school is a fundamental part of the education of students. It provides a basis of knowledge required to enter the workforce or specialize that knowledge further through higher education. Currently, in the general science curriculum, science is taught in a way that "does not stimulate application-based approach of course delivery" or the ability to make conclusions by oneself.[2] Instead it emphasizes memorization over application of material.[2] It has been suggested that this can cause students to lack critical thinking skills and be unable to create causal links.[2] To develop students' abilities in science, research can be used to show them methods by which ideas are discovered, thereby developing their abilities to think critically.

There are numerous ways through which research can be introduced to high school students including the following: science fairs, in-class experimentations, and adding research papers into the science curriculum. Science fairs are science projects that groups, or individuals can work on which will be evaluated by a group of judges. Since there are both competitive and non-competitive science fairs, it is a good way to inspire interest in science education. In-class experimentation is a method that can provide students with experience in the science field by providing opportunities to preform experiments firsthand. Lastly, research papers can be implemented to help students critically think about scientific topics.

There are currently several uncertainties in the area of research in high school education. Firstly, it is unknown which method of research incorporation into the high school curriculum introduces the greatest benefits while also minimizing the drawbacks for the students and faculty. Additionally, the exact effectiveness of each method is also unknown as there is a lack of quantitative studies analyzing the effectiveness of each method. While there is a lack of quantitative assessment, expert opinions have been compiled in this paper. The final area of concern is the gap between successful and struggling students which may be created by introducing a richer curriculum. Given the large amount of uncertainty, a more collaborative effort, and a summary of what has been previously studied is required. It is beneficial to know what the research shows so that new principals, directors, and departments of education will be better equipped to make more informed decisions for future steps.

Early exposure to STEM (science, technology, engineering, mathematics) at the high school level is important as it helps young students direct their steps toward a suitable and fulfilling career. Additionally, providing high school students with

DOI: 10.36838/v4i1.3

the opportunity to gain experience in the healthcare system is another method by which students can discover their interests. In this way, students can receive a holistic view of the roles and responsibilities associated with various healthcare careers before deciding to pursue higher education in the medical field.

This study aims to collect the current data and discuss the efficacy, drawbacks, and future goals for each of these interventions while also posing an outline of how research might be introduced into the high school curriculum and presenting the strengths and limitations of such initiatives.

Methods

This study was written in a scoping review format, which is predominantly used when the topic in discussion has not been well-researched. Scoping reviews are used to organize literature, unlike systematic reviews which address a single question. There are various reasons why scoping reviews are conducted, including covering key concepts, and analyzing and identifying knowledge gaps. The five stages of the proposed approach by Arksey and O'Malley and advanced by Levac, Colquhoun, and O'Brien was used, which is considered a methodologically rigorous scoping review. These five stages are as follows: (1) finding research questions, (2) searching for relevant literature, (3) filtering studies that do not fit the inclusion criteria, (4) inputting the data in a chart, and (5) summarizing, acquiring, and reporting the results.

This literature review searched through various databases to locate studies that documented methods of engaging secondary students in research activities. PubMed and Gale Academic OneFile were searched for articles that have been published between the years 2003 to 2020.

Inclusion criteria for the studies were: (1) the participants had to include high school students and (2) the students were conducting any form of research. Any studies with students in higher education (e.g., undergraduate studies) and articles that were not written in English were excluded. This study searched articles related to the keywords below using the following search criteria: adolescent [MESH and keyword search], students [MESH and keyword search], research personnel [MESH], laboratory personnel [MESH], high school [keyword search], secondary school [keyword search], middle school [keyword search] AND research [MESH and keyword search], science [MESH and keyword search], Proof of Concept Study [MESH], Problem Based Learning [MESH], experiment [keyword search], science fair [keyword search], experimental [keyword search], STEM [keyword search], informal learning environment [keyword search], hands-on [keyword search].

Results

Eleven studies fit the inclusion criteria described above. Three studies analyzed the effectiveness of science fairs in promoting interest and skill development in research and experimentation. These studies used student opinions regarding their experiences to draw conclusions about the benefits and drawbacks of science fairs, and whether or not they should be mandatory. In addition, five studies focused on providing students with real-world research experience. They accomplished this by giving the students a chance to work with three studies focused on unique methods through which high school students can conduct research inside the classroom.

Table 1: Review of data collected on effects of research implementation in the high school curriculum.

Source	Objective/ Goals	Explanation /Method of implementing research	Suggested Pros	Suggested Cons
Rosenbaum, J.T.; Martin, T.M.; Farris, K.H.; Rosenbaum, R.B.; Neuwelt, E.A.[1]	The article sheds light on the "pre-eminence of science in the United States [being] endangered"1 The objective of the article is to understand whether universities, specifically medical schools, can teach high school students' scientific inquiry.	The plan is to teach the class about the processes of scientific inquiry through various methods including partnering each student with a mentor, use of journal club format, a hypothesis proposal, and "hands-on" laboratory experience.[1]	• Provides an opportunity for students to get involved in science and gain experience in the field. • Teaches the students how to conduct research. • Study found that 73% of their graduates were planning careers in science or health.1 • Students were seven times more likely to rank the class as "influencing career or life choices".1 • The experience is given to students throughout the study "dramatically affects one's attitudes towards science".1	• Requires students to spend time outside of general schooling under specific instruction only for science, which removes time from other critical subjects such as English. • Incredibly resource- intensive as each student has a mentor who presumably has their own responsibilities, creating a large amount of workload.
Brill, G.; Yarden, A.[2]	The study uses research papers as a substitute to textbooks in a classroom to stimulate critical thinking and deeper questions for high school students.	To introduce students to scientific inquiry research in developmental biology was adopted into the curriculum. The effect this produced was profound in that students went from asking questions about basic properties to asking questions about causal links and comparisons. The effect of having just one research paper added to the curriculum created a significant increase in the quality of student questions.	• Increased depth of student's questions. • Introduces students to cutting-edge research that increases interest. • Significant increase in critical thinking after reading just one study.[2]	• Studies may req ire prior knowledge. • Hard to implement new research for students. • Can confuse some students forcing them to require more help from teachers.
Grinnell, F.; Dalley, S.; Shepherd, K.; Reisch, J.[3]	This article focuses on the improvement of high school level science by determining the strengths and weaknesses of the high school students regarding science. A survey was done to collect the information on the high school students.	To improve high school level science, the writer proposes to make science fair participation required, and in doing so, provide experience to the students.	• Provides experience to students on how to conduct research. • Is likely to help when getting into universities and colleges. • It was shown in the article that the students who participated in science fairs had an easier time researching, having access to various articles, and not having a hard time finding resources.	• Since the writer proposes to make science fairs mandatory, many students may not be interested in science and as a result, may not benefit from the experience.
Polcino, C.; Jory, B.; Sabety, J.; Jones, L.G.; Ashcroft, J.; Rodriguez, B.[4]	This study introduces the process of making alloys to high school students in an effort to teach scientific inquiry.	The scientific method is introduced through alloys and experimentation involving alloys. Students' existing knowledge was used and expanded upon with inquiry in researching alloys and learning the chemistry, physics, and geology behind metallurgy.	• Alloys are an age-old process that can be meshed with history.. • Easy concept to pick up and use to learn scientific inquiry.	• Difficult to reach a high level of critical thinking with such an established concept. • Concept may not be known to many students and would be redundant unless it completely replaces textbook work.
Brooks, E.; Dolan, E.; Tax, F.[5]	This article talks about providing meaningful research experiences to high school students, scientists, teachers, and the students who work together in order to understand the inner workings of science. PREP (The Partnership for Research and Education in Plants) uses classroom- tested protocols to cooperate with the students in finding the function of a disabled gene in Arabidopsis through a large- scale research project.	First, the teachers must locate the university or college with scientists they wish to collaborate with. Then they formulate a plan for the project and find any additional things they need including materials, responsibilities as well as schedules. The first step for the students is to study Arabidopsis and the gene(s). As the experiment is underway, they begin to collect data and use critical thinking skills to see differences between wild-type and mutant plants. Then after they finish their analysis, the scientist can help them interpret their results.	• Provides a way to present difficult concepts. • A more engaging way of learning. • Provides meaningful researching skills and experiences.	• A lot of money and funding is required to do this research project.
Naujock, J.[7]	This article talks about incorporating field research into the high school science curriculum to give students experience in the real world.	Send students into real-world scenarios that require them to conduct research to answer problems.	• Students are more motivated. • Students gain confidence and a sense of accomplishment. • Classroom dynamics between students and teachers improve.	• It takes a long time.. • General knowledge that is required by the curriculum may overwhelm students that spend time in field research.
Kabacoff, C.; Srivastava, V.; Robinson, D.N.[8]	This article is about giving minority students the chance to apply themselves in a real- world environment and gain more representation in the sciences.	Disadvantaged youth get access to a summer academic research experience that is an academic internship. The goal is to fortify academic and scientific skills.	• Allows students to get a better understanding of science in the real world. • Allows them to learn in a real- world setting.	• Requires students to give up their summers, leading to them losing their break from school, increasing the amount of stress they feel. • This could lead the disadvantaged students, in the process of catching up, to fall further behind.
Paul, J.; Lederman, N.G.; Groß, J.[9]	The study investigates the effectiveness of science fairs as tools to teach scientific experimentation.	Experiments are essential for both doing science and learning science. The aim of the German youth science fair, Jugend Forscht, is to encourage scientific thinking and inquiry methods such as experimentation.	• Science fairs are a universally accessible form of learning experimentation. • Students learn to reflect on their work and develop unique processes to experiment. • Increase interest in science careers.	• Requires student motivation. • Can lead to some students following the wrong track of thinking. • Lack of proper materials and pathways to data leads to falsification and plagiarism of data.
Grinnell, F.; Dalley, S.; Reisch, J.[10]	This article speaks on improvement in high school level science by identifying the strengths and weaknesses of students regarding science.	Surveys are done by the students to collect data on whether students developed an interest in science after their previous experience with science fairs. By proposing to make science fairs mandatory, students will have more experience in the subject and in conducting research.	• The improvements that are to be made can help teachers provide more effective and more. engaging science fairs • Students learn how to conduct research. • Gives data on student opinions on how to improve science fairs.	• More survey responses were filled in by grades 9 and 10 leading to a skew in the data against grade 11 and 12 opinions. • More girls than boys filled out the surveys leading to a skewed result.
Ericsson, J.; Husmark, T.; Mathiesen, C.; Sepahvand, B.; Borck, Ø.; Gunnarsson, L.; Lydmark, P.; Schröder, E.[11]	This article reported on four senior high school students who participated in a computational physics research project. In this project, students worked at a laboratory for one week. They conducted research in computational physics, to understand how research is done in the real world.	Students are taken to a lab where they perform "density functional theory (DFT) calculations to obtain the adsorption energy and structure of the toxic methylbenzene molecule toluene on graphene."[11]	• Allows high school seniors to develop research skills that will be applicable going into university. • Allows advanced students to contribute to society in a meaningful way the year before normally possible.	• Significant knowledge barrier for high school students to research advanced topics. • Time barrier for high-school students. • Requires very high-level students which limits participation.
Peffer, M.E.; Beckler, M.L.; Schunn, C.; Renken. M.; Revak, A.[12]	This article talks about the benefits of SCI simulations in the classroom.	SCI simulations are conducted by accessing a website that has a simulation that you can interact with. You are then to work through the simulation in the same way one might do so in a lab.	• It does not require a lot of resources. • It is very time efficient. • It sheds light on how scientists perform research in the real world.	• Educators would need to be trained to implement this effectively. • It requires access to technology, which may be a challenge in some communities.

Discussion

In this review paper, the need for the inclusion of research in the high school curriculum was identified and several methods to implement research were provided. To determine effective methods for high school students to take part in research, a scoping review was conducted. Three methods were preeminent in providing an avenue to conduct research including science fairs, in-class experimentation, and incorporating research papers into the science curriculum.

One method of engaging high school students in research is through science fairs. During a science fair, students are asked to research and develop an idea that they present to a group of judges. If the science fair is competitive, the judges will evaluate all of the projects and subsequently crown a winner. If the science fair is non-competitive, the judges will give each contestant feedback on their ideas and areas of improvement. Additionally, they will not declare a winner. Each type of science fair has its benefits and drawbacks. Competitive science fairs are shown to work better with students who have already developed an interest in science before competing. This is because these students have a desire to compete and win the competition. This type of science fair generally does not interest students who do not have a passion for science. A study was done which gathered student opinions on science fairs. In this study, one student mentioned that when they were forced to compete, some students could have an advantage as they might potentially have family connections to a scientist or have been exposed to gathering research from academic studies.[3] This leaves the students without these aforementioned advantages feeling that the science fair is futile due to their inability in competing with other students who may have many more resources than them at their disposal.[3] In conclusion, this type of science fair is well suited for students who already display interest in the subject of sciences, lending them valuable background experience in research that could be used beyond secondary school education. However, it can be unwise to force all students to compete in science fairs, since many students who either do not want to win or do not think they can win can feel alienated from the competition.

On the contrary, non-competitive science fairs generally appeal to a wider range of students. They can allow students who have a passion for science to explore their areas of interest and present them to the judges to get feedback on their ideas. However, it does not take advantage of some students' competitive nature in the same way that a competitive science fair might. It also allows students who do not have an interest in STEM (science, technology, engineering, mathematics) to select a topic that they think they would be interested in and develop a project based on that idea. As a result, these students may develop a passion for a new topic while also providing an opportunity to present it to the judges to get feedback on their ideas. Non-competitive science fairs might not present the same challenge that a competition traditionally would, but they can still be considered an opportunity to improve student skills. Both methods of implementing science fairs types of students. A common issue between each of the methods is that they can take an extensive amount of time and resources to implement. The current Ontario curriculum demands students learn a certain amount of core, foundational knowledge to pass the exam stages and acquire a high school diploma. In other words, introducing science fairs into the secondary education module without altering the time spent in other areas would increase the workload on students and render them feeling overwhelmed.

Another method of introducing research to high school students is through in-class experimentation and explanation of ideas. For example, in order for students to learn about alloys, they would be given the methods and materials to create different alloys, then followed by being tasked with answering questions about the process, and finally formulate conclusions as well as potential causal links.

Consequently, students could be able to conduct research and utilize the scientific method in a simpler, friendlier, and more guided manner. This method can be applied in a way to demonstrate the process by which scientific ideas in the curriculum were discovered. Although in-class experimentation has many benefits, there are still limitations as to what it can accomplish. Primarily, most of the concepts introduced through the experiments are well-established concepts. For instance, one of the studies reported on teaching high school students about creating alloys, a process that has been carried out for hundreds of years.[4] As a result, it is possible that levels of critical thinking are lessened. Another challenge is the high financial demand for implementation. This includes difficulties in covering the costs of the materials as well as the costs associated with training teachers.

The final method is to use research papers to showcase to high school students how to appropriately form causal links and critically think about scientific topics. Before being exposed to the way scientists think, high school students "tend to ask only questions of the properties category."[2] To show students what type of questions to ask and how research is conducted, they can read articles and make their own hypotheses while following the research paper introduced to them. This can allow students to ask deeply meaningful questions, form creatively enhanced links and out-of-the-box style of thinking. While this method requires significant alterations to Ontario's high school curriculum and serious effort from teachers to implement, it is flexible in terms of the level of difficulty.[2] Implementing research papers may also be one of the easiest for teachers to incorporate in high schools but could be one of the hardest for students to grasp and understand. Even though it requires no added infrastructure or materials, students will become required to demonstrate effort into reading and understanding advanced educational studies. It is important to note that this method is the most well-documented in terms of results as it has statistical evidence. A study was conducted by Brill and Yarden[2,5] in which secondary students were tasked to create questions and answers. In advance of being introduced to any of the learning, 94% of the students asked declarative questions; however, after they were exposed to a research paper, 21% of the students made causal relationships.[2] The substantial change in the types of questions asked after reviewing only

DOI: 10.36838/v4i1.3

one research paper demonstrates the efficacy of this method of teaching students about science.[2] Notably, this method of implementation can deliver promising benefits, including the following: increased depth of questions, ease of implementation, and an enhanced understanding of the scientific method for students. Due to the lack of studies on this topic, the effects that implementing research papers will have on struggling students are not yet understood and no sufficient analysis can be inferred on individual students.[2] One possible way to implement this method into Ontario's high school curriculum is to introduce a research paper in every unit and guide students through the procedure of learning research work in detail. While reading the papers, students are shown how researchers reach their conclusions and establish facts.

Strengths and Limitations:

A strength of the study includes how the study identifies three ways of integrating research into the school environment, as well as providing the positives and negatives of each method. Identifying this allows the study to be more impartial and less biased. The limitations of the study are that there is a limited volume of academic literature, from which statistical evidence is even more sparse due to which a significant conclusion is hard to reach. Even though there is a limited volume of literature on this topic, significant pros and cons could not be included. It is recommended that future studies focus on the interventions discussed in this review; science fairs, in-class experimentation, and research papers in hopes of providing more concrete statistical evidence to support proper implementation of these interventions. Another limitation of this study is that the criteria of the searched articles may have excluded relevant articles and journals. Furthermore, exploring more education systems outside of the North American countries can help to analyze different methods of implementing research in the high school curriculum.

Future Steps:

To ensure the success of the interventions outlined in this paper, multiple steps can be taken. Firstly, additional studies can be carried out to analyze the different methods of research, specifically the impacts of the methods on individual students. Through conducting further research studies, the statistical efficacy of each proposed method will be made clear. Secondly, through the use of surveys, gathering the opinions of students who have participated in the trials for the interventions will be essential in applying for these programs on a large scale. This will allow students to offer advice on how to improve the programs and limit their drawbacks. Through these surveys, the curriculum can be modified to accommodate students. Lastly, studies can be conducted to determine how research may be implemented into the curriculum while ensuring students will not be overwhelmed by their workload. It is important to manage the load on students to make sure the gap between successful and struggling students is not increased, leading to an unfair working environment that is unrewarding for struggling students.

Conclusion

There are many promising methods that high schools can employ to engage students in the process of research. Each method has its limitations and benefits, which is why implementing multiple methods can help compensate for the weaknesses of each method. Firstly, introducing research to high school students through research papers would be very effective as an introduction because there would be minimal changes to the infrastructure of the school. In addition, exposing students to how experiments are carried out can help them grasp more complicated forms of research. The students who are interested in science can sign up for an optional science fair in which they can gain experience in individually conducting research. The effectiveness of implementing research is corroborated by the consensus of all the studies discussed in this review, that it is beneficial for students. Thus, it can be concluded that integrating research into the high school curriculum can be an important step to improving the level of education in high schools

Acknowledgements

We would like to thank our mentors and supervisors: Abanoub Aziz Rizk, Ahmed Al-Izzi, and Monica Elzawy for catering to our requisites through their knowledge and experience. Furthermore, we appreciate the help and guidance from our senior post-secondary team bestowed in the success of this project. Albeit no funding was provided, we are truly grateful for having the opportunity to conduct this research project.

References

1. Rosenbaum, J.T.; Martin, T.M.; Farris, K.H.; Rosenbaum, R.B; Neuwelt, E.A. Can Medical Schools Teach High School Students to Be Scientists? Federation of American Societies for Experimental Biology Journal 2007,21 (9), 1954-1957.
2. Brill, G.; Yarden, A. Learning Biology Through Research Papers: A Stimulus for Question- Asking by High-School Students. Journal of Cell Biology Education 2003,2 (4), 266-274.
3. Grinnell, F.; Dalley, S.; Shepherd, K.; Reisch, J. High School Science Fair: Student Opinions Regarding Whether Participation Should Be Required or Optional and Why. Public Library of Science one 2018,13 (8), 1-16.
4. Polcino, C.; Jory, B.; Sabety, J., Jones, L.G.; Ashcroft, J.; Rodriguez, B. Advancing Alloys: Bringing Solid Mixtures to The High School Classroom. The Science Teacher Journal 2020,87 (7), 40-49.
5. Brooks, E.; Dolan, E.; Tax, F. Partnership for Research and Education in Plants (PREP): Involving High School Students in Authentic Research in Collaboration with Scientists. The American Biology Teacher 2011,73 (3),137-142.
6. Muncan, B.; Majumder, N.; Tudose, N. From High School to Hospital: How Early Exposure to Healthcare Affects Adolescent Career Ideas. International Journal of Medical Education 2016, 7, 370-371.
7. Naujock, J. Incorporating True Research Opportunities into High School Curriculum: A Research and Design Course. School Science and Mathematics 2009,109 (7),369-370.
8. Kabacoff, C.; Srivastava, V.; Robinson, D.N. A Summer Academic Research Experience for Disadvantaged Youth. Cell Biology Education A Journal of Life Science Education 2013,12 (3), 410-418.
9. Paul, J.; Lederman, N.G.; Groß, J. Learning Experimentation Through Science Fairs. International Journal of Science Education 2016,38 (15), 2367–87.

10.Grinnell, F.; Dalley, S.; Reisch, J. High School Science Fair: Positive and Negative Outcomes. Public Library of Science one 2020,15 (2), 1-17.
11.Ericsson, J.; Husmark, T.; Mathiesen, C.; Sepahvand, B.; Borck, Ø.; Gunnarsson, L.; Lydmark, P.; Schröder, E. Involving High School Students in Computational Physics University Research: Theory Calculations of Toluene Adsorbed on Graphene. Public Library of Science one 2016,11 (8), 1-12.
12.Peffer, M.E.; Beckler, M.L.; Schunn, C.; Renken, M.; Revak, A. Science Classroom Inquiry (SCI) Simulations: A Novel Method to Scaffold Science Learning. Public Library of Science one 2015,10 (3), 1-14.

Authors

Abramo Aziz Rizk was born in Turin, Italy on the 12th of January 2005. He is a junior student at Bishop Reding Catholic Secondary School and is currently in the AP program. Abramo was also a recipient of the science and math award in grade 9.

Mohid Farooqi is a sophomore at Bishop Reding Catholic Secondary School. He has an interest in many fields including physics and neurology. Some of his accolades include high placement in Waterloo math competitions. He has ambitions to create change globally and hopes to do so through academics.

John Sarga was born in Egypt on May 28, 2004. John is a junior taking the AP program at Bishop Reding Catholic Secondary School, who anticipates following a computer science track in university.

Mahmoud Al-Izzi is a junior student at St. Francis Xavier Catholic Secondary School. Aside from his academic achievements in mathematics and science courses, he has participated in Medlife Bites for a Bigger Cause campaign to aid in diminishing the world hunger crisis. His ambition remains paramount in the health sciences field.

Monica Elzawy is currently an undergraduate student studying Biomedical Science at the University of Guelph. She has a continuous desire to learn and a passion for facilitating knowledge transfer in academia.

Ahmed Al-Izzi is a dental student at the University College Cork Faculty of Dentistry. He is constantly eager to keep himself updated on advancements in the healthcare field through attending continuing medical education courses, participating in research activities, and engaging in community services.

Abanoub Aziz Rizk is a medical student at the University of Ottawa Faculty of Medicine. He has a great interest in medical education and wishes to instill love for learning amongst others through research and community initiatives.

DOI: 10.36838/v4i1.3

IJHSR
ijhighschoolresearch.org
■ RESEARCH ARTICLE

Solitary Confinement Resources

Brooke M. Kivel

Hendrick Hudson High School, 2166 Albany Post Rd, Montrose, NY 10548, USA; Brooke.kivel890@gmail.com

ABSTRACT: Solitary confinement is the most severe form of isolation found within the United States. The conditions are so poor that the prisoners suffer horribly in terms of mental health, and their rates of recidivism correspondingly increase. The goal of this research was to determine helpful psychological resources to implement into solitary confinement units to keep prisoners mentally healthy, thus preventing them from reoffending. A survey was distributed to individuals previously in solitary confinement, asking them about their experiences and desired resources. The most desired resources were human interaction, mental health resources, and more time out of cell. These resources should be implemented into all states that continue to use the system of solitary confinement.

KEYWORDS: Behavioral and Social Sciences; Sociology and Social Psychology; Psychology; Prison; Mental Health; Solitary Confinement; Prison Reform.

■ Introduction

Solitary confinement has previously been referred to as "a concentration of some of the most important negative effects of the entire prison complex."[1] Solitary confinement is a form of severe imprisonment in which prisoners are completely isolated from human contact, the outside world, or any form of social interaction. While, according to the National Criminal Justice Service, one of the main goals of prisons is to offer a place of growth and hopeful rehabilitation, solitary confinement accomplishes the complete opposite.[2] Prisoners in solitary confinement have been proven to experience serious negative psychological effects that deteriorate their mental health and make it increasingly difficult to successfully reenter society.[3] They lack access to sufficient mental health resources, leading to severe negative psychological effects, and steadily increasing their rates of recidivism.[4] It is essential to research possible remedies to include in solitary confinement units, since many states are determined to continue this controversial system of incarceration. This would then allow isolated prisoners to stay mentally healthy and successfully reenter society as contributing members. This poses the question, what resources would be the most beneficial to implement into solitary confinement units, from the prisoner point of view, to prevent the development of mental health disorders among isolated prisoners?

Conditions:

Prisoners in solitary confinement are isolated an average of 23 hours a day in windowless cells that range from 60 to 80 square feet in dimension. This small space is responsible for housing the prisoner's bed, toilet, sink, and any other limited possessions they may own.[3] The Liman Program at Yale Law School, joined with the Association of State Correctional Administrators (ASCA), collected information on solitary confinement units by asking the directors of state and federal corrections systems to state their policies about administrative segregation. This was defined as removing a prisoner from the general population to solitary confinement for thirty days or more. The survey was created with the goal of discovering more about the solitary confinement experience. They formed a survey of more than 130 questions and responses were sourced from 46 jurisdictions. The survey revealed that prisoners spent 23 hours in their cells on weekdays and 48 hours straight on weekends. Opportunities for social contact were strictly limited, and time out-of-cell ranged from 3 to 7 hours a week in many jurisdictions. While some prisons have more opportunities than others, there are no regulations set in place to ensure that all prisoners in solitary confinement have access to proper psychological resources and social interaction.[4]

Psychological Effects of Isolation:

Isolation from human contact deteriorates mental health in any circumstance, and the harsh conditions of solitary confinement escalate these effects. Researcher Phillip Zombardo simulated the conditions of prison, and certain forms of solitary confinement, in his experiment titled the "Stanford Prison Experiment," in which psychologically healthy college students were placed in a prison environment, either being guards or prisoners. The "prisoners" in the experiment rapidly deteriorated into emotional breakdowns which was quite revealing, as this involved solitary confinement on a very small and much less severe level. It is essential to note that none of the prisoners in this experiment had any preexisting mental health conditions. Zimbardo's research indicates that socially isolated prisoners in solitary confinement experience "significantly increased negative attitudes and affect, irritability, anger, aggression [...] chronic insomnia, free floating anxiety, fear of impending emotional breakdowns, a loss of control, and panic attacks; [...] discomfort around other people, engage in self-imposed forms of social withdrawal, and suffer from extreme paranoia [...] hypersensitivity to external stimuli (such as noise, light, smells), [...] cognitive dysfunction [...] a sense of hopelessness and deep depression are widespread [...] and symptoms of psychosis, including visual and auditory hallucinations."[3] While the Stanford Prison experiment was not entirely focused on solitary confinement, Keramet Reiter and

DOI: 10.36838/v4i1.4

Joseph Ventura from the University of California came together to specify and measure the prevalence of psychological distress among incarcerated people solely in solitary confinement. Information was collected for this study from in-depth interviews, Brief Psychiatric Rating Scale (BPRS) assessments, reviews of medical disciplinary files for selected individuals in solitary confinement, and 1-year follow-up interviews with certain participants. The interviews included 96 questions that related to the incarcerated people's psychological health. The results of the study revealed 22% of participants attempted suicide, 18% documented other self-harm, 80% documented feelings of extreme isolation, 16% mentioned extreme anxiety, 25% felt loss of identity, and over 50% documented some other form of psychological distress.[1] This research, however, did not obtain information from the prisoners regarding resources to implement into solitary confinement units.

It is also important to note that individuals in solitary confinement are not necessarily the most dangerous in the prison complex. Some are placed in solitary if they are deemed dangerous from previous crimes, however, many are placed in solitary confinement for nonviolent offenses, suspected gang activity, immigration issues, or for their "own protection" if they are homosexual, transgender, or have been raped by other prisoners. Additionally, oftentimes prisoners are placed in solitary for breaking rules in general population prison, not regarding the degree of crime they committed.[5] Thus, the prisoners suffering the horrible psychological impacts of solitary confinement are typically no more "deserving" of their punishments than those in general population prison.

Self-Harm:

The negative mental health effects of solitary confinement can often lead to self-harm. Fatos Kaba, Andrea Lewis, and Sarah Glowa-Kollisch, researched the prevalence of self-harm within solitary confinement. To obtain their results, the researchers analyzed data from medical records on 244,699 incarcerations in the New York City jail system from January 1, 2010, through January 31, 2013. Examples of self-harm include "ingestion of a potentially poisonous substance or object leading to a metabolic disturbance, hanging with evidence of trauma from ligature, wound requiring sutures after laceration near critical vasculature, or death." The results of the study showed that out of 1303 incarcerations "there were 2182 acts of self-harm; in 89 incarcerations there were 103 acts of potentially fatal self-harm." The results showed that inmates assigned to solitary were 2.1 times as likely to commit acts of self-harm. These acts of self-violence are exceedingly dangerous, as prisoners who break property while trying to harm themselves are typically punished and forced to endure more time in solitary confinement, thus damaging their mental health further.[6] Self-harm is one of the most indicative signs of poor mental health, highlighting the incredible psychological disturbances of those in solitary confinement.

Psychological Resources and Recidivism:

Prisoners in solitary confinement lack the psychological resources necessary to prevent psychological damage, and receive treatment as little as every ninety days, or never at all. Oftentimes psychological behavior (self-harm, etc.) is regarded as behavioral issues, not psychological, and therefore not treated effectively. If their actions were approached as a psychological issue, not a behavioral one, interventions would be justified. On the rare occasion that prisoners are admitted for psychiatric help, they are returned to confinement shortly after, and this process becomes a "revolving door cycle." While resources vary between prisons, most prisoners in solitary confinement have no access to therapies, stimulating activities, or any human contact. Many prisoners who leave solitary confinement reoffend when they return home because they have suffered such psychological traumas and lack the necessary social skills to create relationships and succeed in the real world.[7] It has been proven that "many prisoners are significantly handicapped when they attempt to make their eventual transition from prison back into the free world."[3] A study of recidivism in Connecticut revealed that within three years of release from incarceration, 92 percent of prisoners kept in solitary confinement reoffended (about 30 percent higher than the regular prison population).[8] Furthermore, the type of resources needed in the prison complex is rarely studied from the prisoners' point of view. While some prisons have better solitary confinement units than others, there are no regulations set in place to protect the mental health of the prisoners. If prisons do not implement psychological resources into their solitary confinement units, they are contributing to a serious issue within the country and ultimately harming potential successful futures of the incarcerated. Additionally, if the system of solitary confinement is not reformed, the goals of the prison complex, offering rehabilitation to create positive change, will never be fully accomplished.

Methods

The decided method for this study was a survey, which would be distributed to individuals who were previously incarcerated. A survey was the most logical method to use for this research, as it allowed for the collection of information from a wide range of individuals in various states. The larger sample size provided more reliable data and made the recognition of trends clear. Additionally, this was the easiest way to hear first-hand experiences from the prisoners and the resources they wanted to implement. The survey was also kept anonymous, which prompted the participants to answer the questions more honestly and produced stronger data. The survey consisted of fourteen questions designed to confirm the negative psychological health effects of those isolated in prison and identify helpful resources to implement into solitary confinement units.

A portion of this survey was aimed at investigating the effects and conditions of isolation, similar to the ASCA-Liman 2014 National Survey of Administrative Segregation in Prison. Instead of using in-depth interviews, the Liman Program at Yale Law School and the ASCA created a survey to gather information from the largest array of state and correctional institutions in the most efficient and effective manner.[4] The survey used in this study was not completed on such a large scale, due to time and logistical constraints, but the design and reason for choosing this method was very

DOI: 10.36838/v4i1.4

similar to that of the ASCA-Liman National Survey. This study's survey had a different number and format of questions, as the goal was to determine possible resources and not discover psychological issues. In addition, it was not possible to work with current inmates, due to age related requirements and the lengthy process of approval.

To ensure "that appropriate steps [were] taken to protect the rights and welfare of humans participating as subjects in the research," the survey was reviewed and approved by Hendrick Hudson school district's Institutional Review Board.[9] In order to access a study group of individuals who were previously incarcerated the following programs were contacted: a prison reentry program that assists individuals to reintegrate back into their communities in Nevada, a transitional housing reentry center in Alabama, and a transitional housing center for ex-offenders in Alabama. The names of these centers were left out of this paper for confidentiality concerns. These rehabilitation centers all work to help those with criminal records lead successful lives, thus providing them with easy access to individuals who were previously incarcerated. The survey was emailed to the rehabilitation center directors, reviewed, and approved by their administrations, printed for the participants to fill out, and the results were scanned and returned via email. To participate in the survey, participants had to be over the age of eighteen and had to have experienced some form of incarceration in their lifetime.

The beginning of the survey prompted three formality and ethicality questions to make sure that the participant was of age (18 years or older), aware that their anonymous responses were being used for research purposes, and that aspects of mental health would be mentioned in the survey. The suicide hotline was provided to ensure that the participants would have access to mental health resources if necessary. The fourth question confirmed that the participant did experience some form of incarceration. The fifth question asked if the participant ever experienced some form of solitary confinement, however this form of isolation was not required to complete the survey. Only the responses that marked that they experienced some form of solitary confinement would be analyzed later in the research. It was expected that many of the participants would have experienced some form of solitary confinement during their time of incarceration, as previously noted research indicates this is a common occurrence for those who have been incarcerated.[3]

The next section of the survey asked about mental health symptoms that are known to result from isolation and are indicative of negative mental health. Included effects were those accumulated from various studies about the impact of solitary confinement, specifically that of Keramet Reiter and Joseph Ventura, with the Department of Criminology, Law, and Society and the School of Law from the University of California.[1] The symptoms that were chosen to investigate were insomnia, depression, anxiety, anger, and self-harm.

When the participants were asked if they experienced any of these effects, diagnosing terms were not blatantly stated, as participants might have been wary to admit they experienced mental health issues, or unaware of what these mental health issues entailed. Instead of the term insomnia, the phrase "feelings of sadness, emptiness, or lack of energy" was used, and instead of anxiety, the phrase "feelings of worry, panic, or stress" was used. The questions were formatted to ask if the participants experienced any of these symptoms after returning home from their time of incarceration.

Each survey question had five answer choices: "almost never," "sometimes," "about half the time," "most of the time," and "almost always." Each of the answer options correlated to a number that was later used for the analyzation process.

The last section of the survey was aimed at addressing the gap in current research, investigating resources to implement into solitary confinement units. The next question differed from the previous questions, as it was open response and not multiple choice. This question stated that if the participant experienced any or all of the symptoms previously mentioned in the survey, what activities or coping mechanisms did they complete to improve their mental state and alleviate those negative feelings. Inmates in solitary confinement currently lack the psychological resources necessary to stay mentally healthy, and this section of the survey would help to generate possible solutions to that detrimental issue, thus accomplishing the goal of this research study. The next question asked if any of those resources were available to the prisoners during their time incarcerated. This section was created to identify what resources were available to prisoners both in solitary confinement and the general population. The following question asked what resources were not available to them, but that they felt would be helpful. This section will be used to identify resources that should be implemented into prisons that currently are not. The final question outlined the goals of this research to the participants and provided them with space to include anything else they would like to add.

Limitations and Restrictions:

The methods used for this study did have certain limitations, as it was very difficult to obtain a large sample size for this study. Many rehabilitation centers were closed because of COVID-19, did not have the resources or time to print and distribute the survey, or simply did not want to participate. These restrictions made it difficult to access a large sample size. Additionally, the variations of regional policies in different parts of the country may have impacted the experiences of certain prisoners, thus limiting the data, as it was only collected from two states.

Results and Discussion

The survey results were analyzed from the three rehabilitation centers: 26% of the results were from the first center in Nevada, 22% were from the second center in Alabama, and 35% were from the third center in Alabama. Participants' responses were only analyzed if they marked that they experienced some form of social isolation during their time incarcerated. In total, there were 48 responses analyzed.

Quantitative Data:

For the first section of the survey, consisting of the multiple-choice questions, the average of the severity scores was calculated for each mental health symptom. The response of "Almost Never" correlated to a one, "Sometimes" correlated to a two, "Half the Time" correlated to a three, "Most of the

Time" correlated to a four, and "Almost Always" correlated to a five. The average of the severity scores for insomnia was 3.48, depression was 3.35, anger was 3.19, anxiety was 3.42, and self-harm was 2.54. The specific numbers and percentages can be found in Table 1 below. The standard deviation (σ) is also provided, which is the range to indicate the degree of variability in responses.

Table 1: Self-reported severity of mental health problems in survey responses.

Severity	1 "Almost Never"	2 "Sometimes"	3 "Half the Time"	4 "Most of the Time"	5 "Almost Always"	Average of Scores
Insomnia	5 people (10%)	11 people (23%)	3 people (6%)	14 people (29%)	15 people (31%)	3.48
Depression	6 people (13%)	13 people (27%)	3 people (6%)	10 people (21%)	16 people (33%)	3.35
Anger	4 people (8%)	14 people (29%)	9 people (19%)	11 people (23%)	10 people (21%)	3.19
Anxiety	3 people (6%)	10 people (21%)	6 person (13%)	17 people (35%)	11 people (23%)	3.42
Self-Harm	22 people (46%)	1 person (2%)	9 people (19%)	9 people (19%)	7 people (15%)	2.54

Qualitative Data: Section 1:

The next section of the survey included the written response questions, which were analyzed as a whole. Included resources were pulled from Question 11, which asked about activities or coping mechanisms that were helpful in alleviating mental health symptoms outside of the prison complex, but only included if Question 12. Question 12 asked if these resources were available to them in solitary confinement, which confirmed that this resource was not available to the prisoner during their time in solitary confinement. Not a single resource mentioned in Question 11 was said to be available in solitary confinement in Question 12. All resources from Question 13 were analyzed, as this question specifically asked for resources that would have been helpful but were not offered during their time of incarceration. The ten most reoccurring responses served as the basis of comparison and were marked for prevalence. These responses included human interaction, counseling and mental health resources, time out of cell, access to a phone, access to television, access to workout equipment, religious materials, access to books, increased medical attention, and some form of education. "Human interaction" included responses that mentioned "seeing family," "seeing friends," "getting hugs," or simply "seeing other inmates." "Counseling and mental health" included responses that specifically asked for mental health resources, someone to talk to about their feelings, or certain therapies. "Time out of cell" included responses that mentioned spending time in another room or spending more time outdoors. The rest of the included responses were more materialistic desires than experiential, and typically did not vary in response.

"Human interaction" was mentioned by 63% of participants, "counseling and mental health resources" by 56%, "time out of cell" by 44% , "access to a phone" by 31%, "access to television" by 19%, "access to workout equipment" by 10%, "religious materials" by 10%, "access to books" by 8%, "increased medical attention" by 6%, and "some form of education" by 6%. The results of this section of the survey are displayed visually in Graph 1 below.

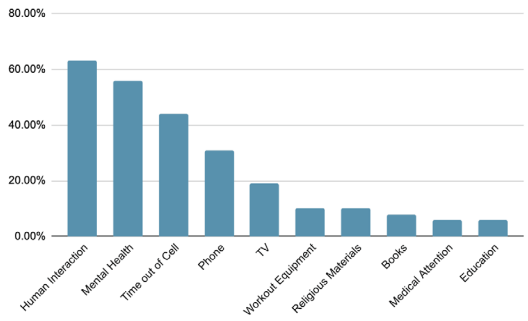

Figure 1: Desired resources of former inmates as determined by related survey questions.

Qualitative Data: Section 2

The last section of the survey included a space for participants to include a personal story or any additional information they felt would enhance this research. The responses varied, but most built upon desired resources in isolation and others detailing memorable experiences. Several of the responses were quite emotional, their tone revealing the desperation for reform in solitary confinement units. Three example responses have been provided below.

Example Response #1

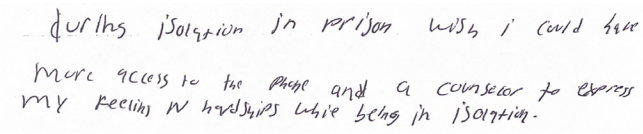
during isolation in prison what I could have more access to the phone and a counselor to express my feelings of hardships while being in isolation.

Example Response #2

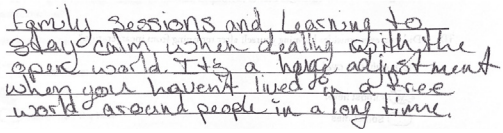
family sessions and learning to stay calm when dealing with the open world. It's a huge adjustment when you haven't lived in a free world around people in a long time.

"family sessions and learning to stay calm when dealing with the open world. It's a huge adjustment when you haven't lived in a free world around people in a long time."

Example Response #3

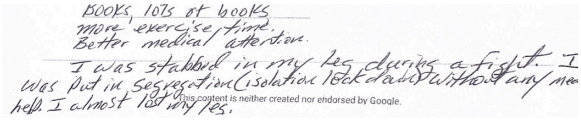

"Books, lots of books. More exercise time. Better medical attention. I was stabbed in my leg during a fight. I was put in segregation (isolation lockdown) without any medical help. I almost lost my leg."

■ Analysis & Discussion

The averages of the severity scores from the multiple-choice section confirm the prevalence of negative mental health among those who left solitary confinement. Each average hovered around the three-value range, corresponding to the response of "Half the Time." To put these values into perspective, 26% of Americans experience some form of mental health disorder, while 100% of the participants in this study claimed they experienced one or more of the symptoms listed, thus indicating they were suffering from certain mental health

DOI: 10.36838/v4i1.4

disorders.[10] This is incredibly concerning and highlights a major flaw within the solitary confinement system, as individuals who leave prison should be working to better themselves and their communities, not being subject to further psychological injury. However, the results of this section of the survey are not unique to the field of research, as negative psychological effects resulting from solitary confinement have been proven through previous research referenced throughout this study.

A new understanding of the matter comes when considering the solution to this issue, a notion addressed by the qualitative portion of the survey. The three most popular responses were "human interaction" (63%), "mental health resources" (56%), and "time out of cell" (44%). "Access to a phone" (31%) was just below these resources but can realistically be considered as an aspect of "human interaction." Resources that could more easily be implemented into solitary confinement units, such as TV (19%), religious materials (10%), and books (8%) fell staggeringly behind the popular resources, indicating that the solutions to solitary confinement cannot possibly be a "quick and easy fix." However, this research in combination with previous research, such as that from Keramet Reiter and Joseph Ventura, illustrates the urgency for reform in solitary confinement units.[1] Action must be taken immediately.

Professional Opinion:

As one of the participants stated in the survey, "It's a huge adjustment when you haven't lived in a free world around people in a long time" (Example Response #2). The lack of human interaction in solitary confinement makes it extremely difficult for prisoners to reenter society. IA criminal justice lawyer based in New Mexico (name withheld due to confidentiality concerns) was contacted to obtain his opinion on the issue of solitary confinement and certain experiences of his clients. He mentioned that many of his clients coming from solitary confinement struggle readjusting to real life, causing many of them to reoffend. He also acknowledged that several of his clients in general population prison had experienced trouble with authority by breaking certain rules but were almost always better behaved after receiving psychological counseling or treatment, highlighting the power of mental health resources. The lawyer expressed his discontent for the system of solitary confinement and the dire need for research in the field regarding solutions and reform.[11] A pseudonym was used in place of the lawyer's real name for confidentiality concerns.

Implications:

Action for reform in solitary confinement units should be based on the three most prevalent responses from the survey: human interaction, mental health resources, and time out of cell. These resources make the most sense to implement, as they were the most desired by individuals who actually spent time in solitary confinement, thus having the best understanding of the topic. In terms of human interaction, prisoners should be provided with the same visitation opportunities as those in general population prison. Familial visits would help prisoners maintain a sense of reality and memories that keep them psychologically grounded. A Vera Institute study of general population prison corroborated with the findings of this research and found that "Incarcerated men and women who maintain contact with supportive family members are more likely to succeed after their release."[12] Previous research has proven that those in solitary confinement are not the most dangerous criminals in the system, thus providing no reasoning to isolate them from family interaction. Humans are social creatures and stripping them of this basic necessity is setting them up for failure. Individuals must be accustomed to social interaction to succeed in society outside of incarceration, thus limiting the rates of recidivism. The overwhelming amount of survey responses that mentioned some form of human interaction in their solution section highlights the detriments of isolation and the difference that human connection can make when considering mental health.

In terms of mental health resources, prisoners in solitary confinement should all be provided with accessible counseling and therapies. Their inability to access these resources increases their vulnerability to mental health disorders and ability to cope with their situations. Those unable to access psychological treatment will inevitably suffer in terms of mental health, making it more difficult for them to reenter society and increasing the rates of recidivism. Previous research within general population prisoners directly supports this research and has established that "cognitive treatment programs delivered with professional standards can reduce recidivism by 25 to 35 percent."[13] If these same programs were implemented into solitary confinement units --the prisoners that need it most-- the results would be immeasurable.

Logistics:

The three most popular responses from the survey would be very logistically possible to implement into solitary confinement units. More time spent outside would be relatively low cost and would improve the mental health of solitary inmates tremendously. Allowing familial visits would also be a cost-efficient solution, as this simple human interaction could serve as psychological treatment. Maintaining supportive family relationships is also a powerful tool for reentry success. Implementing mental health resources and counseling into solitary confinement units would be a financial concern for prisons, but the investment seems worth improving the mental health of prisoners and decreasing the rates of recidivism outside of the prison complex. These improvements are justified as a proactive investment in the prevention of future crimes and additional incarcerations.

Limitations:

While the results of this study were clearly conclusive, the sample size was not representative of the entire population. The responses were only collected from three centers in two different states, which leaves the experiences of a majority of the country unexplored. Additionally, the states in which the data was collected tend to be more conservatively leaning, so their prison policies may differ from other, more liberal, states. Getting information from states in the Northeast, for example, has the potential to include the policies of left leaning states, which may differ from those in the South. This research should be repeated with a larger and more inclusive sample size, making sure to include states from areas like the Northeast.

Importance:

In an ideal world, the system of solitary confinement would not exist in the United States, but the issue is a bit more complex than this absolute solution. A small number of states are slowly working towards the goal of abolishing solitary confinement, and some, like New York, have fortunately achieved this objective. However, a majority of states are hesitant to abolish the system, as they believe that it serves a substantial purpose; whether to limit violence in general population prisons, prevent gang activity, or "protect" certain vulnerable prisoners. New York, a liberal state, was able to achieve such reform, but more conservative states will face increased difficulty passing this legislation. For the time being, regardless of what the future holds, it appears that the system of solitary confinement is engrained in most state legislatures for years to come. The current system clearly cannot continue without reform. The solution, supported by this research, would be to implement certain essential resources into solitary confinement units, almost creating a general population prison on a smaller and more restricted scale. These policies should be implemented within all states that continue to use the system of solitary confinement.

This study was unique in that the responses for prison resources came directly from the opinions and firsthand experiences of individuals who were previously incarcerated. The first section of the survey confirmed that a majority of the participants did experience negative psychological effects, making their experiences and suggested resources extremely valuable for research. By allowing familial visits, providing mental health counseling, and implementing increased time spent outside for prisoners in solitary confinement, the rates of mental health disorders for these inmates would decrease, thus allowing them to more easily integrate into society and lowering their rates of recidivism. Making these changes would create a safer country and ensure that those released from solitary confinement would contribute to society in a positive manner, a reality more in line with the goals of the prison complex.

■ Acknowledgements

I would like to acknowledge my AP Research teacher, Mrs. Gallagher, for supporting me throughout this process and always offering a helping hand. My parents were also incredibly supportive during my research and encouraged me to look further into the topic.

■ References

1. Reiter, K., Ventura, J., Lovell, D. L., & Augustine, D. (2020). Psychological Distress in Solitary Confinement: Symptoms, Severity, and Prevalence in the United States, 2017–2018. *Am J Public Health.* https://doi.org/10.2105/AJPH.2019.305375
2. Kifer, M., Hemmens, C., & Stohr, M. K. (2003). Goals of Corrections: Perspectives From the Line. *Criminal Justice Review*, 28(1), 47-69. https://www.ncjrs.gov/App/Publications/abstract.aspx?ID=201939
3. *Senate Judiciary Subcommittee on the Constitution, Civil Rights, and Human Rights Hearing on Solitary Confinement*, 2012 Leg. (D.C. June 19, 2012) (testimony of Professor Craig Haney). https://www.judiciary.senate.gov/imo/media/doc/12-6-19HaneyTestimony.pdf
4. Gordon, S. E. (2014). Solitary Confinement, Public Safety, and Recidivism. *University of Michigan Journal of Law Reform*, 47.
5. Baumgartel, S., Guilmette, C., Kalb, J., Li, D., Nuni, J., Porter, D., & Resnik, J. (2015, November 10). Time-In-Cell: The ASCA-Liman 2014 *National Survey of Administrative Segregation in Prison* (552). Yale Law School, Public Law Research Paper.
6. *Solitary Confinement Is Cruel and Ineffective*. (2013, August 1). Scientific American. Retrieved January 21, 2021, from https://www.scientificamerican.com/author/the-editors/
7. Kaba, F., Lewis, A., Glowa-Kollisch, S., Hadler, J., Lee, D., Alper, H., Sellings, D., MacDonald, R., Solimo, A., Parsons, A., & Venters, H. (2014). Solitary Confinement and Risk of Self-Harm Among Jail Inmates. *American Journal of Public Health*.
8. Smith, P. S. (2006). The Effects of Solitary Confinement on Prison Inmates: A Brief History and Review of Literature. *Crime and Justice*, 34(1), 441-528. https://www.jstor.org/stable/10.1086/500626?seq=20#metadata_info_tab_contents
9. *Recidivism in Connecticut.* (2001). Connecticut Gov. https://www.ct.gov/opm/lib/opm/cjppd/cjresearch/recidivismstudy/2001recidivisminconnecticut.pdf
10. *Institutional Review Boards Frequently Asked Questions*. (2019, April 18). Food and Drug Administration. Retrieved April 6, 2021, from https://www.fda.gov/regulatory-information/search-fda-guidance-documents/institutional-review-boards-frequently-asked-questions
11. *Mental Health Disorder Statistics*. (n.d.). John Hopkins Medicine. Retrieved March 24, 2021, from https://www.hopkinsmedicine.org/health/wellness-and-prevention/mental-health-disorder-statistics#:~:text=An%20estimated%2026%25%20of%20Americans,substance%20abuse%20and%20anxiety%20disorders
12. Wade, R. (2021, February). [Personal interview by the author]
13. Friedmann, A. (2014, April 15). *Lowering Recidivism Through Family Communication*. Prison Legal News. Retrieved March 7, 2021, from https://www.prisonlegalnews.org/news/2014/apr/15/lowering-recidivism-through-family-communication/
14. Bush, J. (2016, June 26). *To Help A Criminal Go Straight, Help Him Change How He Thinks*. National Public Radio. Retrieved March 22, 2021, from https://www.npr.org/sections/health-shots/2016/06/26/483091741/to-help-a-criminal-go-straight-help-him-change-how-he-thinks#:~:text=More%20recently%2C%20researchers%20have%20established,inmate%20per%20year%20on%20average.
15. Conti, L. (2008, August 1). *How Light Deprivation Causes Depression*. Scientific American. Retrieved March 7, 2021, from https://www.scientificamerican.com/article/down-in-the-dark/
16. *Sour mood getting you down?* Get back to nature. (2018, July). Harvard Health Publishing.

■ Author

Brooke Kivel is a student at Hendrick Hudson High School in Montrose, New York. She has always been passionate about psychology, the criminal justice system, and prison reform. Her research is very reflective of these passions.

DOI: 10.36838/v4i1.4

IJHSR
ijhighschoolresearch.org
■ RESEARCH ARTICLE

Inhibition of ZAR1 Enhances Cancer Cell Proliferation on Non-smoking Lung Cancer Patients

Jana Choe

The Governor's Academy, 1 Elm St, Byfield, MA 01922, 01922, USA; gosyber@suwon.ac.kr

ABSTRACT: Tobacco smoking has long been highlighted as the main cause for lung cancer. However, many cases of lung cancer have also been reported in nonsmokers. Air pollution, chemical exposure, mutations, and other genetic alterations are known to be associated with lung cancer. This research focuses on genetic alterations of lung cancer patients who have never smoked in their lifetime. Using cBioportal, genomic alterations of a total of 1144 patients (111 Lifelong non-smokers and 976 smokers) were analyzed in this study. It was found that lifelong non-smoking patients have a much higher rate of deletion on Chromosome 4 (cytoband position 4p11) compared to that of the smoking patients. Among the 8 genes that are located on 4p11, this research mainly focused on Zygote Arrest 1 (ZAR1) gene because there is a recent discovery of guiding evidence that suggests a potential interconnection between ZAR1 and cancer. To understand the role of ZAR1 on cell proliferation in lung cancer, mRNA expression of ZAR1 was inhibited using small interference RNA (siRNA). When ZAR1 mRNA was depleted, cancer cell proliferation increased in the NCI-H358 cell line. In conclusion, ZAR1 depletion increases cancer cell proliferation, and it can be used as a biomarker for lifelong non-smoker lung cancer.

KEYWORDS: Cellular and Molecular Biology; Molecular Biology; Lung Cancer; ZAR1; Non-smoker.

■ Introduction

Lung cancer is by far the leading cause of cancer related deaths worldwide, accounting for approximately 25 percent of all cancer deaths.[1] Being the leading cause of cancer deaths in men and the second leading cause in women, lung cancer is characterized by a poor five year survival rate of 18.6 %.[2] The two main types of lung cancer are small cell (Small cell lung cancer tends to be more aggressive than the non-small cell cancer) and non-small cell lung cancer, distinguished by the size and characteristics of the cancerous cells.[3]

Tobacco-smoking is believed to be the main cause of lung cancer. However, other causes of lung cancer have been studied by the researchers.[4] Although smokers are more vulnerable to cancer cell developments, lifelong non-smokers can also develop cancer cells. The research of genetic alterations on lung cancer from nonsmokers is very limited.[5] To find the novel genetic alterations in lung cancer from nonsmokers, the gene alteration found mainly in non-smokers from data provided in the cBioportal was analyzed.[6] By analyzing genetic alterations in 1144 patients, it was observed that Human zygote arrest 1 (ZAR1) is one of the genes that is frequently deleted in lifelong non-smokers' lung cancer cells.

ZAR1 is located on chromosome 4 (4p11). ZAR1 is found to have a critical effect on oocyte-to-embryo transition.[7] It is inactivated during the development of the embryo; however, ZAR1 is a maternal gene whose products (RNA or protein) are produced by the oocyte before the embryo development. ZAR1 is found to be mainly expressed in human lungs.[8] Growing evidence points to the possible correlation between the role of ZAR1 and cancer. ZAR1 has recently been brought back to the surface when researchers observed that ZAR1 was inactivated in lung cancer cell lines. [8] It is now suspected to be a potential tumor suppressor gene.[8] To further clarify this correlation, this study investigated whether ZAR1 is a potential tumor suppressor that may affect the development of cancer cells. In order to find the relationship between the deletion of ZAR1 and development of lung cancer, ZAR1 was depleted by siRNA and its subsequent effect on cancer cell proliferation was analyzed.

■ Methods

Cell culture :

NCI-H358 cells were purchased from Korea Cell Line Bank. Cells were routinely cultured in RPMI 1640 medium (Gibco) supplemented with 10 % inactivated FBS (Hyclone), 100 U/mL penicillin and 100 µg/mL streptomycin (Gibco). Cells were maintained at 37 ˚C in a 5 % CO2 humidified environment and prepared for experimental procedures when in log-phase growth.

siRNA transfection :

The small interfering RNA (siRNA) prevents the translation of specific genes with complementary nucleotide sequence, silencing their expression. The siRNA transfection is a process that enables the siRNA to be delivered to the cells. The reagent used within the process forms a complex with the siRNA, helping it to penetrate the membrane. The siRNA, when it enters the targeted cells, incorporates with other proteins to form the RNA-Induced Silencing Complex (RISC). The siRNA unwinds to form single stranded siRNA, which then binds to its complementary nucleotide and induces mRNA cleavage.

With this technique, the expression of ZAR1 of the cancer cell lines can be regulated. Four different samples are used in this study: cell line without any treatment, with 0.3 µl of control siRNA, with 0.3 µl (10 pmol) of siZAR1, and with

DOI: 10.36838/v4i1.5

0.6 µl (20 pmol) of siZAR1. siRNA was transfected with a transfection reagent, RNAimax (Invitrogen). The mole ratio of siRNA:reagent was prepared as 1:3. The cells were transfected with the mixed solution of siRNA and transfection reagent for 48 h.

Total RNA extraction:

RNA extraction is a process used for the isolation of total RNA from a given sample of cell lines or tissues. RNA-spin™ Total RNA Extraction Kit to extract the macromolecules from the cell lines was used. After removing the culture media, we replaced it with a R-buffer, which helps cell lysis. We added 350 µl of 70 % EtOH to the lysate and centrifuged the mixture in a spin column to collect the required RNA. We then purified the extracted RNA using two types of washing buffers (Washing buffer A, B) to cleanse the RNA of possible remnants and used an elution buffer to collect the total RNA.

cDNA synthesis:

cDNA was synthesized from the extracted RNA using TOPscript™ Reverse Transcriptase (Enzynomics). The cDNA reaction was prepared as follows: 5 µl of extracted RNA, 1 µl of oligodT (20 pmol), 2 µl 10x reaction buffer, 1 µl RT enzyme, and water was added up to 20 µl. The cDNA synthesis was performed as follows: 25 °C for 10 min, 42 °C for 1 h, 95 °C for 5 min, and 4 °C for infinite.

Polymerase Chain Reaction:

Polymerase chain reaction (PCR) is a method used to rapidly replicate a specific DNA sample. This allows the scientist to amplify a very small amount of the sample to a larger amount for the better quality and the detail of the research. The PCR reaction was performed in stages: 1) 95.0 °C for 5 minutes, 2) repetition of 95.0 °C for 30 seconds, 55.0 °C for 1 minute, and 72.0 °C for 40 seconds for 40 times, 3) 72.0 °C for 5 minutes, and 4) continuation in 10.0 °C.

Agarose gel electrophoresis:

Agarose gel electrophoresis separates the RNA in a matrix of agarose by length and/or size. The 1.5% Agarose gel was prepared using 1.5 g of agarose mixed with 100 ml of Tris-borate-EDTA (TBE) buffer. The mixture was microwaved for 3 minutes until agarose powder was completely dissolved in the buffer. Then, RedSafe Nucleic Acid Staining Solution (Intron) was added to the solution.

Once prepared, the caste was submerged in a buffer in an electrophoresis tank, before loading RNA samples into the pore. GAPDH was used as a normalizing factor to better quantify the mRNA of target genes. When the process was finished, a blue light transilluminator was used to view the results.

Cell proliferation assay:

The cells were trypsinized at indicated days and the percentage of viable cells was measured by counting cells, which were stained by acridine orange/propidium iodide, an apoptosis indicator, with the Luna-FL Dual Fluorescence Cell Counter (Logos Biosystems).

Results and Discussion

Genome wide analysis of copy number variation on lung cancer in lifelong non-smokers:

As tobacco-smoking is the major cause of lung cancer, people oftentimes disregard other potential causes of cancer.[9] In order to study the factors the contribute to lung cancer other than smoking, the differences in genetic alterations between smokers and lifetime non-smokers were compared. While analyzing, it was noted that several genes in chromosome 4p11 were deleted, which occurred in 6.31 % of lifelong non-smokers and 0.2 % of smokers. (Table 1) From the 8 types of genetic alterations presented in chromosome 4p11, we focused on Zygote Arrest 1 (ZAR1).

Table 1: Copy number deletion on lung cancer in lifelong non-smokers. Gene deletions were mainly found in chromosome 4p11 in lifelong non-smokers.

Gene	Cytoband	Lifelong non-smoker (n=111)	Smoker (n=976)	Log Ratio	P-value
CWH43	4p11	7 (6.31%)	2 (0.20%)	4.94	2.938e-6
FRYL	4p11	7 (6.31%)	2 (0.20%)	4.94	2.938e-6
OCIAD1	4p11	7 (6.31%)	2 (0.20%)	4.94	2.938e-6
OCIAD2	4p11	7 (6.31%)	2 (0.20%)	4.94	2.938e-6
SLAIN2	4p11	7 (6.31%)	2 (0.20%)	4.94	2.938e-6
SLC10A4	4p11	7 (6.31%)	2 (0.20%)	4.94	2.938e-6
TEC	4p11	7 (6.31%)	2 (0.20%)	4.94	2.938e-6
ZAR1	4p11	7 (6.31%)	2 (0.20%)	4.94	2.938e-6

siRNA targeting ZAR1 decreases mRNA of ZAR1 on NCI-H358 lung cancer cells:

To find the effect of siRNA transfection on ZAR1 expression level, mRNA expression level was quantified using agarose gel electrophoresis. The band intensity shows the mRNA expression level of ZAR1 and GAPDH in three samples: the siControl, the siZAR1 (10 pmol), and the siZAR1 (20pmol). (Figure 1A) The siControl samples were transfected with non-targeting siRNA for non-specific effects related to siRNA delivery to provide a baseline for target gene silencing. Two different concentrations of siRNA targeting ZAR1 were tested: 10 pmol and 20 pmol. The ZAR1 expression level was normalized with the expression level of GAPDH. (Figure 1B) Compared to the siControl, expression level of ZAR1 decreased to ~30% in siZAR1 (10 pmol) samples. When siZAR1 was treated with 20 pmol, the expression level of ZAR1 further decreased to 20%. Since the lowest expression level of ZAR1 was achieved by the 20 pmol concentration of siRNA, we used 20 pmol condition for the downstream experiments to find the functional role of ZAR1 depletion on NCI-H358 cells.

ZAR1 depletion increases cell proliferation on NCI-H358 lung cancer cells:

Cancer cell proliferation is a process that results in an increase of the number of cells, which is defined by the balance between cell division and cell death. To find the functional role of ZAR1 in cancer cell proliferation, two samples were compared: siControl (negative control) and siZAR1 with 20 pmol. As shown in Figure 2, the cell number was measured after siRNA transfection in five different timelines: 0 hour, 24 hours, 48 hours, 72 hours, and 96 hours. The relative cell proliferation was quantified and the cell number of 0 hour was used to calculate the relative cell number increase. Even after 72 hours of transfection the cell number did not show a significant

DOI: 10.36838/v4i1.5

difference. However, at 96 hour, cell number was significantly increased in siZAR1 transfected cells. This result indicates that ZAR1 depletion induces NCI-H358 cells to proliferate.

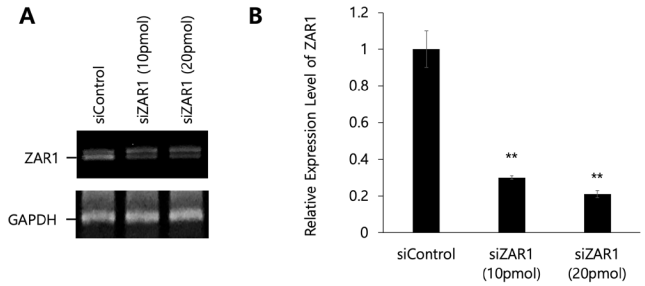

Figure 1: Effect of siRNA targeting ZAR1 on the mRNA expression level of ZAR1. (A) Gel electrophoresis analysis of ZAR1 and GAPDH PCR products. (B) Quantification of ZAR1 mRNA levels 48 h after transfection (n = 3, mean ± SD), student's t-test, ** $p < 0.01$. The sample with higher concentration of siRNA has significantly lower level of ZAR1 expression.

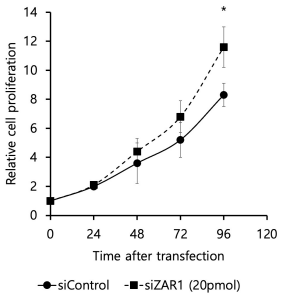

Figure 2: Effect of ZAR1 depletion on cell proliferation on NCI-H358 lung cancer cells. (n = 3, mean ± SD), student's t-test, * $p<0.05$. The sample with siZAR1 transfected cells shows a greater level of cell proliferation than siControl transfected cells.

Conclusions

Copy number variation (CNV) is a phenomenon in which parts of genomes are repeated and the number of repeats on the genome varies between lung cancer patient groups—in this research the CNV difference between the lifelong non-smokers and smokers was investigated.[10] CNV is a type of structural variation which is a type of duplication or deletion event that affects the base pairs in DNA.[11] It was found that the copy number deletion is frequently observed in chromosome 4p11 in non-smoking lung cancer patients. At this chromosomal position, eight genes were deleted including ZAR1. A previous study has discovered that copy number deletion led to decreased gene expression, indicating that the loss of copy numbers in these genes may have low mRNA transcript levels.[12] Since the focus of this research was only on the function of ZAR1 in lung cancer cells, a comparison study with the other seven genes should further be investigated in order to provide a comprehensive understanding about the overall impact of CNV in chromosome 4p11 on lung cancer development.

ZAR1 may have a positive effect on cell proliferation, but the question remains about how. 8A cell cycle is a series of events that allows the growth and the division of a cell.[13] Cell death, on the other hand, is an event in which a cell ceases to perform its functions mostly through apoptosis, programmed cell death.[14] Since both cell cycle and cell death are closely related with cell proliferation, further study is needed to determine whether ZAR1 either regulates cell cycle or promotes cell death in lung cancer.

By silencing the expression level of ZAR1 in a lung cancer cell line with siRNA, this study has analyzed the possible role of ZAR1 in the development of lung cancer. The cell line in which the expression of ZAR1 was inhibited presented a greater rate of cell proliferation than in the control cell line. If the inhibition of ZAR1 promotes the development of lung cancer, it seems reasonable to infer that ZAR1, as suspected, is a potential cancer suppressor gene and therefore can be a promising target for a novel biomarker for lung cancer.

Acknowledgements

I would like to thank my supervisor Dr. Woo Rin Lee for his guidance and advice in this project.

References

1. Cersosimo, R. J., Lung cancer: a review. Am J Health Syst Pharm 2002, 59 (7), 611-42.
2. Torre, L. A.; Siegel, R. L.; Jemal, A., Lung Cancer Statistics. Adv Exp Med Biol 2016, 893, 1-19.
3. Lemjabbar-Alaoui, H.; Hassan, O. U.; Yang, Y. W.; Buchanan, P., Lung cancer: Biology and treatment options. Biochim Biophys Acta 2015, 1856 (2), 189-210.
4. Furrukh, M., Tobacco Smoking and Lung Cancer: Perception-changing facts. Sultan Qaboos Univ Med J 2013, 13 (3), 345-58.
5. Samet, J. M.; Avila-Tang, E.; Boffetta, P.; Hannan, L. M.; Olivo-Marston, S.; Thun, M. J.; Rudin, C. M., Lung cancer in never smokers: clinical epidemiology and environmental risk factors. Clin Cancer Res 2009, 15 (18), 5626-45.
6. Cerami, E.; Gao, J.; Dogrusoz, U.; Gross, B. E.; Sumer, S. O.; Aksoy, B. A.; Jacobsen, A.; Byrne, C. J.; Heuer, M. L.; Larsson, E.; Antipin, Y.; Reva, B.; Goldberg, A. P.; Sander, C.; Schultz, N., The cBio cancer genomics portal: an open platform for exploring multidimensional cancer genomics data. Cancer Discov 2012, 2 (5), 401-4.
7. Wu, X.; Viveiros, M. M.; Eppig, J. J.; Bai, Y.; Fitzpatrick, S. L.; Matzuk, M. M., Zygote arrest 1 (Zar1) is a novel maternal-effect gene critical for the oocyte-to-embryo transition. Nat Genet 2003, 33 (2), 187-91.
8. Richter, A. M.; Kiehl, S.; Koger, N.; Breuer, J.; Stiewe, T.; Dammann, R. H., ZAR1 is a novel epigenetically inactivated tumour suppressor in lung cancer. Clin Epigenetics 2017, 9, 60.
9. Walser, T.; Cui, X.; Yanagawa, J.; Lee, J. M.; Heinrich, E.; Lee, G.; Sharma, S.; Dubinett, S. M., Smoking and lung cancer: the role of inflammation. Proc Am Thorac Soc 2008, 5 (8), 811-5.
10. Qiu, Z. W.; Bi, J. H.; Gazdar, A. F.; Song, K., Genome-wide copy number variation pattern analysis and a classification signature for non-small cell lung cancer. Genes Chromosomes Cancer 2017, 56 (7), 559-569.
11. Lauer, S.; Gresham, D., An evolving view of copy number variants. Curr Genet 2019, 65 (6), 1287-1295.
12. Shao, X.; Lv, N.; Liao, J.; Long, J.; Xue, R.; Ai, N.; Xu, D.; Fan, X., Copy number variation is highly correlated with differential gene expression: a pan-cancer study. BMC Med Genet 2019, 20 (1), 175.
13. Schafer, K. A., The cell cycle: a review. Vet Pathol 1998, 35 (6), 461-78.
14. Elmore, S., Apoptosis: a review of programmed cell death. Toxicol Pathol 2007, 35 (4), 495-516.

Author

Jana Choe is a student of The Governor's Academy in Byfield, Massachusetts. She is interested in studying biology, biomedical research, and genetics, and is hoping to deepen her understanding in these areas of research in the future.

DOI: 10.36838/v4i1.5

IJHSR

ijhighschoolresearch.org

RESEARCH ARTICLE

Evaluating the Effectiveness of Emotion Recognition Software as an Interactional Tool for Individuals with Autism: An Autism Caregiver/Professional Perspective

Aryan Dawer

Modern School Barakhamba Road, New Delhi, Delhi, 110001, INDIA; aryandawer7@icloud.com

ABSTRACT: The aim of this research study was to evaluate the impact of a self-formulated video on a self-designed Emotion Recognition Software (ERS) on autism professionals' or family members' perceptions of the effectiveness of ERS. ERS is a tool for enabling people with Autism Spectrum Disorder (ASD) to interpret emotions in daily interactions. In the study, the respondents were given a brief description of the software and asked to rate its effectiveness. Then they were shown a video explaining and displaying the working of the ERS. Out of the seven emotions shown, they were asked to rate the emotions (on a "1-7" scale) on the basis of their perceptions of the software's efficacy at interpreting each of them and asked to give the software an overall rating. The results from the paired t-test revealed that the video was able to change the respondents' perceptions (mean rating changed from 4.8 to 5.5) and after watching the video, less than 3.5% of the respondents rated the ERS a "3 or below" (as opposed to 17.5% before) and more than 82% rated the ERS a "5" or above" (as opposed to 65.5% before). Interestingly, the results showed that only emotions of happiness and fear affected the respondents' final perceptions of the software. The support shown for the software in the quantitative and qualitative data, after watching the video and understanding its functionality and benefits, suggests that people are excited about its use in real life.

KEYWORDS: Behavioural and Social Sciences; Social Psychology; Emotion Recognition Software; Autism Spectrum Disorder; Efficacy Analysis.

Introduction

For most of us who engage in social interactions naturally and spontaneously, a striking feature of autistic individuals is their struggle with affective contact.[1] This means that a person with autism, a condition known formally as the Autism Spectrum Disorder (ASD), is likely to be fascinated with objects, but be indifferent to people, which can come across as being off-putting for most people. An anecdote shared by "Jenny", a mother of her autistic child, who visited her psychology professor at the latter's office, provides a quintessential example of this characteristic. During this office visit, Jenny's then two-year-old autistic son never once looked at the professor. Instead, he stepped all over her couch swinging all her canvases, lost in their swinging motion, utterly uninterested in any human presence (personal communication, May 5, 2021).

Relatedly, ASD is characterized by impairments in social interaction due to deficits and/or atypical features in the areas of verbal and non-verbal communication, as well as difficulties with reciprocating at a social and emotional level.[2] Therefore, autistic individuals find social interactions to be a great source of stress and anxiety, which can make their lives particularly challenging in mainstream society.

It is important to point out that social interactions can be difficult, even in the case of mildly autistic individuals who possess verbal skills of communication and often function independently in mainstream society, due to aspects of non-verbal communication such as facial expressions, gestures, and eye contact. Several studies describe individuals with ASD as being unable to recognize mental and emotional states in others and in themselves.[3,4] A possible reason is that individuals with ASD are themselves lacking in facial expressions: they do not display their emotions outwardly through facial expressions.[1] For instance, when individuals with ASD are happy or angry, they do not display discernible conventional facial expressions of happiness or anger. This could make it difficult for them to read these expressions in others and to be able to assign meaning and intentions to the conversation partners. Other studies have shown that individuals with ASD tend to look less at the eye region of the face,[5,6] engage in less mutual eye gaze behavior,[7] and struggle to follow the gaze,[8] compared to neurotypical individuals. Such a difficulty could thus further add to their sense of anxiety about social interactions.

Since the human face is central in both the expression and communication of emotion, researchers have sought to investigate ASD individuals' ability to identify emotions. Some studies have found children and adults with high-functioning autism (HFA) can recognize basic emotions, such as the six basic universally recognized emotions (happiness, sadness, fear, anger, surprise, and disgust), from pictures[9] and that they only have problems recognizing "complex emotions" (such as embarrassment, insincerity, intimacy, etc.) in both adults and children with ASD.[4,10] However, the ASD spectrum is vast and we need to look for ways to help those on the low-functioning end as well. It is also debatable if pictures can truly capture various portraits of emotions. There is a need for more sophisticated

DOI: 10.36838/v4i1.6

tools either to train autistic individuals in emotion recognition or simply do it for them.

A solution that could address this challenge faced by individuals with ASD is in the development and application of computational tools that enable emotion recognition through facial expressions.[11,14] An ERS is designed to interpret emotions based on facial expressions identified through a video feed, which are transmitted to be processed in the program in real time. It categorizes facial expressions under one of seven emotions: anger, disgust, fear, happiness, sadness, surprise, and neutral. The software has been trained through the use of a neural network by showing images of different people displaying different emotions. This tool has become an ideal way to support individuals with ASD on the entire spectrum.[10]

Several studies have been done using computational tools to try and help individuals with ASD and to measure the efficiency and validity of these tools. For instance, in one study, two groups of 11 children (aged 12-18) with autism participated: one group used the computer program for 10 half-hour sessions over 2 weeks, the other didn't.[21] Within-program data showed a significant reduction in errors made from first to last use. Students were assessed pre- and post-intervention using facial expression photographs, cartoons depicting emotion-laden situations, and non-literal stories. Scores were not related to age or verbal ability. The experimental group made gains relative to the control group on all three measures. Gains correlated significantly with the number of times the computer program was used and results suggest positive effects.

Stanford University's Autism Glass Project uses Google's face-worn computing system to aid autism-affected subjects in understanding appropriate social cues by appending emoticons to those expressions the system is able to recognize (Figure 1).[16]

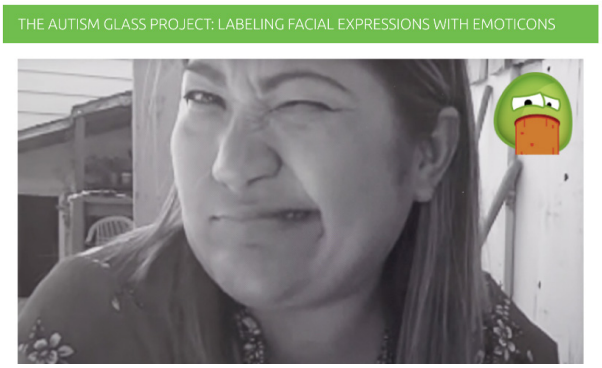

Figure 1: Stanford University's Autism Glass Project.

Note: A display of emotion recognition through emoticons. Reprinted from The Future of Emotion Recognition in Machine Learning. In Iflexicon blog, November 20, 2020, from https://www.iflexion.com/blog/emotion-recognition-software.

The usefulness of ERP tools could thus be tremendous for people with ASD by reducing the aspects of social interactions, which they need to worry about in a conversation. Oftentimes, these programs contain biases not only in the recognition of the emotions themselves but also based on whose emotions are being interpreted. For example, a man and a woman exhibiting the same emotion would be interpreted differently. However, there are concerns regarding the application of this technology in real-life situations. Since it is impossible to guarantee the 100% accuracy of a software that works on a pre-trained model, an autistic person could become unduly distressed by the wrong judgment of the software.

Therefore, to contribute to the evaluation of the perceived pros and cons of using an ERS for ASD individuals, this research study to harness the perceptions of autism professionals or family members regarding this topic by showing them a video created as a part of this research. This video shows a self-designed ERS at work in interpreting the seven common emotions. Since autism professionals and people related to ASD loved ones have first-hand experiences with ASD individuals and ASD individuals' interaction needs, their opinions on the viability of this software could be invaluable.

Methods

Research Aim and Research Approach:

The aim of this research study was to evaluate the impact of a self-formulated video on a self-designed ERS on the perceptions of autism professionals and family members towards the effectiveness of ERS. This study's goal also included examining the ERS in general as a tool for enabling ASD individuals to interpret emotions in daily interactions. More specifically, the respondents were shown the ERS in action, through a video in order to evaluate the efficacy of the software to interpret each emotion.

The hypotheses were as follows:

1a. Null Hypothesis: There is no difference between the mean ratings of the respondents' evaluations of the ERS' efficacy in interpreting the different emotions.

1b. Alternative Hypothesis: There are differences between the mean ratings of the respondents' evaluations of the ERS' efficacy in interpreting the different emotions.

2a. Null Hypothesis: The video has no effect on the respondents' opinions on the effectiveness of ERS for people with ASD.

2b. Alternative Hypothesis: The video has an effect on respondents' opinions on the effectiveness of the ERS for people with ASD.

3a. Null Hypothesis: Respondents' evaluations of the ERS' efficacy in interpreting the different emotions has no effect on their overall rating of its effectiveness for ASD individuals.

3b. Alternate Hypothesis: Respondents' evaluations of the ERS' efficacy in interpreting the different emotions has an effect on their overall rating of its effectiveness for ASD individuals.

Data Collection:

The data collection for this research study consisted of two steps:

1) Design of the Software
2) Design of the Questionnaire

Design of the Software:

The emotional recognition software is a Machine Learning model (MLM) trained on the FER-2013 dataset that consists of 28,709 48x48-pixel training images. The software works on real-time video and identifies emotions by categorizing facial expressions under one of seven emotions:

DOI: 10.36838/v4i1.6

works on real-time video and identifies emotions by categorizing facial expressions under one of seven emotions (Figure2):

- Angry
- Disgust
- Fear
- Happy
- Sad
- Surprise
- Neutral

Figure 2: FER-2013 dataset display.

Note: FER-2013 Learn Facial Expressions from an Image. Kaggle, 2020 https://www.kaggle.com/msambare/fer2013

In the neural network model, a Convolutional Neural Network architecture was followed. Specifically, the program divided an image into different sections and examined them separately to find common features in particular sections of multiple images.[17] For instance, the section focused on one's eyes may show tension in the eyebrows while exhibiting the emotion of anger. The number of dropout layers were increased in this study. Dropout layers, as the name suggests, drop some pixels of the image by a customizable factor, for example, 115 pixels of a 48x48 pixel image (roughly 0.05%) while training the model.[18] This ensured that the model did not get accustomed to seeing the same portions of different pictures. For instance, if the program was identifying anger by examining the tension in one's eyebrows, a person who exhibits anger differently cannot be interpreted correctly. To avoid such a situation, and to prevent any bias in the recognition process, the dropout layers were increased, a very creative idea given that the users of the tool themselves do not have the ability to exhibit emotions through facial expressions.

Design of the Questionnaire:

A questionnaire was designed, which comprised three main sections:

- Respondents' relation to an individual with ASD (professional, parent or sibling)
- Close-ended questions to evaluate respondents' perceptions towards emotional recognition software,
- Before showing the video, the respondents were informed about the function and power of the ERS and asked to assess their perceptions of its effectiveness in helping people with ASD by giving it a rating on a scale of 1 to 7.
- Then the self-prepared video was shown: https://youtu.be/WjKTnTR7EB4
- Then after watching the video, the respondents were asked to rate, on a scale of one to seven, how well the ERS did in in identifying the following emotions: anger, disgust, fear, happiness, sadness, surprise, neutrality.
- Respondents were asked if they think that ERSs could help people with ASD in their daily interactions and rate the software on a scale of 1 to 7 again.
- Open-ended questions to evaluate the respondents' perceptions towards ERS. Respondents were asked to explain their ratings on various questions and give suggestions for improvement in the software. experience of contact by applying force, vibrations, or motions to the user.

An invitation letter was prepared to be sent with the questionnaire, giving background information about the author of the research study. The form was sent to various organizations and support groups for people on the autism spectrum. It was also posted on social media autism communities such as Facebook groups with parents of children with ASD to get a diverse sample group of respondents with unique stories and experiences. Subsequently, the survey was filled by 29 people: 17 parents, one sibling, and 11 professionals.

Data Analysis:

For the analysis of the data, descriptive statistics were used to determine the mean differences between the respondents' ratings. Moreover, a one-way ANOVA test was to evaluate the statistical significance of the mean differences between the ratings that the respondents gave to the efficacy of the ERS to identify each emotion. Next, in order to compare the ratings given by the respondent to the viability of the ERS before and after watching the video, a Paired t-Test was run on the data. After that, a multiple regression analysis was conducted on the group to evaluate the impact of the efficacy of the machine to identify the seven emotions on the respondents' likely overall rating to the viability of the ERS. Then, once the important features were identified, it was run again on them to calculate the percentage of their importance and their coefficients in the equation to predict the respondent's overall rating of the ERS. The responses were graphed on a bar chart to show a clearer picture of the distribution of the proportion of the respondents across the ratings. Finally, qualitative data were analyzed based on the respondents' answers to an open-ended question, asking them to elaborate upon the factors influencing their ratings and suggestions to improve the program.

Results and Discussion

The respondents' ratings of the efficacy of the self-designed facial ERS in recognizing seven basic universal emotions and their evaluation of the viability of the program for ASD individuals before and after watching the video were compared. Moreover, their responses to open-ended questions elicited additional perspectives and suggestions for the improvement in the aforementioned software.

Efficiency in Interpreting Emotions:

Descriptive statistics show that the emotion "Happiness" (Figure 3) (M = 6.21, SD = 1.11) had the highest rating, followed by "Sadness" (M = 5.86, SD = 1.36), "Anger" (M = 5.48, SD = 1.35), "Surprise" (M = 5.31, SD = 1.56), "Fear" (M = 5.24, SD = 1.38), "Neutrality" (M = 5.07, SD = 1.65), and finally Disgust (M = 4.79, SD = 1.61) (see Table 1). It is evident that the standard deviations within the responses of each emotion are almost the same, which suggest that the people's ratings of the efficacy of the program were very similar. Given a scale of

to seven, the ratings given to the program's efficacy (M = 5.43) to interpret various emotions were very impressive.

Table 1: Descriptive Statistics — Comparison of Ratings of Efficiency in Interpreting Emotions.

Groups	*Count*	*Sum*	*Average*	*Variance*	Standard Deviation
Anger	29	159	5.482758621	1.830049261	1.352793133
Disgust	29	139	4.793103448	2.598522167	1.611993228
Fear	29	152	5.24137931	1.903940887	1.379833645
Happiness	29	180	6.206896552	1.24137931	1.114172029
Sadness	29	170	5.862068966	1.837438424	1.355521458
Surprise	29	154	5.310344828	2.435960591	1.560756416
Neutrality	29	147	5.068965517	2.709359606	1.646013246

To determine whether the mean differences were statistically significant, a one-way ANOVA was run. The one-way ANOVA for emotions shows statistical significance: F(6, 196) = 3.20 (higher than the F critical value of 2.15), p < .01 (see Table 2).

Table 2: One-Way ANOVA — Comparison of Ratings of Efficiency in Interpreting Emotions. P-value less than 0.01 and F is more than F-critical showing statistical significance of results.

Source of Variation	*SS*	*df*	*MS*	*F*	*P-value*	*F crit*
Between Groups	39.98029557	6	6.663382594	3.20428652	0.0050451635	2.145071468
Within Groups	407.5862069	196	2.079521464			
Total	447.5665025	202				

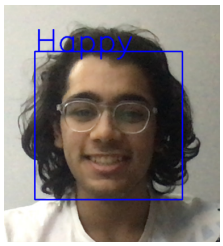

Figure 3: ERS Recognizing the Emotion of Happinesss.

Note: ERP EXPLAINED. Youtube, AD 007, Apr 26, 2021 https://www.youtube.com/watch?v=WjKTnTR7EB4

However, disgust (4.79), a more nuanced and complex emotion, was rated the lowest(Figure 4). Qualitative data offered important insights as to the complexity of guaranteeing the optimal efficacy of the ERS, which is so vital for ASD individuals. First of all, some facial expressions are too ambiguous to predict. Respondents described the emotions as being "too similar", "tricky to predict", and "can overlap". This means that even if the software can detect them correctly, one can never know for sure that it is the intended emotion of the other person because the facial expressions and features used by the ERS to recognize the emotion could be associated with other emotions as well.

Second, people express their emotions through different facial expressions, as stated by one of the survey respondents: "Not everyone shows emotions in the same way." This means that different people have different facial expressions even when they are exhibiting the same emotion. However, this concern of the respondents should have already been accounted for by the usage of FER-2013 dataset in training the model for the software. The FER-2013 dataset included expressions of people of different genders, races, and ethnicities to ensure that precise prediction doesn't only occur for one group of people. Instead, the software was able to categorize different expressions to interpret emotions in people on the basis of the aforementioned factors. However, one can never confirm that every person's way of expressing a particular emotion has been accounted for.

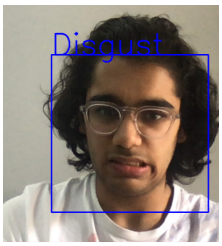

Figure 4: ERS Recognizing the Emotion of Disgust.

Note: ERP EXPLAINED. Youtube, AD 007, Apr 26, 2021 https://www.youtube.com/watch?v=WjKTnTR7EB4

Finally, the fundamental lack of facial affect in individuals with ASD, i.e., their inability to express emotions in their facial expressions means that it may still be cognitively challenging for ASD individuals to use this information to predict emotion, which was pointed out by one of the respondents: "I think the ERP is useful to help ASD individuals recognize facial emotions. However, it doesn't help them to understand WHAT is that emotion or feeling." This statement suggested that the respondents' concern about the use of the ERS does not lie so much with the efficacy of the program, but with the ASD individuals' neurological ability to actually understand emotions. Therefore, they questioned whether the software would be of any use to the ASD individuals in interactions. Nonetheless, most of the respondents showing such a concern were still ready to "give it a shot".

The distribution of the respondents across the ratings on each of the seven emotions was further examined and compared (see Figures 5–11). It was seen that the emotions of happiness and sadness have around 75% of the respondents rating it "6" or above, whereas the more ambiguous emotions such as neutrality, anger and disgust are rated a "5" or "6" by almost 55% of the respondents, thus validating the statistical results that the program performed better with these emotions from the perspective of the respondents.

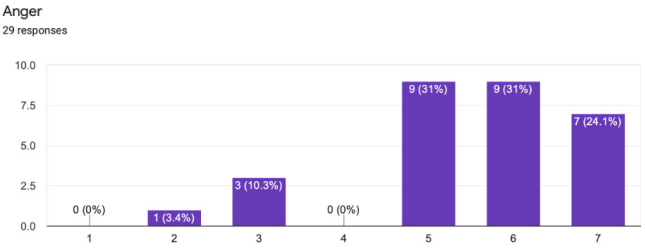

Figure 5: ERS Recognizing the Emotion of Happinesss.

DOI: 10.36838/v4i1.6

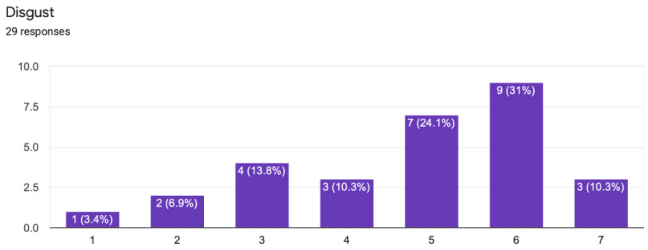

Figure 6: Ratings of Efficiency in Interpreting Disgust.

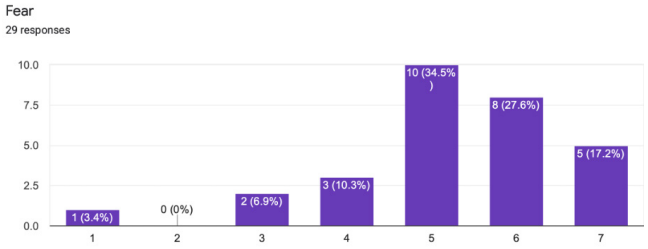

Figure 7: Ratings of Efficiency in Interpreting Fear.

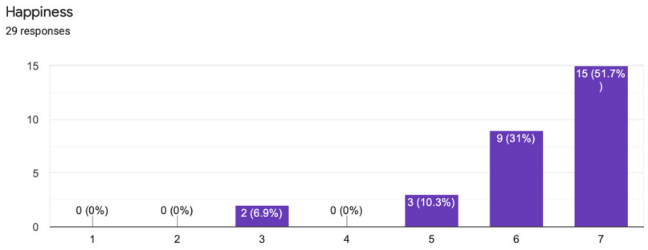

Figure 8: Ratings of Efficiency in Interpreting Happiness.

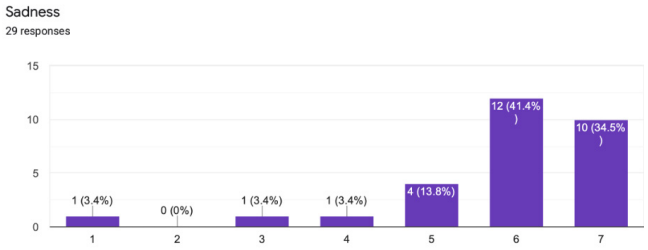

Figure 9: Ratings of Efficiency in Interpreting Sadness.

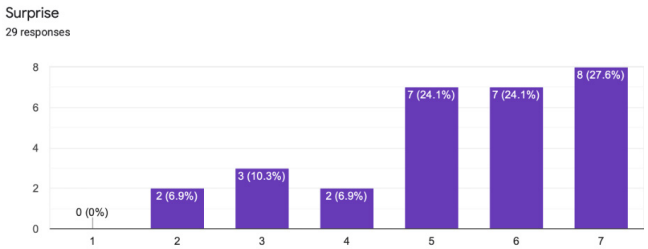

Figure 10: Ratings of Efficiency in Interpreting Surprise.

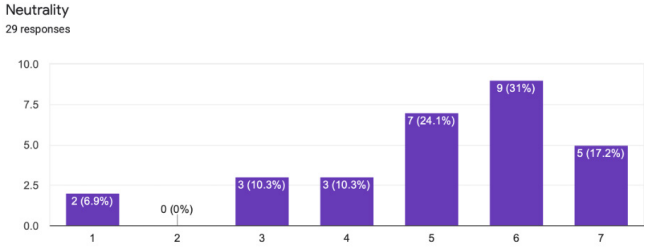

Figure 11: Ratings of Efficiency in Interpreting Neutrality.

Respondents' Perceptions of the Effectiveness of ERS for ASD Individuals:

A paired t-test was run to determine whether the mean difference between the respondents' perceptions and ratings before and after watching the video was statistically significant. Table 3 shows that the mean difference between the ratings was statistically significant, $t(28) = 2.81$ [more than the t critical value of 2.05 (two-tailed)], $p < .01$ (two-tailed). This indicates that the respondents showed a statistically significant change in ratings of effectiveness of the ERS upon watching the video, understanding the concept a little better, and seeing the emotions being interpreted.

Table 3: Respondents' Perception of Effectiveness of ERS for ASD Individuals (Before vs. After). *P-value less than 0.01 and t-stat is more than t-critical showing statistical significance of results.*

t-Test: Paired Two Sample for Means		
	Effectiveness (After)	***Effectiveness (Before)***
Mean	5.482758621	4.75862069
Variance	1.25862069	1.475369458
Observations	29	29
Pearson Correlation	0.298236011730524	
Hypothesized Mean Difference	0	
df	28	
t Stat	2.813429334	
P(T<=t) one-tail	0.004431709	
t Critical one-tail	1.701130934	
P(T<=t) two-tail	0.008863417	
t Critical two-tail	2.048407142	

The fact that the respondents showed a statistically significant change in perception is further examined by looking in the graphs (see Figures 12 and 13). Before watching the video, around 35% of the respondents had rated the effectiveness of ERS as a tool for ASD individuals in the range of 1-4 out of 7. However, after watching the video, this percentage halved to become around 17%.

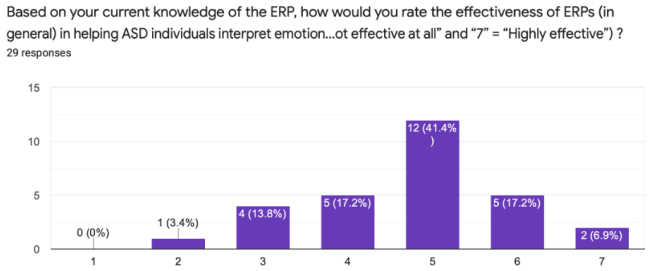

Figure 12: Bar Graph showing Respondents' Rating on the Viability of the Software Before watching the Video.

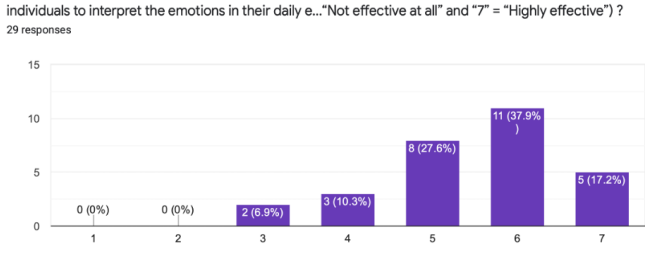

Figure 13: Bar Graph showing Respondents' Rating on the Viability of the Software Before watching the Video. *Note the change in median rating from 5 to 6 which shows the effectiveness of the video.*

It is also important to note that with the responses after watching the video, there wasn't a single respondent who rated the program a "1" or a "2" and more than 82% rated it a "5 or higher". This data indicates that every respondent, on some level, did not dismiss the possibility that ERS could be effective as a tool for ASD individuals. The enthusiasm about this technology, after watching the video, was exhibited through the responses to open-ended questions as well. Respondents were excited about various aspects. Some appreciated the working principle of the software, as in the case of one parent who stated, "My son definitely learns best with pictures. It has helped him tremendously with recognizing different emotions". This highlights the fact that visual media may not only be the best way for learning for autistic individuals but might also be the most comfortable and adaptive medium.

Identification of Ratings of Individual Emotions Impacting Rating of Effectiveness of ERS for ASD Individuals and Extent of Impact :

A multiple regression analysis was conducted to predict the effects of the respondents' ratings of the influencing factors on their ratings of the effectiveness of ERS for ASD individuals after watching the video. Of the seven factors, happiness and fear were found to be statistically significant (see Table 4): Happiness, $b = 0.70$, $t(21) = 3.20$ (higher than the critical value of 2.09), $p < .01$; and Fear, $b = 0.57$, $t(21) = 2.88$ (higher than the t critical value of 2.09), $p < .01$.

Table 4: Regression Analysis: Impact of Efficacy Ratings of Individual Emotions on Effectiveness of ERS for ASD Individuals. P-value of both "fear" and "happiness" is less than 0.05 making them factors in the equation.

Regression Statistics	
Multiple R	0.8589173795
R Square	0.7377390648
Adjusted R Square	0.6503187531
Standard Error	0.6634124299
Observations	29

ANOVA					
	df	SS	MS	F	Significance F
Regression	7	25.99894222	3.714134602	8.438989181	0.0000627063159 5
Residual	21	9.242437095	0.4401160521		
Total	28	35.24137931			

	Coefficients	Standard Error	t Stat	P-value	Lower 95%	Upper 95%	Lower 95.0%	Upper 95.0%
Intercept	0.9012057185	0.830615	1.08498524	0.29022733	0.82615407	2.62856551	0.82615407	2.62856551
Anger	0.1129709058	0.171240	0.65972061	0.51660381	0.46908507	0.24314326	0.46908507	0.24314326
Disgust	0.0480253587	0.105200	0.45651261	0.65270794	0.26680178	0.17075107	0.26680178	0.17075107
Fear	0.5747291244	0.199304	2.88367880	0.00888696	0.16025347	0.98920477	0.16025347	0.98920477
Happiness	0.701466054	0.218934	3.20400308	0.00426372	0.24616733	1.15676477	0.24616733	1.15676477
Sadness	0.3634688226	0.178930	2.03133762	0.05506861	0.73557574	0.00863809	0.73557574	0.00863809
Surprise	0.0321824425	0.139747	0.23028946	0.82009537	0.32280386	0.25843898	0.32280386	0.25843898
Neutrality	0.0722857987	0.124007	0.58291293	0.56615950	0.18560271	0.33017430	0.18560271	0.33017430

A limited regression analysis was done again with the statistically significant variables — happiness and fear. The predictive effect of happiness and fear was confirmed (see Table 5): happiness: $b = 0.59$, $t(26) = 4.53$ (higher than the t critical value of 2.06), $p < .01$; and fear: $b = 0.28$, $t(26) = 2.67$ (higher than the critical value of 2.06), $p = .013$.

Essentially, the rating given to interpretation of happiness and fear aggregated accounted for about 65% of the efficiency rating that the respondents give to the program.

Table 5: Impact of Ratings of Happiness and Fear on Overall Efficiency Rating of the Software. Coefficients of "*fear*" and "*happiness*" (significant factors) are 0.28 and 0.59 respectively.

Regression Statistics	
Multiple R	0.807359643
R Square	0.651829593
Adjusted R Square	0.625047254
Standard Error	0.686966727
Observations	29

ANOVA					
	df	*SS*	*MS*	*F*	*Significance F*
Regression	2	22.97137392	11.48568696	24.33803828	1.10E-06
Residual	26	12.27000539	0.471923284		
Total	28	35.24137931			

	Coefficients	*Standard Error*	*t Stat*	*P-value*	*Lower 95%*	*Upper 95%*	*Lower 95.0%*	*Upper 95.0%*
Intercept	0.327706267	0.757296392	0.432731848	0.668778009	1.228938745	1.884351279	1.228938745	1.884351279
Fear	0.282127031	0.105609104	2.67142717	0.012859088	0.06504441	0.499209652	0.06504441	0.499209652
Happiness	0.592295609	0.130790391	4.528586568	0.000116662	0.323452112	0.861139105	0.323452112	0.861139105

The linear equation to calculate the extent of the impact of the efficacy ratings of these two emotions on the effectiveness rating of the ERS was as follows:

Effectiveness of ERS= 0.33 + 0.59(efficacy rating Happiness) + 0.28*(efficacy rating Fear)*

For example, if an individual were to rate the efficacy rating of happiness at "7", and fear as "6", then his/her likely rating of the overall effectiveness of the software would be 6.14 out of 7. Conversely, if an individual were to rate the efficacy rating of happiness at "1", and fear as "2", then his/her likely rating of the overall effectiveness of the software would be 1.48 out of 7. If an individual were to rate the efficacy rating of happiness at "5", and fear as "4", then his/her likely rating of the overall effectiveness of the software would be 4.04 out of 7 using the equation. These results highlight the importance of these two factors that account for 65% of the impact. Nonetheless, there still are other factors that could be identified to help determine the effectiveness of this video and the self-designed ERS in demonstrating its viability for ASD individuals to people who interact with them.

Conclusion

The research study set out to evaluate the impact of a self-formulated video on a self-designed ERS on the perceptions of autism professionals' or family members of the effectiveness of ERSs as a tool to ASD individuals to interpret facial expressions in daily interactions. All the null hypotheses set out in this research study were rejected due to the statistical significance of the analyses. The results showed that the video featuring a self-designed ERS had a positive effect on the respondents' opinions on the effectiveness of the ERS for people with ASD. The respondents started believing that such a tool could make lives easier which was reflected in a 15% increase in their ratings of the ERS' effectiveness after watching the video. There were differences between the mean ratings of the peoples' perception of the software's efficiency of interpreting different emotions,

DOI: 10.36838/v4i1.6

which were better understood through the analysis of qualitative responses. Some emotions were clearly identified without ambiguity (like happiness, sadness and fear), whereas others were ambiguous (like anger, disgust, and neutrality). Finally, it was found that only happiness and fear out of all the seven emotions had an effect on the respondents' rating on the ERS' effectiveness, which makes sense because they both are easily identified by neurotypicals themselves and have a high mean rating.

While the respondents gave slightly above average to high ratings of the efficacy of individual emotions and the effectiveness of the ERS for ASD individuals, they also pointed out the challenge of this objective. Respondents suggested that their efficacy ratings for different emotions could be biased by their opinions of the ambiguity present. For example, one respondent commented that "the facial expressions for disgust, fear and sadness seem too similar." This means that even neurotypicals struggle to judge certain categories of emotion. In fact, others pointed out that the ERS should include more features like "complex emotions" like "sarcasm", which can be ambiguous, and "condescending behavior", as well as additional features like "body language", to help ASD individuals in interactions. One respondent said, "Some emotions will never be visible." This suggested that there is still a need to generate support for ERS as well as trying to make parents and professionals understand its working better. A good way to do it, as suggested by the respondents, would be by having a way to justify choosing one emotion over the other since neurotypicals themselves get confused with emotions and the only way their brain decides which is which is by providing reason. This might even make the program more relatable for them. It is important to note that these suggestions might make up for the remaining 35% constituent factors or emotions that affect perception of respondents on the viability of the ERS.

Respondents are inclined to give the ERS a try since they already approve of its working principle, that is, it is a visual aid. They wrote about visual aids being a common means in helping the problems of individuals with ASD. One respondent shared that their son/sibling benefited from it. One of them talked about a similar concept saying, "There is something similar in the US where the child wears spectacles that interpret the emotions being observed." This is similar to the Google glass concept discussed in the introduction.[16] Much like the spectacle example above, there are various ways to harness this program in real life, some of them being through physical tools, in the form of a mobile or tablet application, or by using it interlinked with video conferencing platforms like Zoom and Google meet. This tool being available not only during face-to-face interactions, but also during virtual meets, could magnify the potential of its helpfulness for people diagnosed with ASD, with the increase of work from home culture in today's in progressive world.[19] While neurotypicals are chasing efficiency, this tool can help individuals with ASD to maintain, if not improve, their current comfort during interactions.

However, this innovation should not stop here. According to the quantitative data, only the respondents' efficacy ratings of the emotions of happiness and fear predicted their rating on the overall effectiveness of the software. These two emotions together accounted for 65% of the respondents' perception of the software as an effective tool for ASD individuals. This means that the other five emotions do not affect the decision of the respondents effectively, which points towards another opportunity for improvement: the ERS' recognition algorithm and display, and possibly using other ways to interpret emotions, that is, through tone or voice.

Based on the concerns raised by the respondents, the functioning of the ERS as a helpful interaction tool for ASD individuals can possibly be augmented by integrating it with a kind of sound recognition tool. Through the medium of sound and tone, this tool would supplement the evaluation of facial recognition by generating its own output so that a more accurate outcome can be produced. Various ways of integrating the two systems can be explored, working simultaneously, working on the added probabilities from both systems, working alternately, etc. Since facial expressions are not the only thing that determines emotions, such a system could help the computer minimize the error, or ambiguity in the interpretation of facial expressions and give a more reliable prediction of emotions.

References

1. Kanner, L. (1943). Autistic disturbances of affective contact. *Nervous Child*, 2(3), 217-250.http://mail.neurodiversity.com/library_kanner_1943.pdf
2. Faras, H., Al Ateeqi, N., & Tidmarsh, L. (2010). Autism spectrum disorders. *Annals of Saudi Medicine*, 30(4), 295–300. https://doi.org/10.4103/0256-4947.65261
3. Baron-Cohen, S. (1989). The autistic child's theory of mind: A case of specific developmental delay. Journal of Child Psychology and Psychiatry, 30(2), 285-97. https://doi.org/10.1111/j.1469-7610.1989.tb00241.x
4. Baron-Cohen, S., Jolliffe, T., Mortimore, C., & Robertson, M. (1997). Another advanced test of theory of mind: evidence from very high functioning adults with autism or Asperger syndrome. *Journal of Child Psychology and Psychiatry*, 38, 813-822. https://doi.org/10.1111/j.1469-7610.1997.tb01599.x
5. Dalton, K. M., Nacewicz, B. M., Johnstone, T., Schaefer, H. S., Gernsbacher, M. A., Goldsmith, H. H., Alexander, A. L., & Davidson, R. J. (2005). Gaze fixation and the neural circuitry of face processing in autism. *Nature Neuroscience*, 8(4), 519–526. https://doi.org/10.1038/nn1421
6. Klin, A., Jones, W., Schultz, R., Volkmar, F., & Cohen, D. (2002). Visual fixation patterns during viewing of naturalistic social situations as predictors of social competence in individuals with autism. *Archives of General Psychiatry*, 59(9), 809–816. https://doi.org/10.1001/archpsyc.59.9.809
7. Volkmar, F. R., & Mayes, L. C. (1990). Gaze behavior in autism. *Development and Psychopathology*, 2(1), 61–69. https://doi.org/10.1017/S0954579400000596
8. Leekam, S. R., López, B., & Moore, C. (2000). Attention and joint attention in preschool children with autism. *Developmental Psychology*, 36(2), 261–273. https://doi.org/10.1037//0012-1649.36.2.261
9. Grossman, R. B., Bemis, R. H., Skwerer, D. P., & Tager-Flusberg, H. (2010). Lexical and affective prosody in children with high-functioning autism.*Journal of Speech, Language, and Hearing Research* : JSLHR. 53. 778-93.https://doi.org/10.1044/1092-4388
10. Baron-Cohen, S., Wheelwright, S., Spong, A., Scahill, V., & Lawson, J.(2001). Are intuitive physics

and intuitive psychology independent? A *test with children with Asperger Syndrome. Journal of Developmental and Learning Disorders,* 5. https://docs.autismresearchcentre.com/papers/2001_BCetal_kidseyes.pdf.
11. Golan, O., Sinai-Gavrilov, Y., & Baron-Cohen, S. (2015). The Cambridge Mindreading Face-Voice Battery for Children (CAM-C): Complex emotion recognition in children with and without autism spectrum conditions. *Molecular autism*, 6, 22. https://doi.org/10.1186/s13229-015-0018-z
12. Hopkins, I. M., Gower, M. W., Perez, T. A., Smith, D. S., Amthor, F. R., Wimsatt, F. C., & Biasini, F. J. (2011). Avatar assistant: improving social skills in students with an ASD through a computer-based intervention. *Journal of Autism and Developmental Disorders*, 41(11), 1543–1555. https://doi.org/10.1007/s10803-011-1179-z
13. LaCava, P. G., Rankin, A., Mahlios, E., Cook, K., & Simpson, R. L. (2010). A single case design evaluation of a software and tutor intervention addressing emotion recognition and social interaction in four boys with ASD. *Autism: The International Journal of Research and Practice*, 14(3), 161–178. https://doi.org/10.1177/1362361310362085
14. Simmons, E. S., Paul, R., & Shic, F. (2016). Brief report: A mobile application to treat prosodic deficits in autism spectrum disorder and other communication impairments: A pilot study. *Journal of Autism and Developmental Disorders*, 46(1), 320-327. https://doi.org/10.1007/s10803-015-2573-8
15. Silver, M., & Oakes, P. (2001). Evaluation of a new computer intervention to teach people with autism or Asperger syndrome to recognize and predict emotions in others. Autism: *The International Journal of Research and Practice*, 5(3), 299–316. https://doi.org/10.1177/1362361301005003007
16. Washington, P., Voss, C., Haber, N., Tanaka, S., Daniels, J., Feinstein, C., ... & Wall, D. (2016, May). wearable social interaction aid for children with autism. In Proceedings of the 2016 *CHI Conference Extended Abstracts on Human Factors in Computing Systems*. https://doi.org/10.1145/2851581.2892282
17. Wu, J. (2017). Introduction to convolutional neural networks. *National Key Lab for Novel Software Technology,* 5, 23. https://cs.nju.edu.cn/wujx/paper/CNN.pdf
18. Maklin, C. (2019, June 3). *Dropout neural network layer in keras explained*. Towards data science. https://towardsdatascience.com/machine-learning-part-20-dropout-keras-layers-explained-8c9f6dc4c9ab
19. Saltiel, F. (2020). Who can work from home in developing countries. *Covid Economics*, 7(2020), 104-118. http://econweb.umd. edu/~saltiel/files/wfh_mostrecent.pdf

Author

Aryan Dawer is a 12th grader at Modern School Barakhamba Road, New Delhi, India. He is 17 years old, and very interested in Computer Science and Psychology. His passion for designing tools found purpose in his work with individuals with ASD. Previously, he has designed software to recognize emotions through tone and facial expressions to aid them in daily conversations. He is also an environmentalist and is founding member and CTO of DropCount, a water-saving initiative that uses innovative technology to save water. In his free time, Aryan likes to analyse tv show/movie/novel characters, and put himself in their shoes to enhance his logical reasoning skills as well as experience diverse situations.

DOI: 10.36838/v4i1.6

IJHSR
ijhighschoolresearch.org
■ RESEARCH ARTICLE

Antifungal Activity of Lemongrass Oil Against Pathogenic Fungi

Yashwanth Gangavarapu, Suhas Palwai

Adlai E Stevenson High School, 1 Stevenson Dr, Lincolnshire, Illinois, 60061, USA; gangavarapuyash@gmail.com

ABSTRACT: Plant pathogenic fungi cause diseases in plants and have a devastating impact on the global food security within our ever-growing population. The damage to crops not only results in low crop yields but also leaves millions of people starving due to food shortages. Various essential oils have been tested for antifungal activity *in vitro* and *in vivo*, and some demonstrate considerable promise as antifungal agents. Therefore, to prevent the further loss of crops and resistance buildup, we propose to test the bio-fungicidal properties of lemongrass oil as an alternative to chemical fungicides in controlling plant pathogenic fungi. We tested the antifungal efficacy of lemongrass oil against *Alternaria solani, Botrytis cinerea, Fusarium oxysporum, Pythium ultimum* and *Rhizoctonia solani*, using a mycelial radial growth inhibition assay. The results of the study reveal that lemongrass oil has potent *in vitro* action against all these fungal species.

KEYWORDS: Plant Pathogens; Antifungal activity; Growth inhibition; Fungicide; Essential Oils.

■ Introduction

Plant pathogens cause severe diseases and ultimately reduce the productivity and quality of crop and sometimes even destroy the entire crop.[1] Plant pathogens can have terrible consequences if they are not prevented or suppressed.

Botrytis cinerea, commonly known as gray mold, affects over 200 crops such as grapes and strawberries resulting in monetary losses ranging from $10 billion to over $100 billion throughout the world.[2] *Alternaria solani* is an air borne fungal sporulating ascomycetes known as early blight fungi. It causes a wide range of diseases mainly in tomatoes and potatoes that can result in up to 79% crop loss.[3] *Rhizoctonia solani*, considered a soil borne pathogen, causes various plant diseases like root rot, damping off, wire stem, stem lesions, etc.[4] *Pythium ultimum* is soil borne fungal plant pathogen which is the cause of damping off and root rot on many plants. Most plants are killed by *Fusarium oxysporum*, and by the time a plant shows any visible signs of infection, it is too late to combat, and the plant will die.[5]

The threat of antimicrobial resistance to chemicals and antibiotics has increased tremendously due to the excessive reliance on chemicals to control the plant pathogens either through growth inhibition or by killing plant pathogens.[6] This threat has displayed the importance of using natural substances for controlling pathogens. *Cymbopogon citratus*, lemongrass, is an essential oil with a growing reputation due to its antimicrobial properties.[7] Cymbopogon, commonly known as lemongrass or citronella, is a grassy plant found in tropical regions like South Asia, where people have utilized it for practices ranging from traditional medicine to food preservation.[8] These plants are perennials that grow during the summer in moist and rich soils and can grow up to ten feet tall. They are well known for their aroma which has a similar smell to lemons. Cymbopogon is a genus of around 55 species with *Cymbopogon citratus* being primarily used for an essential oil which can be extracted from the leaf of the plant by steam distillation process.[9,10]

Lemongrass oil has been used for a variety of medicinal purposes such as pain relief, fevers, and gastrointestinal disorders for centuries. The effects of lemongrass on various pathogens have been investigated in several studies, and it is shown that it has antimicrobial, antibacterial, and antifungal properties. Studies have shown that lemongrass has demonstrated the ability to inhibit both plant and human pathogens.[11]

Citral is a key component when discussing the antimicrobial properties of lemongrass. Major compounds and its percentages present in lemongrass oil are Citral α-40.8%, Citral β-32%, Nerol- 4.18%, Geraniol-3.104%, Citronellal-2.10%, Terpinolene-1.23% and Geranyl Acetate-0.83%.[12]

The mode of action of lemongrass oil against foliar and post-harvest pathogens is not fully understood. Some studies have indicated that mycelium exposed to lemongrass oil go through morphological injury such as vesiculation, and cytoplasmic commotion besides folding of hyphae.[13] The oil contains a high content of Citral composed of general and geranial isomers which may be the reason for their effective antifungal activity. Some of these active components present in essential oils can act on the pathogen directly or activate defense responses in host plants leading to a reduction in disease progress or can act directly through antagonism, which still requires further research.[14]

■ Results and Discussion

For a long time, medicinal plants and crude herbal products have been used in conventional medicines and household remedies. Not all herbal preparations have undergone scientific scrutiny. The antifungal activity of lemongrass oil against pathogenic fungi was investigated in this study, and the results indicate that lemongrass oil has substantial antifungal activity. These fungal species are associated with some common infections of plant species. The data shown in Figure 1 and Table 1 clearly indicates that all fungal strains tested were completely suppressed by lemongrass oil at 1.0% concentration.

DOI: 10.36838/v4i1.7

The inhibitory effect of lemongrass oil was proportional with concentrations used. Decreased effect of radial growth was observed when concentration was lowered to 0.5%, 0.25% and 0.1% respectively in all pathogens. At a concentration of 0.25%, lemongrass oil was effective only against *Alternaria solani* and *Fusarium oxysporum*.

Table 1: Diameter of mean radial growth of various plant pathogens on agar plates after 5-7 days of incubation.

Plant Pathogen	Lemongrass oil concentration (%)	Mean radial growth (mm)	Mean radial growth inhibition (%)
Alternaria solani	Control	32	0.00
	Soybean oil	34	0.00
	0.1	13	59.4
	0.25	12	62.5
	0.5	0	100
	1.0	0	100
Botrytis cinerea	Control	35	0.00
	Soybean oil	35	0.00
	0.10	35	0.00
	0.25	35	0.00
	0.5	10	71.4
	1.0	0	100
Fusarium oxysporum	Control	35	0.00
	Soybean oil	35	0.00
	0.1	15	57.1
	0.25	13	62.9
	0.5	0	100
	1.0	0	100
Pythium ultimum	Control	35	0.00
	Soybean oil	35	0.00
	0.10	35	0.00
	0.25	35	0.00
	0.5	17	51.4
	1.0	0	100
Rhizoctonia solani	Control	35	0.00
	Soybean oil	35	0.00
	0.10	35	0.00
	0.25	35	0.00
	0.5	30	14.3
	1.0	0	100

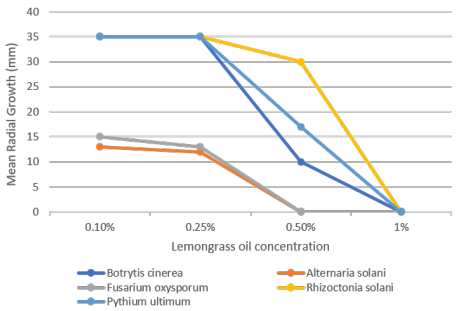

Figure 1: Mean radial growth of various fungal species at varying concentration of lemongrass oil. The graph shows a clear dose response among the concentrations tested.

Several essential oils have been tested for antimycotic activity *in vivo* and *in vitro*, with some showing promise as antifungal agents. Their mechanism of action focuses on the fungal cell membrane, destroying its structure and inducing cell death; spore germination, fungal proliferation, and cellular respiration are all inhibited; and membrane synthesis is prevented.[15] Due to their high volatility and lipophilicity, essential oils bind easily to the cell membrane and exert their biological impact.[16] Antifungal susceptibility varies among fungal organisms, and numerous resistance mechanisms have antifungal sequestration in organelles like vacuoles, or chromosomal alterations, resulting in differential susceptibility of various fungal species to antimicrobial agents in this study.

The effect of lemongrass oil against *Alternaria solani* was studied using 1.0% concentration to determine the mycelial growth inhibition. Dose response studies were also conducted against *Alternaria solani* using various concentrations of lemongrass oil and results are shown in Figure 2. The results showed that lemongrass oil is highly effective against *Alternaria solani*, with a 100% reduction of growth observed at 1.0% and 0.5% followed 65% and 60% in 0.25% and 0.1% concentrations. These results clearly indicate that *Alternaria solani* is sensitive to lemongrass oil. The Minimum Inhibitory Concentration (MIC) value for *Alternaria solani* in this study was found to be 100 µL per mL. Similar results have been reported in the previous studies of antimicrobial activities essential oils against *Alternaria solani*.[17,18]

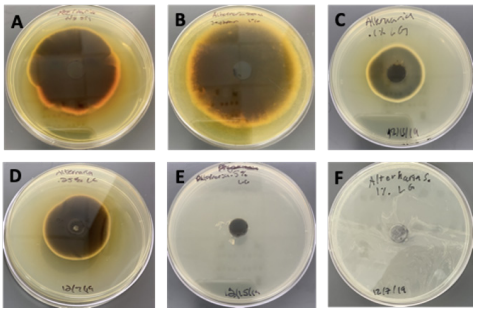

Figure 2: *In vitro* activity of lemongrass oil against *Alternaria solani* by radial growth inhibition. (A) *Alternaria solani* control (B) *Alternaria solani* with 1.0% soybean oil (C) *Alternaria solani* with 0.1% lemongrass oil (D) *Alternaria solani* with 0.25% lemongrass oil (E) *Alternaria solani* with 0.5% lemongrass oil (F) *Alternaria solani* with 1.0% lemongrass oil. Lemongrass oil is highly effective against *Alternaria solani*, 100% reduction of growth observed at 1.0% and 0.5% concentrations.

The antifungal activity of lemongrass oil was evaluated against *Botrytis cinerea* by measuring the radial growth on potato dextrose agar medium. Dose response studies were also conducted, and those results are shown in Figure 3. The lemongrass oil was found to be very effective and showed a 100% reduction of mycelial growth at 1.0% concentration. More than 70% reduction of growth was observed at 0.5% concentration and no effect observed at 0.25% and 0.1% concentrations respectively. These results indicate that lemongrass oil affect mycelial growth of *Botrytis cinerea* in a concentration dependent manner.

The effect of lemongrass oil against *Fusarium oxysporum* was studied using 0.1% to 1.0% concentrations to see the mycelial growth inhibition and the results are reported in Figure 4. The dose response study showed that lemongrass oil is highly effective against *Fusarium oxysporum* similar to *Alternaria solani*. 100% reduction of growth observed at 1.0% and 0.5%, followed by around 62% and 57% in 0.25% and 0.1% concentrations. These results clearly indicate that *Fusarium oxysporum* is very sensitive to lemongrass oil. According to the results reported in Figure 5, the complete inhibition/reduction of mycelial growth of *Pythium ultimum* was observed at 1.0% concentration and a more than 50% reduction at 0.5%

DOI: 10.36838/v4i1.7

concentrations. Full radial growth means no effect on radial growth was observed at 0.25% concentration of lemongrass oil on *Pythium ultimum*.

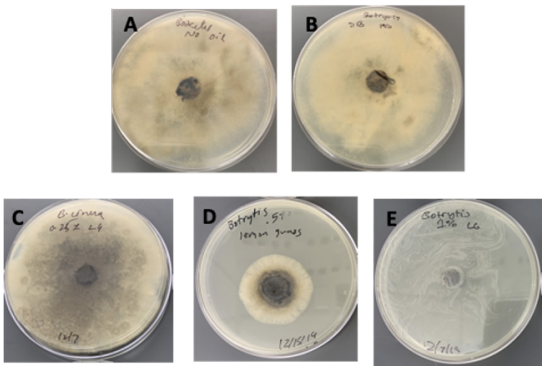

Figure 3: *In vitro* activity of lemongrass oil against *Botrytis cinerea* by radial growth inhibition. (A) *Botrytis cinerea* control (B) *Botrytis cinerea* with 1.0% soybean oil (C) *Botrytis cinerea* with 0.25% lemongrass oil (D) *Botrytis cinerea* with 0.5% lemongrass oil (E) *Botrytis cinerea* with 1.0% lemongrass oil. The lemongrass oil was found to be very effective showed 100% reduction of mycelial growth at 1.0% concentration.

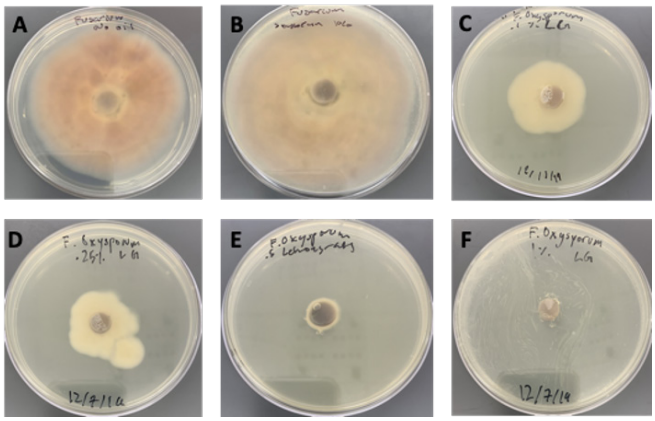

Figure 4: *In vitro* activity of Lemongrass oil against *Fusarium oxysporum* by radial growth inhibition. (A) *Fusarium oxysporum* control (B) *Fusarium oxysporum* with 1.0% soybean oil (C) *Fusarium oxysporum* with 0.1% lemongrass oil (D) *Fusarium oxysporum* with 0.25% lemongrass oil (E) *Fusarium oxysporum* with 0.5% lemongrass oil (F) *Fusarium oxysporum* with 1.0% lemongrass oil. The picture clearly shows a dose response with different concentrations of lemongrass oil.

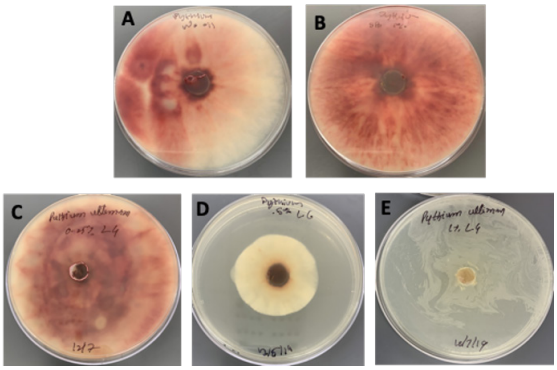

Figure 5: *In vitro* activity of Lemongrass oil against *Pythium ultimum* by radial growth inhibition. (A) *Pythium ultimum* control (B) *Pythium ultimum* with 1.0% soybean oil (C) *Pythium ultimum* with 0.25% lemongrass oil (D) *Pythium ultimum* with 0.5% lemongrass oil (E) *Pythium ultimum* with 0.1% lemongrass oil. The picture clearly shows *Pythium ultimum* growth was completely inhibited at 1.0% concentration of lemongrass oil.

Similarly, the effect of lemongrass oil on mycelial growth of *Rhizoctonia solani* was studied and results shown in Figure 6. *Rhizoctonia solani* did not respond to lemongrass oil the same way as other pathogens. The complete inhibition of growth was observed at a 1.0% concentration of lemongrass oil, but not at lower doses. At a 0.5% concentration, there was only 15% mycelial growth reduction, while lemongrass oil displayed no effect at 0.25% and 0.1% concentrations.

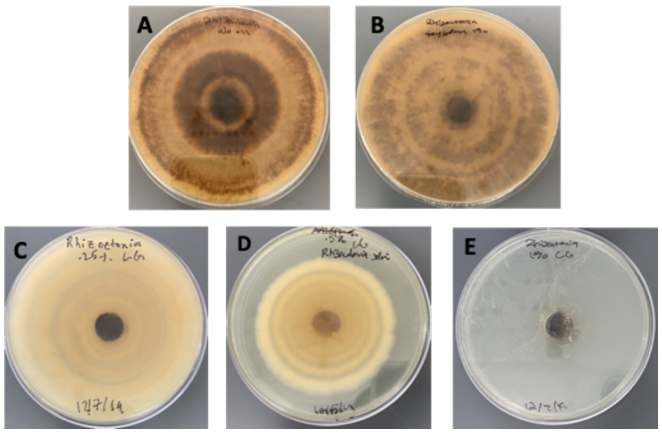

Figure 6: *In vitro* activity of lemongrass oil against *Rhizoctonia solani* by radial growth inhibition. (A) *Rhizoctonia solani* control (B) *Rhizoctonia solani* with 1.0% soybean oil (C) *Rhizoctonia solani* with 0.25% lemongrass oil (D) *Rhizoctonia solani* with 0.5% lemongrass oil (E) *Rhizoctonia solani* with 1.0% lemongrass oil. The picture shows *Rhizoctonia solani* growth was completed inhibited at 1% concentration of lemongrass oil.

We hypothesized that if lemongrass oil is used to control plant pathogenic fungi as an alternative to chemicals, then it will inhibit or minimize the mycelial or spore germination of the plant pathogens stated. The data showed that a 1.0% lemongrass oil concentration was able to inhibit all the pathogens tested completely. Dose-response studies were conducted to optimize the optimal concentration of lemongrass required to control and inhibit the growth of pathogens. These studies determined that a lower concentration of lemongrass oil increased the radial growth of all pathogens means decreased the effectiveness of pathogenicity. Thus, the findings of this study showed that lemongrass oil is an effective deterrent for plant pathogens alternative to chemical fungicides. However, lemongrass oil had greater radial growth inhibition in *Alternaria solani* and *Fusarium oxysporum* rather than *Botrytis cinerea*.

Citral and lemongrass oil had similar antifungal activity, which is consistent with previous research that related the effect to the occurrence of citral in lemongrass.[19] Citral in lemongrass is a fungicidal agent, according to the literature, since it can form a charge transfer complex with a fungal electron donor, causing fungal death.

Conclusion

The results of this investigation showed lemongrass oil has significant antimicrobial activity against plant pathogens. The fungi tested were *Botrytis cinerea, Alternaria solani, Rhizoctonia solani, Fusarium oxysporum*, and *Pythium ultimum*. The aim of this investigation was to find whether lemongrass is effective against plant pathogens and could be used as a viable alternative candidate to chemical fungicides. Lemongrass oil was proven to have antimicrobial properties, and several researchers reported

the use of medicinal purposes mainly for treating human diseases. Limited research was done against plant pathogens mainly against *Pythium ultimum* and *Fusarium oxysporum*.

Because of its antifungal efficacy, low cost, and low toxicity, these findings suggest that lemongrass oil could be used in pharmaceutical preparations for the control and treatment of fungal plant pathogens. Further research is required to test the unique antifungal properties of lemongrass oil and broad-spectrum activity against other fungal and bacterial pathogens.

Methods

Pure natural steam-distilled lemongrass (*Cymbopogon citratus*) oil was obtained from SVA Organics. Plant Pathogen namely *Botrytis cinerea Alternaria, solani, Rhizoctonia solani, Pythium ultimum* and *Fusarium oxysporum* were obtained from American Type Culture Collection (ATCC). Potato Dextrose Agar (PDA) was prepared using premix agar medium obtained from Carolina Biosciences. PDA plates with lemongrass oil (1%, 0.5, 0.25%, 0.1%) concentrations were made following the standard protocol, autoclaving the medium, cool down to 50˚C and make plates by transferring 20 ml to each plate manually.[20] Plates of various concentration for experimental and control groups were labeled.

Making of PDA plates with various lemongrass oil (1%, 0.5, 0.25%, 0.1%) concentrations:

We added 500 ml of tap water to 20 grams of free mixed, commercially available potato dextrose agar powder into a 1.0 Liter flask and mixed and stirred with a magnetic bar. Then 5.0mL of lemongrass oil was added into the medium before autoclaving to create 1.0% lemongrass oil concentration. The media was then autoclaved at 121˚C (15psi) for 15 minutes and transferred to water bath at 50˚C so the media did not solidify. The flask from the water bath was taken out and moved to a biosafety cabinet. 20 ml of the medium was dispensed into each petri plate and plates were allowed to solidify overnight completely. The same procedure was used to make 0.5%, 0.25% and 0.1% concentration plates. For controls, the same media preparation procedure was used as mentioned above with/without adding soybean oil to the medium.

Antifungal Assay (Radial Growth inhibition):

The antagonistic activity of lemongrass oil on radial growth of the test organisms was measured by placing a mycelial agar plug on the center of the PDA plates with various concentrations of lemongrass oil. The plate containing only PDA medium without lemongrass/soybean oil used as pathogen control and a plate containing 1.0% soybean oil was used as a negative control. Three plates of each concentration for each pathogen were used. Each experiment was performed in triplicates.

To transfer the mycelial plugs from plate to plate, a cork borer and forceps were used to extract an agar plug from the middle of each potato dextrose agar plate. The same step was repeated to extract agar plugs for all the plates. Then, a slightly larger cork borer was used to cut the mycelial plug from the pathogenic plate. All plates were sealed with parafilm and incubated in a biological incubator at 28˚C. After 5-7 days, the radial growth of each of the pathogens was measured by calculating the colony diameter on each replicate. Photographs were taken using camera and the radial growth inhibition was assessed by computing the width of the soybean oil and no oil controls on a regular ruler. All plates were disposed of in a biohazard autoclave bag and autoclaved at 121˚C for 30-60 minutes prior to disposal.

Acknowledgements

We thank American Type Culture Collection (ATCC) and Carolina Biosciences for providing cultures and media plates. We sincerely thank Mrs. Christina Palffy, Adlai E Stevenson High School, IL for her continuous assistance, critical review of this manuscript, and feedback throughout the study. We also thank our parents for their continuous moral support, helpfulness, and encouragement of our ideas during these studies.

References

1. Lamichhane, J. R.; Venturi, V. Synergisms between Microbial Pathogens in Plant Disease Complexes: A Growing Trend. *Front. Plant Sci*. 2015, 6, 385.
2. Williamson, B.; Tudsynski, B.; Tudzynski, P.; Van Kan, J l. *Botrytis cinerea*: the cause of grey mould disease. *Molecular Plant Pathology*. 2007, 8 (5), 561-580.
3. Adhikari, P.; Oh, Y.; Panthee, D. R. Current Status of Early Blight Resistance in Tomato: An Update. *International Journal of Molecular Science.* 2017, 18 (10).
4. Ralph Baker and C. A. Martinson. Epidemiology of Diseases Caused by *Rhizoctonia solani*, University of California Press, Berkeley. 1970, pp 172-188.
5. Arie Tsutomu. Fusarium diseases of cultivated plants, control, diagnosis, and molecular and genetic studies. *Journal of Pesticidal Science*. 2019, 44 (4), 275-281.
6. Chandra, H.; Bishnoi, P.; Yadav, A.; Patni, B.; Mishra, A. P.; Nautiyal, A. R. Antimicrobial Resistance and the Alternative Resources with Special Emphasis on Plant-Based Antimicrobials—a Review. *Plants*. 2017, 6 (2), 16.
7. De Silva, B. C. J.; Jung, W. G.; Hossain, S.; Wimalasena, S.; Pathirana, H.; Heo, G J. Antimicrobial Property of Lemongrass (Cymbopogon citratus) oil against Pathogenic Bacteria Isolated from Pet Turtles. *Lab. Anim. Res*. 2017, 33 (2), 84–91.
8. Ekpenyong, Ch.E., Akpan, E.E. Use of Cymbopogon citratus essential oil in food preservation: Recent advances and future perspectives. *Critical Reviews in Food Science and Nutrition*, 2017, 57(12), 2541-2559.
9. Baruah, J.; Gogoi, B.; Das, K.; Ahmed, N. M.; Sarmah, D. K.; Lal, M.; Bhau, B. S. Genetic Diversity Study amongst Cymbopogon species from NE-India Using RAPD and ISSR Markers. *Ind. Crops Prod*. 2017, 95, 235–243
10. Schaneberg, B.T., Khan, I.A. Comparison of extraction methods for marker compounds in the essential oil of lemongrass by GC. *Journal of Agricultural and Food Chemistry.* 2002, 50 (6), 1345–1349.
11. Balakrishnan, B.; Paramasivam, S.; Arulkumar, A. Evaluation of the Lemongrass Plant (Cymbopogon Citratus) Extracted in Different Solvents for Antioxidant and Antibacterial Activity against Human Pathogens. *Asian Pacific J. Trop. Dis*. 2014, 4, S134–S139.
12. Tyagi, A. K.; Gottardi, D.; Malik, A.; Guerzoni, M. E. Chemical Composition, in vitro Anti-Yeast Activity and Fruit Juice Preservation Potential of Lemongrass oil. *LWT-Food Sci. Technol*. 2014, 57 (2), 731–737.
13. Tak, J. H.; Isman, M. B. Metabolism of Citral, the Major Constituent of Lemongrass oil, in the Cabbage Looper,

DOI: 10.36838/v4i1.7

Trichoplusia Ni, and Effects of Enzyme Inhibitors on Toxicity and Metabolism. *Pestic. Biochem. Physiol*. 2016, 133, 20–25.
14. Mbili, N. C.; Laing, M. D.; Yobo, K. S. Integrated Control of *Penicillium expansum* and *Botrytis cinerea* of Apples Using Potassium Silicate, Yeast Antagonists and YieldPlus®. *In XXX International Horticultural Congress IHC2018: II International Symposium on Innovative Plant Protection in Horticulture*. 2018 1269, pp 75–80.
15. Kryvtsova, M. V.; Kohuch, T. T.; Salamon, I.; Spivak, M. J. Antimicrobial Activity of Some Essential Oils on Candida Genus Clinical Isolates. *Мікробіологічний журнал*. 2018, Vol 80 (4), 3–12.
16. Chouhan, S.; Sharma, K.; Guleria, S. Antimicrobial Activity of Some Essential Oils—Present Status and Future Perspectives. *Medicines (Basel)*. 2017 Sep; 4(3): 58.
17. Hassanein, R. A.; Salem, E. A.; Zahran, A. A. Efficacy of Coupling Gamma Irradiation with Calcium Chloride and Lemongrass oil in Maintaining Guava Fruit Quality and Inhibiting Fungal Growth during Cold Storage. *Folia Hortic*. 2018, 30 (1), 67–78.
18. Ragupathi, K. P.; Renganayaki, P. R.; Sundareswaran, S.; Kumar, S. M.; Kamalakannan, A. Evaluation of Essential Oils against Early Blight (*Alternaria solani*) of Tomato. *Int. Res. J. Pure Appl. Chem*. 2020, 164–169.
19. Gupta, A. K.; Ganjewala, D. A Study on Biosynthesis of "Citral" in Lemongrass (C. Flexuosus) Cv. Suvarna. *Acta Physiol. Plant*. 2015, 37 (11), 1–8.
20. Erin R. Sanders. Aseptic Laboratory Techniques: Plating Methods. *J Vis Exp*. 2012; (63): 3064.

Author

Yashwanth Gangavarapu is a rising senior student studying at Adlai E. Stevenson High School, Lincolnshire, IL, USA. He is interested in research, designing, and understanding basic concepts of science, especially in artificial intelligence and machine learning, and applying those technologies in plant and human diseases. He plans to pursue his undergraduate degree either in electrical, biomedical, or aeronautical engineering. His other interests include lacrosse, soccer, and volunteering to teach young kids.

Suhas Palwai is a rising senior student studying at Adlai E. Stevenson High School, Lincolnshire, IL. He is interested in pursuing Computer Science. Suhas enjoys writing code, exploring techniques, and learning new principles to write simpler and efficient code. His other interests include fencing, playing chess, baking, and keeping himself fit.

IJHSR
ijhighschoolresearch.org
REVIEW ARTICLE

Alzheimer's Disease and Musical Training: A Low-Cost Therapeutic?

Tiffany J. Ho

Cupertino High School, 10100 Finch Ave, Cupertino, CA, 95014, USA; tiffany.ho.cali@gmail.com

ABSTRACT: Alzheimer's disease (AD) affects over 50 million people worldwide and is the most prevalent neurodegenerative disease in the world. The CDC reported that in 2014, 5 million people were living with AD in the United States. This number has been projected to rise to 14 million by 2050. AD is one of the top 10 leading causes of death in the United States; therefore, finding treatments and cures for these patients is crucial. Musical training has been observed to induce positive effects on brain development and plasticity, especially in regions of the medial temporal lobe. Providing a strong therapeutic approach in the improvement and restoration of neuroplasticity in the hippocampus, musical training holds the potential to alleviate neurological conditions in which the hippocampus is damaged, such as AD. Here the potential of musical training as a low-cost medium with no known negative side effects by which patients may alleviate neurodegenerative symptoms is reviewed.

KEYWORDS: Behavioral and Social Sciences; Neuroscience; Alzheimer's Disease; Therapeutic; Musical Training.

Introduction

Alzheimer's disease (AD), the most prevalent neurodegenerative disease and the most common form of dementia in the world, primarily affects adults over the age of 65. While the main risk factor of AD is age, other factors such as cardiovascular disease and genetics have been found to play significant roles in the pathogenesis of AD. Studies have also shown that AD is most notably associated with the formation of amyloid plaques, neurofibrillary tangles of tau protein, and hippocampal synapse loss.[1] While different neurodegenerative diseases negatively impact different regions of the brain and, therefore, different cognitive functions, AD has shown the most prominent neuron loss in CA1 of the hippocampus.[2] Other widely observed psychological symptoms of AD include depression, irritability, confusion, and paranoia. Nevertheless, the most common symptom of AD is memory loss. If damage to the hippocampus can be delayed or even restored, patients with AD may observe improved memory functions and reduced symptoms. Through neuronal networks connecting the auditory cortex and the hippocampus, musical training offers a potential medium by which hippocampal plasticity can be improved.

Through the stimulation of interconnected regions across the brain, music can alter brain function, generating a range of outcomes including lowered stress[3] and feelings of excitement due to emotional arousal.[4] Numerous networks work collaboratively to process and respond to musical inputs. These intricate connections allow for music's powerful effect on memory, learning, and emotion.[5] Music first enters the brain through the ear in the form of sound waves.[6] These sound waves hit the tympanic membrane, commonly known as the eardrum, causing a vibration that is transferred through the oval window and into the cochlea, a spiral-shaped cavity in the inner ear that resembles a snail shell. Higher frequencies with shorter wavelengths are responded to earlier compared to lower and longer wavelength frequencies, which are responded to farther along the cochlea. As vibrations pass through the cochlea, circular bundles of stereocilia–tiny hairs found on the inner surface of the cochlea–sway, allowing stimulatory neurotransmitters to flow from the Organ of Corti to the brainstem via the vestibulocochlear nerve. From the brainstem, signals are passed to the thalamus and on to the primary auditory cortex of the inner temporal lobe via neurons of the medial geniculate nucleus. Finally, at the auditory cortex, information is processed and sent to other brain regions for the formation of a response. The flow of this information to the hippocampus allows for the formation of auditory and musical memories.

The hippocampus is found in the medial temporal lobe of both hemispheres of the brain. Resembling the shape of a seahorse, the hippocampus consists of subregions including the cornu ammonis (CA), the dentate gyrus (DG), and the subiculum. The CA, shaped like rams' horns, can be further divided into four subregions called CA1, CA2, CA3, and CA4, each playing a distinct role in the brain's limbic system. Often recognized as a gateway and a relay station within the medial temporal lobe system, the entorhinal cortex (EC) has been found to convey highly processed sensory inputs from the neocortex into the hippocampus.[7,8] It has also been shown that in the anterior temporal neocortex, a pathway involved in auditory object processing computes similarities and variations among the acoustic features of different instruments and objects.[9] Through this pathway, auditory information is processed and sent to the hippocampus for long-term memory formation. Although the connectivity between the auditory cortex and the hippocampus is not yet fully understood, studies have suggested that the auditory cortex projects directly into the parahippocampal cortex, which is known to project into the posterior hippocampus.[10] Neuronal connections between the auditory cortex and the hippocampus act as vehicles by which

DOI: 10.36838/v4i1.8

music and musical training can directly influence hippocampal function.

The hippocampus is involved in two main circuits: the trisynaptic circuit and the monosynaptic circuit. These circuits both allow information to flow from the EC to the hippocampus; however, the information that is passed differs. In the trisynaptic circuit, information is first passed from the EC to the DG via the perforant path. The signals then flow from the DG to CA3 via the mossy fiber pathway, and are finally transported from CA3 to CA1 along Schaffer collaterals. The monosynaptic circuit, on the other hand, transports information directly from the EC to CA1, providing a bypass circuit. In a 2015 study, Basu and Siegelbaum found that there is a 15-20 millisecond delay between the transmission of information through the trisynaptic circuit and the monosynaptic circuit.[11] Studies have also shown that CA1 integrates spatial and nonspatial sensory information in the trisynaptic circuit, suggesting that CA1 compares spatial sensory information and stored mnemonic information. This mechanical design allows for the integration of inputs that contribute to the encoding of episodic memory–the memory of experiences and past events.

Damage to or degeneration of the hippocampus can result in the inability to form new declarative memories. A widely known case of this defect was that of H.M., or Henry Molaison, who suffered epileptic seizures of the temporal lobe. An example of this is the case of the widely known patient H.M. or Henry Molaison, who suffered epileptic seizures of the temporal lobe. To treat his epilepsy and the induced seizures, Molaison had most of his hippocampus as well as surrounding parts of his temporal lobe removed in bilateral temporal lobe resection. As a result of this surgical procedure, Molaison lost the ability to form new episodic memories. Patients similar to Molaison were all severely impaired in the ability to form long-term memories, though most other cognitive functions, including short-term memory, seemed to be fully intact.[12] This condition, known as anterograde amnesia, has been observed in AD, traumatic brain injury, and several other neurological conditions. From these case studies, scientists have found that AD severely impacts both long-term and short-term memory through hippocampal deterioration.

Due to the intricate connections between the auditory cortex and the hippocampus, musical training has the capacity to influence the hippocampus. The hippocampus receives signals from the auditory cortex to form memories of timbres and pitch patterns, which allow most, regardless of musical experience, to recall songs and musical pieces they have heard before. When an auditory input is received and processed by the auditory cortex, its pitch, timbre, and duration are sent to the hippocampus where a memory of the sound is formed. Then, through the monosynaptic and trisynaptic circuits of the hippocampus, synaptic plasticity converts commonly heard sounds, such as voices and musical instruments, into long-term memory.[2] The flow of information through these pathways allow for the activation of other structures in the brain such as the nucleus accumbens and amygdala, which are strongly associated with retrospection and emotional responses.[13] Since AD most prominently affects CA1 of the hippocampus,[14] musical training holds potential as a therapeutic by which hippocampal damage can be improved.

Discussion

Hippocampal defects can severely affect one's cognitive abilities and quality of life. Due to hippocampal neuron loss in neurodegenerative diseases such as AD, neurogenesis–the growth and development of new neurons in the brain–poses a potential solution. Neuropeptides including nerve growth factor (NGF) and brain-derived neurotrophic factor (BDNF) have been shown to facilitate neurogenesis, but this occurs at a rate much slower than that of hippocampal volume loss in moderate to severe AD.[15] This poses a significant obstacle in the treatment of neurological conditions similar to AD. If hippocampal plasticity can be improved, patients suffering hippocampal damage may lead improved lives. Therefore, further research on the mechanisms of hippocampal repair is vital to the development of more effective treatments for AD.

AD significantly affects memory, thinking, and other cognitive functions. Due to hippocampal atrophy, Alzheimer's patients often suffer memory loss and the inability to maintain new memories for long periods of time. In recent years, researchers have explored the effects of music on memory formation and retrieval, both of which are negatively impacted in AD. In 2010, Simmons-Stern and colleagues compared levels of memory encoding and recognition in Alzheimer's patients when presented with sung lyrics versus spoken lyrics.[16] The research found that patients with AD observed a higher accuracy of lyric recognition when presented with sung lyrics compared to spoken lyrics. This supports that musical mnemonics–musical patterns used to aid in memorization–have the ability to help patients with AD learn new information. In addition, studies have investigated the connections between musical training and working memory (WM). Defined as short-term memory in which a limited amount of information is held in the brain for a short period of time, WM is crucial for the appreciation of musical experiences, as it allows for predictions of upcoming events. Differences between one's predictions and what is actually heard give music its ability to evoke memories and emotional responses. Scientists have discovered that musicians possess an enhanced ability to retrieve and process information using WM over non-musicians,[17,18] suggesting that long-term exposure to musical training increases the plasticity of neuronal networks encoding auditory memory. From these studies, it is inferred that music offers a potential medium by which patients with AD may improve memory functions.

Diminished ability to form and retrieve memories in Alzheimer's patients is a direct result of grey matter volume loss in the hippocampus. In a 2014 study, musical training was found to increase the grey matter volumes of several brain areas in musicians. Groussard and colleagues observed that changes gradually appear in the hippocampus and several other regions of the temporal lobe and motor cortex during musical training.[19] While neuroplasticity occurred in the left hippocampus and the right middle and superior frontal cortices shortly after engaging in musical training,

modifications in the left posterior cingulate cortex, the superior temporal areas, the right supplementary motor area, and the insular cortex required several years of consistent training. Since all participants in the study were of the same age and education level, the observed results support that musical training induces structural changes in the brain, particularly the hippocampus. Further research is needed to establish how distinct brain regions and neural circuits are affected by musical training and whether Alzheimer's-induced atrophy to the brain may be reduced or improved by musical training.

Potential of Musical Training as a Therapeutic for Alzheimer's Disease:

Due to the observed ability of musical training to enhance memory and improve plasticity in certain brain regions, researchers have begun exploring the effects of musical training on AD. In a 2015 study, vocal training was evaluated for its effects on patients with mild to moderate AD. Patients in the experimental group attended 1-hour training sessions once a week for 6 months and were required to practice singing at least 3 times a week at home. From their research, Satoh and colleagues found that patients in the experimental group experienced improvements in psychomotor speed and decreases in symptoms of dementia after the 6-month vocal training program.[20] In addition, a 2017 literature review supported that improved attention, memory, and executive functions were increasingly observed in AD patients after music therapy.[21] Collectively, research suggests that musical training is associated with increased plasticity in motor and executive regions of the brain as well as decreased symptoms of dementia.

Previous studies concerning the effect of music on AD and related diseases have involved music listening and music therapy; however, the effects and efficacy of instrumental and vocal training have yet to be fully explored. With evidence that musical training improves hippocampal plasticity and other cognitive functions impaired in AD, we propose to formally employ vocal and instrumental music training as a treatment option for improving Alzheimer's-induced hippocampal degeneration. Musical training using different instruments and training programs offers an unexplored research direction that may unlock new methods for alleviating symptoms of AD and other neurological disorders, producing a far-reaching impact on the millions of people living with AD.

Conclusions

Studies show that musical training can improve hippocampal plasticity and increase grey matter volume in the hippocampus, presenting a potential treatment for Alzheimer's-induced hippocampal neuron loss. These improvements, resulting in refined WM, highlight the potential for therapeutic applications in neurological conditions that damage the hippocampus. Patients suffering from AD are a prime candidate for this therapeutic option, as they often observe impairments in both memory and hippocampal function. Studies have shown musical training to alleviate AD symptoms; however, the mechanisms underlying these benefits remain to be fully elucidated. Musical training sits poised as a potential therapeutic in the treatment of AD and associated neurodegenerative diseases.

Acknowledgements

I would like to thank Mr. Stephen Weber for his guidance and support in the preparation of this paper.

References

1. Scheff, S. W.; Price, D. A.; Schmitt, F. A.; Mufson, E. J. Hippocampal synaptic loss in early Alzheimer's disease and mild cognitive impairment. https://doi.org/10.1016/j.neurobiolaging.2005.09.012 (accessed Jul 1, 2021).
2. Levitin, D. J. This is your brain on music; Plume Books: New York, New York, 2007.
3. Linnemann, A.; Ditzen, B.; Strahler, J.; Doerr, J. M.; Nater, U. M. Music listening as a means of stress reduction in daily life. https://doi.org/10.1016/j.psyneuen.2015.06.008 (accessed Jul 1, 2021).
4. Salimpoor, V. N.; Benovoy, M.; Longo, G.; Cooperstock, J. R.; Zatorre, R. J. The Rewarding Aspects of Music Listening Are Related to Degree of Emotional Arousal. https://doi.org/10.1371/journal.pone.0007487 (accessed Jul 1, 2021).
5. Lehmann, J. A. M.; Seufert, T. The Influence of Background Music on Learning in the Light of Different Theoretical Perspectives and the Role of Working Memory Capacity. https://doi.org/10.3389/fpsyg.2017.01902 (accessed Jul 1, 2021).
6. Peterson, D. C. Neuroanatomy, Auditory Pathway. https://www.ncbi.nlm.nih.gov/books/NBK532311/ (accessed Jul 1, 2021).
7. Canto, C. B.; Wouterlood, F. G.; Witter, M. P. What Does the Anatomical Organization of the Entorhinal Cortex Tell Us? https://doi.org/10.1155/2008/381243 (accessed Jul 1, 2021).
8. Schultz, H.; Sommer, T.; Peters, J. The Role of the Human Entorhinal Cortex in a Representational Account of Memory. https://doi.org/10.3389/fnhum.2015.00628 (accessed Jul 1, 2021).
9. Zatorre, R. J.; Bouffard, M.; Belin, P. Sensitivity to Auditory Object Features in Human Temporal Neocortex. https://doi.org/10.1523/JNEUROSCI.5458-03.2004 (accessed Jul 1, 2021).
10. Kumar, S.; Joseph, S.; Gander, P. E.; Barascud, N.; Halpern, A. R.; Griffiths, T. D. A Brain System for Auditory Working Memory. https://doi.org/10.1523/JNEUROSCI.4341-14.2016 (accessed Jul 1, 2021).
11. Basu, J.; Siegelbaum, S. A. The Corticohippocampal Circuit, Synaptic Plasticity, and Memory. https://doi.org/10.1101/cshperspect.a021733 (accessed Jul 1, 2021).
12. Rubin, R. D.; Schwarb, H.; Lucas, H. D.; Dulas, M. R.; Cohen, N. J. Dynamic Hippocampal and Prefrontal Contributions to Memory Processes and Representations Blur the Boundaries of Traditional Cognitive Domains. https://doi.org/10.3390brainsci7070082 (accessed Jul 1, 2021).
13. Cheung, V. K. M.; Harrison, P. M. C.; Meyer, L.; Pearce, M. T.; Haynes, J.-D.; Koelsch, S. Uncertainty and Surprise Jointly Predict Musical Pleasure and Amygdala, Hippocampus, and Auditory Cortex Activity. https://doi.org/10.1016/j.cub.2019.09.067 (accessed Jul 1, 2021).
14. Kril, J. J.; Hodges, J.; Halliday, G. Relationship between hippocampal volume and CA1 neuron loss in brains of humans with and without Alzheimer's disease. https://doi.org/10.1016/j.neulet.2004.02.001 (accessed Jul 1, 2021).
15. Peng, L.; Bonaguidi, M. A. Function and Dysfunction of Adult Hippocampal Neurogenesis in Regeneration and Disease. https://doi.org/10.1016/j.ajpath.2017.09.004 (accessed Jul 1, 2021).
16. Simmons-Stern, N. R.; Budson, A. E.; Ally, B. A. Music as a memory enhancer in patients with Alzheimer's disease. https://doi.org/10.1016/j.neuropsychologia.2010.04.033 (accessed Jul 1, 2021).

DOI: 10.36838/v4i1.8

17.Burunat, I.; Alluri, V.; Toiviainen, P.; Numminen, J.; Brattico, E. Dynamics of brain activity underlying working memory for music in a naturalistic condition. https://doi.org/10.1016/j.cortex.2014.04.012 (accessed Jul 1, 2021).
18.George, E. M.; Coch, D. Music training and working memory: An ERP study. https://doi.org/10.1016/j.neuropsychologia.2011.02.001 (accessed Jul 1, 2021).
19.Groussard, M.; Viader, F.; Landeau, B.; Desgranges, B.; Eustache, F.; Platel, H. The effects of musical practice on structural plasticity: The dynamics of grey matter changes. https://doi.org/10.1016/j.bandc.2014.06.013 (accessed Jul 1, 2021).
20.Satoh, M.; Yuba, T.; Tabei, K.-ichi; Okubo, Y.; Kida, H.; Sakuma, H.; Tomimoto, H. Music Therapy Using Singing Training Improves Psychomotor Speed in Patients with Alzheimer's Disease: A Neuropsychological and fMRI Study. https://doi.org/10.1159/000436960 (accessed Jul 1, 2021).
21.Fang, R.; Ye, S.; Huangfu, J.; Calimag, D.P. Music therapy is a potential intervention for cognition of Alzheimer's Disease: a mini-review. https://doi.org/10.1186/s40035-017-0073-9 (accessed Jul 1, 2021).

Author

Tiffany Ho is a senior at Cupertino High School in Cupertino, California. She holds a deep passion for neuroscience and hopes to one day make a difference in the scientific community by conducting neurodegenerative disease research. She aims to pursue a career in clinical neuroscience.

IJHSR
ijhighschoolresearch.org
■ RESEARCH ARTICLE

Therapeutic Effect of Changing Working Environment on Musculoskeletal Disease

Hyunje Lee

Seoul International School, 15 Seongnam-daero, 1518 beon-gil, Sujeong-gu, Seongnam-si, Gyeonggi-do, 13113, South Korea; 1101brian.lee@gmail.com

ABSTRACT: Laborers required to do repetitive manual work are often diagnosed with musculoskeletal diseases and are advised by doctors to change their working environments. However, laborer patients tend to rely more heavily on medicines for immediate pain relief than changing their working environment due to job requirements, habits, short-term approach to alleviation, or lack of awareness. The therapeutic efficacy of changing working environments seems to be high, but to date, there has been no empirical or statistical study to support and prove this point. This paper seeks to quantify the pain relief and symptom alleviation achieved by the change in working environment of physical laborers, independent of medication. During the course of patients' treatments, the degree of change in working conditions and the degree of pain were recorded, and a correlation analysis was conducted to examine the relation between the two variables. Results show that improvements on patients' working conditions lead to a statistically significant degree of pain and symptom alleviation (R^2 value of 0.511 when $p<0.01$). This verifies empirically that the patients who changed their working conditions more actively had greater pain relief. Implications of the results and suggestions for further study are discussed.

KEYWORDS: Translational Medical Sciences; Disease Prevention; Musculoskeletal disease; Occupational medicine; Working environment.

■ Introduction

The musculoskeletal diseases that laborers tend to have are studied in the field of occupational medicine.[1] Occupational medicine aims to improve the health of people working in industrial fields and prevent diseases among them,[2] whether that be occupational diseases or non-occupational diseases. As society became increasingly competitive after industrialization, there was a rapid spread of occupational diseases such as pneumoconiosis in coal mines, which became a big problem and instilled in people an awareness of occupational diseases.[3]

In the past, occupational diseases revolved around chemical addiction and cancer caused by carcinogenic environments. However, as the awareness of musculoskeletal diseases widened, people not only started to care about harmful environmental factors in workplaces, but also personal disposition and daily activity habits of workers that the workplace builds.[4]

Musculoskeletal disorders refer to physical disorders caused by factors such as repetitive movements, use of excessive force, mechanical stress, static or improper posture, local vibrations, and body contact with sharp surfaces. They usually occur in muscles and ligaments of the neck, shoulder, waist, and upper and lower limbs. The high-risk occupational groups include computer users, packaging workers, polishers and craftsmen, sheet metal workers, parts assemblers, auto mechanics, and manual workers. Patients who visit the hospital for musculoskeletal disorders are usually at a stage in which the pain recurs even after several days and weeks, and causes difficulty in performing their work. Common types of musculoskeletal disorders include lateral epicondylitis of elbow, chronic shoulder and lumbar, cervical sprain, shoulder rotator cuff disease, myofascial pain syndrome, and chronic ankle sprain.[5]

Since the main cause of Work-related Musculoskeletal Diseases (WMSD) is the patients' working environment, patients are often prescribed actions to adjust their working environment as well as to take medication. However, the majority of patients are either unaware of the necessity of adjusting their working environment or unable to make those adjustments due to the nature of their occupation.[6] Moreover, there are numerous patients who believe that taking medication would be better than making fundamental changes in their working environments to relieve their pain.

Previous studies and guidelines have issued multiple potential causative factors and preventive measures of WMSDs. This includes their relationship to adjusting working conditions; however, it is not easy to find studies that have reviewed the specific influence of change in working conditions in regard to the therapeutic effect in WMSDs. The aim of this study, therefore, was to empirically understand how improvement of the working environment affects pain relief in musculoskeletal disorders. This study is not an invasive experiment, but an observational study that analyzes the statistical correlation of pain relief and the degree of change in working environment during the treatment process of musculoskeletal disorders.

■ Literature Review

Work-related Musculoskeletal diseases (WMSDs) are defined as an illness that results from physical risk factors such as repetitive action, biomechanical overload, and inappropriate working postures in the course of occupational activities.[7] Their

DOI: 10.36838/v4i1.9

symptoms often comprise pain, stiffness, loss of strength, and neuromuscular control in body parts like neck, shoulder, spine, as well as upper and lower extremities.[8]

There are three main causative characteristics of WMSDs. The first causative characteristic is repetitiveness and use of excessive force.[7,9] Strong muscle contraction and repetitive motion causes injuries in both muscular and tendinous tissues as well as inflammation. Examples of WMSDs associated with these characteristics include Carpal Tunnel Syndrome, Rotator Cuff Tendinitis, and Trigger Finger. Another characteristic is posture and physical stress. Inappropriate posture and physical stress during occupational activities cause the build-up of intramuscular pressure and ultimately trigger chronic pain in certain regions.[7,9] Examples of WMSDs caused by this characteristic include Visual Display Terminals (VDT) syndrome and chronic neck sprain. The last causative characteristic is psychological stress, which plays a significant role in certain WMSDs in developing into chronic pain.[10] The ultimate goal of the WMSD treatments is to relieve the associated symptoms and to enable the workers to return to work under good health conditions. Those treatments include symptom relief with the use of an anti-inflammatory medicine, resting, use of ice or heating pad, and continuous joint exercise.[11] The prognosis of WMSDs is good in the initial stage with conservative treatment, but those symptoms are highly likely to develop into a chronic disease due to the difficulty in changing the working environments. Thus, consistent monitoring and care are necessary for the good prognosis of the patients.[12]

The Center for Disease Control and Prevention in the US has investigated the preventive measures for each cause of WMSDs. In the case of having to complete a series of repetitive motions, patients should make use of mechanical assist devices, or find a less stressful position that requires an alternative form of motion. Secondly, in the case of performing strength-requiring work, patients should use mechanical devices that reduce the physical stress.[13] For example, using a drilling machine instead of a punch grip device to complete work. Third, in the case of inappropriate working stature, patients should avoid extreme range of motion of certain body parts and adjust the working facilities to alleviate musculoskeletal stress. For example, a person who holds a job that demands precise use of fingers should provide support on his or her forearm to reduce stress that is applied on his or her arm and elbow muscles.[14] For patients with lower back pain, lifting an object should be done by bending their knees instead of bending their spine.

Previous studies have addressed the multiple causative factors and preventive measures of WMSDs including their relationship to adjusting working conditions as described above. However, it is hard to find a study about how the change in working conditions is statistically connected with the pain relief of WMSD patients. If there is no statistically significant difference in pain relief between the group with an improved working environment and the group without a change in working environment, factors that have a greater impact on treatment than a changed working environment can be prioritized more in treatment. For example, it could be the case that the more important consideration is how early the medication is administered, or the strength of the medication. On the other hand, if there is a statistically more significant correlation between the degree of working condition change and pain scale, then the empirical data could be presented to patients who want to rely solely on medication to urge the willingness to improve their working environment.

Methods

Subject:

Data collection for this study was conducted at Central Hospital located in Siheung, Gyeonggi province, South Korea, from December 2020 to April 2021, based on doctors' cooperation and patients' consent to participate in this research. The study population comprised patients who visited the Orthopedic Outpatient Department of the Central Hospital that had exhibited the following WMSDs; medial and lateral epicondylitis of the elbow (tennis elbow), shoulder joint rotator cuff tendinitis, Visual Display Terminals (VDT) syndrome, chronic wrist sprain, chronic back sprain (lumbar disc herniation), and Carpal tunnel syndrome (CTS). The WMSDs investigated in this study are:

- Medial/Lateral Epicondylitis of elbow: swelling of the tendons that bend your wrist backward away from your palm, commonly known as tennis elbow[15]
- Shoulder joint rotator cuff tendinitis: pain and swelling of the cuff tendons and the surrounding bursa caused by repetitive overload in the shoulder[16]
- Visual Display Terminals (VDT) syndrome or chronic neck sprain: pain in neck and shoulders associated with shoulder-arm-neck syndrome, fatigued eyes and foreign sensation, skin conditions and neuropsychiatric problems and other musculoskeletal symptoms[17]
- Chronic wrist sprain: repeated injury to the ligaments of the wrist commonly caused by repetitive overuse of the wrist[18]
- Lumbar Disc Herniation: problem with one of the rubbery cushions (disks) that sit between the individual bones (vertebrae) that stack to form the spine[19]
- Carpal tunnel syndrome: pain in the wrist that occurs when the median nerve is compressed as it passes through the carpal tunnel[20]

Procedure (Data Collection):

All patients who visited the orthopedic outpatient department were educated on ways to adjust their occupational conditions and received medication treatment and physiotherapy as per usual. Analgesics were prescribed as medication to all patients, but they were guided to take it only when in severe pain and not regularly. Since analgesics are a temporary pain killer, they do not cure the root cause of the disease. The patients who agreed to participate in this study were followed up every week for the successive 6 weeks for data collection. Any patient who did not visit the hospital regularly was followed up by a phone call. All information was collected with the consent of each patient after IRB (Institutional Review Board) approval.

The data collected in this research included age, sex, occupation, contact, diseases, symptom, degree of pain which

was measured in Numeric Pain Scale(NPS), and degree of working condition change in a scale of 1~3 in which "1" indicates barely changed and "3" indicates actively changed. The patient's pain scale was measured in a scale of 0 to 10, in which 10 is the most painful and 0 is not painful at all, and the degree of pain was recorded starting from the first day of the visit. Every week afterward, the patients were asked about their pain scale in-person, through phone calls, or via text messages, and the degree of change in their pain was recorded for six weeks. Figure 1 is the Numeric Pain Scale used in this study, and Figure 2 is an example of a text message sent to patients in this study.

Figure 1: Numeric Pain Scale used in this study.

Dear OOO,

Hello, this is the research team for pain relief of musculoskeletal disorders at Dept. of Orthopedic Surgery, Central Hospital. To examine your pain, we are investigating the degree of your symptoms. Please text the answers to the following 3 questions.

A. Please enter your pain level in the numeric pain scale from 0 (not at all painful) to 10 (very painful).

In the doctor's office, the doctor initially asked what level your pain was, for example, if your pain level was 8 at that time, and if your symptoms have improved compared to the day you met the doctor, your answer would be a number lower than 8.

B. Have you changed your working conditions according to the doctor's recommendation?

The doctor has told you that if one elbow hurts you should try using the other elbow more or use a heating pad, massage cream, or compression band. The question is whether you changed your conditions as you were told by the doctor.

(1) I could not change it almost at all
(2) I changed it to some extent
(3) I changed a lot

We wish for the best of the health of our patients, and if you have any questions, please contact Hyunje Lee (010-xxxx-xxxx) or Dr. Homin Lee (031-xxxx-xxxx) of the research team for musculoskeletal diseases at the Central Hospital. Thank you for your sincere reply.

Figure 2: Text message to monitor patients' working condition change and NPS.

Analysis Methodology:

1. Main data collection was the NPS and the change in working conditions for each patient in the span of six weeks, in addition to their symptoms.

2. For the NPS, the difference between week one and week six was used for analysis as NPS indicates the degree of pain relief of a patient. The patient who had his or her pain relieved the most in the six weeks the study took place would have a relatively greater NPS than other patients.

3. The data for change in working condition, where the patients rated their own changes in working conditions from 1 (barely changed) to 3 (actively changed), was used in the analysis by calculating the average of the numerical data over the six weeks. The calculated average value indicates how active the patient was in changing their working conditions.

4. The correlation of NPS vs Average Working Condition Change was graphed as a scatterplot of 52 data points. The derived line of best fit of the scatterplot was used to calculate the p-value to determine the statistical significance of the data.

5. Data were collected from December 2020 and took place for the following five months until six weeks' length of data for all of the participants was recorded.

Results and Discussion

Data from a total of 62 patients including 46 males and 16 females were collected initially. During the six-weeks span, 10 patients whose follow-up data were not sufficiently collected were excluded from the study; hence 52 patients were subjects in the final study. Average age of the patients was 46 years old. Occupations of the patients were mainly laborers such as factory workers, cooks, and computer workers, who are required to complete repetitive manual work. Types of musculoskeletal disease included 50% of the patients with elbow lesion (lateral epicondylitis of elbow in 26 patients), 17% with shoulder lesion (rotator cuff disease in 3 patients, chronic shoulder sprain in 6 patients), 15% with foot and ankle lesion (plantar fasciitis in 3 patients, chronic ankle sprain in 5 patients), 10% with wrist and hand lesion (chronic wrist sprain in 4 patients, trigger finger in 1 patient), 6% with lumbar lesion (Herniated intervertebral disc in 3 patients), and 4% with cervical lesion (Visual Display Terminal syndrome in 1 patient, chronic neck sprain 1 patient). Data collected from the 52 patients are shown in Table 1. Data include their sex, age, occupation, disease, as well as their Numeric Pain Scale, which is the pain difference between week one and week six, and the Average Working Condition Change ranging from 1(barely changed) to 3 (actively changed) (Table 1).

Table 1: Collected Data.

No	Sex	Age	Occupation	Diesease	Delta NPS	AVG WC
1	M	35	factory worker	Lateral epicondylitis	2	2.17
2	M	36	factory worker	Lateral epicondylitis	4	2.50
3	F	37	factory worker	Lateral epicondylitis	3	2.17
4	M	38	welder	Lateral epicondylitis	4	2.33
5	M	42	fisherman	Lateral epicondylitis	5	2.50
6	F	42	factory worker	Lateral epicondylitis	3	2.20
7	M	50	factory worker	Lateral epicondylitis	4	2.33
8	M	43	chef	Carpal tunnel syndrome	5	2.33
9	M	40	Production manager	Lateral epicondylitis	4	2.50
10	F	57	factory worke	Lateral epicondylitis	5	2.67
11	M	42	factory worker	Lumbar HIVD	5	2.50
12	F	60	housewife	Lateral epicondylitis	4	2.50
13	M	38	factory worker	Lateral epicondylitis	4	2.33
14	M	26	machine transporter	Chronic shoulder sprain	3	2.33

DOI: 10.36838/v4i1.9

15	M	44	factory worker	Lateral epicondylitis	4	2.67
16	M	42	factory worker	Lateral epicondylitis	5	2.17
17	M	58	cycling	Rotator cuff disease	3	2.25
18	M	55	factory worker	Chronic wrist sprain	3	2.50
19	M	47	gas station	Lateral epicondylitis	0	1.17
20	M	46	factory worker	Lateral epicondylitis	2	2.50
21	M	54	factory worker	Lateral epicondylitis	1	1.50
22	M	26	carpenter	Chronic shoulder sprain	3	2.00
23	F	49	computer worker	Chronic shoulder sprain	1	1.75
24	F	48	computer worker	Chronic neck sprain	2	1.50
25	F	46	computer worker	Chronic back sprain	5	2.17
26	M	49	factory worker	Chronic ankle sprain	5	2.17
27	F	42	factory worker	Rotator cuff disease	1	1.67
28	F	53	factory worker	Rotator cuff disease	2	2.00
29	M	23	engineer	Ankle sprain	5	2.33
30	M	58	factory worker	Plantar fasciitis	3	2.33
31	M	41	delivery service	Chronic shoulder sprain	2	2.00
32	F	53	athlete	Chronic shoulder sprain	6	2.00
33	M	26	computer worker	Chronic knee sprain	3	2.00
34	M	52	factory worker	Chronic wrist sprain	2	2.00
35	M	38	factory worker	Chronic wrist sprain	1	2.00
36	M	58	factory worker	Lateral epicondylitis	4	1.33
37	M	26	factory worker	Chronic shoulder sprain	5	2.50
38	M	57	factory worker	VDT, Cervical-HIVD	4	2.50
39	M	50	factory worker	Plantar fasciitis	4	2.50
40	M	64	factory worker	Lateral epicondylitis	3	1.83
41	M	37	factory worker	Lateral epicondylitis	3	2.00
42	F	41	factory worker	Plantar fasciitis	5	2.25
43	M	57	computer worker	Lateral epicondylitis	1	1.75
44	F	58	driver	Lumbar HIVD	3	2.25
45	M	36	fcomputer worker	Lumbar HIVD	2	1.67
46	M	50	factory worker	Trigger finger	1	1.75
47	M	61	animal breeding	Lateral epicondylitis	3	2.3
48	M	52	factory worker	Lateral epicondylitis	0	1.25
49	M	60	factory worker	Lateral epicondylitis	1	1.25
50	M	41	factory worker	Lateral epicondylitis	0	1.00
51	M	26	factory worker	Lateral epicondylitis	4	2.33
52	F	47	teacherr	Lateral epicondylitis	3	2.50

*** NPS: Numeric Pain Scale Difference between week one and week six given that 10 is the most painful and 0 is not painful at all**

**** AVG WC: Average change made in working conditions given that '1' is the least change and '3' is an active change.**

After having followed the data collection and analysis steps stated in the methodology, the result showed that this data set has a R2 value of 0.511 when the p-value is < 0.01, making the correlation of the dataset statistically significant. Figure 3 shows the scatterplot between the change in NPS and average working conditions. It shows that the patients who changed their working conditions more actively had greater pain relief.

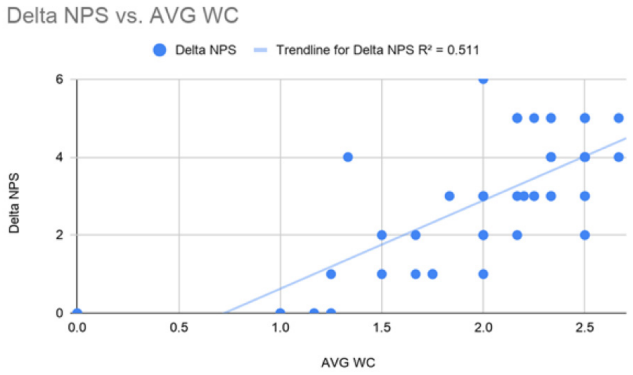

Figure 3: Scatterplot between Delta Numeric Pain Scale(NPS Difference between week one and week six given that 10 is the most painful and 0 is not painful at all) and Average working condition change. (Average change made in working conditions given that '1' is the least change and '3' is an active change.)

Conclusion

The study aimed to analyze how improved working conditions affect pain relief in people with musculoskeletal disorders caused by repetitive labor, biomechanical overload, and inappropriate working postures. Studies have shown that working condition change is significantly correlated with the

pain relief in musculoskeletal diseases, implying that the better the working environment, the more pronounced the pain relief, independent of medication intake. This study was significant in that it helped convince patients of the need to improve their working environment by providing clear empirical data to patients who tend to rely more on painkillers than improving their working environment.

In addition, it has been reconfirmed that the cause of pain in musculoskeletal diseases is a repetitive working environment, so it indicates a need for flexible working environment policies for workers. Even when the patients try to take the advice of improving their working environment, it is often difficult to do by themselves because the working environment is institutionally inflexible, or because of the patients' habits or lack of awareness. In order to reduce the incidence of musculoskeletal diseases among workers in industrial or working sites, the mechanical environment and the physical space for an individual worker needs to allow for different postures and patterns. This would ensure that working posture could be changed from time to time rather than continuously repeating a fixed motion. Decreasing repetition will eventually increase the working productivity, benefiting the employers as well as the workers. Hence, it is necessary to develop public health and labor policies in consideration of such universal benefits. Also, patients may be provided with a campaign or brochure-like announcements to individually learn about certain requirements of working environments for their health.

There are a few limitations to this study. First of all, the NPS and the 1, 2, 3 scale in which the patients rated the extent of change in working condition do not have a standardized or scientific method to distinguish the meticulous difference between "1" and "2". The numeric scales were employed to derive the extent of patients' perception into quantitative indicators. People who are sensitive to pain might rate a higher score in the NPS than those who are less sensitive.

The second limiting factor is that there could be a notable difference in the data between patients who physically visited the hospital more often and the patients who participated in the data collection mostly through mobile phone communication after their first visit to the hospital. The patients who physically visited the hospital more often may generally have had greater decrease in the NPS as time passed, perhaps because they would have been more proactive in curing the disease.

Another limitation is that there were multiple patients during the study who failed to consistently follow up with the data collection due to their personal schedule, government safety protocols due to the pandemic, and financial difficulties caused by COVID-19. These data were excluded from the analysis, reducing the number of subjects in the study.

Lastly, in this study, painkillers were prescribed in addition to changing working conditions, to allow patients to take them intermittently if not regularly. Painkillers may have contributed to the natural healing of the disease over time by temporary pain relief, even without fundamental treatment or a change in working condition.

More sophisticated and concrete analysis by supplementing these limitations could be suggested for further studies. In the future, it would be interesting to study various reasons why patients cannot change their working conditions easily. If the pain decrease mechanism in each reason is investigated, more personalized treatment and consulting would be possible. In additon, it would be meaningful if the dose of medication was analyzed as a variable to measure the impact on pain decrease. Analysis between groups that only change their working environment without medication treatment and groups that take painkillers intermittently, or comparing patients' pain relief with working condition changes only among a group with the same number of visits to the hospital, would garner more insight into the degree of impact of changing working environment and provide more specific implications in further treating musculoskeletal disorder.

Acknowledgements

I would like to express my gratitude to my AP Chemistry teacher Dr. Rose Tyvand from Seoul International School and Dr. Homin Lee from Siheung Central Hospital for advising and supporting me with data collection and analysis in the study.

References

1. Magnavita, N.; Elovainio, M.; De Nardis, I.; Heponiemi, T.; Bergamaschi, A. Environmental Discomfort and Musculoskeletal Disorders. *Occup. Med. (Lond.)* 2011, 61 (3), 196–201.
2. Zenz, C. Occupational Medicine: Principles and Practical Applications. *Year Book Medical Publishers* 1989, 17 (1), 1273. https://doi.org/10.1177/140349488901700119.
3. Laney, A. S.; Weissman, D. N. Respiratory Diseases Caused by Coal Mine Dust. *J. Occup. Environ. Med.* 2014, 56 (Supplement 10), S18–S22.
4. Rom, W. N., & Markowitz, S. B. *Environmental and Occupational Medicine*; Lippincott Williams and Wilkins: Philadelphia, PA, 2007.
5. Hong, J. Y., & Koo, J. W. Medical Approach of Work-Related Musculoskeletal Diseases. *Journal of the Ergonomics Society of Korea* 2010, 29 (4), 473–478. https://doi.org/10.5143/JESK.2010.29.4.473.
6. Sell, L., Lund, H. L., Holtermann, A., & Søgaard, K. The Interactions between Pain, Pain-Related Fear of Movement and Productivity. *Occupational Medicine* 2014, 64 (5), 376–381. https://doi.org/10.1093/occmed/kqu056.
7. Punnett, L. & Wegman, D. Work-Related Musculoskeletal Disorders: The Epidemiologic Evidence and the Debate. *Journal of Electromyography and Kinesiology* 2003, 14, 13–23. https://doi.org/10.1016/j.jelekin.2003.09.015.
8. Visser, B.; van Dieën, J. H. Pathophysiology of Upper Extremity Muscle Disorders. *J. Electromyogr. Kinesiol.* 2006, 16 (1), 1–16.
9. McCauley-Bush, P. *Ergonomics: Foundational Principles, Applications, and Technologies*; CRC Press: London, England, 2011.
10. Hagberg M., Silverstein B., Wells R., Smith M., Hendrick H., Carayon, P., & Perusse, M. *Work Related Musculoskeletal Disorders (WMSDs): A Reference Book for Prevention*; Taylor & Francis: London, England, 1995.
11. Lavdaniti, M., Tsiligiri, M., Sarpetsa, S., Tousidou, E., & Chatzi, M. The Concept of "Care" as Perceived by Greek Nursing Students: A Focus Group Approach. *International Journal of Caring Sciences* 2013, 6 (3), 392–401.
12. Descatha, A., Roquelaure, Y., Chastang, J. F., Evanoff, B., Cyr, D., & Leclerc, A. Work, Prognosis Factor for Upper Extremity Musculoskeletal Disorders? *British Medical Journal* 2009, 66 (5),

DOI: 10.36838/v4i1.9

351–352. https://doi.org/10.1136/oem.2008.042630.
13. Silvia, C. E., Bloswick, D. S., Lillquist, D., Wallace, D., & Perkins, M. S. An Ergonomic Comparison between Mechanical and Manual Patient Transfer Techniques. *Work* 2002, 19 (1), 19–34.
14. Dennerlein, J. T., & Johnson, P. W. Different Computer Tasks Affect the Exposure of the Upper Extremity to Biomechanical Risk Factors. *Ergonomics* 2006, 49 (1), 45–61. https://doi.org/10.1080/00140130500321845
15. Vaquero-Picado, A.; Barco, R.; Antuña, S. A. Lateral Epicondylitis of the Elbow. *EFORT Open Rev*. 2016, 1 (11), 391–397.
16. Factor, D.; Dale, B. Current Concepts of Rotator Cuff Tendinopathy. *Int. J. Sports Phys. Ther*. 2014, 9 (2), 274–288.
17. Parihar, J. K. S.; Jain, V. K.; Chaturvedi, P.; Kaushik, J.; Jain, G.; Parihar, A. K. S. Computer and Visual Display Terminals (VDT) Vision Syndrome (CVDTS). *Med J. Armed Forces India* 2016, 72 (3), 270–276.
18. van Vugt, R. M.; Bijlsma, J. W.; van Vugt, A. C. Chronic Wrist Pain: Diagnosis and Management. Development and Use of a New Algorithm. *Ann. Rheum. Dis.* 1999, 58 (11), 665–674.
19. Amin, R. M.; Andrade, N. S.; Neuman, B. J. Lumbar Disc Herniation. *Curr. Rev. Musculoskelet. Med*. 2017, 10 (4), 507–516.
20. Genova, A.; Dix, O.; Saefan, A.; Thakur, M.; Hassan, A. Carpal Tunnel Syndrome: A Review of Literature. *Cureus* 2020, 12 (3), e7333

Author

Hyunje Lee is a senior at Seoul International School in Korea. His experience of volunteering at a public clinic for underinsured immigrant workers in Korea for 5 years led to his passion for understanding the intricacies of Public and Global Health, the field in which he intends to study in the future.

IJHSR
ijhighschoolresearch.org
RESEARCH ARTICLE

The Psychological Effects on IT Professionals During COVID-19 in the United States and Internationally

Dhanya Janga, Tanishka Aglave

John F. Kennedy Memorial High School, 200 Washington Ave, Iselin, NJ, 08830, U.S.A.; djanga040@gmail.com

ABSTRACT: The mental health of IT professionals in the corporate world has been an increasing concern during the lockdown of the Coronavirus pandemic. The current circumstances societies face have thrown this fragile demographic back into the spotlight. This study aims to conduct a timely assessment of the effects of the COVID-19 pandemic on the mental health of IT professionals within the United States and as well as the rest of the world. To help understand the impact of the pandemic on IT professionals' mental health and well-being, interviews with 64 IT employees were within the United States and 21 interviews with international IT employees were conducted. Quantitative and qualitative approaches were used to interpret the results.

KEYWORDS: COVID-19; pandemic; IT professionals; mental health.

Introduction

Business in the IT world is often hampered by mental health problems. Mental health disorders may affect IT professional's motivation, attention, and social experiences, all of which are critical in business in the IT world. According to the US Bureau of Labor Statistics, the year started with a bang for IT workers, with 25,300 tech workers added to U.S. payrolls in the first two months (BLS). However, by March, this figure had fallen to just 6,000 new IT workers, and by April, the BLS had recorded a staggering net loss of 181,300 tech jobs in the United States.[1] Joe Pinker's (2020) Atlantic post, "The Pandemic will cleave America in Two," highlights two contrasting pandemic perspectives.[2] One is an insight shared by those with advanced degrees who work in stable occupations that allow for telework. People's lives have become more complicated, their jobs have been turned upside down, childcare has been difficult, and leaving the house feels ominous. The other is an experience shared with the majority of the working population – those who are unable to work at home and therefore put themselves in danger every day, whose careers have been lost or downsized, and who are concerned not just about contracting the virus but also about having the opportunity and money to survive.[3] Internationally COVID-19 had many effects on the employee's mental health in the IT industry well. Many workers either lost their jobs or had their salaries reduced. The unemployment rate has risen in all global economies.[3] According to the International Monetary Fund (IMF), the number of workers out of jobs in the United States reached an all-time high of 8.9% last year, marking the end of a decade of employment growth. When sectors of the economy, such as tourism and hospitality, have come to a halt, millions of jobs have been put on government-sponsored job relation programs. In many countries, the amount of new career openings is still very limited. Job openings in Australia have returned to the same number as in 2019, but in France, Spain, the United Kingdom, and many other nations, they are still falling short. [5] This is affecting the mental health of people. No employment is equal to no money which clearly brings up a lot of problems.

Information technology is one of the biggest industries in the world with considerable employment. The IT industry plays a vital role in managing other businesses, exchanging information, and developing technology for everyday lives. Apart from this, many IT professionals have families of their own to tend to. The pandemic has posed many challenges adding additional stressors to many IT employees. The pandemic has caused mental health concerns to skyrocket, and this survey will focus on IT professionals' mental health to learn how one of the biggest job sectors worldwide had been influenced by the Covid-19 pandemic.

Methods

Study Design :

A semi-structured interview survey guide was created with the aim of quantitative and qualitatively measuring the mental health status of IT professionals. In addition, the interview was designed to learn about how IT professionals have dealt with the stress of the pandemic situation. The survey consisted of questions pertaining to IT professionals' daily habits, changes in their mental health, work ethics, screen time, how they dealt with the changes, and etc. The objective of this study is to assess the psychological changes that took place. The survey helped answer the essential question of this article: What are the psychological effects of COVID-19 on IT professionals' health in the US and internationally?

Results and Discussion

Data Collection :

In this study, the effects of COVID-19 on both the employees who work in the United States as well as the employees who work in other countries were examined. First, participants were asked to answer from which state or country they are from. Most of the IT professionals were from the state of New Jersey and in the international survey, most of the participants were from India. Secondly, IT professionals were asked what designations they have in their company. The participants

DOI: 10.36838/v4i1.10

in the international survey were developers, administrators, and project managers. Others were testers, network engineers, operation workers, and technical architects. Most of the participants in the US survey were project managers, developers, business analysts, administrators, or worked in the quality department. Other participants were testers, worked in the production department, network engineers, operations, maintenance, architects, program managers, SAP consultants, product managers, lead engineers, system analysts, and worked in the construction department. The third question asked participants whether working from home affects productivity. This situation is becoming popular in the United States as the number of people working from home increases. Companies have been motivated to give workers the possibility of working from home as a result of the need for flexible working conditions and technological advancements. Furthermore, due to the coronavirus pandemic, many businesses have moved to an entirely remote workforce. According to a United States census bureau survey, 5.2% of full-time employees in the United States worked from home in 2017, up 3.3% since 2000. To put that in context, there were 3.7 million people employed from home in 2000, up to 6.5 million today. In addition, the US Bureau of Labor Statistics estimated that 23.7% of Americans served from home for at least several hours in 2018. While studies to see how COVID-19 will impact these figures are underway, Global workplace analytics reports that 56% of the US population has a career that is at least partly consistent with remote jobs and that 25-30 percent of the workforce will be working from home for more than one day per week in the next two years.[6] In this survey, most of the participants in the US have responded with a positive reply for the productivity of working from home. In an international IT professionals survey, responses from IT professionals were positive as well. Few responded that it had negative effects. The survey's fourth question was "do participants feel better working at home than working at an office?" The international survey participants' reply to this question was yes as well as no. Most of the participants said they feel better working at home than working in an office as there is no time limit and they can take their time to do the daily routine. Some of them said no because of the many distractions at home which led them not to be able to focus on work. In the US survey, participants' responses to this question were similar to those in the international survey. Their reasons for why they enjoyed working from home better was that there was no commute time, more flexibility, and people felt more relaxed. The participants who replied "no" enjoyed working in an office, working with people, working together. According to Sarah Archer's survey, 90% of remote employees want to work from their homes for the remainder of their careers. 61% of workers have quit or considered quitting a workplace due to a lack of employment versatility. [4]

The fifth question of the survey related to some of the advantages of working from home. Respondents from the US survey replied that they have a flexible schedule, save money, zero commuting, no office distractions, it is easier to make calls, no need for formal clothes, more productivity, work, and

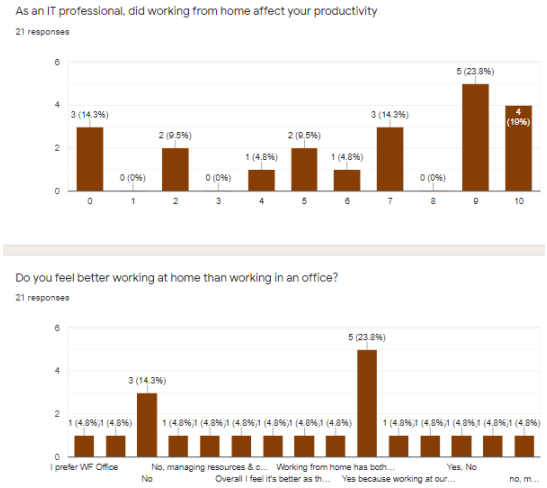

Figure 1: IT professionals were asked how working from home affected their productivity on a scale of 1-10 (1 being negatively and 10 resulting positively). Although responses varied, 70% of the employees reported an increased level of productivity.

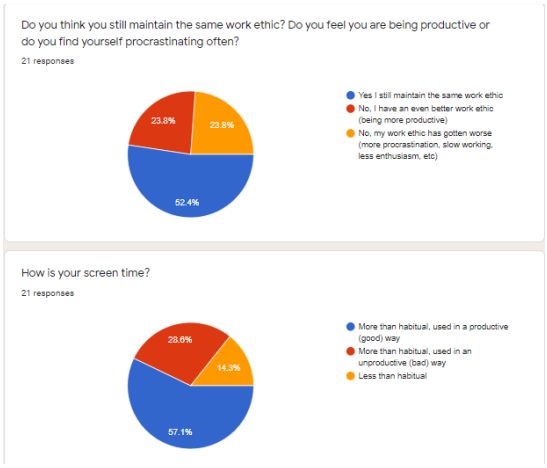

Figure 2: Participants were surveyed on their screen time as well as whether or not they maintained the same work ethic working from home. According to the graphs, more than 50% of IT professionals maintained the same work ethic prior to working from home and reported an increase in screen time.

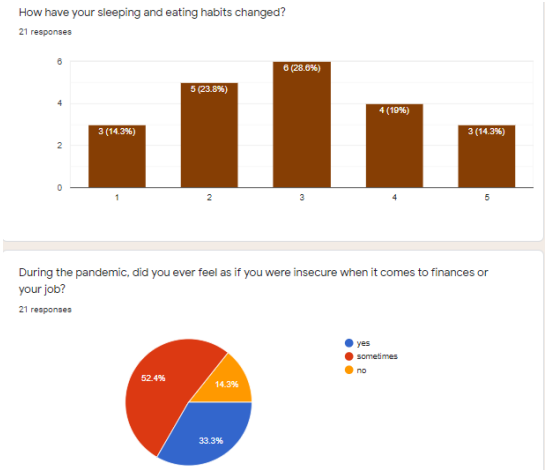

Figure 3: Candidates were also questioned about a change in eating/ sleeping habits as well as job insecurity. Since the majority of the respondents answered "3" on the scale it shows that their eating & sleeping habits haven't significantly changed. In regard to job security, 86% of the IT professionals responded that they do feel insecure to some extent about jobs or finances.

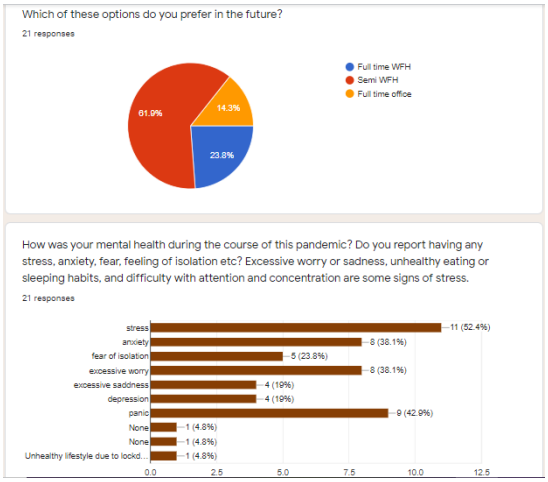

Figure 4: The graphs above show one of the most important aspects of this study: the mental health during the pandemic of IT professionals. They were also asked what work option they prefer for the future. More than half preferred semi-work from home for the future. Surrounding mental health concerns, workers reported increased levels of stress, anxiety, and excessive worries.

family balance, they get time to learn new things and less workload. Over 75% of the participants said they have a flexible schedule and 85.9% of the participants benefited from zero commuting. The next question asked was about the disadvantages of working from home. In the international survey, 57.1% of participants responded that there is difficulty or lack of communication, 42.9% of participants replied that there is difficulty in the working environment and motivational challenges, 38.1% of participants replied that there is difficulty in managing and maintaining accounts and loss of productivity. Some other disadvantages are ergonomic issues, and low reliability and retention. The disadvantages of working from home were a lack of community and differences in culture, difficulty or lack of communication, low reliability and retention, difficulty managing and maintaining accountability, issues with payment and logistics, loss of productivity, and security concerns.[7] As seen from the survey responses, the participants' difficulties were similar to the disadvantages mentioned in the article. In the US survey, the responses of participants were quite similar to what they are in the international survey. Some other disadvantages mentioned by the participants were more working hours, no lunch break, and technical issues. According to the next question on how participants managed time and workflow, most participants in the international survey responded that they prioritize their work and do proper planning. In the US survey, most of the participants responded as they take frequent breaks, scheduling, proper planning, maintain a routine, sticking to the regular office routine, possess a dedicated office room, and other replies were similar to the one mentioned above (Figures 1 and 4). The eighth question to the participants was "do you think you still maintain the same work ethic? Do you feel you are being productive, or do you find yourself procrastinating often?" More than fifty percent of the participants that is 79.7% responded that "yes, I still maintain the same work ethic", 12.5% responded that "no, I have even better work ethic" (being more productive), been worsened i.e., more procrastination, slow working, and less enthusiasm (Figures 1 and 2).

Conclusion

Working at home has been a challenge for many. Moreover, a global pandemic taking place is no way to lighten the load. "We are facing a health threat unlike any other in our lifetimes. Meanwhile, the virus is spreading, and day-to-day lives are being severely tested. Adapting to this new lifestyle can be difficult for some. This resulted in the mental health of IT professionals being challenged. This is a time for prudence, not panic".[8] Everyone has been affected differently by the COVID-19 pandemic. Whether that be adjusting to a new work-life situation, the loss of a job, or a loved one, the weight of these unprecedented times can be heavy, and significantly impact our mental health.[9] In terms of the data gathered, all results from the survey portray that there was indeed a negative effect of the pandemic on IT professionals' mental health. The dramatic changes encountered by all during the face of the pandemic, including changes in society and daily life, resulted in a severe mental health decline that included stress, anxiety, and even depression.

Acknowledgements

We would like to express our heartfelt gratitude to Dr. Balaji Aglave for constantly looking out for opportunities and platforms for us to present this project. We would also like to thank all the participants around the world who took part in this survey and made this research article possible.

References

1. U.S Bureau of Labor Statistics. Current employment statistics - CES (National). https://www.bls.gov/ces/ (accessed Aug 16, 2021).
2. Pinsker, J. The pandemic WILL CLEAVE America in two. https://www.theatlantic.com/family/archive/2020/04/two-pandemics-us-coronavirus-inequality/609622/ (accessed Aug 16, 2021).
3. Blustein, D. L.; Duffy, R.; Ferreira, J. A.; Cohen-Scali, V.; Cinamon, R. G.; Allan, B. A. Unemployment in the Time of COVID-19: A Research Agenda. J. Vocat. Behav. 2020
4. Foote, D. How the pandemic is affecting tech jobs, skills and certifications. Insider Pro. 2020
5. Jones, B. L.; Brown, D. P. &. Coronavirus: How the Pandemic Has Changed the World Economy. BBC. January 24, 2021.
6. 30+ work from home statistics https://www.yourbestdigs.com/work-from-home-statistics/ (accessed Jun 17, 2021)
7. Go, R. 7 Disadvantages of Working from Home and How to Counter Them. Hubstaff.com, 2018.
8. COVID-19: We will come through this together https://www.un.org/sg/en/content/sg/articles/2020-03-16/covid-19-we-will-come-through-together (accessed Jun 17, 2021).
9. Mental health in the workplace during COVID-19: How can employers help? https://healthblog.uofmhealth.org/wellness-prevention/mental-health-workplace-during-covid-19-how-can-employers-help (accessed Jun 17, 2021).
10. Digital Class. Importance of information technology in today world - digital class. https://www.digitalclassworld.com/blog/importance-of-information-technology/ (accessed Aug 2, 2021).
11. Giorgi, G.; Lecca, L. I.; Alessio, F.; Finstad, G. L.; Bondanini, G.; Lulli, L. G.; Arcangeli, G.; Mucci, N. Covid-19-related mental health effects in the workplace: A narrative review. https://www.ncbi.nlm.nih.gov/pmc/articles/PMC7663773/ (accessed Aug 2,

DOI: 10.36838/v4i1.10

2021).
12. Kamal, R. Both remote and on-site workers are grappling with serious mental health consequences of covid-19. https://www.kff.org/policy-watch/both-remote-and-on-site-workers-are-grappling-with-serious-mental- health-consequences-of-covid-19/ (accessed Aug 2, 2021).
13. Foundation, N. I. H. C. M. COVID-19's impact on mental health and WORKPLACE WELL-BEING. https://nihcm.org/publications/covid-19s-impact-on-mental-health-and-workplace-well-being (accessed Aug 2, 2021).

Authors

Dhanya Janga is a student at John F. Kennedy Memorial High School in Iselin, NJ. She has developed a passion for biomedical engineering and psychology through the research projects and literature reviews she has done. Dhanya has a keen interest in medicine and health sciences and aspires to work as a pediatrician in the future.

Tanishka Aglave is a student at Williams Middle Magnet School in Tampa, Florida. She has also developed an interest in science and STEM studies. One of her greatest accomplishments was winning first place at regional STEM competitions in Cellular and Molecular Biology. Her hobbies include volunteering at a community garden and a biology research lab.

IJHSR
ijhighschoolresearch.org
■ RESEARCH ARTICLE

Development of Multiplex Allele-specific PCR Assay for BRAFV600E Mutation Detection in Human Cancer Cells

Young Doo Kim

St. Johnsbury Academy Jeju, 1159, Gueok-ri, Daejeong-eup, Seogwipo-si, Jeju-do, Republic of Korea; gosyber@suwon.ac.kr

ABSTRACT: BRAF mutation is commonly found in many types of human cancers. To detect the BRAFV600E mutation in cancer cells, a low-cost detection method was developed using multiplex allele-specific PCR assay. This method was designed to amplify three different size products in a single reaction: a 403-base pair (bp) for PCR amplification control, a 300 bp for wild-type (wt) allele-specific product, a 151 bp for BRAFV600E allele-specific product. The method was further validated in three different cancer cell lines with or without the BRAFV600E mutation: A172 (BARFwt), SK-MEL2 (BRAFwt), and A375SM (BARFwt/V600E), which was confirmed by Sanger sequencing. After genomic DNA was extracted from all three cell lines, an allele-specific PCR assay was performed. Genomic DNA from A172 and SK-MEL2 amplified only 403 bp (PCR amplification control) and 300 bp (BRAFwt) products, but not 151 bp (BRAFV600E) products. However, genomic DNA from A375SM successfully amplified all three sizes of products, including 151 bp (BRAFV600E), indicating that A375SM harbors BRAFwt/V600E heterozygous mutation. These results indicate that this novel multiplex allele-specific PCR is sensitive enough to detect BRAFV600E harboring cancer cells. Overall, this method not only provides a new tool for the rapid detection of the BRAFV600E mutation but also can be used for early detection of point mutations of various biomarker genes.

KEYWORDS: Molecular Biology; Cancer; Melanoma; BRAF mutation.

■ Introduction

Among many genetic diseases, this study focuses on detecting the BRAFV600E mutations in human cancers. BRAF mutations occur in about 8% of all human cancers.[1] Especially, 80% of melanoma harbor BRAFV600E mutation[2] and over 90% of these are a single nucleotide substitution of glutamic acid for valine.[3] BRAF gene encodes a kinase protein, which can activate the mitogen activated protein kinase (MAPK) pathway. This signal can be activated by epidermal growth factor (EGF) through binding to the EGFR receptor.[4] The mutations in BRAF allows constitutive MAPK pathway to mediate the cellular growth and metastasis in cancer cells.[5] Furthermore, BRAFV600E has been known to be involved in melanoma progression through various mechanisms. Such mechanisms include, evasion of apoptosis, unchecked proliferation, angiogenesis, metastasis, and evasion of immune response (Figure 1).[6] In order to detect this mutation as early as possible, a sensitive, specific, and low-cost assay needs to be developed. According to a market trend analysis report, the market for cancer diagnostic is increasing rapidly at an annual growth rate of 42 %.[6,7] and of different methods, polymerase chain reaction (PCR) is known as one of the most reliable and efficient ways to detect cancer at early stages.[7] This study is, therefore, focused on developing an accurate and efficient method for detecting BRAFV600E mutation using PCR method.

■ Methods

Cell culture and maintenance:

Three human cancer cell lines, A172 (brain), SK-MEL2 (skin), and A375SM (skin), were obtained from the Korean Cell Line Bank (Seoul, Korea). Gibco RPMI-1640 medium supplemented with 10 % FBS (Thermo Fisher) and 1 % penicillin and streptomycin were used. The cells were kept at 37 ºC in a CO2 incubator.

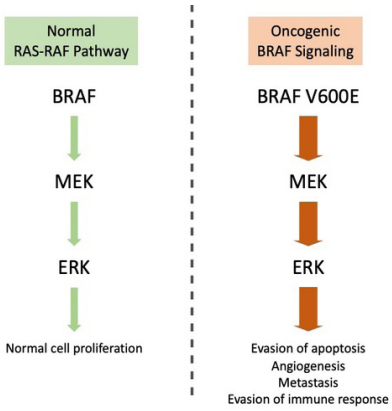

Figure 1: Comparison of RAS-RAF pathways in normal and BRAF mutation-derived oncogenic conditions. Mutation in BRAFV600E leads to upregulation of MEK-ERK pathway, which in turn, triggers various oncogenic conditions.

DNA extraction:

After human cancer cell lines were harvested, DNA was purified by QIAamp DNA Mini kit (Qiagen). Firstly, the cancer cells were suspended with 200 µL PBS. Then, 200 µL buffer AL was added. After the samples were incubated at 56 ºC for 10 min, 200 µL ethanol was added. Then, the samples were moved to AIAamp Mini spin column. After the centrifugation was applied for 1 min, the flow-through solutions were removed. Then, the column was washed with 500 µL buffer AW1 and 500 µL buffer AW2. Finally, the purified DNA was eluted with 200 µL AE buffer.

DOI: 10.36838/v4i1.11

Allele-specific PCR:

The primer sequences are indicated in Figure 2. PCR was performed in a 20 µL final volume containing 1 x buffer, 2 mM MgCl2, Taq DNA polymerase (Bioneer), 250 uM of each dNTP, 1 pmol of each primer, and 100 ng genomic DNA template. The following condition was used for PCR amplification: 95 ºC for 5 min, 35 cycles of 95 ºC for 20 sec, 56 oC for 30 sec, and 72 ºC for 30 sec with a final extension at 72 ºC for 5 min as shown in Figure 1.

Agarose gel electrophoresis :

PCR products were analyzed by 2 % agarose gel electrophoresis. The gels were run at 100 V for 30 minutes. Red-safe (intron) was used to stain the DNA products. Blue light illuminator (B-box) was used to visualize the DNA products.

CSanger Sequencing:

1 microliter of the genomic DNA samples were subjected to PCR amplification. The changes in the genomic DNA sequences of the cancer cells were analyzed by Sanger sequencing analysis (Bioneer, Korea) of a PCR fragment that was amplified from the BRAF gene.

Results and Discussion

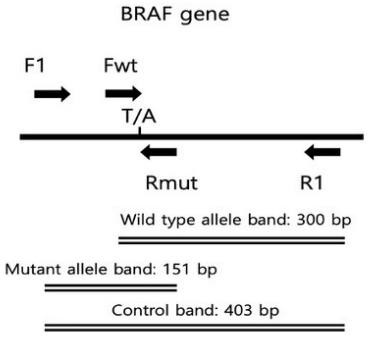

F1: 5'- ACTCTTCATAATGCTTGCTCTGATAGG -3'
R1: 5'- TGTTTGAAATACACTGAAACTGGT -3'
Fwt: 5'- GGTGATTTTGGTCTAGCTACAGT -3'
Rmt: 5'- ATGGGACCCACTCCATCGAGATTTCT -3'

Figure 2: Primer design of multiplex BRAFV600E allele-specific PCR. Forward Primer 1 (F1) and Reverse primer 1 (R1) generates the control band (403 bp). Forward primer for wild type (Fwt) and R1 generates the wild type allele band (300 bp). F1 and Reverse primer for mutation (Rmt) generates the mutant allele band (151 bp). The wild type sequence is T and the mutant sequence is A. The position of the mutation is indicated as T/A in the figure.

The multiplex BRAFV600E allele-specific PCR contained 4 primers in a single PCR reaction tube (Figure 2). Two external primers, F1 and R1, were designed to amplify the control fragment of 403 bp, spanning through the entire region including the wild type and mutant allele bands. Two internal primers, Rmut and Fwt, were designed with either specificity for the mutant sequence or the wild-type sequences, respectively. The mutant and wild-type allele bands were differentiated by the size of the fragment so that the bands would be visibly distinguishable in agarose gel electrophoresis analysis: the amplified wild type fragment was 300 bp and amplified mutant fragment was 151 bp (Figure 2). The optimal PCR condition was determined by varying the parameters, such as annealing temperature and PCR cycle numbers, through multiple experiments.

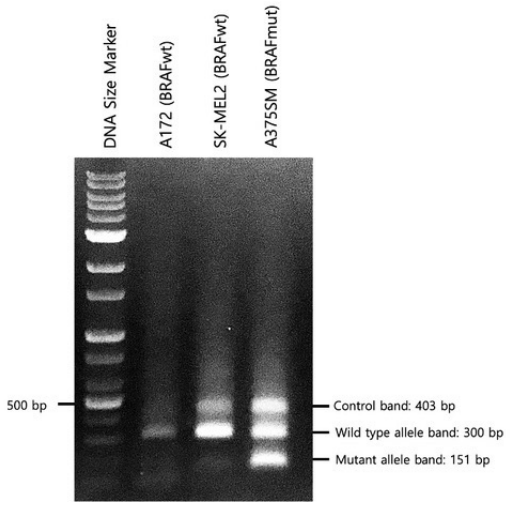

Figure 3: Specificity of BRAFV600E allele-specific PCR was analyzed using three different human cancer cell lines: A172 (BRAFwt), SK-MEL2 (BRAFwt), and A375SM (BRAFV600E). A172 and SK-MEL2 contains wild type allele and A375SM contains both wild type and mutant allele band.

To assess the analytical specificity of the assay, one BRAFV600E mutation containing cell line (A375SM) and two BRAF wild type containing cell lines (A172 and SK-MEL2) were used in this multiplex PCR assay. 403 bp of control bands and 300 bp wild type allele bands were detected in all three cell lines. A 151 bp mutant allele band was detected in only A375SM suggesting that A375SM had a heterozygous mutation (BRAFwt/V600E) (Figure 3). Also, the size of the products can be clearly separated, and no amplified bands overlapped in the agarose gel. A higher percentage of agarose gel and low molecular weight DNA marker will enhance the resolution.

When the DNA sequence of each cell line was also validated with Sanger sequencing, the results were identical to our BRAFV600E allele-specific PCR result (Figure 4), in-

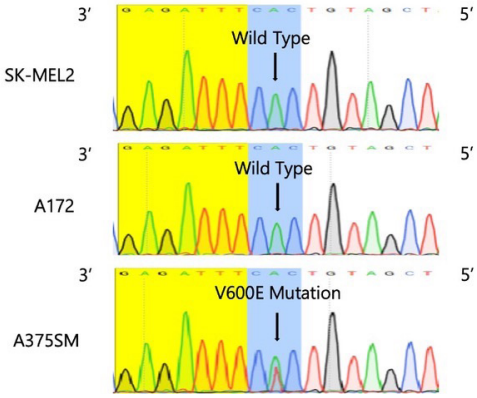

Figure 4: Sanger sequencing result showing wild type and BRAFV600E DNA sequence from SK-MEL2, A172, and A375SM cell lines. The reverse complement sequence is indicated in this figure. The reverse complement sequence of CAC is GTG, which encodes valine (V) on SK-MEL2 and A172. The reverse complement sequence of CTC is GAG, which encodes glutamic acid (E). This result indicates SK-MEL2 and A172 has homozygous wild type allele. A375SM sequence shows that both type of nucleic acids, A and T, were shown at the position of V600E. This result indicates that A375SM has a V600E heterozygous mutation: contains a mutation of one allele and a wild type of another allele.

Conclusions

Even though BRAFV600E mutation testing is widely used in various types of cancer patient samples, the previous method was very limited by its high cost and requirement of expensive lab equipment.[8] Therefore, the need for simple BRAF mutation testing is increasing to apply for genetic testing and chemotherapy drug development. To develop a fast and specific detection of BRAFV600E mutation in many types of cancer cells, a multiplex PCR reaction was designed. After performing hundreds of PCR reaction, the primer and PCR conditions were finally optimized. Also, many different concentrations of primers were tested to increase the specificity. Finally, the most optimized condition was discovered. This sensitive, low-cost, and fast PCR assay amplifies a control fragment of DNA and serves as a positive control for PCR reaction and DNA quality. When the PCR product was analyzed, three different size products were detected in agarose gels.

In this study, the DNA extracted from only three different human cancer cell lines was used to detect BRAFV600E. Therefore, more cancer cells with BRAFV600E should be tested in future to confirm this method. In addition, this novel assay can be easily performed by many basic molecular laboratories. This method can be potentially applied to detect many other point mutations found in cancer tissues and genetic disease. Also, it is applicable to detect the cancer cells with BRAFV600E in the peripheral blood.

Acknowledgements

I would like to thank Dr. Woo Rin Lee from University of Suwon for his advice and support for this research.

References

1. Dong, J.; Phelps, R. G.; Qiao, R.; Yao, S.; Benard, O.; Ronai, Z.; Aaronson, S. A., BRAF oncogenic mutations correlate with ' progression rather than initiation of human melanoma. *Cancer research* 2003, 63 (14), 3883-3885.
2. Menzies, A. M.; Lum, T.; Wilmott, J. S.; Hyman, J.; Kefford, R. F.; Thompson, J. F.; O'Toole, S.; Long, G. V.; Scolyer, R. A., Intrapatient homogeneity of BRAFV600E expression in melanoma. *The American journal of surgical pathology* 2014, 38 (3), 377-382.
3. Ascierto, P. A.; Kirkwood, J. M.; Grob, J.-J.; Simeone, E.; Grimaldi, A. M.; Maio, M.; Palmieri, G.; Testori, A.; Marincola, F. M.; Mozzillo, N., The role of BRAF V600 mutation in melanoma. *Journal of Translational Medicine* 2012, 10 (1), 85.
4. Sumimoto, H.; Imabayashi, F.; Iwata, T.; Kawakami, Y., The BRAF–MAPK signaling pathway is essential for cancer-immune evasion in human melanoma cells. *The Journal of experimental medicine* 2006, 203 (7), 1651-1656.
5. Tian, Y.; Guo, W., A review of the molecular pathways involved in resistance to BRAF inhibitors in patients with advanced-stage melanoma. Medical science monitor: *international medical journal of experimental and clinical research* 2020, 26, e920957-1.
6. Maurer, G.; Tarkowski, B.; Baccarini, M., Raf kinases in cancer–roles and therapeutic opportunities. *Oncogene* 2011, 30 (32), 3477-3488.
7. Seo, J. H.; Lee, J. W.; Cho, D., The market trend analysis and prospects of cancer molecular diagnostics kits. *Biomaterials Research* 2018, 22 (1), 2.
8. Tan, Y. H.; Liu, Y.; Eu, K. W.; Ang, P. W.; Li, W. Q.; Tellez, M. S.; Iacopetta, B.; Soong, R., Detection of BRAF V600E mutation by pyrosequencing. *Pathology* 2008, 40 (3), 295-298.

Author

Young Doo is currently attending Saint Johnsbury Academy in Jeju. He is interested in studying biology and plans to major in molecular biology in university. He is interested in the function of genetic material or genomes in organisms and wants to explore it more deeply.

DOI: 10.36838/v4i1.11

IJHSR
ijhighschoolresearch.org
RESEARCH ARTICLE

Determining the Association Between COVID-19 Cases and Congressional District Affiliation in the United States

Divya Kumar

The Academy of Science, 42075 Academy Drive, Leesburg, Virginia 20175, USA; 812180@lcps.org

ABSTRACT: Understanding the association between congressional district affiliation and COVID-19 cases provides a greater insight into the public health response and helps interpret the effect political affiliation has on the ability to follow public health measures. Estimated congressional district level data for COVID-19 confirmed cases were aggregated using a dasymetric interpolation method. Affiliation was measured using election data to calculate the partisan index. Five dates with significance to the public health perspective of the COVID-19 pandemic were chosen, and COVID-19 congressional district level cases were measured two weeks prior to these dates and the subsequent two weeks. Confounders were considered to create a more accurate model because they cause a spurious association. A paired t-test supported that most of the dates did have a significance in affecting the COVID-19 case rate, and that right leaning districts respond less to those critical dates compared to left leaning districts. Left leaning districts had a higher case rate towards the beginning of the pandemic, however right leaning districts saw a larger increase in cases. This model could help predict how certain politically affiliated groups act and respond during health outbreaks and which groups have a higher chance of being infected.

KEYWORDS: Behavioral and Social Sciences; Sociology and Social Psychology; Public Policy; COVID-19.

Introduction

COVID-19 (Coronavirus disease 2019) is a newly discovered infectious disease, which emerged in China and was declared a global pandemic by the World Health Organization. As of June 8th, 2021, there have been 33.4 million confirmed coronavirus cases and 598,000 related deaths in the United States. Multiple polls and data suggest that COVID-19 is profoundly a partisan issue in the United States. Political partisanship has been steadily increasing in the United States and substantially impacts behavior and beliefs (Gollwitzer *et al.* 2020).[1] This has completely changed the perception and response of the pandemic to be political. Numerous polls have shown that political party affiliation has an effect on support for preventative health behaviors and perception of risk for the coronavirus. A survey conducted by NBC News/Wall Street Journal found that more than 68% of democrats reported being concerned about the coronavirus compared to only 40% of republicans.[2] Another poll conducted by Gallup found that republicans were significantly less likely to take COVID-19 precautionary measures such as social distancing and wearing masks.[3] This partisan divide has affected perceptions of public health. A congressional district is a "a territorial division of a state from which a member of the US House of Representatives is elected" (Congressional District).[4] One of the main reasons that COVID-19 cases for congressional districts are not routinely available is because congressional districts are not straight-forward aggregations of already existing geographical data, for example counties or cities. By having congressional districts statistics, it can help evaluate and monitor programs specifically. They are also helpful geographically because they have roughly similar populations. Partisan differences can be expected, not because of certain policies, but rather because of individual behaviors. As mentioned before, different political parties view the seriousness of the pandemic differently and also view the necessary precautionary measures against COVID-19 differently. This could be due to homophily or herding behaviors because those in similar groups or political parties may feel the need for sameness. Similar rhetoric of political figures and in social media can be seen by corresponding political parties, which leads to imitating the certain political party's behavior.

Literature Review

Neelon *et al.*[5] (2020) conducted a longitudinal analysis examining COVID-19 incidence and death rates from March 1 through September 30, 2020 for the 50 states and DC. They obtained daily COVID-19 incident case and death data from a well validated source and aggregated county data to obtain state-level data. They found that gubernatorial party affiliation did drive policy decisions and polarized the attitude towards the pandemic. DeSouza and Subramanian[6] (2020) mapped COVID-19 deaths and cases across United States Congressional districts. There is an omnipresence of COVID-19 statistics at the state- and county-levels because of the importance of analysis and significance of public policy. However, a critical geographic unit for which COVID-19 mortality and case statistics have not been presented are the US congressional districts. They used county-level COVID-19 cases, deaths data, and census block data. In every county, COVID-19 cases and deaths per capita were assigned to census blocks in an unweighted manner. Then collection of block-level rates in a CD was summed using the weighted congressional district and census block to obtain congressional district estimates of the difference in every congressional district.

DOI: 10.36838/v4i1.12

Data can be adjusted for potential confounders chosen *a priori* from the US Census Bureau and the Robert Wood Johnson Foundation. Which includes state population size to compute population density, the percentage of state residents aged 65 and older, the percentage of Black and Hispanic residents, the percentage below the federal poverty line, the percentage in poor or fair health, and the number of primary care physicians per 100,000 residents (Johnson *et a*l. 2020).[7]

Wang and Yang[8] (2016) inspected the performance of regularized linear mixed effect models when multiple confounding factors coexist. They found that the Sparse Linear Mixed Models under sequence method of multiple confounding factors correction performed the best consistently compared across all the other combinations. They also used two log likelihood functions, MLE and REML, which both measure the goodness of fit to a sample of data for given values of the unknown parameters and found that MLE and REML methods did not distinguish from each other. The study also suggests that concatenation is the simplest way of correcting multiple confounding factors because it maintains the intuitiveness of integrating different categories into a universal one.

Neelon *et al*.[5] (2020) conducted statistical analysis, by fitting the Bayesian negative binomial models with daily incident cases and deaths for each state as the outcomes. They stratified states by governors' affiliation and graphed the posterior mean incidence and death rates daily for the reference covariate group, as well as the 95% posterior intervals (PIs). Wei[9] (2021) analyzed the Relation Between Government Anti-Contagion Policy Severity and United States COVID-19 Epidemiological Data. Tweets were used as a way to introduce an approach to assess United States policy severity using a random forest ensemble model. Wei found a significant correlation between the state policy severity and hospitalization, death, and case rates.

Coronavirus cases in association with the percentage of political affiliation of the congressional district have not been researched yet and could be an informational insight on COVID-19 precautions. DeSouza and Subramanian[6] (2020) did map coronavirus cases and deaths per congressional district, however, they did not take political affiliation into account, unlike this research. Neelon *et al*. [5] (2020) studied the association between governor political affiliation and COVID-19 cases and deaths in the United States, this research will be similar, however, instead of looking at states and governor political affiliation, this study will be looking at congressional district and the political affiliation of those who reside in that particular congressional district. Other studies used a Bayesian negative binomial model because they did not use percentage votes, instead they used governor political affiliation, so they had a definite variable, unlike this research. This study will be using a linear mixed regression model which allows for external confounding variables and the two main variables that will not be fixed. Gollwitzer *et al*.[1] (2020) studied the partisan difference and its effect on social distancing during the coronavirus pandemic. This study will examine confirmed COVID-19 cases instead of COVID-19 precautions like physical distancing. Wang and Yang[8] (2016) studied the effectiveness of multiple confounding variables and used the method of concatenation, which is similar because this research will be incorporating multiple variables into a linear mixed regression model. However, Wang and Yang[8] (2016) used their regression model as an application in biological processes, while this project will be applicable to COVID-19 congressional district level cases and political affiliation. Wei[9] (2021) used policy severity as a variable, but this research will be looking at political affiliation and will only be focusing on confirmed cases, while they looked at hospitalization rates, cases, and death rates. By being able to associate confirmed COVID-19 cases and congressional districts it can provide further insight to public policy and public perception of the pandemic.

In this research, COVID-19 congressional district level cases for multiple dates will also be measured to understand how certain politically affiliated groups react to those specific changes in federal guidelines, changes in public reaction, or changes in the response to the pandemic. The dates that will be utilized to measure COVID-19 confirmed cases are April 16, 2020; July 14, 2020; November 30, 2020; January 20, 2021; and March 19, 2021. April 16, 2020 was the day that new federal government guidelines, outlining a three-phase plan to reopening the country, were first introduced. This plan included thresholds and requirements for a state to move onto the next phase. It had broad criteria but aimed to reduce COVID-19 cases and deaths. By understanding the number of cases up to this day we can measure the impact of this policy. July 7, 2020 was the day that the United States infection rates reached over 3 million and it was also the day that the United States began its withdrawal from the World Health Organization. By understanding if June 7, 2020 had a significance in effecting COVID-19 cases, it provides further insight into whether an increase in cases or a significant number of cases had an impact in the public's reaction. November 30, 2020 is the day after the Thanksgiving weekend, where there is data to support that there was an uncontrolled amount of travel and not following federal suggested guidelines. Many experts warned about a surge in COVID-19 cases because of Thanksgiving travel. Air travel reached over 1.2 million people the day before, despite warnings and guidelines that discourage traveling. This could help quantify who followed federal suggestions to not travel during the pandemic. January 20, 2021 is the day that the presidential administration changed, therefore many policies changed as well. One of the first executive orders signed by the new administration was a mask mandate on all federal properties. This furthers the study to measure the extent of political affiliation and its effect on COVID-19 cases because of the change in presidential party administration on this day. March 19, 2021 was the day that the United States reached the goal of administering 100 million doses of the Coronavirus vaccine. On this day, over 75 million Americans had at least one dose, while over 40 million have both doses of the vaccine. Measuring cases for this date could aid in the understanding of how the increase in vaccinations and prevention methods affects congressional district COVID-19 cases. COVID-19 confirmed cases will be measured 14 days prior to the certain date and compared to the subsequent two weeks to determine

DOI: 10.36838/v4i1.12

weeks to determine if the date had a significance in affecting COVID-19 case data. It was hypothesized that right leaning districts would have a higher COVID-19 case rate, based on the general rhetoric by specific groups surrounding the pandemic. It was also hypothesized that all the chosen dates would have significance in affecting the number of COVID-19 confirmed cases because they all had an impact in public perception. In this research, congressional district level cases will be mapped using a dasymetric interpolation method and a regression analysis will be run, with COVID-19 congressional district level cases and political affiliation as the variables.

Methods

Congressional district level COVID-19 cases were measured using population-weighted methodology, specifically the dasymetric interpolation method that accounts for the spatial distribution. County level cases were obtained from Kaggle and census block data was retrieved from IPUMS.org. County level COVID-19 cases were first used, and then were then multiplied by the census block population in proportion to the total congressional district population. Census blocks were used as the smallest common factor between congressional districts and counties. They are the source zones and rates are disaggregated into spatial units that are common to both the source and target zone. This then led to the census block COVID-19 case rate in proportion to the congressional district. Then all the census block rates in the congressional district were summed to get the final congressional district COVID-19 case rate. Essentially, the county's rate is distributed to the congressional district via the census block using the block embedded in both target zones, and then the estimated rate is the output by aggregating proportionalized rates.

Congressional district affiliation was measured using 2020 House of Representative election data, which allowed for a moving variable to measure the partisan index of congressional districts. The winning representative's vote count was taken as a percentage of the total number of votes in that certain congressional district. Then, the percentage was subtracted from 50 percent so get the political index. For example, a district with an equal number of democratic and republican votes would have an affiliation of zero. So, the primary independent variable was the congressional district vote share. In congressional districts where the democratic candidate won, the affiliation was negated because democrats are traditionally considered left leaning. The districts in which republican candidates won were kept positive because they are considered right leaning. Affiliation was measured very straightforwardly because there are no current third-party representatives in the House of Representatives in the 117th United States Congress. So, only the two major parties, democrat and republican, affiliation was measured. 2018 Midterm Election Results, The Cook Partisan Voter index, and FiveThirtyEight elasticity scores were taken into account to ensure that there were no electoral outliers. For example, candidates who ran unopposed in the congressional elections in 2020 and/or 2018, candidates who faced more than one other major candidate who received or write in votes, or the personality and/or policy of the candidate significantly differ from the political norm which could affect the results of an election. The extent of political affiliation was labeled as the political index.

The confounding variables included the congressional district's population, median household income, population above the age of 65, population living below the federal poverty line, population with no health insurance coverage, and population density (number of people per square mile). All datasets for the confounding variables came from the United States Government Census website. The confounding variables were weighted according to population or countrywide averages, so that political affiliation would still be the main independent variable.

A linear regression model was used to model the relationship between the two main variables, political affiliation and COVID-19 cases, and the confounding variables as well. Since there were more than two variables, it was a multiple linear regression. The confounding variables were scaled for population, so that they would not be the main independent variables, rather they would be confounders to make a more accurate model. A paired T-test was conducted to compare two population means where there are two samples in which observations in both can be paired. In this case it would be 2 weeks before and after observations.

Results and Discussion

Understanding the Figures:

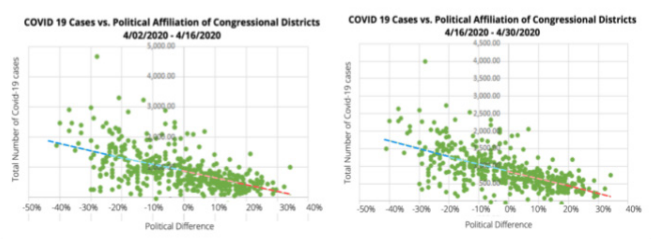

Figure 1: Regression analysis for COVID-19 cases and political affiliation for two weeks before and after April 16, 2020.

In Figure 1, the figure visualizing COVD-19 cases and political index, with confounding variables considered, for the dates of April 2, 2020 to April 16, 2020 has a slope of -2204.7. For the figure graphing out cases between April 16, 2020 and April 30, 2020, the slope is -2152.5. Both graphs have a decreasing slope, which shows that left leaning districts had a higher case rate when compared with right leaning districts.

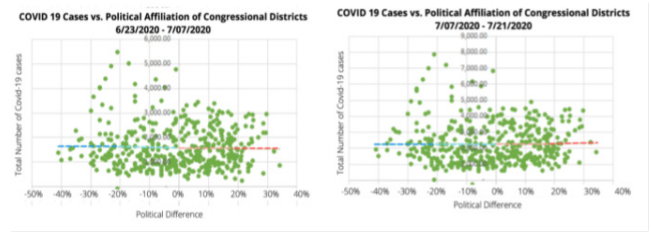

Figure 2: Regression analysis for COVID-19 cases and political affiliation for two weeks before and after July 7, 2021.

In Figure 2, the figure visualizing COVID-19 cases and political index, with confounding variables considered, for the dates of June 23, 2020, to July 7, 2020 has a slope of -125.3.

For the figure graphing out cases between July 7, 2020 and July 21, 2020, the slope is 115.9. The graphs change from decreasing slope to an increase in slope, which shows that right leaning districts saw more of an increase in cases than left leaning districts.

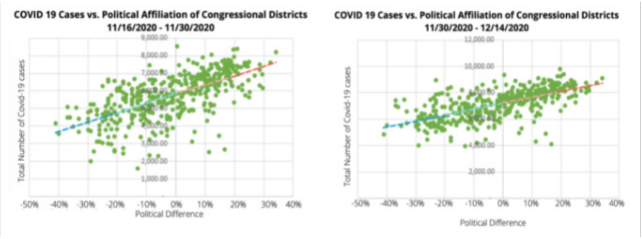

Figure 3: Regression analysis for COVID-19 cases and political affiliation for two weeks before and after November 30, 2020.

In Figure 3, the figure visualizing COVID-19 cases and political index, with confounding variables considered, for the dates of November 16, 2020 to November 30, 2020 has a slope of 5300.2. For the figure graphing out cases between November 30, 2020 and December 14, 2020, the slope is 4530.4. Both graphs have an increasing slope, which shows that right leaning districts had a higher case rate when compared with left leaning districts.

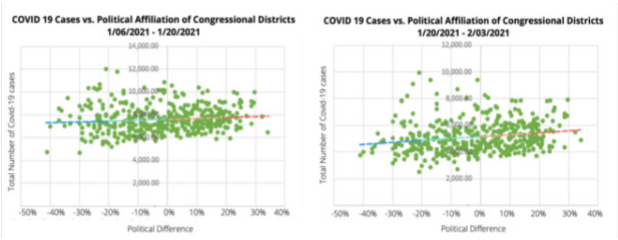

Figure 4: Regression analysis for COVID-19 cases and political affiliation for two weeks before and after January 20, 2021.

In Figure 4, the figure visualizing COVID-19 cases and political index, with confounding variables considered, for the dates of January 6, 2021 to January 20, 2021 has a slope of 783.8. For the figure graphing out cases between January 20, 2021 and February 3, 2021, the slope is 1430.1. There is a significant increase in slope from the first to second graph, which shows that right leaning districts saw more of an increase in cases than left leaning districts.

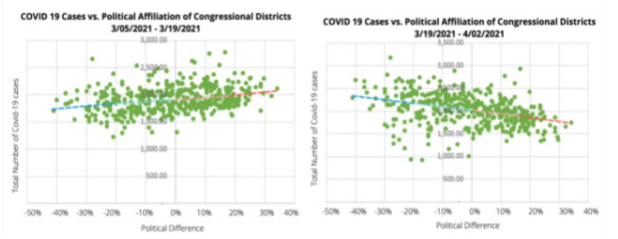

Figure 5: Regression analysis for COVID-19 cases and political affiliation for two weeks before and after March 19, 2021.

In Figure 5, the figure visualizing COVID-19 cases and political index, with confounding variables considered, for the dates of March 5, 2021 to March 19, 2021 has a slope of 438.8. For the figure graphing out cases between March 19, 2021 and April 2, 2021, the slope is -817.7. The graphs change from increasing to decreasing, which shows that left leaning districts saw more of an increase in cases than right leaning districts.

Left leaning districts had a higher case count towards the beginning of the pandemic in the month of April as shown by the negative trendline (shown in Figure 1). Left leaning districts could have had a higher case rate towards the beginning of the pandemic due to lack of information or resources. There were less prevention measures that were recommended by the government to the general public. For example, face masks were not recommended until April, which could be the reason behind why left leaning districts had a higher case rate towards the very beginning of the pandemic. However, as more restrictions and guidelines were put in place, there was a shift in the number of cases in right and left leaning districts. Another reason that left-leaning districts saw more of an improvement in the number of cases could be because they hit a ceiling of cases early. By the date of July 07, 2020, COVID-19 cases did not have a significantly positive or negative trend when compared with congressional district political affiliation (shown in Figure 2). It can be inferred that right leaning districts did not respond to the significance of the date when compared to left leaning districts because the change of rate in the slope increased from the two weeks before to the two weeks after. The date of November 30, 2020 shows that right leaning districts had a higher number of cases. It can be presumed that right leaning districts did not heed to the advice of government agencies such as the CDC, when compared to left leaning districts. As mentioned before there was an abundance of guidance and policies from the government in the fall months, especially against traveling during the holidays. However, the slope does decrease in the two weeks after the date, so all political affiliations responded more to the date of November 30, 2020 (shown in Figure 3). The date of January 20, 2021 showed right leaning districts still having higher case rate. However, the slope decreased when compared to the November date. In the two weeks after the inauguration, there was an increase in slope when compared to two weeks before which shows that right leaning districts responded less to this date. Although, overall, the number of cases decreased significantly for all political affiliations (shown in Figure 4). It can be inferred that the change in political party of the executive branch did show a decrease in COVID-19 cases, which could be because of the policies implemented. The date of March 19, 2021 showed right leaning districts having higher case rate in the two weeks before and left leaning districts having a higher case rate in the two weeks after. Since this date was a milestone for the number of vaccines administered, one of the reasons left leaning districts had a higher case rate could be vaccine disparity. At this point in time there was no complete vaccine roll out by the government. Certain groups did not have the resources or access to be able to get a vaccine at that point in time, which could explain the inverse change in slopes (shown in Figure 5). The percent change formula was used to calculate the difference in slopes and see how right and left leaning districts responded to the significant date. The date of April 16, 2020 had a percent change, from two weeks before to two after, of 2.5 %. The date of June 7, 2020 had a percent change

DOI: 10.36838/v4i1.12

of 190%. The date of November 30, 2020 had a percent change of 14.5%. The date of January 20, 2021 had a percent change of 82%. The date of March 19, 2021 had a percent change of 286%. From this data it can be concluded that the change in the number of cases in regard to congressional district affiliation did not particularly sway one way or the other. However, the data also suggests that right leaning districts responded less because the percent changes are higher and lean more positive, which are the x-values representing right leaning districts.

Understanding the Tables:

Table 1: Regression analysis, Pearson correlation, and paired t-test results for April 16, 2020.

	4/16/2020	4/30/2020
Mean	888.656	896.059059
Variance	412231.9665	294044.704
Pearson Correlation	0.977125557	
Hypothesized Mean Difference	0	
t Stat	-0.948564889	
P(T<=t) two-tail	0.343382278	
t Critical two-tail	1.965574698	

Table 1 shows the results for the paired t-test and regression analysis, with the two different groups being the two weeks before April 16, 2020 and the two weeks after. The t-statistic is around -0.949 and the t critical value is around 1.966. The Pearson correlation coefficient is around 0.977.

Table 2: Regression analysis, Pearson correlation, and paired t-test results for July 7, 2020.

	6/23/2020 – 7/07/2020	7/07/2020 – 7/21/2020
Mean	1595.656941	2272.4418
Variance	763544.1845	1525026.7
Pearson Correlation	0.991503208	
Hypothesized Mean Difference	0	
t Stat	-36.17717243	
P(T<=t) two-tail	1.09E-131	
t Critical two-tail	1.965574698	

Table 2 shows the results for the paired t-test and regression analysis, with the two different groups being the two weeks before July 7, 2020 and the two weeks after. The t-statistic is around -36.177 and the t critical value is around 1.966. The Pearson correlation coefficient is around 0.992.

Table 3: Regression analysis, Pearson correlation, and paired t-test results for November 30, 2020.

	11/16/2020 – 11/30/2020	11/30/2020 – 12/14/2020
Mean	5745.101882	7161.795
Variance	1655141.072	1222659
Pearson Correlation	0.931062593	
Hypothesized Mean Difference	0	
t Stat	-61.05557035	
P(T<=t) two-tail	3.52E-212	
t Critical two-tail	1.965574698	

Table 3 shows the results for the paired t-test and regression analysis, with the two different groups being the two weeks before November 30, 2020 and the two weeks after. The t-statistic is around -61.056 and the t critical value is around 1.966. The Pearson correlation coefficient is around 0.931.

Table 4: Regression analysis, Pearson correlation, and paired t-test results for January 20, 2021.

	1/06/2021 – 1/20/2021	1/20/2021 – 2/03/2021
Mean	7620.076706	5166.212235
Variance	1298856.076	1370160.661
Pearson Correlation	0.887853353	
Hypothesized Mean Difference	0	
t Stat	92.33439381	
P(T<=t) two-tail	6.57E-283	
t Critical two-tail	1.965574698	

Table 4 shows the results for the paired t-test and regression analysis, with the two different groups being the two weeks before January 20, 2021 and the two weeks after. The t-statistic is around 92.334 and the t critical value is around 1.966. The Pearson correlation coefficient is around 0.888.

Table 5: Regression analysis, Pearson correlation, and paired t-test results for March 19, 2021.

	3/05/2021 – 3/19/2021	3/19/2021 – 4/02/2021
Mean	1914.674353	2027.7471
Variance	55337.11838	113704.01
Pearson Correlation	0.062301914	
Hypothesized Mean Difference	0	
t Stat	-5.843042497	
P(T<=t) two-tail	1.02E-08	
t Critical two-tail	1.965574698	

Table 1 shows the results for the paired t-test and regression analysis, with the two different groups being the two weeks before March 19, 2021 and the two weeks after. The t-statistic

is around -5.843 and the t critical value is around 1.966. The Pearson correlation coefficient is around 0.062.

When running a paired t-test, having a t-statistic greater than the t-critical value means that there is a significant difference in the data. The date of April 16, 2020 did not have a significant impact on COVID-19 cases because of a lesser t-value (Table 1). This was still very early in the pandemic where there was not a lot of information available, which could explain why April 16, 2020 did not affect the public's actions and infection rates. July 7, 2020 did have a greater t-value, so it did have a significant impact on COVID-19 cases (Table 2). Overall, there was less of a response to the date, for example the number of cases increased by less than two percent, but it still impacted the number of cases. November 30, 2020 had an incredibly high t-value, so it did have a significant impact on the number of cases (Table 3). This again shows the effect the holiday time had on the pandemic. January 20, 2021 also had a high t-value, so it did have an impact on the number of cases. This shows that the inauguration could have had an impact on the number of COVID-19 cases. Lastly, the date of March 19, 2021 also had a t statistic greater than the critical value, which shows that the date was significant. This supports the idea that the number of vaccines administered significantly impacted the COVID-19 case rate. There are other factors that could have influenced the data, but these conclusions can be made from looking at the significance of date.

The Effect of Confounding Variables:

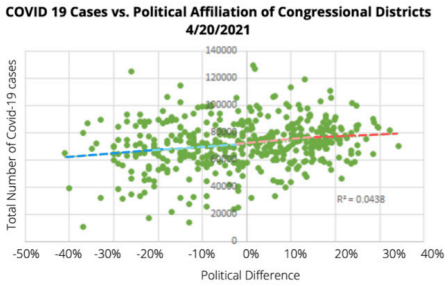

Figure 6: Regression analysis for COVID-19 cases and political affiliation from the beginning of the pandemic to April 20, 2021, but without the inclusion of confounding variables.

Figure 6 shows the graph of the total number of COVID-19 cases and political index, with no confounding variables considered. It has an R2 value of 0.0438.

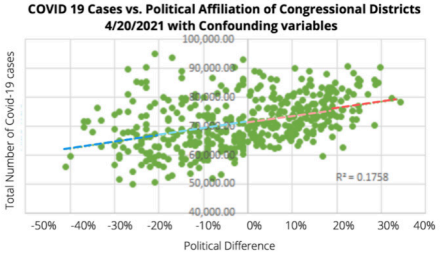

Figure 7: Regression analysis for COVID-19 cases and political affiliation from the beginning of the pandemic to April 20, 2021, but without the inclusion of confounding variables.

The data without confounding variables had a wider variance associated with it, when compared to the data that have confounding variables to cause a spurious association. The data points are much more spread out; however, it does not alter the trendline of the data to a great extent (as shown in Figure 6 and 7). The R2 value for the data without confounding variables is 0.0438 as seen in Figure 6, and the R2 value for the data with confounding variables is 0.1758 as seen in Figure 7. Since this research is based on human behavior, the R2 value is closer to zero, however it can be interpreted that the data with confounding variables has less variance and therefore is a better fit to the regression line when compared to the data without confounding variables because it has a higher R2 value. This confirms that the confounding variables - congressional district's population, median household income, population above the age of 65, population living below the federal poverty line, population with no health insurance coverage, and population density - had an influence on both political affiliation and the number of COVID-19 confirmed cases. Adding confounders strengthened the applicability of the data, and helps researchers understand the distinct relationship between COVID-19 cases and political affiliation.

Interpreting the Conclusions:

Many of these conclusions support the validity of many statements heard on the news and the internet. There are polls and data that have found that right leaning individuals do not follow government suggested health policies as well as left leaning individuals do. There is also an innate difference in these groups as they perceive the virus in different ways. One reason for this is that the right leaning media has facilitated the spread of misinformation from the early stages of the pandemic. Polling has found that only 38 percent of Fox News viewers, a right-wing media outlet, are worried about the virus compared to over 70 percent of CNN viewers, a left-wing media outlet. Right leaning media was also more likely to make inaccurate claims about the treatment of COVID-19. Although, it is hard to specify who exactly consumed these types of media, it can be inferred that right leaning individuals consumed right leaning media. (Motta *et al.* 2020).[10] As mentioned previously, right leaning districts did not follow public health measures, such as social distancing, as well as left leaning districts, which could have led to them having a higher number of COVID-19 cases (Gollwitzer *et al.* 2020).[1] Right leaning individuals are less likely to wear masks because they don't feel as threatened by the virus itself (Nowlan *et al.* 2020).[11] This could explain why there is less of a response from right leaning districts to those specific dates. The data, taken together, suggests that right leaning districts had a higher number of cases throughout the pandemic, and they also responded to policies and significant days of the pandemic much less.

Conclusion

A paired t-test supported that most of the dates did have a significance in affecting the COVID-19 case rate, and that right leaning districts responded less to those critical dates compared to left leaning districts. Specifically, the dates of July 14, 2020, November 30, 2020, January 20, 2021, and March 19, 2021 had a significance in affecting COVID-19 cases, while the date of April 16, 2020 did not have a significant impact on the case rate. Based on the data, left leaning districts had a

DOI: 10.36838/v4i1.12

higher case rate towards the very beginning of the pandemic, however right leaning districts saw a larger increase in cases overall. Right leaning districts had less of a response to the significant dates and saw a significantly greater increase as there was an increase in time and an increase in information. In the future, this model could help predict how certain politically affiliated groups act and respond during health outbreaks and which groups have a higher chance of being infected.

Future research could include adding other confounding variables, for example the presence of racial minorities, availability of resources to protect themselves from the virus because they have an effect on the COVID-19 case rate. Furthermore, future research could include considering time series methods and controlling for existing or cumulative cases, and it could also explicitly account for the spillover of cases across adjacent congressional districts.

Another source of error that needs to be implemented in the future is vaccine numbers and disparities. Some districts have more availability to obtain the vaccine and it could be another confounding factor that could affect the COVID-19 case rate more recently because of the high vaccination rates throughout the country. Overall, it can be interpreted from the data that right leaning districts responded less to the COVID-19 prevention measures placed when compared to left leaning districts. The fact that left-leaning districts initially had higher case rates instead of comparable case rates to right-leaning districts makes the shift over time even more marked.

Acknowledgements

I would like to thank my research teacher, Mr. Proffitt. He provided guidance throughout the research process, and I am so grateful for him. I would also like to thank the Academy of Science for giving me the opportunity and resources to conduct my research project.

References

1. Gollwitzer, A., Martel, C., Brady, W.J. Paernamets, P., Freedman, I,G, Knowles, E.D., Van Bavel, J. J. Partisan differences in physical distancing are linked to health outcomes during the COVID-19 pandemic. *Nat Hum Behav* 4, 1186–1197 (2020). https://doi.org/10.1038/s41562-020-00977-7
2. *NBC News/Wall Street Journal Survey Datasets* (Hart Research Associates/Public Opinion Strategies, 2020); https://www.documentcloud.org/documents/6810602-200149-NBCWSJ-March-Poll-Final-3-120-Release.html
3. Bird, R. & Ritter, Z. Is the media creating division on COVID-19 health practices? *Gallup* https://news.gallup.com/poll/312749/media-creating-division-covid-health-practices.asp (2020).
4. *Congressional District*. https://www.merriam-webster.com/dictionary/congressional district.
5. Neelon, B., Mutiso, F., Mueller, N. T., Pearce, J. L., & Benjamin-Neelon, S. E. (2020). Associations between governor political affiliation and COVID-19 cases and deaths in the United States. *medRxiv : the preprint server for health sciences*, 2020.10.08.20209619. https://doi.org/10.1101/2020.10.08.20209619
6. DeSouza PN, Subramanian SV. COVID-19 across United States congressional districts. *J GlobHealth Sci*. 2020;2:e22. https://doi.org/10.35500/jghs.2020.2.e22
7. Johnson, K., Khayyat-Kholghi, M., Johnson B., Tereshchenko, L. (2020). The Association Between the Rate of Angiotensin-Converting Enzyme Inhibitors and Angiotensin Receptor Blockers Use and The Number of Covid-19 Confirmed Cases and Deaths in the United States: Geospatial Study. *medRxiv,* 2020.05.31.20118802. https://doi.org/10.1101/2020.05.31.20118802
8. Wang, H., & Yang, J. (2016). Multiple Confounders Correction with Regularized Linear Mixed Effect Models, with Application in Biological Processes. *BioRxiv*, 14, 9. https://doi.org/10.1101/089052
9. Wei, J. (2021). Analyzing the Relation Between Government Anti-Contagion Policy Severity and United States COVID-19 Epidemiological Data.
10. Motta, M., Stecula, D., & Farhart, C. (2020). How Right-Leaning Media Coverage of COVID-19 Facilitated the Spread of Misinformation in the Early Stages of the Pandemic in the U.S. *Canadian Journal of Political Science*, 53(2), 335-342. doi:10.1017/S0008423920000396
11. Nowlan, L., Zane, D (2020). Getting Conservatives and Liberals to Agree on the COVID-19 Threat. *Journal of the Association for Consumer Research*, 2020; https://doi.org/10.1086/711838

Author

Divya Kumar is a junior at Freedom High School and The Academy of Science, where she is a student researcher. She loves doing research and enjoys learning about social sciences. She hopes to major in public policy in the future.

IJHSR
ijhighschoolresearch.org
RESEARCH ARTICLE

Discovery of an Antibody Against SARS-CoV-2-RBD (Receptor Binding Domain)

Claire Lee, Seungjae Kim, Ha Ryeong Eo, Christine Yi

Seoul International School, Dong pangyo-ro 155, Bundang-gu, Seongnam-si, Gyeonggi-do, 13525, South Korea;
christine.yi22@stu.siskorea.org

ABSTRACT: The novel SARS-CoV-2 is the causative agent of the recent COVID-19 pandemic and has claimed more than 3 million lives worldwide. The spike protein is a viral transmembrane protein of the SARS-CoV-2 that binds to receptors on target cells, making it responsible for cell entry. The S1 subunit of the Spike protein contains the receptor-binding domain (RBD), which strongly binds to the angiotensin-converting enzyme 2 (ACE2) receptor of human cells. Therefore, the purpose of this study was to discover a neutralizing antibody against SARS-CoV-2-RBD that could potentially be used to develop a combined post-exposure therapy for SARS-CoV-2 infection. Phage display biopanning and ELISA assays were performed to isolate single chain variable fragment (scFv) antibodies binding to SARS-CoV-2-RBD from the phage display library. The ELISA assays resulted in a total of nine positive binders, and of those nine, two scFv antibodies carrying unique DNA sequences were identified. However, additional protein sequence analysis by ExPASy revealed the presence of stop codons in both antibody sequences, making the antibodies inapplicable for further therapeutic development. Taken together, the phage display biopanning strategy described here provides a promising basis for isolating a clinically applicable neutralizing antibody against SARS-CoV-2-RBD.

KEYWORDS: Biomedical and Health Science; Genetics and Molecular Biology of Disease; Phage display; SARS-CoV-2; RBD.

Introduction

Coronaviruses (CoV) are a large group of viruses that can cause a range of illnesses in vertebrates.[1] Within the past two decades, two highly pathogenic coronaviruses with zoonotic origin — severe acute respiratory syndrome coronavirus (SARS-CoV) and Middle East respiratory syndrome coronavirus (MERS-CoV) — have caused large-scale outbreaks of infectious diseases.[2] The novel severe acute respiratory syndrome coronavirus[2] (SARS-CoV-2), the causative agent of the recent COVID-19 pandemic, first emerged in Wuhan, China, at the end of 2019. It is a highly transmissible virus and the third most pathogenic coronavirus that causes mild to severe respiratory infections in humans. On January 30th, 2020, the World Health Organization (WHO) declared COVID-19 as the sixth public health emergency of international concern, and as of April 18th, 2021, about 130 confirmed cases and 3 million deaths have been reported worldwide.

SARS-CoV-2 is an enveloped virus with a positive-sense, single-stranded RNA genome.[3] SARS-CoV-2 entry into host cells is mediated by its transmembrane spike (S) glycoprotein. The S glycoprotein is responsible for binding to the host cell receptor and for the fusion of the viral and cellular membranes.[4] The S1 subunit of the S glycoprotein contains the receptor-binding domain (RBD), which binds to the host cell receptor angiotensin-converting enzyme 2 (ACE2), initiating viral cell entry.[5] Therefore, this receptor interaction site on the S1 subunit is considered the main target for therapeutic monoclonal antibodies.[6]

Accordingly, the main objective of this study is to discover and isolate an antibody that will bind to the receptor-binding domain (RBD) of SARS-CoV-2. Herein, the phage display technique was utilized to present the peptide sequences on the surface of bacteriophages, and the scFv antibody sequences were inserted into a vector, creating a phagemid that was placed inside the bacteriophage. An antibody that strongly binds to the receptor-binding domain of SARS-CoV-2 would function as a neutralizing antibody that prevents the infectivity of SARS-CoV-2 and potentially serve as a therapeutic agent in the development of a combined post-exposure therapy against SARS-CoV-2 infection.

Methods

Phage display technique and ELISA screening were used to isolate specific scFv antibodies against SARS-CoV-2-RBD. A phage display library containing bacteriophages each displaying different scFv antibodies was constructed prior to the experiment. The scFv library was subjected to three rounds of biopanning, and positive phage clones were identified through ELISA screening. The DNA and protein sequences of the positive scFv clones were analyzed (Figure 1).

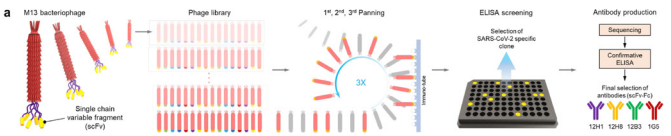

Figure 1: Description of the overall methodology.[7]

Selection of scFv antibodies using phage display:

scFv phage display library, Escherichia Coli TG1 strain, and M13 helper phage were obtained from YntoAb. In each round of panning, 5μg of SARS-CoV-2-RBD in 1mL of sodium carbonate buffer (pH 9.2) was coated on an immune tube 7 and

DOI: 10.36838/v4i1.13

incubated at 4 ˚C overnight. The following day, the tube was blocked with 3% skim milk (1XPBS) for 30 minutes at room temperature. Phage particles were pre-incubated with 3% skim milk for 30 minutes to remove their reactivity against skim milk proteins and were added directly to the RBD-coated immune tube. After washing five times with 1XPBS containing detergent, bound phages were eluted with 1 ml 100 mM TEA for 8 minutes at room temperature and neutralized with 500 µl 1 M Tris-Cl (pH 7.4). 8.5 ml of E.coli TG1 strain was then infected with the eluted phage particles and incubated at 37 ˚C, 130 rpm for 60 minutes (the TG1 strain was cultivated in an LB agar plate containing Ampicillin and Kanamycin prior to this step to check for contamination). 1 µl of infected TG1 was placed in a 100 µl growth medium and spread on a 90 mm LB agar plate containing Ampicillin, which was later used to approximate the number of infected colonies. The remaining bacterial culture was pelleted by centrifugation at 3000 rpm for 5 minutes, spread on a 150 mm LB agar plate containing Ampicillin, and incubated overnight at 37 ˚C. 4 mL of growth medium was then added to the 150 mm plate to scrape the bacterial colonies. After re-suspending the solution, 50 µl of infected bacteria were inoculated into 20 mL of SB-ampicillin growth medium and placed in a shake incubator 37 ˚C, 220 rpm for 1.5 hours for bacterial growth. The remaining bacterial culture was kept at -80 ˚C in 50% glycerol for long-term storage.

Following incubation, the phage library was rescued by infection with 1 ml of M13 helper phage. Kanamycin (1:1000) was added directly to the TG1 strain during the rescue process and incubated overnight at 30 ˚C, 200 rpm to increase efficiency by removing uninfected bacteria. The following day, the bacterial cells were removed from the medium by centrifugation (3500 rpm, 15 min, 4 ˚C). Escaped phage particles bound to 5X PEG (Figure 2) were pelleted by centrifugation (15,000 Xg, 30 min, 4 ˚C). 550 µl of 1X PBS (with protease inhibitor cocktail without EDTA, pH 7.4) was added to the phage particles to inhibit the breakdown of proteins. The phage particles were once again pelleted by centrifugation (12,000 rpm, 5 min, 4 ˚C) and filtered through a 0.2 µM filter syringe to remove any possible bacteria debris. Succeeding rounds of panning were performed following the identical procedure but with increased washing stringency. The RBD output for the first, second, and third rounds of panning was 8 x 105, 4.4 x 105, and 6.26 x 107, respectively.

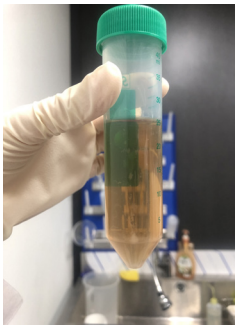

Figure 2: Escaped phage particles bound to 5X PEG pelleted by centrifugation.

Seeding and Induction:

After the third round of selection, individual bacterial colonies were inoculated into 96-well-plates each containing 100 µl SB-ampicillin (Figure 3), followed by overnight incubation at 220 rpm, 30 ˚C. 15 µl from each well was moved to a new set of 96-well-plates each containing 165 µl SB-ampicillin and incubated at 37 ˚C, 220 rpm for 90 minutes. The remaining bacteria in the original well-plate was stored at -80˚C with 40 µl of 50% glycerol to prevent rapid re-crystallization. 20 µl IPTG was added to the incubated 96-well-plates to inactivate the repressor for continuous transcription and incubated overnight at 30 ˚C, 200 rpm.

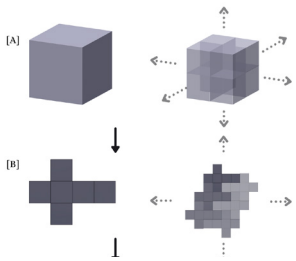

Figure 3: Individual bacterial colonies incubated with SB-ampicillin.

Periplasmic Sup Preparation:

The incubated bacterial culture induced with IPTG was centrifuged at 3,000 rpm for 10 minutes at 4 ˚C. 80 µl of 1X TES buffer was added and vortexed, followed by incubation on ice for 30 minutes. Then, 120 µl of 0.2X TES buffer was added and vortexed, followed by incubation on ice for 30 minutes. Centrifugation was carried out at 3,000 rpm for 10 minutes at 4 ˚C, and the supernatant (periplasmic sup) containing soluble scFvs was taken directly for ELISA screening.

Periplasmic Sup Preparation:

The incubated bacterial culture induced with IPTG was centrifuged at 3,000 rpm for 10 minutes at 4 ˚C. 80 µl of 1X TES buffer was adde

Enzyme-linked Immunosorbent Assay (ELISA):

5 µg of SARS-CoV-2-RBD was coated on a 96-well ELISA plate following the same immobilization method described above. The RBD-coated wells were each blocked with 150 µl 3% skim milk (1X PBS) for 30 minutes at room temperature. Additionally, a negative control was prepared by coating the 3% skim milk on a separate empty ELISA plate. 50 µl of periplasmic sup was added to each of the wells in both the RBD-coated plate and the negative control. The plates were left at room temperature for 30 minutes. The plates were washed 3 times with 150 µl of 1X PBS detergent to remove any unbound or nonspecific binding proteins. 50 µl of secondary antibody (anti-HA peroxidase)[8] suspended in 3% skim milk was added to the wells and incubated for 30 minutes. The addition of the secondary antibody to the primary antibody produces a fluorescent signal due to the reaction between the HA Tag and the Anti-HA peroxidase.[9] After washing 3 times with 150 µl of 1X PBS detergent, 50 µl of TMB substrate was added to each of the wells and left at room temperature for 5 minutes. The substrate reaction was stopped with 50 µl of sulfuric acid (Figure 4). The optical density (OD) values were measured at 450 nm using the ELISA

reader (Table 1, Table 2). The positive clones were identified with OD450nm values above 1.0. Overall, the ELISA assays resulted in 9 positive binders.

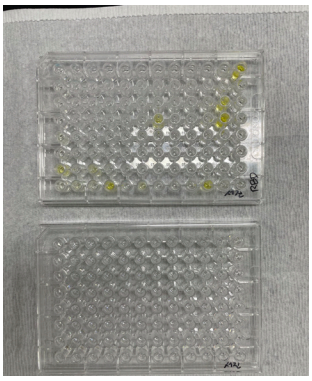

Figure 4: 96-well-plates after the addition of H_2SO_4.

Table 1: RBD ELISA results (using ELISA reader from BIOTECH).

RBD	1	2	3	4	5	6	7	8	9	10	11	12
A	0.081	0.056	0.05	0.086	0.047	0.631	0.048	1.121	0.052	0.049	0.061	1.028
B	0.101	0.06	0.313	0.046	0.047	0.047	0.046	0.049	1.213	0.048	0.367	0.054
C	0.107	0.049	0.045	0.047	0.048	0.533	0.606	0.383	0.048	0.047	0.048	0.051
D	1.301	0.046	0.046	0.188	0.048	1.17	0.047	0.048	0.161	0.046	0.05	0.055
E	0.181	0.046	0.047	0.048	0.045	0.044	0.045	0.046	0.047	0.05	0.049	0.214
F	0.054	0.046	0.046	0.045	0.046	0.047	1.316	0.049	0.047	0.05	0.049	0.121
G	0.067	0.466	0.05	0.05	0.047	0.048	0.207	1.033	0.475	0.049	0.051	0.055
H	0.066	0.63	0.056	0.06	0.052	0.056	1.22	1.621	0.06	0.056	0.056	0.062

Table 2: 3% skim milk ELISA results (negative control)..

3% skim milk	1	2	3	4	5	6	7	8	9	10	11	12
A	0.06	0.051	0.048	0.057	0.048	0.047	0.046	0.045	0.048	0.048	0.05	0.056
B	0.052	0.046	0.047	0.048	0.046	0.047	0.054	0.049	0.05	0.047	0.048	0.051
C	0.059	0.047	0.045	0.046	0.046	0.047	0.047	0.05	0.046	0.048	0.05	0.052
D	0.056	0.047	0.045	0.05	0.048	0.053	0.044	0.047	0.045	0.046	0.046	0.05
E	0.059	0.047	0.046	0.066	0.052	0.046	0.046	0.05	0.051	0.046	0.049	0.053
F	0.063	0.049	0.047	0.05	0.046	0.049	0.05	0.046	0.048	0.049	0.052	0.056
G	0.073	0.055	0.056	0.049	0.05	0.05	0.048	0.05	0.051	0.05	0.049	0.059
H	0.079	0.065	0.058	0.063	0.058	0.059	0.056	0.06	0.057	0.056	0.059	0.063

OD450nm values above 1.0 were identified as positive. The negative control did not yield any positive binders, verifying that the antibodies with OD_{450nm} > 1.0 in Table 1 bind specifically to RBD. A total of 9 samples were carried on to the sequencing stage.

Seeding:

The 96-well stock stored at -80 ˚C was allowed to thaw at room temperature. 5 µl of each of the 9 positive binders were taken from the 96-well stock and mixed with 2 ml of SB-ampicillin in 15 ml tubes, followed by incubation overnight at 37 ˚C, 200 rpm.

DNA Minipreparation:

1.4 ml from each bacterial culture was moved to 1.5 ml tubes. The bacterial cells were pelleted by centrifugation at 12,000 rpm for 5 minutes at 4 ˚C. 250 µl of P1 buffer containing EDTA was added to destabilize the cell walls. 250 µl of P2 buffer containing NaOH was added for alkaline lysis, which disrupts the hydrogen bonding between the DNA bases and causes both bacterial and phage DNA to denature. 350 µl of P3 buffer containing acetic acid was added for neutralization, allowing the DNA to precipitate. Centrifugation was carried out at 12,000 rpm for 10 minutes at 4 ˚C to separate the phage DNA from the bacterial DNA. The supernatant containing the phage DNA was filtered through a miniprep tube column (provided by YntoAb) and centrifuged at 12,000 rpm for 60 seconds at 4 ˚C. The filtrate was thrown away, and 500 µl of ethanol-based EW buffer was added to the tube column, followed by centrifugation. The same procedure was repeated with 700 µl of ethanol-based PW buffer. After replacing the tube with a new one, 50 µl of DW was added directly to the column and centrifuged at 12,000 rpm for 60 seconds at 4 ˚C. The filtrate containing the phage DNA was quantified using TAKE3 (Table 3) and sent for sequencing.

Table 3: DNA quantification results (using TAKE 3 equipment from BIOTECH). *Concentration (ng/µL) based on Beer-Lambert's law, concentration=absorbance x constant (50 ug/ml for DNA) x dilution factor.

Sample ID	Absorbance_260	Absorbance_280	O.D. Ratio (260/280)	DNA Concentration (ng/µL)*
A8	0.089	0.046	1.951	88.919
A12	0.044	0.021	2.148	44.15
B9	0.056	0.027	2.06	55.963
D1	0.178	0.095	1.872	178.043
D6	0.269	0.145	1.864	269.384
F7	0.2	0.107	1.863	200.132
G8	0.025	0.014	1.805	24.788
H7	0.485	0.263	1.842	484.598
H8	0.317	0.168	1.893	317.233

Using the quantification results, DNA purity and DNA concentration were measured. DNA is quantified at 260 nm, and proteins are quantified at 280 nm.[10] DNA to protein (260/280) ratios greater than 1.6~1.8 were considered high DNA purity.[10]

Results and Discussion

Results:

The 9 positive binders identified by the ELISA assays were carried on to the sequencing stage. DNA from individual phage clones was isolated to obtain specific nucleotide sequences, represented by four-color chromatograms. Of the 9 positive binders, only 2 of the scFv antibodies displayed regular, evenly spaced peaks (Figure 5, Figure 6).

Figure 5: B9 sequencing results.

Figure 6: H8 sequencing results.

DOI: 10.36838/v4i1.13

Antibodies with irregular peaks were omitted at this stage. Antibodies with regular peaks as shown in Figure 5 and Figure 6 were further processed. ExPASy, an online translational tool, was used to deduce the protein sequences as shown in Figure 7 and Figure 8.

GND-
NEKTAIAIAVALAGFATV**AQAA**ELVMTQSPSSLSASVGDRVTITCRASQSISSYLNWYQQKP
GKAPKLLIYAASSLQSGVPSRFSGSGSGTDFTLTISSLQPEDFATYYCQQSYSTPPTFGQGT
KVEIKGGSSRSSSSGGGGSGGGGQV-
LVQSGAEVKKPGSSVKVSCKASGGTFSSYTISWVRQAPGQGLEWMGRIIPILGIPHYAQKFQ
GRVTITADKSTSTAYMELSSLRSEDTAVYYCATTQWELPKRGTFDIWGQGTMVTVSSASTQS
PSVTS**GQAGQ**HHHHHHGAYPYDVPDYAS-
EGGGSEGGGSEGGGSEGGGSGGGSGSGDFDYEKMANANKGAMTENADENVLQSDAKGKLDSV
ATDYGAAIDGFIGDVSGLLMVMGLLVILLALIPKGSSR-
RGKFTFKENFRQNYLPSSTGEGALLLWAGKPMNFFFWNKNFSGGFCFFLSPL

Figure 7: B9 protein sequence.

VDQ-
KTAIAIAVALAGFATV**AQAA**ELVMTQSPSSLSASVGDRVTITCRASQSISSYLNWYQQKPGK
APKLLIYAASSLQSGVPSRFSGSGSGTDFTLTISSLQPEDFATYYCQQSYSTPPTFGQGTKV
EIKGGSSRSSSSGGGGSGGGGQV-
LVQSGAEVKKPGSSVKVSCKASGGTFSSYTISWVRQAPGQGLEWMGRIIPILGIPHYAQKFQ
GRVTITADKSTSTAYMELSSLRSEDTAVYYCATTQWELPKRGTFDIWGQGTMVTVSSASTQS
PSVTS**GQAGQ**HHHHHHGAYPYDVPDYAS-EGGGSEGWRF-GWRL-GRRFRWWLWFR-F-L-
KDGKR--GGYDRKCR-KRATV-R-RQT-FCRY-LRCCYRWVHW-RFRPC-
GEGATGGFCGAQFPKGQVGEGEIPL-
EKIRPNYFLPTPVEGGPLFLGGEKKKFFLLGKKKIPGAWFFFIPPFIFFFLTPEKGGHFLPP
PGGGRGGVILFFFFFPFTPHPSL-GSK

Figure 8: H8 protein sequence.

AQAA and GQAGQ mark restriction enzyme sites.[11] The his6-tag, linker, and HA-tag were all successfully translated in both Figure 7 and Figure 8. However, the stop codons (represented by a dash) between the restriction enzyme sites make both sequences inapplicable for mammalian cells.[12] Bacteria TG1 can convert stop codons so that the gene can be expressed, which suggests why positive ELISA results were yielded in experimental conditions. However, mammalian cells cannot translate stop codons and therefore this sequence is not applicable to mammalian cells.[11] To summarize, sequences containing stop codons between restriction enzyme markings do not code for a viable antibody against RBD.[11] In other words, sequences that do not contain stop codons between restriction enzyme markings must be discovered in order for them to be applicable to mammalian cells.

Discussion:

Two RBD-specific scFv antibodies carrying unique sequences were isolated from the phage display library. Positive ELISA results confirm that both antibodies bind specifically to SARS-CoV-2-RBD and not to 3% skim milk. However, additional protein sequence analysis by ExPASy revealed the presence of stop codons in both antibody sequences. Thus, despite their specificity to the RBD, both scFv antibodies are inapplicable for further therapeutic development or diagnostic tests against SARS-CoV-2. Nevertheless, the results of this study highlight the possibility of isolating clinically applicable neutralizing antibodies specific to SARS-CoV-2-RBD by phage display biopanning. These antibodies would be considered promising candidates for the development of a post-exposure therapy against COVID-19 infection.

As a modification, following the same procedure but with a different phage display library or with additional panning can help isolate RBD-specific scFv antibodies with intact protein sequences. Increasing the number of washing or increasing the washing stringency can also increase the selectivity and hence exclude weakly binding antibodies. Further investigation can involve a slight modification in methodology such as substituting the immune tube coating stage with immobilized proteins on beads.

Conclusion

In this study, we sought to discover an antibody against SARS-CoV-2-RBD. From our scFv library, no viable antibodies were found. While 2 RBD-specific antibodies carrying unique sequences were isolated and characterized, the presence of stop codons in their protein sequences make them inapplicable to mammalian cells. Further attempts to isolate an scFv antibody that is ultimately applicable to mammalian cells will be made using a different phage display library.

Acknowledgements

We thank YntoAb for providing us with an equipped laboratory.

References

1. Hu, B., Guo, H., Zhou, P. et al. Characteristics of SARS-CoV-2 and COVID-19. *Nat Rev Microbiol* 19, 141–154 (2021). https://doi.org/10.1038/s41579-020-00459-7
2. Andersen, K.G., Rambaut, A., Lipkin, W.I. et al. The proximal origin of SARS-CoV-2. Nat Med 26, 450–452 (2020). https://doi.org/10.1038/s41591-020-0820-9
3. SARS. https://www.cdc.gov/sars/index.html (accessed Feb 17, 2021).
4. Schoeman, D., Fielding, B.C. Coronavirus envelope protein: current knowledge. Virol J 16, 69 (2019). https://doi.org/10.1186/s12985-019-1182-0
5. Machhi, J., Herskovitz, J., Senan, A.M. et al. The Natural History, Pathobiology, and Clinical Manifestations of SARS-CoV-2 Infections. *J Neuroimmune Pharmacol* 15, 359–386 (2020). https://doi.org/10.1007/s11481-020-09944-5
6. Kruse RL. Therapeutic strategies in an outbreak scenario to treat the novel coronavirus originating in Wuhan, China [version 2; peer review: 2 approved]. F1000Research 2020, 9:72 (https://doi.org/10.12688/f1000research.22211.2)
7. Kim, H.-Y.; Lee, J.-H.; Kim, M. J.; Park, S. C.; Choi, M.; Lee, W.; Ku, K. B.; Kim, B. T.; Park, E. C.; Kim, H. G.; Kim, S. I. Development of a SARS-CoV-2-Specific Biosensor for Antigen Detection Using ScFv-Fc Fusion Proteins. Biosensors and Bioelectronics 2021.
8. Clark, M. F.; Lister, R. M.; Bar-Joseph, M. ELISA Techniques. Methods in Enzymology 2004, 742–766. https://doi.org/10.1016/0076-6879(86)18114-6
9. Lin A.V. (2015) Indirect ELISA. In: Hnasko R. (eds) ELISA. Methods in Molecular Biology, vol 1318. Humana Press, New York, NY. https://doi.org/10.1007/978-1-4939-2742-5_
10. Haque, K.A., Pfeiffer, R.M., Beerman, M.B. et al. Performance of high-throughput DNA quantification methods. BMC Biotechnol 3, 20 (2003). https://doi.org/10.1186/1472-6750-3-20
11. Gasteiger, Elisabeth & Gattiker, Alexandre & Hoogland, Christine & Ivanyi, Ivan & Appel, Ron & Bairoch, Amos. (2003). ExPASy: The proteomics server for in-depth protein knowledge and analysis. Nucleic acids research. 31. 3784-8. 10.1093/nar/gkg563.
12. DNA Miniprep protocol handbook, 2020.

Authors

Claire Lee is currently a senior at Chadwick International, an international school located in Incheon, South Korea. As her interests lie in biological sciences, her choices for majors

are biology and/or pre-dentistry.

Seungjae Kim is a current junior that attends Chadwick International School. He is interested in neuroscience and molecular biology. He has received awards in International Genetically Engineered Machine (IGEM) 2019 and Korean Science and Engineering Fair (2020). He is also a participant of Genius Olympiad 2021.

Haryeong Eo is currently a sophomore attending Shanghai American School Puxi. It was her pleasure to participate in this amazing research for the first time and serve as a team member. She hopes this experience will help set the groundwork for studying biomedical engineering.

Christine Yi is a junior at Seoul International School in South Korea. She is heavily interested in neuroscience, medicine, and molecular biology, and has partaken in various research projects. As an aspiring pre-med student, she spends her time volunteering in nursing homes and professional laboratories.

DOI: 10.36838/v4i1.13

IJHSR
ijhighschoolresearch.org
RESEARCH ARTICLE

A Hypercube unfolding that Tiles R^2 (and R^3)

Trun V. Ramteke

Private International English School, Mussafah, Sector 9, Shabiya, Abu Dhabi, P.O. Box: 39972, UAE; trunvishal.ramteke@gmail.com

ABSTRACT: In their pioneering work, G. Diaz and J. O'Rourke[1] show that the four-dimensional hypercube has an unfolding that tiles three-dimensional space, and can be further unfolded to tile two-dimensional space. This paper presents an alternative path to unfolding the hypercube to tile lower-dimensional space.

KEYWORDS: Mathematics; Geometry and Topology; Computational Geometry; Dimension Descending Tilers; Hypercube Unfoldings; Octocube Unfoldings.

Introduction

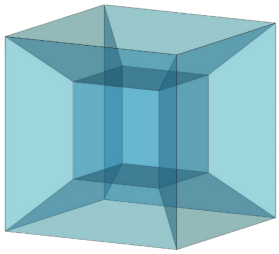

Figure 1: The 4-D hypercube's shadow in 3-D.

The hypercube is the 4-dimensional analog of the cube (Figure 1). Unfolding the hypercube will give its 3-D net like in Figure 2(a); analogous to how unfolding a cube will give its 2-D net (Figure 2(b)).

A 3-D cube has 11 distinct nets and each net is a monohedral tile (monohedral, a tessellation where each tile is congruent). A beautiful pattern emerges, the cube (that obviously tiles $\mathbb{R}^3$) has unfoldings that tile $\mathbb{R}^2$. This entitles the cube to be a dimension descending tiler (DDT).

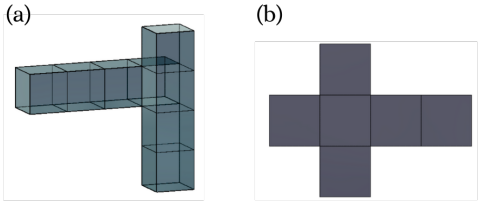

Figure 2: (a) A net of the Hypercube· (b) A net of the cube.

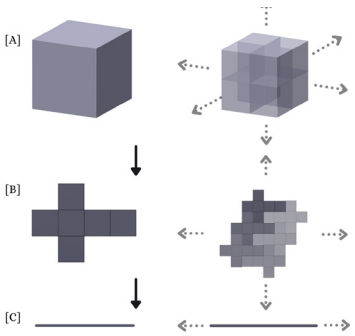

Figure 3: A DDT descending dimensions. (Let an alphabet mark the rung on the ladder) The DDT at [A], its net down a dimension at [B] and so on.

The hypercube – which itself tiles 4-D space – has 261 distinct 3-D nets that tile $\mathbb{R}^3$,[2] analogous to the previous example of the 3-D cube. *Following this pattern, will these 3D nets, in turn, have edge-unfoldings that will tile* $\mathbb{R}^2$?

Diaz and O'Rourke showed the hypercube indeed has a net (that tiles $\mathbb{R}^3$) whose edge-unfolding (an unfolding that cuts along the edges of the polycube) perfectly tiles $\mathbb{R}^2$. Stefan Langerman and Andrew Winslow also showed that the 'Dali Cross' – one of the 261 unfoldings of the hypercube – has an edge-unfolding that tiles the plane.[3] Thus, showing the tesseract to be a dimension descending tiler, from $\mathbb{R}^4$ to $\mathbb{R}^1$. {Note that the unfolding of the 2-D net is a line that obviously tiles $\mathbb{R}^1$} This paper explores another path to unfold the 4-D hypercube to tile lower-dimensional spaces.

Results and Discussion

A 3-D cube has 6 faces and its net is a 6-square polysquare (refer to Figure 2); similarly, the tesseract has 8 cubes, and its net is an 8-cube polycube, termed an octocube (In this paper, an octocube specifically refers to the 8-cube polycube face-unfolding of the hypercube). All 261 octocubes have been shown to tile $\mathbb{R}^3$. Of which, this paper will focus on the edge-unfolding of octocube #72. (The octocubes are numbered according to Moritz Firsching's list of octocubes).[4] Do note that octocube #72 is quite similar to octocube #120 in Figure 2 of Diaz and O'Rourke's paper.

Net of the hypercube tiling R^3:

First, it can be observed that octocube #72 tiles $\mathbb{R}^3$. The proof for this tiling was first shown by Jose A. Gonzalez.[5] This paper will briefly describe how octocube #72 tiles $\mathbb{R}^3$, in a simpler but tweaked way. The following stacking procedure is very similar to that in Figures 3 and 4 of Diaz and O'Rourke's paper.

1. First it is observed that the octocubes can be 'inserted' into each other to form a stack of 3 octocubes (Figure 4). This forms a uniform 'staircase' on the back left and back right side (back right side not visible in Figure 4), and the front bottom and front top sides. {Of course, choosing three octocubes is arbitrary. Three were chosen for simplicity; it can be imagined as an infinite number of octocubes to be stacked in such a way to form an infinite diagonal from south-west to north-east}.

DOI: 10.36838/v4i1.14

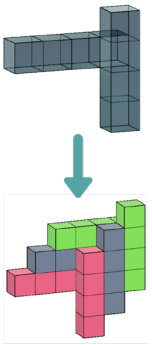

Figure 4: 3 stacked octocube #72s.

2. Stack two of these structures to get the structure in Figure 5. Here, the red block's back left staircase is nestled into its 'negative' in the blue stack (present behind and below, not visible in Figure 5). Again, an infinite diagonal of this structure can be imagined.

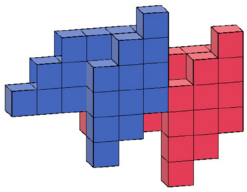

Figure 5: Stacked triplets of octocube #72s.

3. A larger portion of the infinite diagonal stack is shown in Figure 6. Stacking this infinite diagonal on the top and the bottom, infinite times, will result in a 2-cube thick slab that runs forever in the X-Z plane. Just as in Figure 4 of Diaz and O'Rourke's paper.

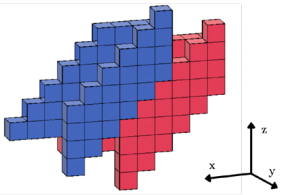

Figure 6: A portion of the infinite diagonal stack.

4. It is obvious that layering these 2-cube thick slabs (in the y-direction) will tile $\mathbb{R}^3$ perfectly. Hence proved the octocube tiles 3-dimensional space (proved first by Jose A. Gonzalez).

This is the first descent down a dimension.

The net of Octocube #72:

Now it is necessary to introduce the net of this Octocube that will tile 2D space. This is the second descent down a dimension.

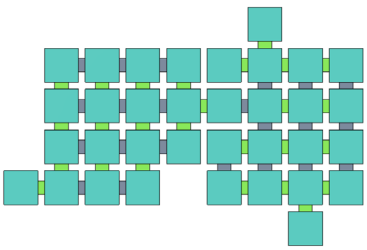

Figure 5: Net of octocube #72. The green joints between squares are all valley-folds, and the blue joints do not hinge.

A step-by-step transformation of the net of octocube #72 is shown in Figure 8.

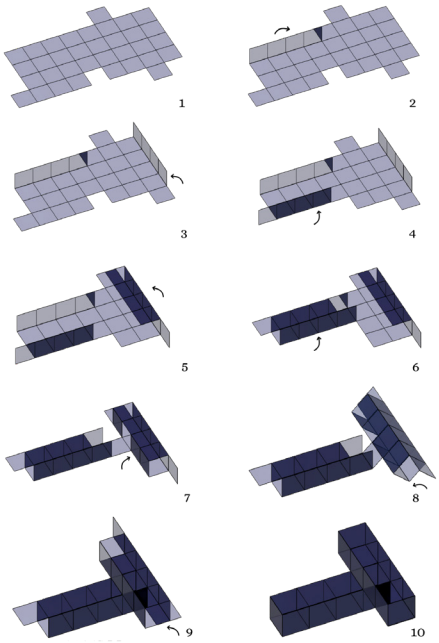

Figure 8: A step-by-step transformation of the net to octocube #72.

Not all nets are Valid:

All octocubes tile $\mathbb{R}^3$, so do all the unfoldings of an octocube tile $\mathbb{R}^2$? The answer is no. Not all nets of octocube #72 tile $\mathbb{R}^2$. The following are (two of many) valid nets, but do not tile $\mathbb{R}^2$ (Figures 9 and 10).

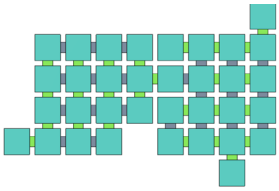

Figure 9: A slight modification of the net in Figure 7, that makes it not tile $\mathbb{R}^2$.

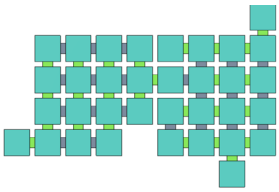

Figure 10: Another net of octocube #72 that does not tile $\mathbb{R}^2$.

Net of the Octocube #72 tiling R^2:

The net of octocube #72 tiling $\mathbb{R}^2$ is shown in Figure 11.

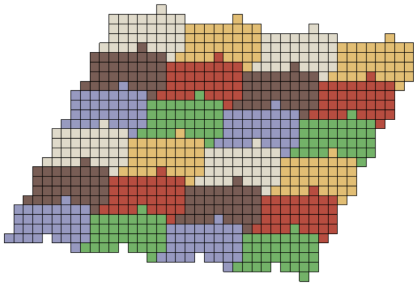

Figure 11: A net of the octocube shown tiling $\mathbb{R}^2$.

DOI: 10.36838/v4i1.14

Conclusions

The paper has presented an alternative path than what has been by G. Diaz, J. O'Rourke, and S. Langerman, and A. Winslow to unfolding the hypercube to tile lower-dimensional space. However, it is still left to answer (besides what has not been answered in Diaz and O'Rourke's paper):

• How many nets of an octocube are there that do tile $\mathbb{R}^2$; or does only one net tile $\mathbb{R}^2$?

• What is the ratio between the nets that do and those that do not tile $\mathbb{R}^2$?

• What is this ratio when a higher dimensional DDT (if they exist) descends the ladder (the ladder as was in Figure 3)?

Acknowledgements

I would thank Matt Parker and all mathematicians and scientists for doing great things every day and inspiring young minds.

References

1. Diaz, G., O'Rourke, J. Hypercube Unfoldings that Tile R^3 and R^2. *arXiv*. 2015, arXiv:1512.02086 [cs.CG].
2. Whuts. https://whuts.org/ (accessed 2021-07-10).
3. Andrew Winslow, *dali-cross-unfolding-pnc* https://andrewwinslow.com/images/dali-cross-unfolding-pnc.pdf (accessed 2021-08-5).
4. *Moritz Firsching unfoldings of the hypercube*. https://mo271.github.io/mo/198722/unfoldings.html (accessed 2021-07-10).
5. *Whuts Unfolding* 72, https://whuts.org/unfolding/72 (accessed 2021-07-10).

Author

Trun loves physics and recreational math. He is passionate about exploring new ideas and breaking barriers. Being an avid inventor and entrepreneur, he has ventured into advancing miniature satellite technology. Trun aspires to advance Quantum Computing to accelerate technological development and solve the world's biggest challenges.

IJHSR
ijhighschoolresearch.org
■ RESEARCH ARTICLE

Utilizing Coffee Ground Waste to Enhance Polyhydroxyalkanoates (PHA) Derived from Soil Bacteria

Eunice Rhee

Seoul International School, 15, Seongnam-daero 1518 beon gil, Sujeong-gu, Seongnam-si, Gyeonggi-do, 13113, Republic of Korea; gosyber@suwon.ac.kr

ABSTRACT: Bioplastics are known to have many benefits for the environment, such as slowing down global warming by reducing greenhouse gases and preventing environmental pollution caused by plastic waste. Due to these advantages, it is considered a future-oriented industry, with diverse studies progressing for its widespread use. However, despite its numerous actual and potential uses, the high production costs hinder bioplastic from completely replacing conventional plastics. Therefore, the focus of this research was to develop a method to increase the production efficiency of PHA (Polyhydroxyalkanoates), a natural polymer with high similarity to synthetic plastic, using coffee extract waste. This not only solves the existing environmental problems caused by coffee waste, but also serves as a rich carbon source for bacteria to increase the PHA production rate. Through this experiment, *B. Megaterium* was successfully selected as our choice of PHA producing soil bacteria. Also, coffee oil was efficiently extracted using a stovetop espresso maker and the inclusion of 3 % coffee oil was found to significantly increase PHA production in *B. Megaterium*. In conclusion, this research not only provides a solution for this coffee waste problem, but also improves the production of PHA in bacteria and possibly reduces the production costs of bioplastics.

KEYWORDS: Microbiology; Environmental Microbiology; Soil Bacteria; Bioplastic; PHA.

■ Introduction

Lack of nutrients in an environment can often lead to competition within bacterial populations. In these conditions, bacteria utilize numerous strategies, one of which is storing nutrients not only for the enhancement of their own survival, but also to deprive its competitors of them.[1] PHA (Polyhydroxyalkanoates) is able to fulfill their role as storage units for cells in challenging environmental conditions by storing excess carbon and energy.[2] Thus, harsh conditions or presence of nutrients may be a determining factor in the frequent occurrence of PHA in bacteria.

PHA, a type of natural polymer, is a prokaryotic storage macromolecule, which is collected as water insoluble granules in bacteria cytoplasm.[3] PHA is composed of repeating monomers of β-hydroxyalkanoic acids joined by bonds between the carboxyl group and the hydroxyl group.[4] *Scl*-PHA consists of monomers of three to five carbon atoms, exhibiting thermoplastic properties. *Mcl*-PHA consists of monomers of six to 16 carbons and demonstrates latex-like features. Blends of these properties help make up for the unfavorable drawbacks that may be present when produced as bioplastic. Still, PHA has numerous benefits, such as biodegradability, biocompatibility, availability in numerous renewable resources, and the highest similarity to standard chemically synthesized plastics, and this has led to the popularity of its integration in the production of sustainable products.[5]

In order to become an adequate replacement for normal plastics, the production costs need to be minimized, while the productivity is maximized.[6] When producing biodegradable plastic from soil bacteria, one major problem that greatly increases the costs is the lack of a sufficient carbon source.[7] This causes the need for more bacteria in the production of bioplastic.[8]

Due to this reason, many researchers have been searching for a prospective, inexpensive substrate that may provide fatty acids, as they are utilized during a β-oxidation pathway that directly produces acetyl-CoA, a precursor of PHA production.[4] Plant oils are highly suitable because out of the other inexpensive carbon sources, the theoretical yield of PHA production from plant oils is found to be up to 1.0 g of PHA per gram of plant oil, which is a much higher quantity than others.[9]

As a substance derived from a plant, coffee oil is composed of high quantities of carbon atoms per weight.[10] Therefore, it was utilized in the experiment because it had the greatest production of PHA out of the other possible waste or inexpensive oils.[11] In the coffee industry, most of the ground coffee wastes are either burned or discharged into the environment.[12] As the industry grows, the burden of disposal also seems to be exacerbated. The use of coffee oil as a carbon source can therefore be beneficial in multiple ways, as it not only provides a solution for the coffee waste problem, but also improves the production of PHA in bacteria and possibly reduces the production costs of bioplastics.

■ Methods

Agar plate preparation for soil bacteria:

Nile red staining was used to specify the types of bacteria that would contain PHA. 5 mg per 1 mL of the solvent, DSMO, was first used to make the Nile red stock solution.[13] Then, 1.5 g of agar, 2.5 g of LB, 50 mL of water, and 50 µL of the Nile Red stock solution were combined and microwaved to make the solution on an agar plate. To ensure that all plates had an equal amount of solution, 9 mL was poured in each

DOI: 10.36838/v4i1.15

of the 5 agar plates. and the elbow movement. A micro servo was positioned on the wrist part and a high torque servo on the elbow part.

Optimization of culture condition:

In order to determine the most favorable concentration, three different concentrations were tested on separate plates. A soil sample containing about 40-50 g was first collected in a 50 mL tube from Seoul, Dogok-dong. Then, 0.1 g of this soil sample was measured and moved to a labeled 15 mL tube. 10 mL of deionized water was then added into this tube using a pipet to create a solution with a soil concentration of 1:100. To mix thoroughly, the solution was vortexed for 30 min. Then, 1 mL of the solution was evenly distributed on an agar plate using a spreader to make a 1:1,000 sample. The remaining solution was used to further dilute the sample to 1:10,000, 1:50,000 and 1:100,000 plate samples. After slightly drying them, the agar plates were placed in a 37 ºC incubator for approximately 16 hours.

Coffee oil extraction from coffee ground:

To prepare the extraction, coffee grounds were dried at 60 ºC for 72 hours. Then, to extract hydrophobic coffee oil, 50 mL of N-hexane, which is also a hydrophobic solvent, was placed in the water tank of a stovetop espresso maker. The filter basket contained 20 grams of the dried coffee grounds, while the upper chamber was left empty. The maker was placed on a hot plate stirrer at 69 ºC for 10 minutes to prevent overheating the N-hexane, which has a boiling point of 68 ºC.

Selection of PHA producing bacteria:

When the Nile red agar plates were placed under blue light, the bacteria containing PHA turned pink or red. Out of the hundreds of bacterial colonies, five of the most vibrant pink or red colonies were selected, making sure some of these had varying qualities to guarantee different bacterium types. As a negative control, one colony, which was neither pink nor red, was selected to show the difference in PHA producing rates. These 6 selections were then labeled with a marker on the back of the plate.

PHA extraction from soil bacteria:

To extract the PHA, first, 1 mL of LB solution was placed in 1.5 mL tubes. Then, frozen bacteria stocks were thawed to room temperature and seeded into the 1 mL LB media, along with 0 %, 1.5 % and 3 % coffee oil. Once the bacteria were cultured in a 37 ºC shaking incubator for 16 hours, the tubes were centrifuged for 5 minutes at 4,000 g. After 5 minutes, bacteria were collected as a pellet and the remaining solution was carefully removed. Then, 100 µL of chloroform was added to resuspend the bacteria. Once the chloroform was removed, 500 µL of chloroform was added. Bacteria were then incubated at 60 ºC to completely dissolve the pellet. The samples were further vortexed for 10 min, centrifuged at 13,000 g for 5 min. and then carefully moved to a new 1.5 mL tube. 500 µL of chilled methanol was added to the solution to obtain pure PHA by methanol precipitation. When the final solution was dried in the drying oven for 60 ºC overnight, PHA was obtained in a form of white powder.

Identification of bacteria strain with BLAST sequence alignment:

DNA was extracted and 16S ribosomal RNA gene was specifically amplified by polymerase chain reaction (PCR). After the amplified sequence was analyzed by Sanger sequencing, about 700 bp of nucleotide sequence were identified. Then, this DNA sequence was inserted in nucleotide BLAST as a query sequence.

Results and Discussion

Optimizing the concentration of bacteria to grow on an agar plate:

The objective of this experiment was to determine the optimal concentration of bacteria when cultured on an agar plate. This was an essential step to be established prior to the rest of the study because if the concentration of bacteria was too high, lack of space would inhibit the growth of different bacterial colonies. On the other hand, if the concentration of bacteria was too low, the chance of the agar plate containing bacteria with PHA would be decreased. Determining the optimal condition would also be essential because the concentrations that are either too high or too low would make it difficult to extract the bacteria after the Nile Red Staining. The soil was diluted in water with concentrations of 1:1,000, 1:10,000, 1:50,000, and 1:100,000. After the four solutions were spread evenly on agar plates and placed in the incubator for 16 hours, the optimal concentration was determined to be within 1:10,000 and 1:50,000 (Figure 1).

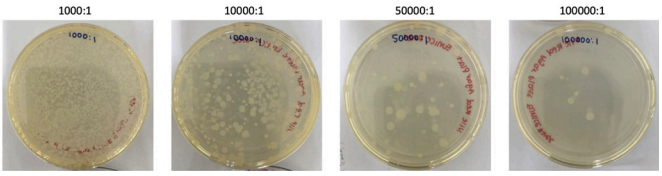

Figure 1: Effect of four different dilution conditions on the number of colonies in an agar plate. The optimal dilution condition was found to be between 1:10,000 and 1:50,000, which shows that more than 40 bacterial colonies were clearly separated from one another.

Selection of PHA producing bacteria:

When shone under the light, differences in fluorescence were able to be classified. Smaller colonies seemed to have stronger shades of red, while larger groups tended to have lighter shades. Overall, the colonies that exhibited red shades seemed to have a comparably faded outline. (Figure 2)

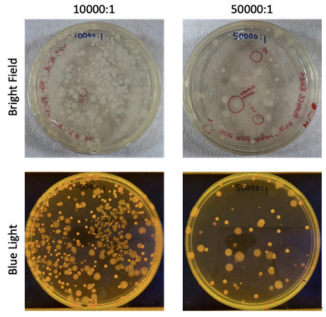

Figure 2: Selection of PHA-producing bacteria by Nile red staining. The figure illustrates the two most suitable concentrations under a blue light. PHA-producing bacteria can be distinguished by red colonies.

Images of selected bacteria:

Next, the tip of a pipet was used to select six isolated single colonies: 5 colonies exhibiting red or pink color and 1 negative control colony. These colonies were diluted in 1 mL of water. 2 µL of each selected colony was placed under the microscope to confirm that each sample exhibited only one phenotype, as it would help guarantee that there was no cross contamination. For the experiment, colony #1 was used due to its highest vibrancy in redness from the Nile red staining. As shown in Figure 3, the bacteria from colony #1 have long, string-like figures, and when zoomed in further, short sticks-like shapes joined to create its twisting figure.

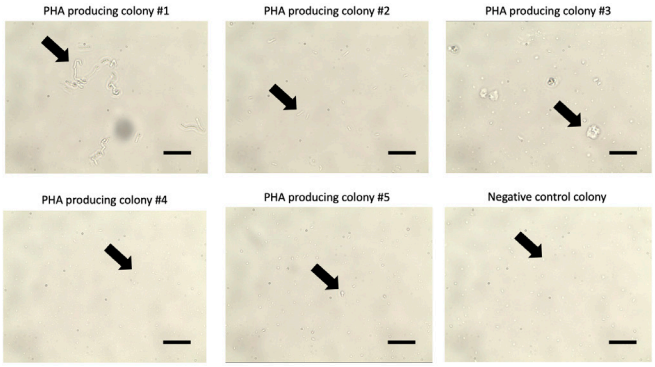

Figure 3: Microscope images of six selected bacterial colonies exhibiting different phenotypes. Each colony had one corresponding shape, indicating no cross contamination occurred. The arrow indicates the position of bacteria in the image. Scale bar = 10 µm.

Coffee oil extraction from coffee grounds:

The stovetop espresso maker that was used for the extraction had three compartments: the water tank, where the N-hexane solvent was placed, the filter basket, where the coffee grounds were placed, and the upper chamber, where the coffee oil would be collected. (Figure 4).

The lid in the upper chamber had a small hole that allowed air to pass through, while the water tank was tightly sealed to generate pressure difference. To summarize how the stovetop espresso maker works, when heated, the hydrophobic solution would vaporize in the water tank, attracting the oil in the coffee grounds as it passes through the filter basket, then it turns back into liquid form as the pressure drops in the upper chamber, creating coffee oil.

Once the coffee oil was extracted by a stovetop espresso maker, N-hexane, which originally had a clear color, now had a brown tint to it, which darkened each time the extraction process was repeated three times.[12]

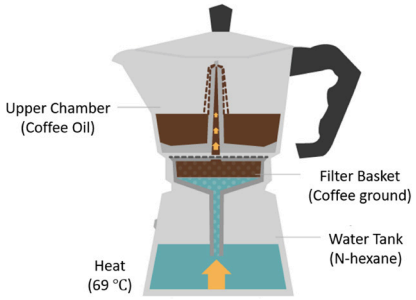

Figure 4: Schematic drawing of stovetop espresso maker as an extractor for coffee oil.

Effect of coffee oil on PHA production:

The white powder in each petri dish in Figure 5A shows the extracted PHA from the bacteria. Figure 5A shows how the white powder increases as the percentage of coffee oil supplementation increases. This indicates that the coffee oil enhances PHA production in bacteria.

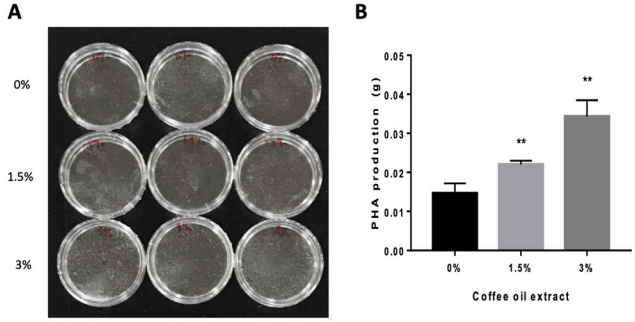

Figure 5: Enhanced PHA production in bacteria by coffee oil supplementation. (A) The image of purified PHA from bacteria. (B) Quantification of PHA production after supplementation with 0%, 1.5%, 3% coffee oil extract. Unpaired t-test was used to identify the statistical significance. (** indicates p-value less than 0.01).

When the extracted coffee oil was added to the LB solution, it was found that PHA production increased as the percentage of coffee oil increased. When the coffee oil was absent, the PHA production was about 0.015 g, but when 1.5 % of the solution was coffee oil, the PHA production increased to 0.023 g. The PHA production increased even further with 3 % coffee oil to 0.035 g. (Figure 5B) In this experiment, 3% coffee oil supplementation during bacterial culture showed the highest PHA production.

Bacillus megaterium strain A6-G 16S ribosomal RNA gene, partial sequence

Sequence ID: MT588737.1 Length: 1290 Number of Matches: 1

Range 1: 19 to 718 GenBank Graphics Next Match

Score	Expect	Identities	Gaps	Strand
1293 bits(700)	0.0	700/700(100%)	0/700(0%)	Plus/Plus

```
Query  1    GCAGTCGAGCGACTGATTAGAAGCTTGCTTCTATGACGTTAGCGGCGGACGGGTGAGTAA  60
            ||||||||||||||||||||||||||||||||||||||||||||||||||||||||||||
Sbjct  19   GCAGTCGAGCGACTGATTAGAAGCTTGCTTCTATGACGTTAGCGGCGGACGGGTGAGTAA  78

Query  61   CACGTGGGCAACCTGCCTGTAAGACTGGGATAACTTCGGGAAACCGAAGCTAATACCGGA  120
            ||||||||||||||||||||||||||||||||||||||||||||||||||||||||||||
Sbjct  79   CACGTGGGCAACCTGCCTGTAAGACTGGGATAACTTCGGGAAACCGAAGCTAATACCGGA  138

Query  121  TAGGATCTTCTCCTTCATGGGAGATGATTGAAAGATGGTTTCGGCTATCACTTACAGATG  180
            ||||||||||||||||||||||||||||||||||||||||||||||||||||||||||||
Sbjct  139  TAGGATCTTCTCCTTCATGGGAGATGATTGAAAGATGGTTTCGGCTATCACTTACAGATG  198

Query  181  GGCCCGCGGTGCATTAGCTAGTTGGTGAGGTAACGGCTCACCAAGGCAACGATGCATAGC  240
            ||||||||||||||||||||||||||||||||||||||||||||||||||||||||||||
Sbjct  199  GGCCCGCGGTGCATTAGCTAGTTGGTGAGGTAACGGCTCACCAAGGCAACGATGCATAGC  258

Query  241  CGACCTGAGAGGGTGATCGGCCACACTGGGACTGAGACACGGCCCAGACTCCTACGGGAG  300
            ||||||||||||||||||||||||||||||||||||||||||||||||||||||||||||
Sbjct  259  CGACCTGAGAGGGTGATCGGCCACACTGGGACTGAGACACGGCCCAGACTCCTACGGGAG  318

Query  301  GCAGCAGTAGGGAATCTTCCGCAATGGACGAAAGTCTGACGGAGCAACGCCGCGTGAGTG  360
            ||||||||||||||||||||||||||||||||||||||||||||||||||||||||||||
Sbjct  319  GCAGCAGTAGGGAATCTTCCGCAATGGACGAAAGTCTGACGGAGCAACGCCGCGTGAGTG  378

Query  361  ATGAAGGCTTTCGGGTCGTAAAACTCTGTTGTTAGGGAAGAACAAGTACAAGAGTAACTG  420
            ||||||||||||||||||||||||||||||||||||||||||||||||||||||||||||
Sbjct  379  ATGAAGGCTTTCGGGTCGTAAAACTCTGTTGTTAGGGAAGAACAAGTACAAGAGTAACTG  438

Query  421  CTTGTACCTTGACGGTACCTAACCAGAAAGCCACGGCTAACTACGTGCCAGCAGCCGCGG  480
            ||||||||||||||||||||||||||||||||||||||||||||||||||||||||||||
Sbjct  439  CTTGTACCTTGACGGTACCTAACCAGAAAGCCACGGCTAACTACGTGCCAGCAGCCGCGG  498

Query  481  TAATACGTAGGTGGCAAGCGTTATCCGGAATTATTGGGCGTAAAGCGCGCGCAGGCGGTT  540
            ||||||||||||||||||||||||||||||||||||||||||||||||||||||||||||
Sbjct  499  TAATACGTAGGTGGCAAGCGTTATCCGGAATTATTGGGCGTAAAGCGCGCGCAGGCGGTT  558

Query  541  TCTTAAGTCTGATGTGAAAGCCCACGGCTCAACCGTGGAGGGTCATTGGAAACTGGGGAA  600
            ||||||||||||||||||||||||||||||||||||||||||||||||||||||||||||
Sbjct  559  TCTTAAGTCTGATGTGAAAGCCCACGGCTCAACCGTGGAGGGTCATTGGAAACTGGGGAA  618

Query  601  CTTGAGTGCAGAAGAGAAAAGCGGAATTCCACGTGTAGCGGTGAAATGCGTAGAGATGTG  660
            ||||||||||||||||||||||||||||||||||||||||||||||||||||||||||||
Sbjct  619  CTTGAGTGCAGAAGAGAAAAGCGGAATTCCACGTGTAGCGGTGAAATGCGTAGAGATGTG  678

Query  661  GAGGAACACCAGTGGCGAAGGCGGCTTTTTGGTCTGTAAC  700
            |||||||||||||||||||||||||||||||||||||||
Sbjct  679  GAGGAACACCAGTGGCGAAGGCGGCTTTTTGGTCTGTAAC  718
```

Figure 5: Nucleotide Blast DNA sequence alignment analysis shows that colony #1 bacteria DNA is identical to *B. Megaterium* 16S ribosomal RNA. Query is an input sequence analyzed from colony # 1 bacteria. Subject (Sbjct) is a sequence searched within a database.

DOI: 10.36838/v4i1.15

BLAST program allows DNA sequences from all organisms including bacteria to be searched.[7] Since many organisms' genomic sequences are already identified and saved in the genome databases, BLAST is able to provide the best matching sequence from these databases for bacterial identification. When the best matching sequence result was analyzed, the DNA sequence from colony #1 was found to be identical to *B. Megaterium* 16S ribosomal RNA (Figure 6). This DNA analysis result indicates that the identity of colony #1 is *B. Megaterium*.

Conclusion

When conducting this experiment, the concentration of bacteria that would be ideal for growth on the agar plate was first determined. While these were left to grow, the coffee ground waste was utilized to extract coffee oil. Once the optimized concentration was specified, the soil bacteria was left to grow in the Nile red agar plate. The reddest colony, which has been identified as *B. Megaterium* by DNA sequencing, was then selected and prepared for PHA isolation. Three trials of three different concentrations of coffee oil were conducted for reliable results. Through procedures including centrifugation, chloroform washing, and methanol precipitation, pure PHA was obtained. Once this final solution was dried, the PHA was in a form of powder in petri dishes. As the percentage of coffee oil increased, the PHA production also increased, indicating that coffee oil increased the efficiency of the PHA production.

Like most experiments, however, this experiment also had some limitations and compromises. One was the utilization of N-hexane during the coffee oil extraction process. N-hexane is commonly used to extract oils but is also known to have harmful effects on humans. Exposure to such substances may result in damage ranging from central nervous system effects to polyneuropathy in humans.[14] In future studies, finding a substitute for N-hexane will help enhance the quality of this bioplastic.

To conclude, not only is this method both a highly efficient and cost-effective way to produce PHA, but it also reuses wasted coffee grounds during the production of coffee oil. This issue pertains highly to the authors, as South Korea is ranked third in producing the most plastic waste per person and has coffee consumption rates increasing by 20.3%.[15] In the future, this innovative solution may help alleviate the detrimental effects of such problems in South Korea, and possibly, the Earth's environment.

Acknowledgements

I would like to express my special thanks to my parents and my mentor who gave me the opportunity to work on this wonderful project. Additionally, they helped me in learning more about the scientific procedure and the sustainable production of biodegradable substances.

References

1. Haruta, S.; Kanno, N., Survivability of Microbes in Natural Environments and Their Ecological Impacts. *Microbes Environ* 2015, 30 (2), 123-5.
2. Chen, G. Q.; Jiang, X. R., Engineering bacteria for enhanced polyhydroxyalkanoates (PHA) biosynthesis. *Synth Syst Biotechnol* 2017, 2 (3), 192-197.
3. Somleva, M. N.; Peoples, O. P.; Snell, K. D., PHA bioplastics, biochemicals, and energy from crops. *Plant Biotechnol J* 2013, 11 (2), 233-52.
4. Sabapathy, P. C.; Devaraj, S.; Meixner, K.; Anburajan, P.; Kathirvel, P.; Ravikumar, Y.; Zabed, H. M.; Qi, X., Recent developments in Polyhydroxyalkanoates (PHAs) production - A review. *Bioresour Technol* 2020, 306, 123132.
5. Anjum, A.; Zuber, M.; Zia, K. M.; Noreen, A.; Anjum, M. N.; Tabasum, S., Microbial production of polyhydroxyalkanoates (PHAs) and its copolymers: A review of recent advancements. *Int J Biol Macromol* 2016, 89, 161-74.
6. Zhao, K.; Deng, Y.; Chun Chen, J.; Chen, G. Q., Polyhydroxyalkanoate (PHA) scaffolds with good mechanical properties and biocompatibility. *Biomaterials* 2003, 24 (6), 1041-5.
7. Amaro, T.; Rosa, D.; Comi, G.; Iacumin, L., Prospects for the Use of Whey for Polyhydroxyalkanoate (PHA) Production. *Front Microbiol* 2019, 10, 992.
8. Luengo, J. M.; Garcia, B.; Sandoval, A.; Naharro, G.; Olivera, E. R., Bioplastics from microorganisms. *Curr Opin Microbiol* 2003, 6 (3), 251-60.
9. Budde, C. F.; Riedel, S. L.; Willis, L. B.; Rha, C.; Sinskey, A. J., Production of poly(3-hydroxybutyrate-co-3-hydroxyhexanoate) from plant oil by engineered Ralstonia eutropha strains. *Appl Environ Microbiol* 2011, 77 (9), 2847-54.
10. Cruz, M. V.; Paiva, A.; Lisboa, P.; Freitas, F.; Alves, V. D.; Simoes, P.; Barreiros, S.; Reis, M. A., Production of polyhydroxyalkanoates from spent coffee grounds oil obtained by supercritical fluid extraction technology. *Bioresour Technol* 2014, 157, 360-3.
11. Rathbone, S.; Furrer, P.; Lubben, J.; Zinn, M.;Cartmell, S., Biocompatibility of polyhydroxyalkanoate as a potential material for ligament and tendon scaffold material. *J Biomed Mater Res A* 2010, 93 (4), 1391-403.
12. Gigliobianco, M. R.; Campisi, B.; Peregrina, D. V.; Censi, R.; Khamitova, G.; Angeloni, S.; Caprioli, G.; Zannotti, M.; Ferraro, S.; Giovannetti, R.; Angeloni, C.; Lupidi, G.; Pruccoli, L.; Tarozzi, A.; Voinovich, D.; Martino, P. D., Optimization of the Extraction from Spent Coffee Grounds Using the Desirability Approach. *Antioxidants (Basel)* 2020, 9 (5).
13. Spiekermann, P.; Rehm, B. H.; Kalscheuer, R.; Baumeister, D.; Steinbuchel, A., A sensitive, viable-colony staining method using Nile red for direct screening of bacteria that accumulate polyhydroxyalkanoic acids and other lipid storage compounds. *Arch Microbiol* 1999, 171 (2), 73-80.
14. Ono, Y.; Takeuchi, Y.; Hisanaga, N., A comparative study on the toxicity of n-hexane and its isomers on the peripheral nerve. *Int Arch Occup Environ Health* 1981, 48 (3), 289-94.
15. Je, Y., Jeong, S., & Park, T. Coffee consumption patterns in Korean adults: The Korean national health and nutrition examination survey (2001-2011). Asia Pacific Journal of Clinical Nutrition 2014, 23(4), 691–702.

Author

Eunice Rhee is currently a student at Seoul International School. She enjoys traveling to new places and trying new foods. She has interests in biology, environmental science, and data science and hopes to major in these fields.

IJHSR
ijhighschoolresearch.org
RESEARCH ARTICLE

Detecting Lymphotoxin-alpha Gene Mutation, a Genetic Risk Factor in Community-acquired Pneumonia, Using Allele-specific PCR

Seyun Bang

Choate Rosemary Hall, 333 Christian St, Wallingford, CT, 06492, USA; gosyber1@gmail.com

ABSTRACT: Genetic mutation in the Lymphotoxin-alpha (LTA) gene, LTA 250G>A (Substitution, position 250, G→A) is known to cause severe inflammatory responses to infectious diseases, and one of the major inflammatory conditions this mutation is known to cause is enhanced risk of septic shock in community-acquired pneumonia. Previously proposed methods for detecting this mutation are time consuming and require special instruments. To readily detect this mutation while preserving high accuracy, we used multiplex PCR. The results indicate that the PCR condition proposed in this study allows us to detect both LTA wildtype (wt) and LTA 250G>A with high accuracy. Both genotypes can be distinguished by different sizes of DNA amplification in gel electrophoresis. We were able to confirm this using four different human cell lines: A172 (LTAwt), SK-MEL2 (LTAwt), A375sm (LTAwt), and MCC13 (LTA 250G>A). This novel method can be used for rapid and accurate detection of LTA 250G>A, which is a genetic risk factor for community-acquired pneumonia. This is a simple and inexpensive method for mutation detection, which is accessible to minimally equipped laboratories.

KEYWORDS: Molecular Biology, Genetic Mutation, LTA mutation, community-acquired pneumonia, allele-specific PCR.

Introduction

Community-acquired pneumonia (CAP) encompasses cases of infectious pneumonia in patients who live in a community.[1] The disease is commonly caused by pathogens such as *Streptococcus pneumoniae*, influenza A, *Mycoplasma pneumoniae* and *Chlamydophila pneumoniae*.[2] It is the third most common reason for hospital admission for adults, and in the United States, it is the leading cause of death from infectious diseases. CAP is also one of the leading causes of severe sepsis, which has a considerably high fatality rate.[3]

Proinflammatory genes such as lymphotoxin-alpha (LTA) code for pro-inflammatory cytokines that play a central role in inflammatory diseases of infectious origin, such as CAP. Overexpression of proinflammatory cytokines can have a deleterious effect on the host, leading to several disorders including sepsis, ischemia, and hemorrhage.[4] LTA 250G>A has been identified as an important genetic mutation that worsens the severity of different inflammatory conditions. Among the many inflammatory conditions that it is known to exacerbate, LTA+250 AA genotype predisposes community-acquired pneumonia patients at greater risk for septic shock.[5] A previous study also indicates that LTA+250 AA genotype site is associated with higher serum tumor necrosis factor-alpha levels and a higher mortality rate in children with bacteremia.[6]

Allele-specific polymerase chain reaction (ASPCR) is a technique of polymerase chain reaction (PCR) that allows the direct detection of any point mutation in human DNA by amplified products in agarose gel electrophoresis. ASPCR is designed with a set of oligonucleotide primers that generates a 3' mismatch with the DNA template, which does not allow the primer extension by DNA polymerase.[7]

Genetic mutation in the LTA (250G>A) is known to be one of the greatest risk factors for septic shock in community-acquired pneumonia.[8] However, previous methods for detection require extended workflow time and sophisticated equipment, making it more difficult for the patients to readily access pre-diagnosis. Here, a novel method of LTA mutation detection using allele-specific PCR is proposed. This method only requires four DNA primers, a PCR machine, and minimal agarose gel electrophoresis equipment, which enables molecular diagnostic assays to be analyzed rapidly in 3 hours without any need for expensive lab equipment.

Methods

Cell culture of human cell lines:

Four human cell lines were obtained from Korea Cell Line Bank (Seoul, Korea): A172, SK-MEL2, A375SM, and MCC13. RPMI-1640 medium with 10% FBS and 1% penicillin and streptomycin supplements were used. The cells were maintained at a 37 ˚C in a CO2 incubator.

Genomic DNA purification from human cell lines:

1.2 x 106 of human cells were harvested for genomic DNA extraction. DNA was isolated using QIAamp DNA Mini Kit (Qiagen). After the cells were resuspended with 200 μL phosphate-buffered saline (PBS), 200 μL lysis buffer was added. After incubating the lysate at 56 ˚C for 10 min, 200 μL of ethanol was added. Then, samples were loaded on the Mini spin column. After the centrifugation was applied for 1 min, the flow-through solution was removed. Then the column was washed with 500 μL AW1 buffer and 500 μL AW2 buffer. The purified DNA was eluted with a 200 μL AE buffer.

DOI: 10.36838/v4i1.16

Allele-specific PCR:

The primer sequences are presented in Figure 1. 20 µL PCR reaction was performed as follows: 1 x reaction buffer, 2 mM MgCl2, Taq DNA polymerase, 250 uM of each dNTP (Bioneer), 1 pmol of each primer, and 100 ng genomic DNA template. Then, the following PCR condition was used for the target gene amplification: 95 ℃ for 5 min, 35 cycles of 95 ℃ for 20 sec, 56 ℃ for 30 sec, and 72 ℃ for 30 sec with a final extension at 72 ℃ for 5 min.

Agarose gel electrophoresis:

After 1.5% agarose gel was prepared with Red-safe (Intron) staining solution, the samples were loaded onto the gel with 6X DNA loading buffer (Bioneer). After the gel was run at 100 V for 30 min, the gel was visualized by a Blue light illuminator (B-box).

Results and Discussion

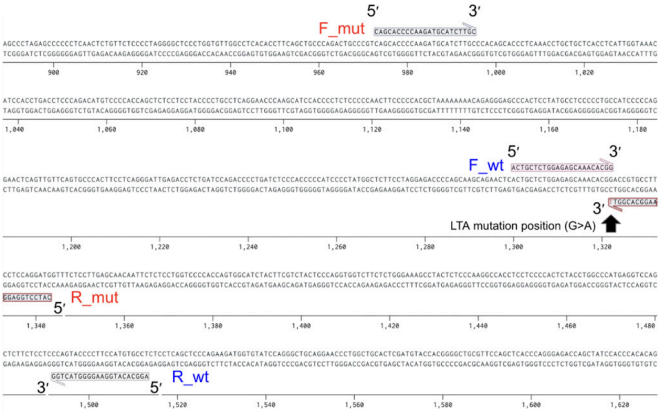

Figure 1: Primer design of LTA 250 G>A allele-specific PCR. Forward primer wild type (F_wt) and Reverse primer wild type (R_wt) generate 214 bp for detecting wild-type allele G. Forward primer mutant (F_mut) and Reverse primer mutant (R_mut) generate 371 bp for detecting mutant allele A.

The method presented here allowed efficient discrimination of LTA mutation by allele-specific PCR in a single reaction with standard PCR conditions. A common reverse primer and two forward allele-specific primers with different tails amplify two allele-specific PCR products of different lengths: 214 bp for detecting wild-type allele G and 371 bp for detecting mutant allele A (Figure 1).

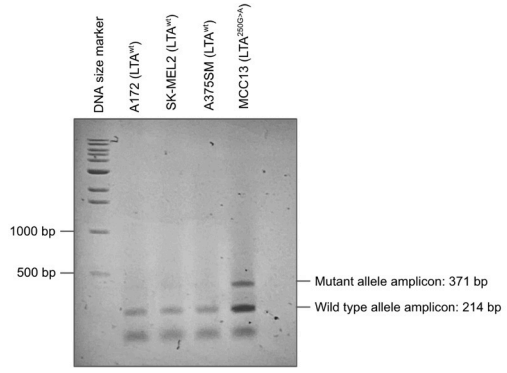

Figure 2: Allele-specific PCR results using four different human cell lines: A172 (LTAwt), SK-MEL2 (LTAwt), A375SM (LTAwt), and MCC13 (LTA 250G>A). The mutant allele amplicon was only detected in an MCC13 DNA sample.

To confirm the specificity of the assay, one LTA 250G>A mutation containing cell line (MCC13) and three cell lines with LTA wild type (A172, SK-MEL2, A375SM) were used in this allele-specific assay. A wild type allele band (214 bp) was detected in all four cell lines. A 371 bp mutant allele band was detected only in MCC13 indicating that MCC13 had heterozygous mutation (LTAwt/250G>A) (Figure 2). This result was consistent with the mutation data provided by the Catalogue Of Somatic Mutations In Cancer (COSMIC) which is a mutation database that includes about 6 million coding mutations across 1.4 million tumor samples.

Conclusion

ASPCR has been used in DNA-based diagnostic techniques for the diagnosis of genetic and infectious diseases. In this research, the accuracy and specificity of our novel ASPCR was confirmed by the detection of LTA 250G>A by analyzing the PCR products in agarose gel electrophoresis. Our result was consistent with the mutation database provided by COSMIC. This novel assay can be easily performed by using basic laboratory equipment. This method can potentially be applied to detect many other single nucleotide polymorphisms or point mutations found in genetic diseases. To fully confirm the applicability of this result, it would be necessary to test more than four cell lines and corroborate the specificity of LTA 250G>A mutation detection. Also, there are numerous other mutations that are associated with community-acquired pneumonia. Further studies may be carried out to detect a more comprehensive set of CAP-associated mutations in one single PCR reaction.

Acknowledgements

I would like to thank all of my previous and current science teachers who have allowed me to find my passion in science and helped me build a strong scientific foundation to pursue in-depth scientific research. I would also like to thank my mentor, Dr. Woo Rin Lee, for providing guidance throughout this research process.

References

1. Ticona, J. H.; Zaccone, V. M.; McFarlane, I. M., Community-Acquired Pneumonia: A Focused Review. *Am J Med Case Rep* 2021, 9 (1), 45-52.
2. Rider, A. C.; Frazee, B. W., Community-Acquired Pneumonia. *Emerg Med Clin North Am* 2018, 36 (4), 665-683.
3. Jose, R. J.; Periselneris, J. N.; Brown, J. S., Community-acquired pneumonia. *Curr Opin Pulm Med* 2015, 21 (3), 212-8.
4. Yamada, Y.; Ichihara, S.; Nishida, T., Proinflammatory gene polymorphisms and ischemic stroke. *Curr Pharm Des* 2008, 14 (33), 3590-600.
5. Sole-Violan, J.; de Castro, F.; Garcia-Laorden, M. I.; Blanquer, J.; Aspa, J.; Borderias, L.; Briones, M. L.; Rajas, O.; Carrondo, I. M.; Marcos-Ramos, J. A.; Ferrer Aguero, J. M.; Garcia-Saavedra, A.; Fiuza, M. D.; Caballero-Hidalgo, A.; Rodriguez-Gallego, C., Genetic variability in the severity and outcome of community-acquired pneumonia. *Respir Med* 2010, 104 (3), 440-7.
6. McArthur, J. A.; Zhang, Q.; Quasney, M. W., Association between the A/A genotype at the lymphotoxin-alpha+250 site and increased mortality in children with positive blood cultures. *Pediatr Crit Care Med* 2002, 3 (4), 341-4.

7. Gaudet, M.; Fara, A. G.; Beritognolo, I.; Sabatti, M., Allele-specific PCR in SNP genotyping. *Methods Mol Biol* 2009, 578, 415-24.
8. Schueller, A. C.; Heep, A.; Kattner, E.; Kroll, M.; Wisbauer, M.; Sander, J.; Bartmann, P.; Stuber, F., Prevalence of two tumor necrosis factor gene polymorphisms in premature infants with early onset sepsis. *Biol Neonate* 2006, 90 (4), 229-32.

Author

Seyun is a senior at Choate Rosemary Hall in Wallingford, CT. She serves as the Editor-in-Chief of a magazine that uncovers healthcare disparities, Head Copy Editor of Choate Public Health, Vice President of Biology Club, and more in an effort to pursue her passion in medicine, science, and health equity.

DOI: 10.36838/v4i1.16

IJHSR
ijhighschoolresearch.org
RESEARCH ARTICLE

Testing the Efficacy of Nanoparticles, Biological Formulation with the qPCR Technique to Improve HLB Management

Shloke Patel

Hillsborough Highschool, 2218 Branch Hill Street, Tampa, Florida, 33612, USA; shlokep8@gmail.com

ABSTRACT: Citrus phloem bacteria, Candidatus *Liberibacter asiaticus* (CLas), causes the citrus greening disease, Huanglongbing (HLB). In 2019, this devastating disease caused a 21% decrease in the fresh citrus fruit market and a 72% decline in the commercially grown production of oranges in Florida. The number of Florida industry jobs dropped by 59% compared to previous years. HLB has no cure; global orange juice production is expected to fall by double digits in the coming years. Typical symptoms include yellowing of the leaves, as well as lopsided, premature, and bitter fruits. Since, CLas hides deep within the citrus phloem, commercial antibiotic sprays often cannot reach the bacteria. A biological solution for the prevention of the detrimental effects of HLB was used; the formulations tested were combined with copper nanoparticles which would potentially increase the penetration and the longevity of the formulation to mitigate the effects of the greening disease. The formulations included Firewall and Fireline, two approved and readily available antibacterial solutions, and a bioformulation, curry leaf extract.

The experiment was conducted in a greenhouse with 42 infected plants with five leaf samples being collected from each plant. The DNA of the leaves was extracted using the GeneJET DNA purification Kit. 6 formulations: Firewall with and without nanoparticles, Fireline with and without nanoparticles, curry leaf extracted with and without nanoparticles were prepared and injected into six plants. After 3 months, the bacterial DNA concentration was determined, and 4 physical parameters of the plant were measured. The formulations were injected again, and after 70 days, qPCR assay and physical parameters were measured. Then, both the CT values and physical parameters were collected and compared.

The bacterial count remained unchanged in the treatment and control variables, the three physical parameters, trunk diameter, plant height, and width all improved compared to the control variable.

KEYWORDS: Biology; Agriculture; Huanglongbing; *Candidatus liberibacter*; Nano formulation; GeneJET.

Introduction

The Citrus production in Florida is limited by the impact of various biotic and abiotic factors. Of all the citrus limiting factors, Huanglongbing (HLB) or citrus greening is the most prominent and rampant in spreading throughout a grove in just matter of weeks. Although Florida has favorable conditions and is best suited for citrus production, it is very prone to HLB. Citrus greening disease has devastated millions of acres of citrus crops throughout the United States and abroad.[1] Florida is the largest orange-producing state in the United States and the third-largest orange producer in the world behind Brazil and China. The citrus industry makes roughly 45,000 full time and part-time jobs and contributes 8.6 billion a year to Florida's economy.[1] Since HLB was first found in 1998, orange acreage and yields in Florida have decreased by 26% and 42%, respectively.[2] Orange production dropped from 242 million to 104.6 million boxes in 2014 and if this negative trend continues, Florida will not have a profitable orange industry soon.[2] In the current scenario, farmers are faced with the threat of losing their orange grove to this disease. Currently, the only short-term viable solution entails antibiotics which wash away after a month or two with devastating effects on the soil. Additionally, many unknown side effects are caused by these antibiotics. However, Florida has still allowed these chemicals to be sprayed on the orange plants without any proven utility of the Firewall and Fireline solutions being demonstrated. Many researchers have been experimenting with the use of minuscule particles called nanoparticles. These 100-nanometer particles can easily penetrate a cell wall allowing the antibiotic to seep through phloem.[3] These particles are currently used in medical and technological fields but are scarcely used in the agricultural field.

Citrus greening disease (Huanglongbing) is caused by a bacterial infection (*Candidatus liberibacter*), which spreads through an insect vector called Asian Citrus Psyllid (ACP). Psyllid adults feed on citrus greening-infected trees and acquire the bacteria through the bacterial residue on the vector's mouth. The psyllid then carries the bacteria from an infected plant to a healthy plant. Next, the psyllid injects the bacteria onto a healthy plant while feeding and transfers the greening disease into the plant's phloem, affecting the vascular system and limiting nutrient uptake.[4] The disease reduces yield, fruit size, and quality and increases tree mortality and production costs. Once the orange tree is infected with the greening disease, the tree eventually dies within a few years.[5] Currently, many nanoparticles are being used as fungicides due to the elements' antibacterial properties.[6]

Nanoparticles are made of many conventional materials that change mechanical properties when they are formed into nanoparticles. Nanoparticles have a greater surface area per weight than larger particles, which causes them to be more reactive to large particles. These small particles usually come in

DOI: 10.36838/v4i1.17

the form of metals for the agricultural sciences because many phloem or xylem-limited bacteria are not easily penetrable by regular antibiotics.[7] Nanoparticles such as copper bind to the bacteria, and because of copper's antibacterial properties, they eliminate the bacteria. Research shows that engineered nanoparticles that are metalloids have demonstrated an activity that kills harmful plant bacteria. Many metalloids are known for being bactericides and or fungicides but are not used conventionally. Nano-fertilizers have also been very useful in improving plant health by entering the phloem of the plant. Some nanoparticles act as antimicrobial agents, while others alter the nutrition of the plant. Penetration of the vascular tissue occurs when a particle is sufficiently small so that it can seep through the cell wall. During a process called adhesion, the nanoparticle bends the cell wall, and eventually, the cell wall wraps around the nanoparticle.[8] In large quantities, the penetration can be beneficial and can play a role in mitigating disease, which might lead to a reduction in the use of heavy metals and other chemicals.

Methods

Analysis and Procedure:

The experiment was conducted in a greenhouse with 42 infected plants. The psyllid repellency was determined by the prevention of the reinfection of the plant, validated through the CT value. Since this was a short-term experiment, immediate symptoms were tested through the measurement of the physical parameters. Fireline and Firewall have extremely toxic chemicals such as oxytetracycline hydrochloride[16] in Fireline and Streptomycin[13] in Firewall which are helpful in killing the bacteria. Samples were collected from each plant to determine the concentration of the greening bacteria through qPCR assay. DNA was extracted using the Gene JET DNA purification Kit.

The initial PCR measurements were used to ensure that all the plants had the same CT value to provide consistent data.

Plant Measurements:

The trunk diameter was measured using the vernier caliper for each of the 42 plants. Plant width was determined by the spread of the leaves that are the farthest from each side of the plant. The plant height was measured by the trunk of the plant that was above soil level to the tip of the plant, vertically. The plant width and plant height were measured using a measuring tape.

Plant Vigor:

The plant vigor is a researcher-based observation on the total fullness of the plant. Variables such as the color of the leaves are taken into consideration. In this experiment a 0-10 scale was used to calibrate the plant vigor.

Chlorophyll Measurements:

The chlorophyll concentrator meter used was the Apogee Meter which measures the content in µmol per m². To measure the chlorophyll content, a leaf was placed between the arm of the meter and the base of the meter, and the leaf was pressed against by the arm which detected the chlorophyll. The data then was gathered in the appendix of the system and was uploaded to excel.

qPCR preparation :

The qPCR technique provided an essential piece of data when determining the bacterial count, the CT value. There are 3 steps in the process of the qPCR technique which include the denaturation, primer annealing, and extension. The qPCR solution requires 10 µL of TAQMAN qPCR buffer which is comprised of 8.6 µL of sterile deionized water, CQUL Primer and the leaves of the plants.

Arbo Jet Injection Preparation:

An opening in the trunk is required to inject the 6 solutions into the plants. A 4 mm hole was drilled into each of the 42 plants using the drilling machine. Once the path into the plant was created, 60 mL of the desired solution was injected into a one-year-old plant. The injection was slowly administered to prevent the disruption of the flow of nutrients in the phloem and xylem. The process took approximately 8 hours for the solution to be fully administered.

Psyllid Repellency:

The psyllid repellency was determined by the CT value, which was an indicator for the bacterial count. The physical parameters also helped in validating the CT value results.

Results and Discussion

The psyllid repellency was tested using 7 treatments including the control variable. Treatment 1 was the controlled variable, and treatments 2 and 3 were the industry standards, Fireline and Firewall, respectively. Treatments 4 and 5 were the industry standards with the nano formulation, and treatments 6 and 7 were the bioformulation, curry leaf extract, without the nano formulation and with the nano formulation, respectively.

The following parameters were studied during the evaluations of the results. The parameters monitored include, increase in the height, increase in the width of the stem, increase in the trunk diameter, increase in the chlorophyll content as a measure of the overall plant health and average increase in the plant vigor (Table 1 through Table 7).

Table 1: Average Increase in Plant Traits of the 42 Citrus Plants through 2 Growing Seasons.

Treatment	Trt 1	Trt2	Trt 3	Trt 4	Trt 5	Trt 6	Trt 7
(6 replications)							
Avg. increase in ht (ft) (6 replications)	0.35	0.55	0.73	0.7	0.57	0.6	0.52
Avg. increase in width (ft) (6 replications)	0.2	0.38	0.53	0.43	0.37	0.52	0.53
Avg. increase in Trunk diameter (ft)	0.17	0.27	0.31	0.42	0.39	0.21	0.27
Avg. increase in Chlorophyll content (µmol m^-2)	41.2	25.83	32.33	33.5	33.17	32	34.16
Avg. increase Plant vigor (0-10 scale)	-0.37	0.47	0.53	0.47	-0.27	-0.16	0

Table 1 shows the average increases of all the plant traits taken for the 7 treatments and 6 replications, through the 2 growing seasons.

DOI: 10.36838/v4i1.17

Table 2: Average Plant Vigor of the 42 Citrus Plants through 2 Growing Seasons (0-10 scale).

Treatments / Time	Trt 1	Trt 2	Trt 3	Trt 4	Trt 5	Trt 6	Trt 7
Start	8.2	8.2	8.3	8.2	8.6	7.83	8
3 months	7.83	8.33	7.5	7.67	7.83	8	7.5
5.5 months	7.83	8.67	8.83	8.67	8.33	7.67	8
Percent Increase	0.37	0.47	0.53	0.47	0.27	0.16	0
Standard Deviation	0.21	0.24	0.67	0.50	0.39	0.17	0.29

Table 2 shows the average plant vigor on a 0-10 scale for the 7 treatments for the 6 replications. There was a significant increase in treatment 3 with an increase of plant vigor of 1.33.

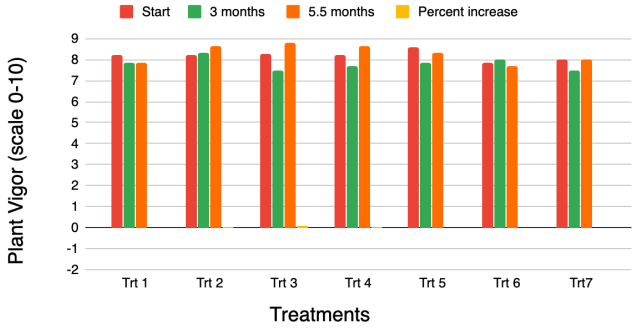

Figure 1: Average increase in Plant Vigor..

Most of the treatments started with a plant vigor of around 8. As the bacteria moved towards the phloem the plant vigor decreased and at 5.5 months the plant vigor started to increase. Treatment 3 had the highest plant vigor at 5.5 months (Figure 1).

Table 3: Average Height of the 42 Citrus Plants through 2 Growing Seasons(ft).

Treatment / Time	Trt 1	Trt 2	Trt 3	Trt 4	Trt 5	Trt 6	Trt 7
Start	1.8	1.82	1.87	1.92	1.92	1.78	1.8
3 months	1.94	2.01	2.05	2.11	2.23	2.1	2.1
5.5 months	2.13	2.37	2.6	2.67	2.7	2.38	2.32
Percent Increase	18.33%	30.22%	39.04%	39.10%	0.60%	33.71%	28.89%
Standard Deviation	0.17	0.28	0.38	0.39	0.35	0.30	0.26

Table 3 and Figure 2 shows the average height of the 42 citrus plants through the two growing seasons, approximately 5.5 months. Treatment 4 had an average percent increase of 39.10%, which was the largest increase of all the 7 treatments.

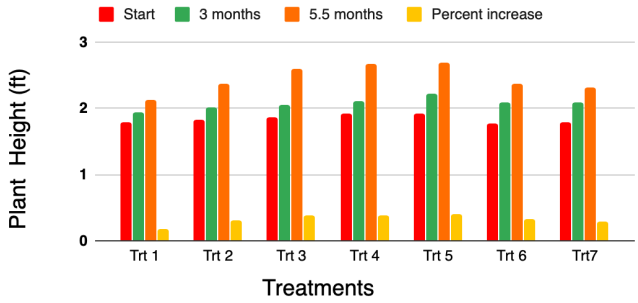

Figure 2: Average height increase.

As shown by the Table 3 above after a period of 5.5 months a more drastic increase was shown compared to the interval of the start to 3 months of the experiment.

Table 4: Average Width of the 42 Citrus Plants through 2 Growing Seasons (ft).

Treatments / Time	Trt 1	Trt 2	Trt 3	Trt 4	Trt 5	Trt 6	Trt 7
Start	1.3	1.3	1.32	1.28	1.3	1.3	1.35
3 months	1.35	1.42	1.45	1.4	1.45	1.52	1.5
5.5 months	1.5	1.68	1.85	1.73	1.67	1.82	1.82
Percent Increase	15.39%	29.23%	40.15%	35.16%	28.46%	40%	9.82%
Standard Deviation	0.10	0.19	0.28	0.23	0.19	0.26	0.24

Table 4 shows the average width of the 42 citrus plants through the 2 growing seasons (approximately 5.5 months). Over the span of 2 growing seasons treatment 3 showed the largest percent increase in the width of all the treatments.

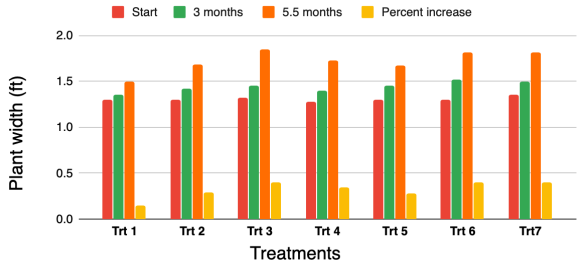

Figure 3: Average Width increase.

The average width percent increase is shown in the Figure 3 of all the treatments for the 6 replications.

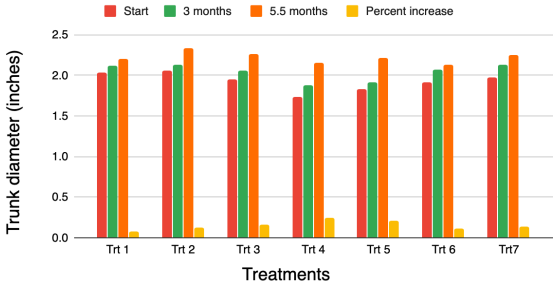

Figure 4: Average Trunk Diameter increase.

There was a positive trend between the amount of time and the increase in the trunk diameter in the 7 treatments.

Table 5: Average Trunk Diameter of the 42 Citrus Plants through 2 Growing Seasons (inches).

Treatments / Time	Trt 1	Trt 2	Trt 3	Trt 4	Trt 5	Trt 6	Trt 7
Start	2.03	2.06	1.95	1.73	1.83	1.92	1.98
3 months	2.12	2.13	2.06	1.88	1.91	2.07	2.13
5.5 months	2.2	2.33	2.26	2.15	2.22	2.13	2.25
Percent Increase	8.30%	3.11%	5.90%	24.28%	21.31%	10.94%	13.84%
Standard Deviation	0.09	0.14	0.47	0.21	0.21	0.11	0.14

This data was significant because there was a significant increase of growth between 3 months and 5.5 months showing that the treatments had an effect, which was allowing the phloem and xylem to expand. Treatment 4 had the highest percent increase of the average trunk diameter of 24.28%.

Table 6: Average Chlorophyll Content of the 42 Citrus Plants through 2 Growing Seasons.

Treatments / Time	Trt 1	Trt 2	Trt 3	Trt 4	Trt 5	Trt 6	Trt 7
Start	288	275.67	285	284.5	290.33	287.5	285.67
3 months	302.5	286.83	296.33	297.12	303.67	301	297.33
5.5 months	329.2	301.5	317.33	318	323.5	319.5	319.83
Percent Increase	11.31%	9.37%	11.39%	11.77%	11.43%	11.13%	11.96%
Standard Deviation	20.90	12.95	16.40	16.92	16.69	16.06	17.36

Due to the large standard deviations, the abnormal production of chlorophyll and chlorophyll deficiency are seen in later stages of HLB so fewer conclusions can be made from this data.

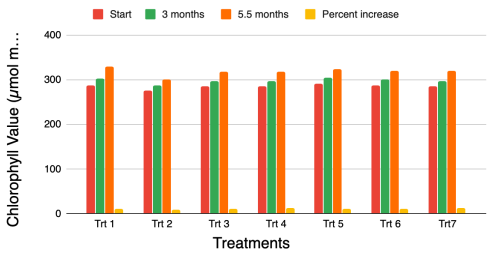

Figure 5: Average Chlorophyll content.

The plant is producing the required nutrients at the higher rate as it has more chlorophyll which is displayed by data in the table (Figure 5 and Table 6).

qPCR Assay:

The controlled environment in the greenhouse provided more controlled variables than experimenting in the field because the CT value did not change before and after 3 months. The physical parameters were measured using the qPCR technique. A scale of the acceptable CT values in relation to the bacterial population was created. A CT value below 17 indicates high levels of bacterial infection and a CT value of above 32 indicates that there is little to no bacteria present

Table 7: Average CT value of the 42 Citrus Plants through 2 Growing Seasons.

Treatments / Time	Trt 1	Trt 2	Trt 3	Trt 4	Trt 5	Trt 6	Trt 7
Start	26.96	25.98	25.16	25.69	25.69	23.55	24.7
3 months	24.33	25.53	25	23.93	24.62	24.62	23.98
5.5 months	25.65	25.76	24.15	24.96	25.16	24.09	26.19
Standard Deviation	1.32	0.23	0.54	0.88	0.54	0.54	1.23

The difference between the starting CT value and the CT value after 5.5 months roughly stayed between 0 and 1 showing that the bacterial count remained consistent.

The CT value might have changed over time (Table 7) because of the bacteria's behavior concerning the temperature, but not enough time was given to access this variable. To see more accurate results of the bacteria usually 6 months is needed.[2] During the 6 months either the plant will show significant symptoms or display no signs of symptoms. The hypothesis was accurately tested due to the data given by the 4 physical parameters. The physical parameters provided an accurate method to measure the bacterial content by examining characteristics including whether the plant was displaying or not displaying early symptoms such as blotchy mottle, yellowing of the leaves and veins.

The standard deviation was between 1.32 and 0.23 for the CT values, which shows that the data varies between 1.32 and 0.23 units from the mean CT value on average. In the experiment, the CT value of each plant was recorded before experimenting. 42 out of the 49 plants that had similar CT values were selected for this experiment. The change in the CT values should be comparable if all the plants have identical CT values.

Many researchers have tested the effectiveness of curry leaf extract on different vectors and the results have been positive due to azacytidine, an active antibacterial compound found in curry leaf.[17] The expected results of this experiment were that since copper nanoparticles are also anti-bacterial, they would improve the efficacy. Currently, the efficiency of the addition of nano formulation in the plant vascular system is unknown.

The CT value in the table shows the number of cycles it takes for the PCR to detect the bacteria. Treatment 7 had the highest increase of the CT value which means the bacterial content decreased the most over the period of 5.5 months.

DOI: 10.36838/v4i1.17

Conclusion

The hypothesis was contradicted because the introduction of the nanoparticles did not prove to have a large impact on the CT value. According to the data collected in this experiment, the amount of *Candidatus liberibacter* bacteria stayed constant with the treatment of the six formulations injected in the infected citrus plants.

Currently, the treatments seem to have little effect on the CT value of the bacteria. As per the data collected the CT value has remained consistent with the highest standard deviation of 1.32 units over a period of 5.5 months. The treatment that showed the most improvement over the time span of 5.5 months was treatment 7, the bioformulation with nano particles.

The change in the CT values did not prove that the nanoparticles helped with penetration of the antibiotics or curry leaf extract at 5.5 months, but there was a positive trend in the physical traits. Because of the flush formation process when the sap from the xylem tissue moves to the phloem tissue, the CT value remains the same, but it causes a better development of plant foliage. When the sap flows from the phloem to the xylem tissue, the bacterial concentration might decrease in the leaf, resulting in the increase in the CT value. Continuing this experiment for one full year might allow more time to see a difference in the CT value, since it covers the 4 cycles of the sap movement.

Acknowledgements

My sincere gratitude to my mentor Dr. Balaji Aglave for guiding me through this project and offering his insight and expertise on this topic. I could not have completed this experiment without the help of Florida Agricultural Research. I sincerely thank them for permitting me to conduct my experiment on their premises. I also thank my science teacher Ms. Mishell Thomas-King for taking her time out of her day to help me with my project by giving me tips on my research plan. I thank my mom and dad for taking me to the research center.

References

1. Asian Citrus Psyllid and Huanglongbing in California. https://californiacitrusthreat.org/pest-disease/
2. http://entnemdept.ufl.edu/creatures/citrus/acpsyllid.htm
3. Asian Citrus Psyllid. https://www.aphis.usda.gov/aphis/resources/pests-diseases/hungry-pests/the-threat/asian-citrus-psyllid/asian-citrus-psyllid
4. Grafton-Cardwell, B., n.d. *The Asian Citrus Psyllid and the Citrus Disease Huanglongbing.* [ebook] Available at: <https://ucanr.edu/sites/mgfresno/files/133416.pdf>
5. Useche, A. S. and P. Impact of Citrus Greening on Citrus Operations in Florida. https://edis.ifas.ufl.edu/fe983
6. Food and Resource Economics Department (FRED). https://fred.ifas.ufl.edu/economicimpactanalysis/publications/2015-citrus-industry/
7. 2021. *Afrox 2017 INTEGRATED REPORT*. [ebook] Available at: <https://www.afrox.co.za/en/images/Afrox_IR_11244_v8b_20180410_LN%20%28002%29_tcm266-468473.pdf>
8. 2021. Safety Data Sheet - *Copper Nanoparticles*. [ebook] Available at: <https://www.acsmaterial.com/pub/media/catalog/product/s/d/sds-copper_nanoparticles.pdf>
9. Ortiz, J.; says:, R. L.; says:, L. B. How do Nanoparticles Enter Cells? https://sustainable-nano.com/2014/08/19/how-do-nanoparticles-enter-cells/
10. Elmer, W., Ma, C. and White, J., 2018. *Nanoparticles for plant disease management*. [ebook] Available at: <https://portal.ct.gov/-/media/CAES/DOCUMENTS/Biographies/Elmer/Elmer-Ma-White-NP-for-Pl-Diseae-Management-2018.pdf?la=en>
11. 2013, W. by A. Z. N. M. 26. *Copper (Cu) Nanoparticles* - Properties, Applications. https://www.azonano.com/article.aspx?ArticleID=3271
12. 2018. Safety Data Sheet - Copper (Cu) Nanoparticles / Nanopowder. [ebook] Available at: <https://n.b5z.net/i/u/10091461/f/MSDS-NANOPOWDERS/US1089.pdf>
13. 2014. *Material Safety Data Sheet* - Firewall. [ebook] Available at: <http://agrosource.net/wp-content/uploads/2018/07/firewall-50-sds-use-this-one.pdf>
14. 2017. *MATERIAL SAFETY DATA SHEET - LIQUID NITROGEN*. [ebook] Available at: <https://www.afrox.co.za/en/images/Nitrogen266_92436_tcm266-401695.pdf>
15. 2016. *Thermo Scientific GeneJET Plant Genomic DNA Purification Mini Kit #K0791, #K0792*. [ebook] Available at: <https://assets.thermofisher.com/TFS-Assets/LSG/manuals/MAN0016131_GeneJET_Plant_Genomic_DNA_Purification_Mini_Kit_UG.pdf>
16. 2011. *Material Safety Data Sheet - FineLine*. [ebook] Available at: https://assets.greenbook.net/M104560.pdf
17. Kumar, J., Sharma, V. K., Singh, D. K., Mishra, A., Gond, S. K., Verma, S. K., Kumar, A., and Kharwar, R. N. (2016, February 4) Epigenetic Activation of Antibacterial Property of an Endophytic Streptomyces coelicolor Strain AZRA 37 and Identification of the Induced Protein Using MALDI TOF MS/MS. *PloS one*. Public Library of Science.

Author

Shloke Patel is a junior at Hillsborough High School. Growing up around farms, Shloke developed a deep understanding of the beneficial effect of farm fresh food on health. From a young age Shloke took inspiration in gardening by creating a backyard garden and enjoying fresh vegetables and fruits. He hopes to make a positive impact in the field of agricultural research.

IJHSR
ijhighschoolresearch.org
RESEARCH ARTICLE

Facile Preparation of Novel Stainless-steel Mesh for Efficient Separation of FOG (Fat, Oil and Grease) and Water

Zhi-Wei Steven Zeng

Obra D. Tompkins High School, 4400 Falcon Landing Blvd, Katy, TX 77494, USA; zengsteven@yahoo.ca

ABSTRACT: Large excesses of fat, oil, and grease (FOG) in food waste enter sewer systems on a daily basis, resulting in "fatbergs" that can lead to significant economic loss due to expensive removal. It is therefore vital to prevent the release of FOG into sewer systems. In this report, a low-cost and convenient method was established to coat the durable stainless-steel mesh with nano-needles and hydrogel, rendering the mesh simultaneously superhydrophilic and superoleophobic. The obtained mesh demonstrated superior capability in separating cooking oil from water, thus, showing immense potential for application.
KEYWORDS: wastewater treatment; fat; oil; grease; separation; superhydrophilic; superoleophobic.

Introduction

As one of the most common cooking ingredients, large amounts of oil are consumed every day, producing excess waste fats and grease that accumulate into a mixture of water and FOG (fat, oil, and grease). Currently, most FOG is released into sewer systems through kitchen sinks. When the FOG accumulates in pipelines, solid deposits that block the flow of drainage and sewer movement are formed. Known as "fatbergs",[1] these FOG blockages can pose a difficult problem for urban communities around the world. Every year, there are 10,000-36,000 sanitary sewer overflow events in the US and 25,000 in the UK, half of which are due to FOG.[2] Moreover, it is very expensive to mitigate the problems caused by fatbergs. In London alone, the annual cost to clean FOG-blockages reaches £18 Million[3] while one major fatberg clogging cost the city as much as £400,000.[4] New York City was forced to spend $19 Million on fat-berg removal in 2018 alone.[5]

Superhydrophobic coatings have excellent water repelling capabilities[6] and have been broadly employed for oil-water separation. For example, superhydrophobic sponges prepared using environmentally friendly and low-cost methods can efficiently remove oil submerged in seawater.[7] However, FOG-water mixtures generated in the kitchen contain water as the majority of the mixture, resulting in the need to continuously separate large amounts of water from oil. In this case, a superhydrophobic mesh or sponge is not ideal because water will rapidly block pores, leading to poor oil-water separation. In contrast, if a filter simultaneously demonstrates super-high affinity to water and super-high repulsion to oil when it is immersed in water, it is highly desired for FOG-water separation because water can quickly pass through the system with the oil components rejected.[8] The so-called superhydrophilic and underwater superoleophobic meshes have become increasingly reported in literature for oil-water separation.[9,10] The key to such materials is the existence of a stable water film kept in nanometer-sized structures on the material's surface. Currently there are two primary methods to prepare superhydrophlic and underwater superoleophobic surfaces:

1) nanometer-sized hydrophilic roughness generated using dipping,[11] spraying,[12] etching,[13] mineralization,[14] electrodeposition,[15] or laser-based methods.[16] A good example is the array of $Cu(OH)_2$ nano-needles on Cu surface based on the etching method using aqueous solution of sodium hydroxide and ammonium sulfate.[13]

2) a thin layer of hydrogel saturated with water which is coated onto the material's surface.[17,20] A popular hydrogel for this purpose is calcium alginate, which is produced from natural products like seaweed.[21]

The majority of literature methods for the preparation of superhydrophilic and underwater superolephobic meshes/membranes rely on expensive chemicals and complicated procedures, making it difficult to expand the scope of implementation in the real world. Simultaneously, there are also limitations in the current primary methods for the preparation of such meshes:

a) Because water film kept in the capillaries or pores can easily be drained due to gravity, the hydrophilic nanostructures (nanoparticles, nano-needles, nanowires, or nanotubes, etc.) may not effectively prevent the drainage of the water film during repeated use.

b) The water-saturated hydrogel is soft and can be damaged easily.

Considering the nanostructures, e.g., nano-needles can protect the hydrogel, and the hydrogel can keep a stable water film, it is reasonable to hypothesize that the combination of hydrophilic nano-needle structures and a coating of hydrogel might achieve synergy and lead to better FOG-water separation.

So far, copper meshes 22–24 and stainless-steel meshes 25–27 have been commonly used in literature studies, although cotton 28 and glass 29 meshes are occasionally reported. Copper mesh suffers from weak strength, low chemical stability, and relatively high cost. On the other hand, it is important to considered that a stainless-steel mesh would offer advantages over copper, in terms of lower cost and mechanical strength, providing that the surface properties can be better tailored accordingly to the application.

DOI: 10.36838/v4i1.18

Therefore, this communication describes results from experiments using surface-modified stainless-steel mesh. It is clearly demonstrated that the synergy of nano-needles and hydrogel leads to significant improvement of oil-water separation performance of the mesh. As a result, strong and durable stainless-steel mesh with excellent oil-water separation capability can be prepared using a very convenient and low-cost method.

Methods

Materials:

Copper sulfate pentahydrate (from Alpha Chemicals), sodium hydroxide (from Belle Chemical), ammonium persulfate (from Eisen-Golden Laboratories), sodium alginate (from Modernist Pantry), calcium chloride (from Pure Organic Ingredients) and stainless-steel woven wire 200 mesh (12"× 40", from Yikai Store) were used as received. The DC power supply (model KPS305DF) was manufactured by EVENTEK. Food color, vegetable oil, distilled water, copper pipe and a 2-inch PVC union socket end ("Solvent Union", manufacture by Homeworks Worldwide LLC., IL, USA) were purchased from a local hardware store. Home-made chili oil was used as dye for vegetable oil.

A pocket optical microscope (ioLight Model 1, manufactured by ioLight Limited, U.K.) was used to examine the meshes.

Modification of stainless-steel mesh:

Figure 1 shows the protocol used to modify the surface of the stainless-steel mesh. In the first step, a layer of copper is coated onto stainless steel mesh. In the second step, the fresh copper layer is modified to grow hydrophilic nanoneedles on the copper surface. Finally, a layer of hydrogel is formed on the surface of either the fresh copper layer or the copper layer with $Cu(OH)_2$ nanoneedles.

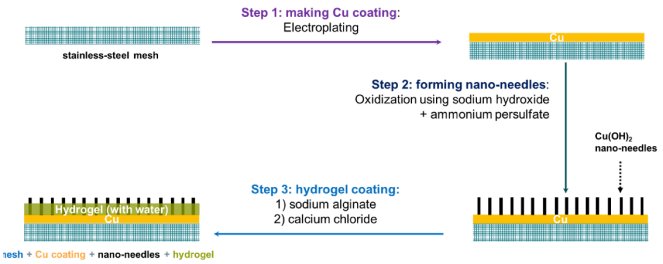

Figure 1: Three steps used for the modification of the stainless-steel mesh. In Step 1, the stainless-steel mesh was coated with a layer of copper using an electroplating method. In Step 2, a layer of copper hydroxide nano-needles was grown on the Cu layer. In Step 3, a layer of calcium alginate hydrogel was deposited on the $Cu(OH)_2$ nano-needles.

All the preparation experiments were conducted at ambient temperature. The details of the procedure are as follows.

Step 1: Coating stainless steel mesh with Copper

First, stainless steel woven wire mesh was cut into an 8-cm (diameter) circle. Then it was rinsed with water. After this cleaning process was repeated three times, the mesh was dried in air. A copper rod was polished with a piece of fine-size sandpaper first. Then, it was washed with water three times and dried in air, too. In the next step, both the stainless-steel mesh and the copper rod were immersed into 500 mL $CuSO_4$ aqueous solution (1 M) in a glass beaker. The distance between the mesh and the copper rod was kept at 5 cm. Then the copper rod was connected to the positive output of DC power supplier using the cord with an alligator lead and the stainless-steel mesh was connected to the negative output of the DC power supplier. After that, the DC power supply was turned on, and the voltage and current values were adjusted to coat a copper layer onto the stainless-steel mesh. The voltage and current used in this experiment are 3 V and 2 A, respectively. The electroplating time was kept at 1 hour for all samples.

Step 2: Growth of Cu(OH)2 needles on Copper layer

This method's details were also described in literature.[13] First, 100 mL aqueous solution containing sodium hydroxide (2.5 M) and ammonium persulfate (0.1 M) was prepared. Then the freshly prepared Cu-coated mesh was meshed with water and immersed into this solution for 1 hour. After the treatment, the copper-coated mesh became dark green. The mesh was then taken out of the solution and washed with water to remove the residual solution.

Step 3: Formation of calcium alginate hydrogel

Details of the procedure can be found in the literature.[21] First, 100 mL aqueous solution of sodium alginate (0.05 wt%) and 100 mL aqueous solution of $CaCl_2$ solution (5 wt%) were prepared, respectively. The mesh obtained after Step 2 was soaked in the sodium alginate solution for 5 minutes. Then it was taken out and washed with water to remove residual sodium alginate solution. After that, it was immersed in the $CaCl_2$ solution for 10 minutes.

Evaluation of the oil-water separation capability of the surface-modified mesh:

The oil-water separation capability of the prepared meshes was evaluated in this experiment. As explained in Figure 2, vegetable oil was doped with chili oil to make a red-colored oil while green food dye was added into water to prepared green-colored water. The colored oil and colored water were mixed in a bottle at 50:50 ratio (v/v) prior to the test. Then a piece of modified mesh was mounted onto in the middle of a Union Socket End ("Solvent Unit") made of PVC (2-inch). After that, the mesh was rinsed with some water. Once the water drained, the solvent union was placed on the top of a cup. The oil-water mixture described above (50 mL oil and 50 mL water) was shaken for 30 seconds, then it was poured into the solvent union. After 10 minutes, the liquid collected in the cup was poured into a volumetric flask. The volume values of the oil layer and the water layer were read after the oil and water had a clear boundary.

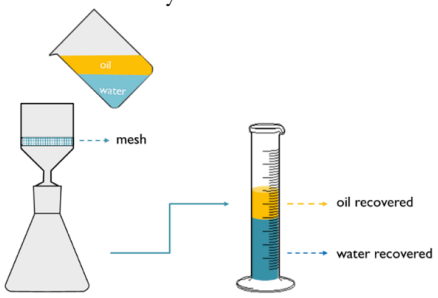

Figure 2: Schematic of the estimation of oil-water separation capability of the mesh.

Two parameters will be calculated to evaluate the performance of the mesh.

$$oil\ rejection\ \% = 1 - \left(\frac{oil\ recoveryed\ by\ tested\ mesh}{oil\ recovered\ by\ steel\ mesh}\right) \times 100 \quad (1)$$

$$water\ recovery\ \% = \left(\frac{water\ recoveryed\ by\ tested\ mesh}{water\ recovered\ by\ steel\ mesh}\right) \times 100 \quad (2)$$

Results and Discussion

A series of meshes were prepared using different modification conditions:

1) Stainless-steel mesh with copper coating.

2) Stainless-steel mesh with copper coating and nano-needles.

3) Stainless-steel mesh with copper coating and hydrogel coating.

4) Stainless-steel mesh with copper coating, nano-needles, and hydrogel coating.

For each modification condition, two independent meshes were prepared for performance evaluation. Images of the tested meshes are given in Figure 3. It is evident that electroplating of copper onto stainless-steel mesh reduces the pore size of the mesh (Figure 3). The growth of nanoneedles further lowered this value. Coating of hydrogel onto the mesh slightly decreased the pore size.

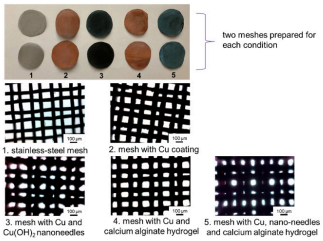

Figure 3: The meshes under evaluation and their microscopic images. The pore size of the mesh was slightly reduced after modification.

A typical result of the recovered water and oil is given in Figure 4.

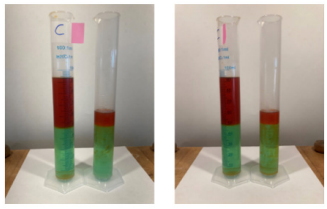

Figure 4: Oil-water separation using stainless-steel mesh (left) or stainless-steel mesh with copper coating (right). The two images represent the results of two independent measurements on individual samples. It is evident that the tests had good repeatability.

The water recovery (%) and oil recovery (%) results are listed in Table 1 and plotted in Figure 5.

Table 1: Water recovery (%) and oil recovery (%) results of the meshes investigated. The synergy of the nano-needle and hydrogel was evident by the complete water recovery as well as full oil rejection.

sample	water recovery, avg. (%)	oil rejection, avg. (%)
base mesh	100.0 ± 0.5	0.0 ± 0.5
base mesh + Cu	100.0 ± 0.5	68.8 ± 3.5
base mesh + Cu + nanoneedles	100.0 ± 0.5	80.0 ± 3.5
base mesh + Cu + hydrogel	100.0 ± 0.5	82.5 ± 5.3
base mesh + Cu + nanoneedles + hydrogel	100.0 ± 0.5	100.0 ± 0.5

The detailed morphology of the original mesh and the modified mesh cannot be examined at sub-micron level, however, the preparation of $Cu(OH)_2$ nano-needle/nanotube using sodium hydroxide-ammonium persulfate has been well documented. Therefore, it is reasonable to assume the desired nano-needle structures were formed on the meshes as reported in literature.

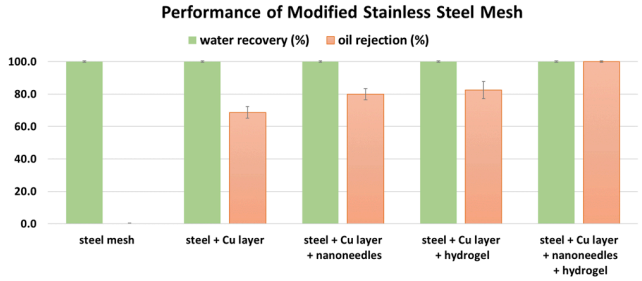

Figure 5: Performance of the original and modified stainless-steel meshes under investigation. Modifying the mesh with nano-needle or hydrogel alone could not lead to full oil rejection. On the other hand, the mesh modified with both nano-needle and hydrogel could completely separate oil and water.

The water recovery results (Table 1, Figure 5) of each tested mesh were all 100%, indicating that all meshes were superhydrophilic. The oil recovery results of these samples, on the other hand, were vastly different. The original stainless-steel mesh did not show any oleophobic properties and all tested oil passed through the mesh. When the stainless-steel mesh was coated with a fresh copper layer via electroplating, only 30% of the oil passed through the mesh, demonstrating certain oleophobic properties. Further modification of the Cu-coated mesh with either nano-needles or hydrogel will enhance the oleophobic properties of the mesh slightly, but none of these methods could completely separate oil from water (Figure 6). When these two treatment methods were combined to get a nano-needle array with a layer of hydrogel, no oil passed through the modified mesh, clearly demonstrating the desired superhydrophilicity and superoleophobicity of the modified mesh (Figure 6).

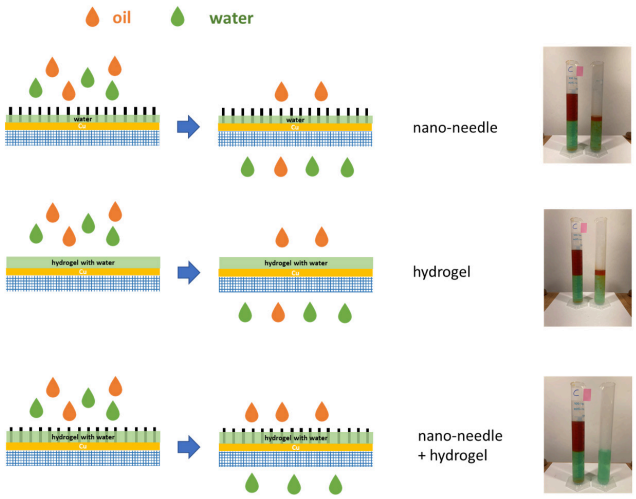

Figure 6: Schematic of the different oil-water separation performance of the meshes with different modification methods. Complete oil-water separation was achieved only when the mesh was modified by nano-needle and hydrogel.

Therefore, the hypothesized synergy of nano-needles and hydrogel regarding oil-water separation capability was demonstrated. Moreover, the meshes with desired performances can be prepared using readily available, low-cost

DOI: 10.36838/v4i1.18

materials and a convenient method. Therefore, it is expected that such meshes can be supplied at affordable prices on a large scale. The wide application of these meshes can significantly reduce the amount of FOG released into wastewater system and markedly minimize the economic loss and negative environmental impact caused by FOG clogs.

Through the approach described in this work, it was evident that a facile and cost-effective method has been established to prepare superhydrophilic and underwater superoleophobic meshes. It is envisioned that these meshes can be conveniently manufactured on an industrial scale to separate FOG from water, leading to the effective elimination of environmental and economic issued caused by FOG.

Although the method detailed in this report is extremely simple, its economic benefit could be significant if it can be applied in large scale. All the materials used in this proof-of-concept experiment purchased from local/internet shops were inexpensive. A single piece of unmodified 200 mesh stainless steel mesh (30 × 60 cm) can be purchased at $10 and the price for bulk purchase will be much lower. The cost of chemical for the modification of one piece of the mesh is less than $0.50, so the cost of the modified mesh (30 × 60 cm) can be controlled at less than $5/piece. Since water co-exists with FOG in the pipeline, the modified mesh can be installed in the pipeline for continuous FOG-water separation. In contrast, current cleaning operation of the pipeline clogged by FOG requires shutting down the water flow to remove the FOG blockage which is significantly more expensive because it involves wages for the workers and economic loss due to shut down. If this convenient and low-cost technique can be used extensively in the world, the financial benefit will be even more dramatic.

Conclusion

It has been shown that a state-of-the-art superhydrophilic and superoleophobic mesh with excellent oil-water separation capability can be conveniently prepared using low-cost materials. The key to this success was the combination of nano-needle structures and hydrogel coating on the mesh. The deployment of this novel method can help to significantly minimize the amount of FOG in sewer systems, leading to a dramatically positive economic and environmental impact.

Acknowledgements

Sincere thanks to my parents for their support and guidance.

References

1. Schaverien, A. Scientists Solve a Puzzle: What's Really in a Fatberg. *The New York Times* https://www.nytimes.com/2019/10/04/world/europe/sidmouth-fatberg.html (2019).
2. Husain, I. A. F.; Alkhatib, M. F.; Jammi, M. S.; Mirghani, M. E. S.; Zainudin, Z. B.; Hoda, A. Problems, Control, and Treatment of Fat, Oil, and Grease (FOG): A Review. *J. Oleo Sci*. 63, 747–752 (2014).
3. Keane, D. 'Disgusting' fatberg size of BUNGALOW removed after clogging London sewer. *The Sun* https://www.thesun.co.uk/news/14098430/fatberg-size-bungalow-removed-sewer/ (2021).
4. Wyllie, I. Fighting the fatbergs: how cities are waging war on clogged sewers. *the Guardian* http://www.theguardian.com/cities/2015/aug/07/fighting-the-fatbergs-how-cities-are-waging-war-on-clogged-sewers (2015).
5. Kary, T. In Fatberg Fight, NYC Goes to War Against Flushable Wipes. *Bloomberg.com* (2019).
6. Ren, G.; Song, Y.; Li, X.; Zhou, Y.; Zhang, Z.; Zhu, X. A superhydrophobic copper mesh as an advanced platform for oil-water separation. *Appl. Surf. Sci*. 428, 520–525 (2018).
7. Zeng, Z. S. & Taylor, S. E. Facile preparation of superhydrophobic melamine sponge for efficient underwater oil-water separation. *Sep. Purif. Technol*. 247, 116996 (2020).
8. Xue, Z.; Wang, S.; Lin, L.; Chen, L.; Liu, M.; Feng, L.; Jiang, L. A Novel Superhydrophilic and Underwater Superoleophobic Hydrogel-Coated Mesh for Oil/Water Separation. *Adv. Mater*. 23, 4270–4273 (2011).
9. Wang, H.; Hu, X.; Ke, Z.; Du, C. Z.; Zheng, L.; Wang, C.; Yuan, Z. Review: Porous Metal Filters and Membranes for Oil–Water Separation. *Nanoscale Res*. Lett. 13, 284 (2018).
10. Yong, J., Chen, F., Yang, Q., Huo, J. & Hou, X. Superoleophobic surfaces. *Chem. Soc. Rev*. 46, 4168–4217 (2017).
11. Zhang, L., Zhong, Y., Cha, D. & Wang, P. A self-cleaning underwater superoleophobic mesh for oil-water separation. *Sci. Rep*. 3, 2326 (2013).
12. Xiong, L.; Guo, W.; Alameda, B. M.; Sloan, R. K.; Walker, W. D.; Patton, D. L. Rational Design of Superhydrophilic/Superoleophobic Surfaces for Oil–Water Separation via Thiol–Acrylate Photopolymerization. *ACS Omega 3*, 10278–10285 (2018).
13. Liu, N.; Chen, Y.; Lu, F.; Cao, Y.; Xue, Z.; Li, K.; Feng, L.; Wei, Y. Straightforward Oxidation of a Copper Substrate Produces an Underwater Superoleophobic Mesh for Oil/Water Separation. *ChemPhysChem* 14, 3489–3494 (2013).
14. Liao, R.; Ma, K.; Tang, S.; Liu, C.; Yue, H.; Liang, B. Biomimetic Mineralization to Fabricate Superhydrophilic and Underwater Superoleophobic Filter Mesh for Oil–Water Separations. Ind. *Eng. Chem*. Res. 59, 6226–6235 (2020).
15. You, Q., Ran, G., Wang, C., Zhao, Y. & Song, Q. A novel superhydrophilic–underwater superoleophobic Zn-ZnO electrodeposited copper mesh for efficient oil/water separation. *Sep. Purif. Technol*. 193, 21–28 (2018).
16. Zhou, R.; Shen, F.; Cui, J.; Zhang, Y.; Yan, H.; Juan Carlos, S. S. Electrophoretic Deposition of Graphene Oxide on Laser-Ablated Copper Mesh for Enhanced Oil/Water Separation. *Coatings* 9, 157 (2019).
17. Matsubayashi, T., Tenjimbayashi, M., Komine, M., Manabe, K. & Shiratori, S. Bioinspired Hydrogel-Coated Mesh with Superhydrophilicity and Underwater Superoleophobicity for Efficient and Ultrafast Oil/Water Separation in Harsh Environments. *Ind. Eng. Chem*. Res. 56, 7080–7085 (2017).
18. Lu, F.; Chen, Y.; Liu, N.; Cao, Y.; Xu, L.; Wei, Y.; Feng, L. A fast and convenient cellulose hydrogel-coated colander for high-efficiency oil–water separation. *RSC Adv*. 4, 32544–32548 (2014).
19. You, Q., Ran, G., Wang, C., Zhao, Y. & Song, Q. Facile fabrication of superhydrophilic and underwater superoleophobic chitosan–polyvinyl alcohol-TiO2 coated copper mesh for efficient oil/water separation. *J. Coat*. Technol. Res. 15, 1013–1023 (2018).
20. Lin, L.; Liu, M.; Chen, L.; Chen, P.; Ma, J.; Han, D.; Jiang, L. Bio-Inspired Hierarchical Macromolecule–Nanoclay Hydrogels for Robust Underwater Superoleophobicity. *Adv. Mater*. 22, 4826–4830 (2010).
21. Wang, Y., Feng, Y., Zhang, M., Huang, C. & Yao, J. A green strategy for preparing durable underwater superoleophobic calcium alginate hydrogel coated-meshes for oil/water separation. *Int. J. Biol. Macromol*. 136, 13–19 (2019).
22. Chen, Y.; Li, X.; Glasper, M. J.; Liu, L.; Chung, H.-J.; Nychka, J. A. A regenerable copper mesh based oil/water separator with switchable underwater oleophobicity. *RSC Adv.* 6, 92833–92838

(2016).
23.Xu, S., Sheng, R., Cao, Y. & Yan, J. Reversibly switching water droplets wettability on hierarchical structured Cu 2 S mesh for efficient oil/water separation. *Sci. Rep*. 9, 12486 (2019).
24.Zhang, E., Cheng, Z., Lv, T., Qian, Y. & Liu, Y. Anti-corrosive hierarchical structured copper mesh film with superhydrophilicity and underwater low adhesive superoleophobicity for highly efficient oil–water separation. *J. Mater. Chem*. A 3, 13411–13417 (2015).
25.Li, J.; Cheng, H. M.; Chan, C. Y.; Ng, P. F.; Chen, L.; Fei, B.; Xin, J. H. Superhydrophilic and underwater superoleophobic mesh coating for efficient oil–water separation. *RSC Adv*. 5, 51537–51541 (2015).
26.Gou, X.; Zhang, Y.; Long, L.; Liu, Y.; Tian, D.; Shen, F.; Yang, G.; Zhang, X.; Wang, L.; Deng, S. Superhydrophilic and underwater superoleophobic cement-coated mesh for oil/water separation by gravity. Colloids Surf. *Physicochem. Eng. Asp*. 605, 125338 (2020).
27.Zhang, Z., Liu, Z. & Sun, J. Facile preparation of superhydrophilic and underwater superoleophobic mesh for oil/water separation in harsh environments. *J. Dispers. Sci. Technol*. 40, 784–793 (2019).
28.Zhou, H.; Wang, H.; Yang, W.; Niu, H.; Wei, X.; Fu, S.; Liu, S.; Shao, H.; Lin, T. Durable superoleophobic–superhydrophilic fabrics with high anti-oil-fouling property. *RSC Adv*. 8, 26939–26947 (2018).
29.Ma, Q.; Cheng, H.; Yu, Y.; Huang, Y.; Lu, Q.; Han, S.; Chen, J.; Wang, R.; Fane, A. G.; Zhang, H. Preparation of Superhydrophilic and Underwater Superoleophobic Nanofiber-Based Meshes from Waste Glass for Multifunctional Oil/Water Separation. *Small* 13, 1700391 (2017).

Author

Zhi-Wei Steven Zeng is a senior at Obra D. Tompkins High School, TX. He has strong interest in environmental science and has worked on three projects (oil spilling, solar energy utilization, and water clean-up), and qualified for ISEF final competition in 2020 and 2021. He won the First Place of YM American Academy Special Award in the 2021 ISEF final competition. He is also passionate in filming and won Third Place in state competition for documentary film.

DOI: 10.36838/v4i1.18

IJHSR
ijhighschoolresearch.org
RESEARCH ARTICLE

Residential Solar Energy: A Mathematical Cost Analysis

Trivedi Mytreyi

Hamilton High School 3700 S Arizona Ave, Chandler, AZ, USA; mnm.trivedi@gmail.com

ABSTRACT: This research studied the way by which residential solar energy production can offset the power drawn from the utility and its overall financial impact on the customer through mathematical cost analysis. A sample annual electricity bill was used as the baseline for the analysis. The publicly available energy generation and pricing structure of Tesla® Solar Solution were used for the calculation. Several rate plans from Salt River Project (SRP) were analyzed for their impact on the electricity bill for the same usage pattern with and without solar generation. Inferences were drawn about the benefit of solar generation with recommendations for maximizing the return on investment.

KEYWORDS: Solar energy generation; utility rate; storage batteries; net energy metering; demand charge.

Introduction

Energy generation in the US is dominated by non-replenishable fossil fuels. Renewable energy has been an active topic of discussion lately due to the real threats of climate change. Renewable energy sources provide an alternative to non-replenishable and polluting fossil fuels by being produced from sources that will not become depleted. The most commonly available renewable energy sources are solar and wind energy. Solar energy is poised to take a lead role in clean and renewable production of energy.[1] It is based on the concept of photovoltaic effect. Solar photovoltaic (PV) energy generates renewable electricity by converting energy from the sun.[2] The energy of the sun is captured by the solar panel, which excites the electrons. The current that flows due to the excited electrons is converted using electronic components into a form that can be utilized by a household to offset the energy drawn from the electric utility. If the solar energy production is greater than the household's needs, the excess energy can be returned to the electrical utility or even be stored in a local rechargeable battery to be used at a later time. The trend is moving toward incorporating solar into more buildings and beyond panels being placed on roofs. Some possible applications include: solar tiles, solar film, solar roadways, and solar windows.[3]

Many states, such as Arizona and California, offer incentives for switching to renewable energy. As part of their commitment to reduce carbon emissions, electric utility companies in the Phoenix Metropolitan area (Salt River Project [SRP] and Arizona Public Service [APS]) are making investments in solar and wind energy farms. Additionally, energy providers have been making changes to their utility plans to encourage homeowners to convert to more renewable energy sources. SRP provides several electricity rate plans to give customers an opportunity to balance their budgets to their electricity consumption. Several commercial residential solar energy solutions are available from vendors like SunRun® and Tesla®. However, consumers remain skeptical about the practicality and benefits of solar energy, as witnessed by the slow adoption of this technology. This begs the question of whether people are oblivious to the financial and other benefits, or uncomfortable with new technology. Although most people understand solar energy production in general, cost-benefit analyses are not freely available to prospective customers particularly with the battery storage option. This research attempts to address the gap using a residential case as an example and deriving a model to explain and de-mystify the factors involved in residential solar energy. The next section explains utility rate plans and presents a simple mathematical model for estimating solar energy generation and electricity consumption for a residential setting. The formulas are then used to understand energy balance patterns and cost projections for various solar energy solution configurations. Finally, inferences are made about the Return-of-Investment (RoI) potential for residential solar energy.

Model for Solar Energy Estimation: Solar Energy Generation

The energy produced by solar panels is very strongly a function of the time of day and season. This is largely dependent on the extent of exposure to the sun. Each solar panel has a limit on the maximum power that can be generated. Depending on the house size and model, there are different sizes of solar panels and different numbers of storage batteries. For instance, Tesla® offers Small, Medium and Large configurations[4] that produce a maximum output of 3.8kWh, 7.6kWh or 11.4kWh, respectively. Similarly, there is an upper limit on the energy storage and the maximum power that can be supported by each power storage battery. Each Tesla® battery (called PowerWall2TM) can store up to 13.5kWh of energy, which can be discharged at a 5kW maximum rate. The battery storage solution can be stacked to meet the needs of the household. They store energy by converting electrical energy into chemical through a chemical reaction. Energy can be stored for a period of time and can be released when required by means of a conversion of chemical energy to a voltage potential across the positive and the negative electrodes that lie in the battery electrolyte.[5]

In order to facilitate a model for energy generation, a simple experiment was conducted to first understand the productive hours of the day and study the pattern of available solar

DOI: 10.36838/v4i1.19

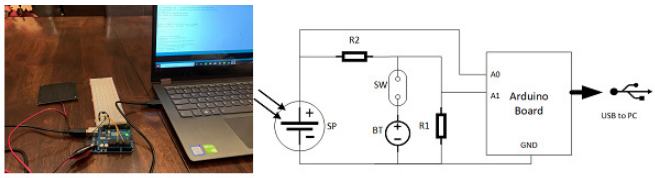

Figure 1: Experimental setup for studying solar energy generation showing a. picture of the setup, and b. electrical circuit connection.

energy. Using a commercially available Solar Panel rated at 5V/100mA, one experiment was to track the current produced by the Solar panel during the day by monitoring voltage across a resistor load. A second experiment was conducted to study how an electric load is shared between solar energy and the utility. A rechargeable battery was used to represent the utility. The measurement was conducted throughout the day over a 12-hour period (6:30am to 6:30pm), which required an automated voltage measurement system for accuracy and repeatability. An Arduino kit6 was employed to measure and record the voltage across the resistor at periodic intervals. Figure 1 shows a picture of the experimental setup for studying solar energy generation along with the electrical circuit diagram. In the first experiment, the switch (SW) was left open. The solar voltage across the panel (SP) was measured at input pin A0 of the Arduino kit and current flow was deduced based on the total resistance (R1+R2). In the second experiment, the switch (SW) was closed to connect the battery (BT). The current through the solar panel (SP) and battery (BT) was calculated by observing the voltage at points A0 and A1. The battery was nominally at 1.5V and discharged into resistor R1 as long as the solar voltage was lower than 1.5V. The panel prevented backflow of current into itself. The measured results of the experiment are described later in this section.

Understanding Electric Utility Rates and Solar Energy Solution:

A sample SRP residential electricity bill over the year 2019 from January to December was used as the control parameter for this study and a reference for further analysis. The various price plans described in SRP's website (www.srpnet.com/menu/electricres/priceplans.aspx) were analyzed and the sample electricity bill was taken to mathematically project the annual bill without and with a Solar Energy Solution by creating equations for each specific price plan. For the analysis, Tesla® (Solar City) was chosen as the solar energy solution provider because of the public information available from their website (www.tesla.com/energy/design) as well as the Google Project Sunroof (www.google.com/get/sunroof) website on the configurations.

Several conventional price plans are offered by SRP, such as Basic, EZ-3 and Time-Of-Use. Most people use the Basic and Time-of-Use plans. The basic rate charges electricity usage at a flat rate throughout the day, whereas the Time-of-Use plan charges at a lower rate during the "Off-Peak" hours and higher rate during the "On-Peak" hours. The off-peak and on-peak hours depend on the season, as shown in the chart in Figure 2. In Arizona, winter months are November-April, summer months are May-June and September-October, and peak summer months are July-August.

Figure 2: Off-peak and On-peak Hours over the year for SRP Rate Plans.

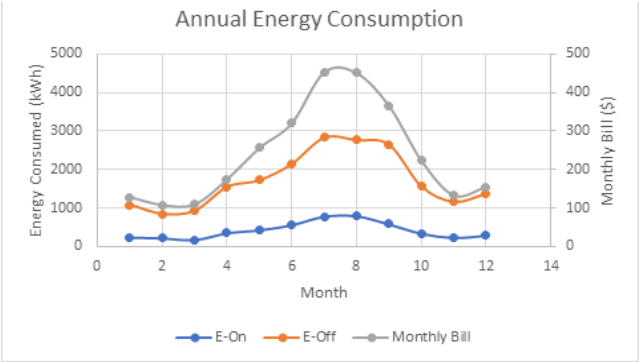

Figure 3: Annual Energy Consumption of a sample household.

The SRP monthly electricity bill and website[7] provide a wealth of information about energy consumption by a subscribing household. The annual energy consumption by the sample AZ household on the Time-of-Use plan being studied in this project was compiled from the monthly SRP electricity bill over a period of 12 months. The data is shown in Figure 3. The energy consumption during on-peak and off-peak hours per month is on the left axis, while the monthly electricity bill on the Time-of-Use plan is shown to the right. The energy consumption is highest during the hot summer months when the AC is running, and lowest through the winter months. This annual energy consumption was used as the baseline reference for studying the various rate plans and solar energy solutions.

SRP also offers various electricity rate plans for consumers that install residential solar energy systems, such as Solar Time-of-Use, Average Demand and Customer Generation Plans. The Solar Time-of-Use and Customer Generation Plans were chosen for study in this project. Key information about various solar and non-solar energy rate plans compiled from SRP's website is summarized in Table 1 below. The table shows the rates in each season as well as the basic service charge for each price plan. Every rate plan has seasonal variations in the on/off-peak rates because the electricity bill for each plan can be different for the same usage pattern. The electricity rate is higher during the summer months than winter months. Coupled with the observation that higher energy is consumed during summer months, the electricity bill during summer months can be four-times that of the winter months (Figure 3). The Time-of-Use plan allows consumers to reduce their bill by moving high energy consuming activity (e.g., laundry, pool pump) to off-peak hours. The Solar Time-of-Use plan has the same rates as the non-solar plan, but the utility provides a flat-rate credit for energy returned to the grid. The Solar Customer Generation plan has the lowest electricity rate, and the credit for energy returned to the utility is the same rate as the charge for energy consumed.

DOI: 10.36838/v4i1.19

This is referred to as 'Net-Metering'. However, this plan has a penalty called 'Demand Charge' which is an extra amount that must be paid each month proportional to the maximum power drawn from the grid during on-peak hours. Table 2 shows the Demand Charge rates as a function of peak power and the season. As shown, the demand charge penalty is significantly higher for higher peak demand. Thus, households with Solar Customer Generation plan must be aware of this penalty if they have equipment that draws high instantaneous (or peak) power. The next section describes the equations that were formulated to model these price plans.

Table 1: Key Information of various Energy Plans under study.

Plan Name	Non-Solar Flat	Non-Solar Time-of-Use	Solar Time-of-Use	Solar Customer Generation
Plan Name	E23	E26	E13	E27
Service Charge ($)	20	20	32.44	32.44
Summer On Peak Rate ($/kWh)	.1134 (>2K)	0.2094	0.2094	0.0462
Summer Off Peak Rate ($/kWh)	0.1091 (<2K)	0.0727	0.0727	0.036
Peak Summer On Peak ($/kWh)	0.127 (>2K)	0.2409	0.2409	0.0622
Peak Summer Off Peak ($/kWh)	0.1157 (<2K)	0.073	0.073	0.0412
Winter On Peak Rate ($/kWh)	0.0782	0.0951	0.0951	0.041
Winter Off Peak ($/kWh)	0.0782	0.0691	0.0691	0.037
Demand Charge ($/kW)	0	0	0	See Table 2
Credit ($/kWh)	0	0	$0.0281	Same as charge

Table 2: Demand Charge Rate for Solar Customer Generation Plan/E27.

Peak Demand	0-3 kW	3-10 kW	> 10 kW
Summer ($/kW)	7.89	14.37	27.28
Peak Summer ($/kW)	9.43	17.51	33.59
Winter ($/kW)	3.49	5.58	9.57

Model for Monthly Bill Estimation for Various Plans :

The objective of this project was to estimate the electricity bill for the plans described in Table 1 for the annual usage pattern shown in Figure 3. The SRP website does not offer equations for any plan, so the first task was to formulate equations that accurately represent each plan. The equations cover the base charge for energy consumption, credit for solar energy generation/storage and applicable power penalty/taxes. The variables describing the monthly base charge for energy consumption are:

- Service_Charge: The base charge for any given plan
- Energyk: Total energy consumed for the month at the rate 'k', where k represents on-peak or off-peak (except Flat Rate plan, where k represents rate <2KWh or >2KWh)
- Ratek: Billing rate for the month at the rate 'k', where k represents on-peak or off-peak (except Flat Rate plan, where k represents rate <2KWh or >2KWh)

The base energy consumption charge for each plan is

$$Energy\ Consumption\ Charge = \left[Service\_Charge + \sum_{k=on-peak,off-peak} (Energy_k * Rate_k)\right]$$

The Flat Rate and Time of Use plans simply account for the service charge and energy consumed at each rate. The Solar energy plans provide a credit to the consumer for the amount of solar energy generated. The energy generated by the solar panels can be used to power the home, offsetting the energy drawn from the utility. With the Solar Time of Use Plan, the excess solar energy may be returned to the grid for a flat-rate credit (2.81c/kWh) which is typically much lower than the rate at which the customer is charged for the energy drawn from the grid. While the Solar Customer Generated plan is similar to the Solar Time of Use concept, a key difference is in the credit for the excess solar energy returned to the grid. Per the Net-Metering concept, the consumer is charged for the net energy drawn from or returned to the grid at on-peak or off-peak rates. Effectively, the customer gets the full credit for all generated solar energy. It is important to estimate the energy generated during on-peak and off-peak hours for both Solar Plans. The method for estimating on-peak and off-peak solar energy generation is described later in this section. The variables describing the solar energy generation credit are defined as:

- Generationk: Total Energy generated for the month at the rate 'k', where k represents on-peak or off-peak for the Customer Generated Plan
- Creditk: Credit rate for the month at the rate 'k', where k represents on-peak or off-peak for the Customer Generated Plan
- Excess Generation: Total energy returned to the grid for the month for the Solar Time of Use Plan
- Flat_Credit: Flat rate credit (2.81c/kWh) for energy returned to the grid in Solar Time of Use Plan

Then, the utility credit for each plan is

$$Customer\ Generation\ Credit = \left[\sum_{k=on-peak,off-peak} (Generation_k * Credit_k)\right]$$

$$Solar\ Time\ of\ Use\ Credit = Excess\ Generation * Flat\ Credit$$

In order to estimate the solar energy generated during on-peak and off-peak hours, the solar cycle over the year must be understood first. The experimental setup described in Figure 1 was used for this purpose, with the results shown in Figure 4. The left graph in Figure 4 shows the Current and Voltage generated by the Solar Panel, showing a bell curve through the day from 6:30am to 6:30pm. This shows that the current and voltage are directly proportional to the amount of sunlight with maximum production at mid-day. The right graph of Figure 4 shows the result of the second experiment, plotting the current drawn from the battery connected in parallel with the solar panel. When the solar production is low, the charge stored in the battery feeds the resistor load. When the curve drops below zero, the battery current is negative, so the solar energy is feeding the load as well as returning charge to the battery. This shows the basic idea of using Solar Panels to offset the energy drawn from the electric utility. The battery is discharging from time 6:30am-10am and 3:30pm-6:30pm. It is charging from 10am-3.30pm.

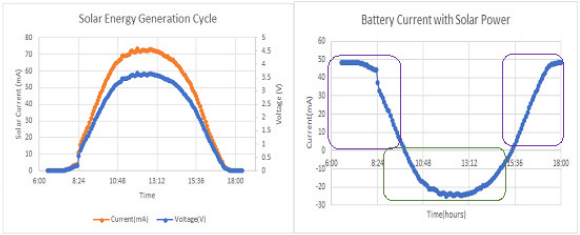

Figure 4: Solar Generation Cycle and Battery Current with Solar Power showing a: Solar panel voltage and current, and b: charge/discharge cycle of the storage battery.

Figure 4 shows that the solar energy generation cycle through the day is highly non-linear. In order to estimate the solar energy generated during on-peak and off-peak hours, the solar cycle must be approximated into a simpler form for a study of the scale. Likewise, domestic energy consumption patterns are also non-linear. For this study, some simplifying assumptions were made regarding the average energy generation and consumption patterns through the seasons in order to analyze the annual bill for various plans. Figure 5 shows a piecewise linear approximation of daily energy generation and consumption patterns for the summer and winter months. The orange lines are a simplification of the bell-curve shaped solar energy generation pattern. The blue lines show a simplified representation of energy usage patterns based on a study of the SRP bill over a twelve-month period. This represents the usage pattern for a typical family that is out of the house during office/school hours. Energy consumption is lower during the middle of the day but higher through the evening and night when the family is home.

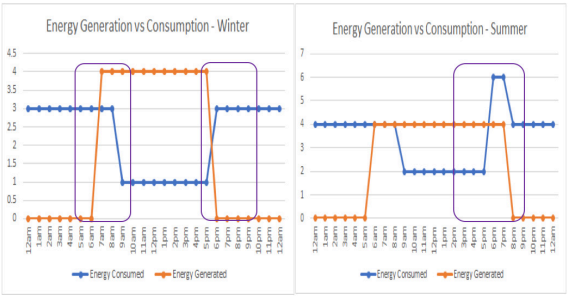

Figure 5: Energy Generation vs. Consumption Patterns-Winter and Summer.

A mathematical spreadsheet model was built for estimating solar energy generation using the simplifying assumptions outlined in Figure 5. The Google SunRoof[8] project site provided an estimate of the total energy generation over the entire year for any solar panel configuration. In order to derive the energy generation for any month, the average daylight time for each month was listed, and the total estimated energy generation was distributed over the months in direct proportion of the daylight time. This simplification does ignore the effect of temperature on efficiency of energy generation, but this should be acceptable for this project. For each month, the energy generated was split into on-peak and off-peak production ($Generation_{on\text{-}peak}$ and $Generation_{off\text{-}peak}$) by mapping the productive hours with the on-peak and off-peak hours chart shown in Figure 2. Weekends and holidays are treated at off-peak rates over the entire day. The Excess Generation for the Solar ToU plan was then computed as:

If $Generation_{on\text{-}peak} > Energy_{on\text{-}peak}$, then $Excess_{on\text{-}peak} = Generation_{on\text{-}peak} - Energy_{on\text{-}peak}$, else = 0

If $Generation_{off\text{-}peak} > Energy_{off\text{-}peak}$, then $Excess_{off\text{-}peak} = Generation_{off\text{-}peak} - Energy_{off\text{-}peak}$, else = 0

$$Excess\ Generation = \sum_{k=on-peak,off-peak} (Excess_k)$$

A downside of the Customer Generation plan is that the utility charges a penalty for the maximum power drawn from the grid over any hour during the on-peak periods of the month, referred to as Demand Charge, listed in Table 2. The penalty is higher if the household has equipment (such as old AC models) that draw higher peak current. Then depending on the peak power, the Demand Charge is:

$$Demand\ Charge = \sum_{k=1,2,3} (Power_k * Charge_k), \text{ where}$$

k=1 represents power between 0-3kW, k=2 is power between 3kW-10kW, k=3 is power >10kW.

All the equations described in this section were used to put together monthly bill estimates for various plans. Figure 6 shows the flow diagram for applying charges and credits towards the monthly bill.

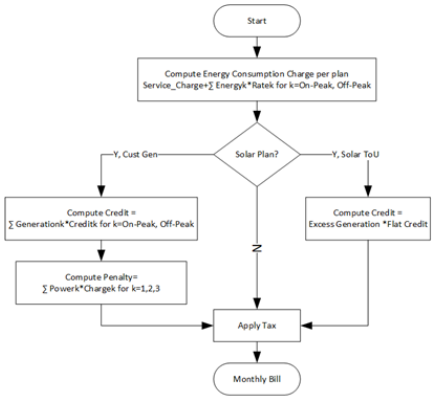

Figure 6: Flowchart for computing the monthly electricity bill for each plan.

Battery Storage:

The piecewise uniform energy model of Figure 5 reveals that periods for peak daily energy consumption and generation are mismatched. It also suggests that less energy is generated during the on-peak hours (marked in purple box) than off-peak hours. A hypothesis is that savings in solar electricity bill may be limited due to this mismatch if the solar energy is instantaneously consumed or returned to the grid. If it is possible to harness the excess energy generated during the cheaper off-peak hours and use it to power the house during the expensive on-peak hours, it would arguably have a greater effect on reducing the electricity bill. Storage batteries may be used to implement this possibility.

Battery storage was considered for the Solar Time-of-Use and Customer Generated plans. This model assumes that during the daylight hours, the solar energy is first used to meet the residential energy consumption. The excess energy is first allocated for battery storage, and once the battery capacity is reached, the residual excess energy is returned to the utility for energy credits. Once the sun is down, the energy stored in the battery is first used to meet the energy consumption during on-peak hours. The residual energy is consumed during off-peak hours. An alternative model could be one where all the solar energy generated during off-peak hours is used to charge the battery, and the battery primarily provides the power during the on-peak hours.

In case of the Customer Generation Plan, the peak power drawn is first serviced by the battery, and the utility only covers the amount of peak power that exceeds the battery's discharge rate. This greatly reduces the demand charge for this plan. For

DOI: 10.36838/v4i1.19

the Solar ToU plan, the utility of the battery is mostly to alleviate the power drawn from the utility during on-peak hours.

Results and Discussion

The flow described in the previous section was used to calculate the net monthly electricity bill. This section presents the results of the comparative analysis across various plans. The annual energy consumption pattern shown in Figure 3 was used in all cases.

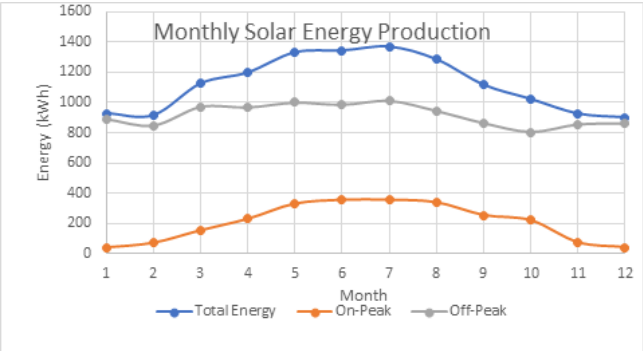

Figure 7: Monthly Solar Energy Production.

The graph in Figure 7 shows the results of the model for energy produced by the Solar Panels over one year, broken out in on-peak and off-peak production. The model is based on a Google Sunroof estimated annual production of 13,500 kWh for a mid-sized 7.6kW Solar System in Arizona. As expected, the highest energy is produced during the summer months. It is interesting to note that most of the energy is produced during off-peak hours, which is consistent with Figure 5. This limits the amount of credit to the customer during on-peak hours. Figure 3 shows that average energy consumption is also lower during the on-peak hours than off-peak hours. However, the offset between energy consumption and generation patterns still results in a penalty for the consumer. This model accounts for varying daylight hours over the seasons. The energy generated during the on-peak hours was considerably (5x-10x) less than the energy generated in the off-peak hours. This shows that it is difficult to offset the price of energy consumed during on-peak hours. Since most of the energy is harvested during off-peak hours, batteries can be a beneficial addition to the solar panels.

Figure 8 compares the annual electricity bill for the two non-solar and two solar plans under study. Additional benefit from battery storage was also studied for the Solar plans. Based on research, SRP does not permit the use of storage batteries without a Solar Energy Generation solution. Among the non-solar solutions, the Time-of-Use plan offers incremental annual savings (~$250) over the flat rate plan. The potential savings incentivize customers to move higher electricity usage to the Off-Peak hours.

As seen from Figure 8, both the Solar Time-of-Use and Customer Generated Plans result in a lower electricity bill than the two non-solar plans by about $500-$750 even without the use of batteries. Use of power storage batteries results in a further reduction of the annual bill. Interestingly, storage batteries yield a greater value with the Customer generation plan than the Solar Time-of-Use plan. With the Solar Time-of-Use plan, batteries provide a fixed amount of offset to the energy consumed by the household, and the credit for energy returned to the utility is very small. On the other hand, Net-Metering in the Customer Generated plan provides credits that are better balanced with the energy consumption. Further, the batteries reduce the peak energy demand from the grid during On-Peak time, directly mitigating the Demand Charge penalty. The Customer Generated Price Plan shows the greatest price drop with the second battery by nearly eliminating demand charge.

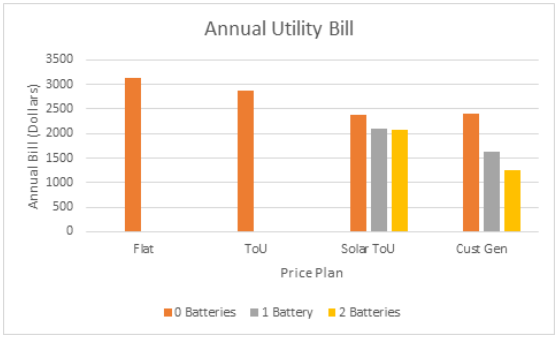

Figure 8: Annual Utility Bill for scenarios under study.

It is clear from Figure 8 that residential solar energy systems yield significant reductions in annual electricity bill (~25%) compared to the non-solar baseline plan. Use of storage batteries can result in even greater savings (~60%). This reduction of electricity bill by 60% seems very attractive. However, the initial cost of solar energy solution installation can be a big deterrent for most families. The Federal government offers tax credits (~26% in 2020) for solar energy installations, with additional rebates from individual states and utility companies. Still, the total installation cost can run into several thousand dollars. For instance, after rebates and incentives, the Tesla® Solar Energy solution can be about $12,000 without batteries, and up to $22,000 with batteries. The expectation, then, is that it would take several years for a customer to recuperate the installation cost even with a substantial reduction in the annual electricity bill. Further, solar energy equipment is typically projected to have a productive lifespan of 12-15 years.

A Total Cost-of-Ownership calculation was performed for all four plans under study to determine the financial merits of a solar energy solution. A cumulative annual bill for 15 years was compiled and added to the initial price of installation of the solar energy solution to project the final cost to the consumer. Cumulative payments were compared to determine if and when the solar price plan is cheaper than just drawing energy from the electrical grid. Figure 9 shows an overlay graph of the cumulative cost of ownership of various energy solutions. It is assumed that the electricity rates charged by the utility have an annual inflation rate of 3%. This is the average rate of inflation over the past 20 years.

All the graphs are slightly non-linear with varying slopes. The Flat rate (Flat) plan and the Time of Use (ToU) plan both started out as the least expensive since there is no upfront capital cost, but the Flat Rate ended up being the second most expensive price plan. The Customer Generated Plan (CustGen) with no batteries and the Time of Use (ToU) plan

ended up with similar cost after 15 years. The Solar Time-of-Use plan with 2 batteries (Batt ToU2) remained the most expensive throughout the 15 years. The Customer Generated plan with 2 Batteries (Batt Cust2) was the most cost effective in the long run as it ended up with the least cumulative price despite having the highest upfront cost. This plan has an 11-year breakeven point with a 40% return of investment in 15 years.

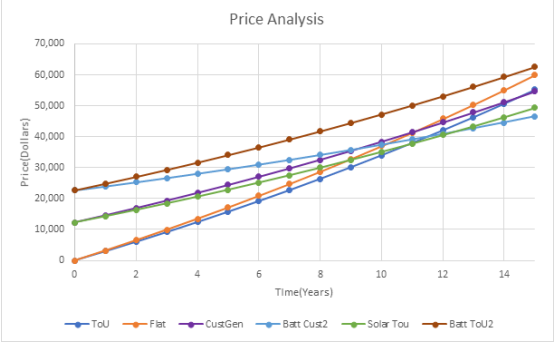

Figure 9: Annual Utility Bill for scenarios under study.

It is clear that Solar energy solutions require a high upfront investment in terms of installation costs. Even with a lower electricity bill, it takes several years to recuperate the cost. Most importantly, the rate of energy reduction is a strong function of the configuration of the solar energy solution and the utility rate plan. If not matched properly, it is possible for some consumers to never achieve a breakeven point. On the other hand, with a wise selection of the energy solution and utility plan, it is possible to break even within 10 years or less. The optimal solution may vary depending on the consumer lifestyle (stay at home all day vs mostly being outside during the daytime hours).

Solar panels should be taken care of regularly and placed strategically to maximize the energy generation. Optimal placement in residential settings is often on rooftops along the side that gets maximum exposure to the sun, preferably towards the south in the US with little surrounding tree cover. The panels should also be washed and wiped at periodic intervals to remove the dust and debris that collects on them over time. With regular care, the solar panels can generate energy for a long time, with little degradation over the years. The energy storage batteries usually do not require maintenance or servicing; however, experts need to be brought in if problems arise.

Conclusion

In conclusion, a thorough mathematical analysis of the electrical utility bill was presented for various configurations of Tesla® solar energy solution and SRP bill pay schemes. It is shown that solar energy generation can significantly reduce the electricity bill and pay for itself over a period of time, but the benefits can be limited by the mismatch between when the energy is generated and when it is consumed. Storing the excess energy in batteries for later consumption was seen to have a greater effect in reducing the electricity bill. The analysis shows that a solar energy solution that utilizes two Powerwall2TM batteries and is on SRP's Customer Generation Price Plan (E27) presents the best opportunity to offset the upfront installation costs in the least amount of time. The spreadsheet tool created in this project was proved out on a specific sample electricity bill but can be used to provide an assessment for a variety of consumption scenarios and solar energy configurations. As shown through the study, policies that dictate rates would heavily influence solar deployment in residential sectors in addition to advances in solar energy technology. Continuous improvements in battery technology and pricing schemes will give a boost to solar energy for increased utility scale deployment.

Acknowledgements

The author would like to thank Dr. Malay Trivedi for his encouragement and constructive suggestions through this project.

References

1. Gme. "Solar Energy: Past, Present and Future." *Green Mountain Energy Company*, 30 Nov. 2018, www.greenmountainenergy.com/2014/06/solar-energy-past-present-future/
2. Shaikh, Mohd Rizwan & Shaikh, Sirajuddin & Waghmare, Santosh & Labade, Suvarna & Tekale, Anil. (2017). A Review Paper on Electricity Generation from Solar Energy. International Journal for Research in Applied Science and Engineering Technology. 887. 10.22214/ijraset.2017.9272.
3. "The Future of Solar Energy." *Main*, energy.mit.edu/research/future-solar-energy/
4. "Design Your Solar." Tesla, www.tesla.com/energy/design
5. "Cucchiella, Federica, Idiano D'adamo, and Massimo Gastaldi. "Photovoltaic energy systems with battery storage for residential areas: an economic analysis." Journal of Cleaner Production 131 (2016): 460-74. Print.
6. "Home." *Arduino*, www.arduino.cc/
7. "Salt River Project Power and Water." SRP, www.srpnet.com/
8. "Project Sunroof." *Google*, Google, www.google.com/get/sunroof

Author

Mytreyi Trivedi is a rising senior at Hamilton High School with a strong desire to learn STEM topics. Over the years, she has participated in and won three State Science Fair Awards related to alternative energy. She is passionate about hands-on learning and research in science topics.

DOI: 10.36838/v4i1.19

IJHSR
ijhighschoolresearch.org
RESEARCH ARTICLE

Implementing Value-Sensitive Machine Learning to Develop a Risk Level Self-Assessment Model for Cervical Cancer

Kaixin Kate Yin

International School of Beijing, 10 An Hua Street, Shunyi District, Beijing, 101300, China; kate.yin@student.isb.bj.edu.cn

ABSTRACT: Cervical cancer begins with cancerous cells in the cervix. Cervical cancer is the third most common cancer worldwide, and 80% of the cases occur in developing countries. The high incidence of this cancer in the developing world is mostly due to a lack of effective screening programs aimed at detecting and treating precancerous conditions. This project aimed to mitigate this issue by developing a self-assessment model based on value-sensitive machine learning. The model would advise if the user should receive a cervical cancer screening based on their lifestyle and disease history. The machine learning model is developed based on dataset with survey responses to enable preliminary assessment on risk level before seeking healthcare resources. The dataset had 858 records; 55 patients had a positive cervical cancer diagnosis, and the remaining 803 patients were healthy. A machine learning approach was adopted, and the samples were divided into two groups randomly as the training and testing groups. 70% (600 patients) of the entire dataset was used to train the machine, and the remaining 30% (258) was assigned as the test dataset. Various classifiers, such as a decision tree, SVM, and logistic classification were also implemented. To evaluate each classification method, a confusion matrix was generated for each method, and classifiers were compared using F1 score and false negative rate. The tradeoff between overall classifier performance and the consequence of false negative rate in this scenario was discussed and an implementation suggestion was provided.

KEYWORDS: Computational Biology and Bioinformatics; Computational Biomodeling; Machine Learning.

Introduction

Cancer stems from normal cells transforming into tumor cells in a multistage process. The chances of survival and treatment for cancer decrease over time; therefore, significant improvements in a patient's chance of survival can be made if diagnoses were made in the early stages and avoiding delays.[1] As in many other diseases, the existence of several screening and diagnosis methods creates a complex ecosystem from a Computer-Aided Diagnosis (CAD) system point of view.[2] However, in developing countries with more limited medical care resources, people may not be able to accurately detect cancer in the early stages, resulting in higher morbidity rates. In addition, the social stigma against women with cervical cancer may be high in developing countries, which can prevent women from seeking medical attention. Therefore, the most critical problems during diagnosis are related to determining the most appropriate screening plan and estimating individual risk for each patient.[3]

To reduce unnecessary screenings and reduce the need for accessing healthcare resources, people who are concerned about their risk of cancer could complete a lifestyle and disease history, which helps determine if they are at risk for developing cancer.[4] Afterward, these patients can seek out screening according to their risk level. Such a risk prediction survey can help developing countries support the targeted group more effectively and reduce the burden on healthcare.[5]

This investigation attempted to develop a risk level self-assessment model using three machine learning methods: decision tree, logistic classification, and support vector machine (SVM). These approaches were chosen due to their renowned high accuracy and efficiency.[6,8] A decision tree model forces the consideration of all possible outcomes of a decision and traces each path to a conclusion. It creates a comprehensive analysis of the consequences along each branch which is suitable for the issue at hand. A cervical cancer dataset contains multiple attributes that need to be taken into account; therefore, all of these factors need to be considered before reaching a conclusion. A logistic classification achieves similar purposes; it estimates the probability of an occurrence of an event based on one or more inputs, which again matches this exploration's objective.[10] A SVM model is known for its kernel trick to handle nonlinear inputs, which could be applied to the case of a cervical cancer dataset that contains Boolean data.[11]

In this study, the cervical cancer risk detection algorithm was built based on a dataset consisting of survey responses and biopsy diagnosis. An algorithm selection was performed based on increasing overall model performance and reducing false negative rates. A discussion on trade-offs between algorithm performance and the consequence of predicting false negative cases was also provided.

Dataset:

The dataset used in this project was collected by Hospital Universitario de Caracas in Caracas, Venezuela. It comprises demographic information, lifestyle, and disease history of 858 patients.[12] There are 35 attributes in total, with 4 types of diagnosis results. The attributes in the dataset are summarized in Table 1.

DOI: 10.36838/v4i1.20

Table 1: Attribute Information.

Feature	Type	Feature	Type
Age	Integer	STDs: pelvic inflammatory disease	Boolean
# of partners	Integer	STDs: genital herpes	Boolean
Age of 1st intercourse	Integer	STDs: molluscum contagiosum	Boolean
# of pregnancies	Integer	STDs: AIDS	Boolean
Smokes	Boolean	STDs: HIV	Boolean
Smokes years	Integer	STDs: Hepatitis B	Boolean
Smokes packs/year	Integer	STDs: HPV	Integer
Hormonal Contraceptives	Boolean	STDs: Number of diagnosis	Integer
Hormonal Contraceptives years	Integer	STDs: Time since first diagnosis	Integer
IUD	Boolean	STDs: Time since last diagnosis	Integer
IUD years	Integer	Dx: Cancer	Boolean
STDs	Boolean	Dx: CIN	Boolean
STDs number	Integer	DX: HPV	Boolean
STDs: condylomatosis	Boolean	Dx	Boolean
STDs: cervical condylomatosis	Boolean	Hinselmann: target variable	Boolean
STDs: vaginal condylomatosis	Boolean	Schiller: target variable	Boolean
STDs: vulvo-perineal condylomatosis	Boolean	Cytology: target variable	Boolean
STDs: syphilis	Boolean	Biopsy: class or target variable	Boolean

Related Work:

Except for the original data, the earliest study conducted based on this dataset was a cost-sensitive classifier, whose accuracy had passed the basic level by a narrow margin.[7] Afterward, more algorithms were developed based on this dataset, such as using two improved support vector machine (SVM) approaches to predict the risk of cervical cancer.[13] Recently, another approach using Firefly Algorithm and Random Forest Classifier was developed.[14] This study was further improved when the synthetic minority oversampling technique (SMOTE) was used to reduce the number of features based on Random Forest classification. Researchers recently managed to achieve an accuracy of 97.25% using a stacked autoencoder with a soft-max layer.

However, all of these studies were optimized for overall classifier performance. There lacks a useful case-sensitive, value-sensitive approach to building classifiers for cervical cancer. Because this dataset was collected in a developing country with highly accessible lifestyle and disease history data, it opens the opportunity to develop a pre-cancer screening, self-assessment tool to raise awareness of women's health. In addition, it gives rise to a possible increase in the early diagnosis rate for women who face challenges for screening for cervical cancer.

In this study, a value-sensitive machine learning approach was implemented. The focus was on the real-world use case and on reducing the false negative rates instead of improving the overall model. The models developed in this study were optimized on false-negative because the project's aim was to develop a pre-screening self-assessment tool, in which false negatives (advising high-risk individuals that there's no need to screen for cervical cancer) leads to much more serious consequence comparing to false positives (advising low-risk individuals to undergo additional screening).

Methods

Value Sensitive Machine Learning:

Value sensitive machine learning is an approach that takes values of ethical importance into account.[15] In this case, human values were taken into account in a well-defined matter throughout the entire modeling process. Quantitative and qualitative data were collected from a survey and the attributes were interpreted under the specific cultural and sociotechnical contexts.[16]

Data Cleaning:

Data dropping and data filling were performed to resolve the missing data in this dataset. First, systematic missing, or cases in which the patients did not provide a response to certain survey questions were identified. This was denoted by Boolean attributes in the dataset, such as whether the patient has a history of STD, or if the patient is under IUD birth control. The missing data could be a result of a reluctance to answer sensitive questions, unknown disease history, difficulty recollecting lifestyle, or no response to survey at all. These data that are missing are completely random, and any filling could bias the original dataset. Thus, the patients who have missing Boolean attributes in any of the survey responses were eliminated. This step produced 728 samples in the dataset.

Regarding the missing Integer attributes, missing responses were filled in with the mean or median of such attributes. Replacing the above with two approximations was a statistical approach of handling missing numerical values. Although this method may add variance to the overall dataset, it was more effective than dropping columns of data. Examples of these attributes include years of smoking, number of pregnancies,

DOI: 10.36838/v4i1.20

number of pregnancies, number of sexual partners, which all have a known correlation with risk for cervical cancer.

Models:

Based on existing work, multiple models were trained using Decision Tree, Logistic Regression and SVM.

Decision tree, as one of the most frequently applied machine learning methods, is trained on a dataset for classification and regression analysis. This model groups the samples into several groups based on a series of questions. The process of classification is like a tree. The root of the tree includes all samples. Then, it divides into several sets of samples using a recursive procedure. The decision tree's key challenge is the selection of the optimal partition attributes, which can be explained by information entropy, gain ratio, or Gini index.[17]

Logistic classification is a binary classification model in which the conditional probability of one of the two possible realizations of the output variable is assumed to be equal to a linear combination of the input variables, transformed by the logistic function.[18]

A SVM is a supervised machine learning model that uses classification algorithms for two-group classification problems. After giving an SVM model sets of labeled training data for each category, it is able to categorize new data points.[19]

First, classifiers optimizing for overall performance with a high F1 score were trained. Afterwards, the best-performing classifier was selected and the selected classifier optimizing for a lower false-negative rate was retrained.

Evaluation:

The dataset was divided into two groups as the training and testing groups randomly. The training dataset was 70% (508 patients) of the cleaned dataset, and the remaining dataset (218 patients) was assigned as the test dataset.

The training dataset was used to train a Decision Tree, an SVM and a Logistic Regression classifier with 10-fold cross-validation. Then, each model was tested on the testing dataset to evaluate its performance.

There are various performance indicators. Since this study only contained two classes, the Percentage of Correctly Classified Instances (PCCI) was used as a performance indicator. In the following expressions, a positive result means that the biopsy test showed positive for cervical cancer and vice versa. The results could be divided into four groups. They were:

- Correctly Classified Class 0 Instances also called as True Negative Class 0 (TNC0)
- Falsely Classified Class 0 Instances also called as False Positive Class 0 (FPC0)
- Falsely Classified Class 1 Instances also called as False Negative Class 1 (FNC1)
- Correctly Classified Class 1 Instances also called as True Positive Class 1 (TPC1)

Results and Discussion

Optimizing for overall performance, the following performance was obtained for the test set:

Decision tree

Using the decision tree method, an F1 score of 92.9% was achieved with the following confusion matrix:

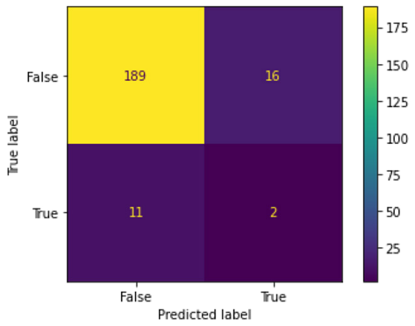

Figure 1: The model generated using the decision tree method with an F1 score of 92.9% and 11 FNC1 cases.

Figure 1 shows the successful identification of 189 TNC0 cases, 2 TPC1 cases, 16 FPC0 cases and 11 FNC1 cases. In cancer screening, it is crucial to avoid false negative cases, also known as Type II errors. Type II errors should be avoided because they could eventually cost a human's life due to mistaken diagnosis.

SVM

Using the SVM method, an F1 score of 92.9% was achieved with the following confusion matrix:

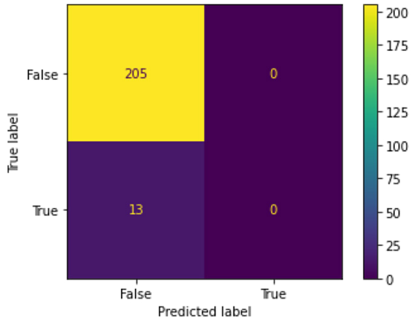

Figure 2: The model generated using the decision tree method with an F1 score of 92.9% and 11 FNC1 cases.

Figure 2 shows the successful identification of 205 TNC0 cases, 0 TPC1 case, 0 FPC0 cases and 13 FNC1 cases.

Though more TNC0 cases were correctly identified through this method, the number of FNC1 cases also increased, which is not ideal.

Logistic Classification

Using the logistic classification method, an accuracy of 93.1% was achieved with the following confusion matrix:

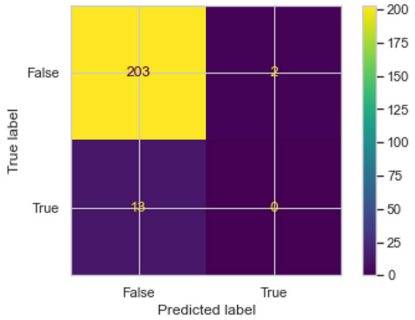

Figure 3: The model generated using the logistic classification method with an F1 score of 93.1% and 13 FNC1 cases.

Figure 3 shows the successful identification of 203 TNC0 cases, 0 TPC1 case, 2 FPC0 cases and 13 FNC1 cases

Though the accuracy improved by 0.2% compared to both

decision tree and SVM, the number of FNC1 cases and FPC0 cases also increased, which is not ideal.

Afterwards, the logistic classification model that would be used for secondary training was chosen because it presented the highest F1 score. A logistic classification classifier was re-trained while optimizing for recall (lowering the false negative rate) and the final classifier was obtained. The final classifier obtained an F1 score of 69.2% and a false negative rate of 0.917% with the following confusion matrix:

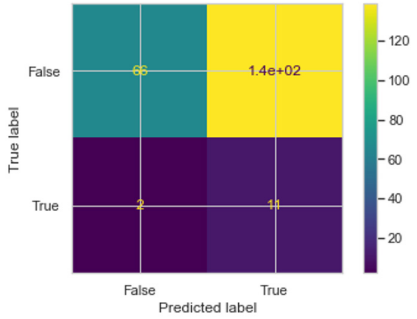

Figure 4: The model generated using the logistic classification method after secondary training with 2 FNC1 cases.

Though the F1 score is much lower than the other two models done using SVM and decision tree, the final classifier using Logistic Regression identifies the least number of FNC1 cases.

Discussion

To evaluate each model's effectiveness, it was more reasonable to assess by examining the number of FNC1 cases rather than the F1 score. FNC1 cases, also known as type II errors, are detrimental to cancer screening because human lives are priceless. Hence, the goal of this risk assessment tool should be to raise awareness and encourage people who are at risk to get tested. As a result, the model should optimize for low FNC1 because if people are at risk of cancer but not aware of their risks, it could cost them their lives.

Though SVM and decision tree models achieve a higher F1 score compared to the logistic classification model (92.9% compared to 69.2%), the confusion matrix of both SVM and decision tree models showed that FNC1 cases were very high: 11 and 13, respectively. On the other hand, the logistic classification model only had 2 FNC1 cases, which was much less than the ones specified by SVM and decision tree models.

Therefore, the logistic classification serves as a more suitable and ideal model designed under the real-world context, successful in getting all people with possible risks to get tested and optimized for the overall medical system efficiency.

Conclusion

It was shown that it is feasible to implement a cervical cancer risk level assessment model using survey responses, enabling self-assessment tools for women in developing countries to perform self-assessment for their risk level before seeking medical resources and biopsy screening. Although the best F1 classification result was obtained by decision tree and SVM, the best model should optimize for a lowering false negative rate due to the detrimental consequences of false negatives in cancer screening. The number of cases classified as false positives indicated that the number of patients with cancer who are not warned. In this study, this number was presented as False Negative (FNC1). For each method, the number of instances classified as false negative was 11, 13, and 2 with decision tree, SVM and logistic classification, respectively. That means that false classified instance rates were 4.26%, 5.04%, and 0.69%, respectively. Because the number of correctly classified instances across all three methods are very similar, the false-negative rates became more critical when determining the best approach. So, in the authors' opinion, the best model for this study is determined to be the logistic classification method.

Acknowledgements

I thank Ms. Zhao and Mrs. Monroe for academic support.

References

1. Cancer Report. February 2017 [cited WHO World Health Organization 25.09.2017]; Available from: http://www.who.int/mediacentre/factsheets/fs297/en/.
2. Ünlerşen, Muhammed & Sabanci, Kadir & Özcan, Muciz. (2017). Determining Cervical Cancer Possibility by Using Machine Learning Methods. International Journal of Latest Research in Engineering and Technology. 3. 65-71.
3. Fernandes, K., J.S. Cardoso, and J. Fernandes, Transfer Learning with Partial Observability Applied to Cervical Cancer Screening, in Pattern Recognition and Image Analysis: 8th Iberian Conference, IbPRIA 2017, Faro, Portugal, June 20-23, 2017, Proceedings, L.A. Alexandre, J. Salvador Sánchez, and J.M.F. Rodrigues, Editors. 2017, Springer International Publishing: Cham. p. 243-250.
4. Cancer Prevention and Control. "Cancer Plan Self-Assessment Tool." Centers for Disease Control and Prevention, www.cdc.gov/cancer/ncccp/pdf/cancerselfassesstool.pdf.
5. Nikpour, Maryam & Hajian-Tilaki, Karimollah & Bakhtiari, Afsaneh. (2021). Risk Assessment for Breast Cancer Development and Its Clinical Impact on Screening Performance in Iranian Women [Corrigendum]. Cancer Management and Research. Volume 13. 3079-3080. 10.2147/CMAR.S311176..
6. P. H. Swain and H. Hauska, "The decision tree classifier: Design and potential," in IEEE Transactions on Geoscience Electronics, vol. 15, no. 3, pp. 142-147, July 1977, doi: 10.1109/TGE.1977.6498972.
7. Dreiseitl, Stephan, and Lucila Ohno-Machado. "Logistic Regression and Artificial Neural Network Classification Models: A Methodology Review." Journal of Biomedical Informatics, vol. 35, no. 5-6, 2002, pp. 352–359., doi:10.1016/s1532-0464(03)00034-0.
8. Pisner, Derek A., and David M. Schnyer. "Support Vector Machine." Machine Learning, 2020, pp. 101–121., doi:10.1016/b978-0-12-815739-8.00006-7.
9. Song, Y. Y., & Lu, Y. (2015). Decision tree methods: applications for classification and prediction. Shanghai archives of psychiatry, 27(2), 130–135. https://doi.org/10.11919/j.issn.1002-0829.215044
10. Castañón, Jorge. "10 Machine Learning Methods That Every Data Scientist Should Know." Medium, Towards Data Science, 5 Sept. 2019, towardsdatascience.com/10-machine-learning-methods-that-every-data-scientist-should-know-3cc96e0eeee9.
11. Suthaharan S. (2016) Support Vector Machine. In: Machine Learning Models and Algorithms for Big Data Classification. Integrated Series in Information Systems, vol 36. Springer, Boston, MA. https://doi.org/10.1007/978-1-4899-7641-3_9
12. Fernandes, Kelwin, Cardoso, S. Jaime and Fernandes, Jessica.

DOI: 10.36838/v4i1.20

"Cervical cancer (Risk Factors) Data Set." UCI, Hospital Universitario de Caracas, 2017, archive.ics.uci.edu/ml/datasets/Cervical+cancer+%28Risk+Factors%29. Accessed 13 Feb. 2021.
13. W. Wu, H. Zhou, Data-driven diagnosis of cervical cancer with support vector machine-based approaches, IEEE Access 5 (2017) 25189–25195.
14. Sawhney, Ramit & Mathur, Puneet & Shankar, Ravi. (2018). A Firefly Algorithm Based Wrapper-Penalty Feature Selection Method for Cancer Diagnosis. 10.1007/978-3-319-95162-1_30.
15. Umbrello, S., van de Poel, I. Mapping value sensitive design onto AI for social good principles. AI Ethics (2021). https://doi.org/10.1007/s43681-021-00038-3
16. Simon, J. & Wong, P.-H. & Rieder, G. (2020). Algorithmic bias and the Value Sensitive Design approach. Internet Policy Review, 9(4). https://doi.org/10.14763/2020.4.1534
17. Rokach, Lior, and Oded Maimon. "Decision Trees." Data Mining and Knowledge Discovery Handbook, Jan. 2005, pp. 165–192., doi:10.1007/0-387-25465-x_9.
18. Maalouf, Maher. (2011). Logistic regression in data analysis: An overview. International Journal of Data Analysis Techniques and Strategies. 3. 281-299. 10.1504/IJDATS.2011.041335.
19. Zhou, Zhi-Hua. "Support Vector Machine." Machine Learning, pp. 129–153., doi:10.1007/978-981-15-1967-3_6.

Author

This is Kaixin Yin, currently a high school senior attending International School of Beijing. I have always been greatly intrigued by the complexity of science, especially bioinformatics. Driven by my passion for programming, I self-studied machine learning and then created a risk level self-assessment model for women in developing countries.

IJHSR
ijhighschoolresearch.org
RESEARCH ARTICLE

A New Decarbonized Energy Station for Hospitals

Yameng (Moe) Zhang

École Argyle Secondary, 1131 Frederick Rd, North Vancouver, British Columbia, V7K 1J3, Canada; moe.zhang2004@gmail.com

ABSTRACT: In 2020, the COVID-19 pandemic caused a significant strain on hospitals around the world. One of the key challenges for hospitals is maintaining a stable energy supply in emergency situations such as the global pandemic. This study proposes a decarbonized energy station based on a coupled reversed Carnot cycle powered by the Carnot cycle, providing a sustainable source to satisfy the various energy needs of hospitals. Carbon dioxide (CO_2) is utilized as the driving medium. Renewable energy powers the energy input, consequently replacing fossil fuels. The only power input of this proposal is work, while the proposed energy station can achieve cooling and heating simultaneously. In the reversed thermodynamic cycle, power input results in the fluid achieving a high relative pressure and temperature that is suitable for the general use of a hospital. As the CO_2 working fluid is in a dense phase, it can achieve a heating function, providing the energy to the heating systems. Next, the fluid reaches low pressure and temperature as it expands and evaporates while absorbing heat to attain a cooling process that is satisfactory for a hospital. Our results show that 4,780,800 tons of carbon emission annually can be reduced if this method is implemented in all Canadian hospitals. Because this energy station will not produce any carbon emissions while providing heating and cooling, it is promising for future hospitals.

KEYWORDS: Physics; decarbonized; natural fluid; energy station; carbon dioxide; hospitals.

Introduction

Due to the COVID-19 pandemic, hospitals are running at full capacity, resulting in significantly heightened levels of energy consumption. Among public and commercial institutions, hospitals are one of the highest consumers of energy. Energy intensity in American hospitals ranks second among all buildings. A Canadian health care institution typically needs 324 gigawatt hours (eGWh) in a year to keep up with the energy demands from various sectors such as ventilation, biomedical material refrigeration, and other specialized medical equipment.[1] In total, Canada needs around 388,800 gigawatt hours(eGWh) a year. Chinese studies delineate that energy consumption by hospitals are 1.6-2.0 times that of other public buildings. Hospitals have higher energy consumption levels due to the distinct features and functions of the buildings. For example, the large construction scale, the complex functions, the concentrated equipment, the diverse energy demand, and the high comfort degree and high infection control requests.

The energy demands of hospitals are diversified, involving two main sectors: heating and cooling. For example, lighting, air conditioning, heating, dehumidification, bathing, refrigeration, freezing, drying, are some of the various energy needs.[2] Figure 1 shows an operating room in a hospital, containing energy demands such as lighting, ventilation, purification, cooling, heating, and dehumidification.

In the energy system of traditional hospitals, electricity -usually produced by coal- and natural gas are the main sources of energy supply. Canada's electricity generation is 60% hydro; however, Canada does still rely on coal and natural gas.[3] Energy supply efficiency is tremendously low as shown in the traditional method of energy supply in Figure 2. In addition, Figure 2A illustrates that the required energy is supplied by power plants, which are usually powered by fossil fuels, such as coal and natural gas. The generated electricity is also used for cooling in hospitals. The heating in hospitals is usually produced by boilers, which are also powered by burning natural gas, but boilers are much more efficient than power plants. This is shown in Figure 2B. Traditional energy stations rely solely on burning fossil fuels to provide energy. It can be seen from Figure 3 that numerous harmful gases especially CO_2 are emitted to the environment during the energy providing process.

Figure 1: Operating room in a hospital.[4]

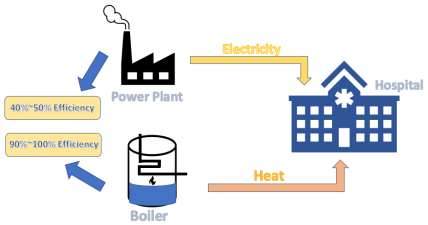

Figure 2A: Traditional method of energy supply for hospitals by power plants (top).
Figure 2B: Traditional method of energy supply for hospitals by boilers (bottom).

DOI: 10.36838/v4i1.21

Figure 3: Traditional Energy Station.[5]

To reduce the level of energy consumption and carbon emissions of hospitals, research has been conducted from two perspectives. One is to optimize the energy output through the adoption of a new cooling and heating energy technology with high efficiency.[6,10] The other is that fossil fuels are replaced with renewable energy to reduce the electricity production from traditional power plants.[11,12] Fossil energy reserves are limited on Earth and face the risk of depletion; the massive and continued use of fossil energy could destroy the environment. Therefore, for future development, it is imperative to use renewable energy as the source for energy stations. Different from the traditional form of energy stations, the proposed energy system is based on the usage of renewable energy, with the goal of converting renewable energy into clean secondary energy.

Thus, in this paper, a new decarbonized energy station system covering energy output and terminal conversion is proposed to solve the problem of high energy consumption and high carbon emissions in hospitals.

Methods

Theoretical study of the new energy station formulation:

Carnot cycle using CO_2 fluid for power output

Carnot cycles are chosen as they are ideal; therefore maximum efficiency can be attained. In comparison with other cycles, the Carnot cycles generate substantially more energy. The basic power output is based on the Carnot thermodynamic cycle shown in Figure 4. In this figure, the heat input from the process 1-2 will produce the power output in the expansion process 2-3 which results in the heat output during the process 3-4. After the compression of the working fluid through the process 4-1, the thermodynamic cycle circulates again. Traditionally, the heat input in the process 1-2 is powered by fossil fuel. However, consider if the heat input from the process 1-2 is supplied by renewable energy, such as solar energy, then the power output from the process 2-3 is achieved exclusively through renewable energy (shown in Figure 4). Based on the Carnot thermodynamic cycle, the existing power is made by using water as the working fluid. Here, it is proposed that not only should water be utilized, but CO_2 should be considered as a working fluid in this power cycle, as depicted in Figure 4; this method effectively uses CO_2 as a useful resource instead of wasting it.[13,14] Furthermore, when there is an excess of renewable energy produced, the captured and transported CO_2 is compressed into the CO_2 storage tank, where it is then stored. If the power generation insufficient and cannot meet the demands of power grid, the compressed CO_2 will drive the turbine impeller to run, push the generator rotor to complete the power generation, releasing energy if energy demands are high, and meet the power generation demand of the power grid. CO_2 involved in energy output powered by renewable energy is presented in Figure 4. The figure on the left is a Pressure Vs. Volume graph of the process, whereas the right is a diagram of the process with real equipment.

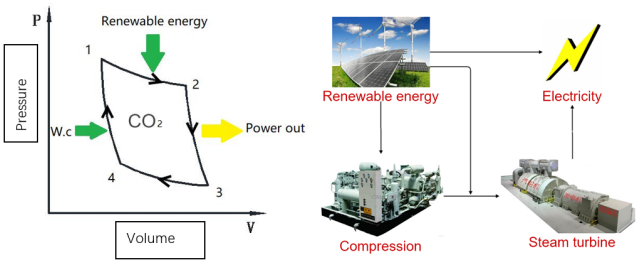

Figure 4: Schematic diagram of the renewable energy powered CO_2 energy output.

* W.c.= Work in.

Reversed Carnot cycle using CO_2 fluid for heating and cooling involved in terminal energy conversion in hospitals

Figure 5 depicts a reversed Carnot cycle. In this thermodynamic cycle, the power input - which can be provided by renewable energy - can form a compression (process 1-2), in which the working fluid is compressed to high pressure and temperature as seen in state 2. The fluid at state 2 is then condensed and releases heat to the user in processes 2-3, which achieves a heating function. Subsequently, the fluid expands to state 4 and is at a low pressure and temperature. At state 4 the fluid evaporates and absorbs heat to achieve cooling during the process 4-1. From Figure 5, it is shown that the only power needed in this cycle is the compression from the work done; however, cooling and heating can be achieved simultaneously.

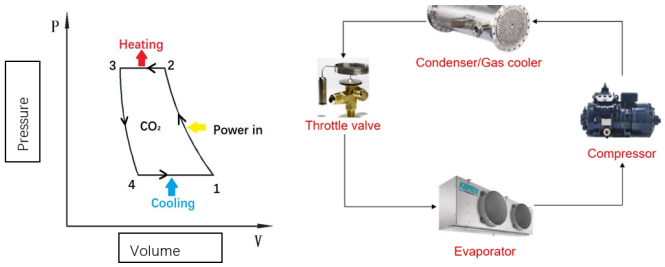

Figure 5: Schematic diagram of the transcritical CO_2 refrigeration and heat pump system.

This basic cycle, meeting different cooling and heating demands, is an effective energy-saving system because the cooling and heating generated is several times larger than the work consumed in the compression process. Based on the efficiency of the reversed Carnot cycle, the generated cooling and heating quantity is more than several times of the consumed work. Furthermore, regarding environmental issues, the mainstream usage of Freon working fluids in the thermodynamic cycle (Figure 5) is a contributing factor to global warming and ozone layer depletion. CO_2 is a natural

refrigerant, ODP (Ozone Depletion Potential) =0 and GWP (Global Warming Potential) =1 and can be used in the cycle shown in Figure 5 to replace the Freon fluids. It is important to use CO_2 because the rapidly increasing CO_2 levels have become a global concern. With this proposed system, the CO_2 is regarded as a useful material, not waste. As transcritical CO_2 compression cycles have high discharge temperatures and large temperature slips during condensing, it is suitable for heating while cooling.[15,19] The viscosity of CO_2 is lower than Freon fluids, but the thermal conductivity and heat capacity are much higher than Freon fluids. This is helpful for industrial and commercial fields that require refrigeration and heating concurrently. By using the reverse Carnot cycle theory, CO_2 achieves high temperatures at the supercritical state post compression, and supercritical fluids release heat in gas coolers to meet the heat demand of various terminals. After throttling, CO_2 enters a low-temperature and low-pressure state, which can absorb heat from lower temperature mediums to meet the cooling requirements. The transcritical CO_2 cycle system, where the pressure is higher than a critical cycle, achieves a simultaneous heating and cooling. This solves the problem of meeting the various energy needs of hospitals and drastically reduces the loss of energy in the conversion process.

Renewable energy powered CO2 cycle for terminal energy conversion in hospital

Figure 6 shows the renewable energy powered CO_2 cycle for energy demands in a hospital. At the first stage, CO_2 uses renewable energy to generate electricity (Figure 4), and the generated power is used to power the transcritical CO_2 reversed Carnot thermodynamic cycle (Figure 5) in facing the terminal needs at the second stage, which includes heating, drying, hot water, cooling, air conditioning, freezing, cold storage etc. Accordingly, CO_2, participates in the initial energy output and the terminal conversion process of various energy grades. From the analysis above, it is delineated that this novel energy station will not produce carbon emissions and utilizes CO_2 as a useful resource and driving medium. Therefore, it is an exceedingly green energy station.

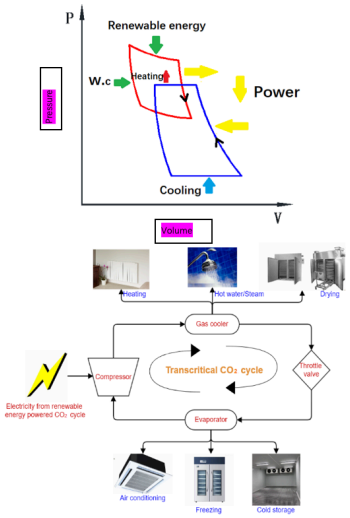

Figure 6: Transcritical CO_2 combined cooling and heating system powered by renewable energy.

Methods for Calculations

All the energy consumption for cooling and heating comes from the renewable energy powered CO_2 energy output system. The energy consumption of transcritical CO_2 combined cooling and heating system is calculated according to the following method.

$$W = M(h_{c,2} - h_{c,3}) = \frac{Q}{COP} \quad (1)$$

W-Annual energy consumption of the CO_2 combined cooling and heating system *M*-Total mass of CO_2 participating in energy output, $h_{c,2}$, $h_{c,3}$ corresponds to the enthalpy of each state point in Figure 4, *Q*-Total cooling / heating load of hospital. The COP can be determined according to the operating environment of the combined heating and cooling system and the enthalpy of each point in the P-H diagram.

Summer condition $COP = \frac{h_1 - h_4}{h_2 - h_1}$ (2)

Winter condition $COP = \frac{h_2 - h_3}{h_2 - h_1}$ (3)

Where, h_1, h_2, h_3, h_4 corresponds to the enthalpy of each state point in Figure 5

The carbon emission of all the schemes is calculated by the following formula.

$$M_{co2} = 0.10118 \times 2.1622 \times W \quad (4)$$

The 0.10118 is the conversion coefficient between electricity and natural gas, and 2.1622 is conversion coefficient between natural gas and CO_2 emission. The comparison of carbon emissions of different schemes is shown in Figure 7.

Results

Perspective of engineering application:

The following is an engineering case of a hospital's energy system design, which is used to predict the possible benefits of adopting this new decarbonized CO_2 energy station. The selected hospital is in Shenzhen, China.[20] According to the survey, the energy system not only solves the electricity supply of medical equipment, but also solves the demand of cooling and heating. The cooling and heating load of the hospital per year is shown in Table 1.

Table 1: Cooling and heating load in hospital per year.

Needs	Load	Hours	Load factor
Cooling	11930kW	5040h	0.17
Heating	2850kW	2160h	0.58

To meet the needs of cooling and heating in hospitals, three possible energy supply methods are provided, which are listed respectively in Table 2, Table 3, and Table 4. A water chiller is a device that consumes electricity to generate cold water. An air source heat pump is a device that absorbs heat from the air to generate heating. In the first scheme, the water chiller is responsible for the cooling, and the air source heat pump is responsible for the heating, both of which use freon as working fluid. In the second scheme, the heating is driven by a boiler burning natural gas. In the third scheme, the lithium bromide water chiller is a device that can produce cold water by burning natural gas. Because the device burns natural gas, it can also produce hot water at the same time to meet the heating demand. It is illustrated that these systems' design schemes are all based on the traditional form of an energy station, in

DOI: 10.36838/v4i1.21

which both have immense energy consumption and carbon emissions. The equipment described is depicted in Figure 7

Figure 7: Diagram of the Equipment used.[21,26]

Table 2: The first scheme of Freon water chiller + Air cooled heat pump unit.

Item	Energy consumption
Water chiller	1939300 (kW.h/a)
Chilled water pump	696780 (kW.h/a)
Cooling water pump	1124928 (kW.h/a)
Cooling tower	347508 (kW.h/a)
Air source heat pump	3054996 (kW.h/a)
Hot water pump	149688 (kW.h/a)

- a- - represents annual average. The same below.

Table 3: The second scheme of Freon water chiller + Gas boiler.

Item	Energy consumption
Water chiller	1939300 (kW.h/a)
Chilled water pump	696780 (kW.h/a)
Cooling water pump	1124928 (kW.h/a)
Cooling tower	347508 (kW.h/a)
Gas boiler	natural gas 652670 (m3/a)
Hot water pump	118843 (kW.h/a)

Table 4: The third of scheme of direct-fired lithium-bromide absorption chiller.

Item	Energy consumption
Direct-fired lithium-bromide absorption chiller	65360 (kW.h/a) + natural gas 3685435 (m3/a)
Chilled water pump	696780 (kW.h/a)
Cooling water pump	1124928 (kW.h/a)
Cooling tower	347508 (kW.h/a)
Hot water pump	102643 (kW.h/a)

If the energy station put forward in this paper is employed, both hot and cold water can be obtained through only utilizing the transcritical CO2 cycle system. According to the needs of the hospital for cooling and heating, the energy consumption of transcritical CO2 system is calculated as shown in Table 5.

Table 5: The Fourth Scheme of Transcritical CO_2 System Combined Cooling and Heating.

Item	Energy consumption
Transcritical CO2 combined cooling and heating system	4789396 (kW.h/a)
Chilled water pump	696780 (kW.h/a)
Cooling water pump	1124928 (kW.h/a)
Cooling tower	347508 (kW.h/a)
Hot water pump	102643 (kW.h/a)
Carbon emission: 0t/a	

From Figure 7, it is delineated that the carbon emissions are 1188t/a, 2336t/a, 8469t/a respectively for schemes 1, 2, and 3. The carbon emissions in scheme 4 is 0t/a here, because all the cooling, heating, and electricity consumptions are supplied by renewable energy. Furthermore, carbon dioxide is also employed as the working fluid in the scheme 4, but no carbon emissions exist in this new energy station proposed in this paper. The annual average value of the scheme 1, 2, and 3 is 3984t, which represents the carbon emission from a traditional energy station in one hospital. For example, if there are 1,200 hospitals in Canada, carbon emissions of 4,780,800t[27] can be cut per year if the proposed energy station is used. Therefore, it can be concluded through these theoretical results that this new energy station should be popularized nationally and globally as it is exceptionally clean and environmentally friendly.

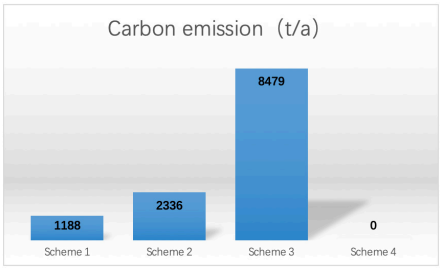

Figure 8: Carbon Emissions of Different Schemes.

Conclusion

The development of renewable energy stations in hospitals is shown to be advantageous in this study. The proposed system with the natural fluid CO_2 is demonstrated to be capable of supplying all the energy demands of a hospital. In detail, a new decarbonized energy station is proposed in this paper to meet the energy demands of a hospital. Specifically, This method is theoretically examined and a comparison of the energy consumption and carbon emission levels between the proposed system and the conventional energy supply schemes. The theoretical results show that the annual CO_2 emissions of the hospital can be cut around 1188t～8469t. An average value of 3984 t CO_2 emissions can be reduced per hospital. This study concludes that this decarbonized energy station is promising in the future of renewable energy implementations in hospitals, which contributes to the carbon- neutralization process.

References

1. Green Care 2019 Environmental Performance Accountability Report. 2019. https://bcgreencare.ca/sites/default/files/VCH_EPAR2019Report_FINAL_Sept1.pdf
2. Katsanis J S , Tsarabaris P T , Bourkas P D , Halaris P G. Estimating water and energy consumption of hospital laundries. AATCC Review, 2008, 8(7):32-36.
3. Provincial and Territorial Profiles. https://www.cer-rec.gc.ca/en/data-analysis/energy-markets/provincial-territorial-energy-profiles/provincial-territorial-energy-profiles-canada.html (accessed April 6th, 2021)
4. "The Surgical Setting." Johns Hopkins Medicine. https://www.hopkinsmedicine.org/health/treatment-tests-and-therapies/the-surgical-setting (accessed December 12, 2020).
5. Sheppard, Kate. "Nebraska Utility Is Phasing out Some Coal Units, and It Won't Cost That Much." https://grist.org/business-technology/nebraska-utility-is-phasing-out-some-coal-units-and-it-wont-cost-that-much/. (accessed December 20,2020)
6. Shi Y ,Yan Z F, Lv Z P. An empirical study on the effect of energy saving measures against hospital energy consumption. DEStech

Transactions on engineering and technology research. 10.12783/dtetr/icaen201/29044.
7. Okamoto S . Energy consumption and technical potential of energy saving in a hospital. International Conference on Energy Sustainability Collocated with the Heat Transfer. 2009.
8. Esmaeil M A, Jahromi A, Twomey J, Yildirim B, Overcash M, Elsken T, Dominquez F, Thomas N, and Mcadam A. Energy consumption of VA hospital CT scans. Proceedings of the 2011 IEEE international symposium on sustainable systems and technology, Chicago, IL, 2011, pp. 1-5, doi: 10.1109/ISSST.2011.5936892.
9. Rundle M . Designing for reduced hospital energy consumption. Hospital engineering, 1982, 36(3):12-14.
10. Roulo C . HVAC system reduces hospital's energy consumption by 32%[J]. Contractor, 2011, 58(3):p.5,53.
11. Szklo A S , Scares J B , Tolmasquim M T . Energy consumption indicators and CHP technical potential in the Brazilian hospital sector. Energy Conversion & Management, 2004, 45(13/14):2075-2091.
12. Pop O G , Abrudan A C , Adace D S , Pocola A G, and Balan M C. Potential of HVAC and solar technologies for hospital retrofit to reduce heating energy consumption. E3S Web of Conferences, 2018, 32:01016.
13. Dostal V , Hejzlar P , Driscoll M J . The Supercritical Carbon Dioxide Power Cycle: Comparison to Other Advanced Power Cycles. Nuclear Technology, 2006, 154(3):283-301.
14. Turchi C S , Ma Z , Neises T W , Wagner M. Thermodynamic Study of Advanced Supercritical Carbon Dioxide Power Cycles for High Performance Concentrating Solar Power Systems. Asme International Conference on Energy Sustainability Collocated with the Asme International Conference on Fuel Cell Science. 2012.
15. Lorentzen G. Revival of carbon dioxide as a refrigerant, International Journal of Refrigeration. 17 (5) (1994) 292–301.
16. Neksa P, Rekstad H, Zakeri G R, Schiefloe P A. CO2-heat pump water heater : characteristics, system design and experimental results. International Journal of Refrigeration, 1998, 21(3): 172-179.
17. Ma Y, Liu Z, Tian H. A review of transcritical carbon dioxide heat pump and refrigeration cycles. Energy, 2013, 55(55): 156-172.
18. Rony UR, Yang H, Krishnan S, Song J. Recent advances in transcritical CO2 (R744) heat pump system: a review. Energies 2019;12(3):457.
19. Tsimpoukis D , Syngounas E , Petsanas D , Mitsopouulos G, Anagnostatos S, Bellos E, Tzivanidis C, Vrachopoulos M G. Energy and environmental investigation of R744 all-in-one configurations for refrigeration and heating/air conditioning needs of a supermarket[J]. Journal of Cleaner Production, 2020:123234.
20. Wang S Y, Yu Z F, Zhao W. Technical and economic analysis of cold and heat source scheme in Shenzhen general hospital. Contamination Control & Air-Conditioning Technology, 2019, 000(004):90-94. (In Chinese)
21. Cooling Water Pump. https://www.ksb.com/centrifugal-pump-lexicon/cooling-water-pump/191520/ (accessed April 6th, 2021)
22. Commercial Water Pump Repair. https://propumpcorp.com/chill-water-pump-repair/ (accessed April 6th, 2021)
23. What is a Water Chiller? https://www.labrotovap.com/what-is-a-water-chiller-how-does-it-work%EF%BC%9F/ (accessed April 6th, 2021)
24. Hyperbolic Cooling Tower with Rope Access. https://www.industrialaccess.com/blog/hyperbolic-cooling-tower-maintenance-rope-access/ (accessed April 6th,2021)
25. Air Source Heat Pumps. https://www.cse.org.uk/advice/renewable-energy/air-source-heat-pumps/ (accessed April 6th, 2021)
26. China Hot Water Pump. https://sanchangpump.en.made-in-china.com/product/qZMmkyLAZEWe/China-Hot-Water-Pump-Heating-Network-Circulating-Pump-Split-Case-Pump-for-Hot-Water-Cos600-560-980rpm-.html (accessed April 6th, 2021)
27. Michas, Frédéric. "Number Hospitals Canada by Province 2019." Statista, September 15, 2020. https://www.statista.com/statistics/440923/total-number-of-hospital-establishments-in-canada-by-province/#:~:text=In%20total%2C%20there%20were%20over,highest%20in%20less%20populated%20territories (accessed November 25, 2020)

Author

Yameng (Moe) Zhang has been captivated by the intricate elements of physics since the first time she became familiar with the field. In this paper, she proposed a decarbonized energy station after recognizing the great energy strains on hospitals during the COVID-19 pandemic. In the future, she hopes to pursue a degree in physics to help others through her research.

DOI: 10.36838/v4i1.21

GENIUS OLYMPIAD

"Let's build a better future together"

www.geniusolympiad.org

International Environment Project Fair For Grades 9-12

Rochester, New York

Hosted by Rochester Institute of Technology

RIT Rochester Institute of Technology

@GeniusOlympiad

terra science and education

IJHSR International Journal of High School Research

is a publication of

terra science and education

N.Y. based 501.c.3 non-profit organization
dedicated for improving K-16 education